Norwegian University of Life Sciences
Faculty of Science and Technology

Philosophiae Doctor (PhD)
Thesis 2018:43

Optimisation of Wastewater Treatment Systems with Data Mining and Process Modelling

Optimalisering av avløpsrensesystemer ved bruk av data mining og prosessmodellering

Xiaodong Wang

Optimisation of Wastewater Treatment Systems with Data Mining and Process Modelling

Optimalisering av avløpsrensesystemer ved bruk av data mining og prosessmodellering

Philosophiae Doctor (PhD) Thesis

Xiaodong Wang

Faculty of Science and Technology

Norwegian University of Life Sciences

Ås (2018)

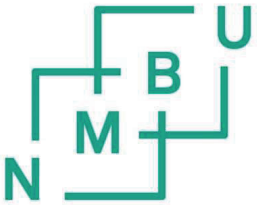

Thesis number 2018:43

ISSN 1894-6402

ISBN 978-82-575-1515-7

Supervisory team

Harsha Ratnaweera (main supervisor)
Professor, Faculty of Science and Technology (REALTEK),
Norwegian University of Life Sciences (NMBU)

Arve Heistad (co-supervisor)
Associate Professor, Faculty of Science and Technology (REALTEK),
Norwegian University of Life Sciences (NMBU)

Lars John Hem (co-supervisor)
Chief engineer, Oslo Water and Sewerage Works
Professor, Faculty of Science and Technology (REALTEK),
Norwegian University of Life Sciences (NMBU)

Knut Kvaal (co-supervisor)
Professor emeritus, Faculty of Science and Technology (REALTEK),
Norwegian University of Life Sciences (NMBU)

Evaluation committee

Martin Oldenburg (first opponent)

Professor, Ostwestfalen-Lippe University of Applied Sciences, Hoexter, Germany

Hallvard Ødegaard (second opponent)

Professor emeritus, Norwegian University of Science and Technology, Trondheim, Norway

CEO, Scandinavian Environmental Technology AS (SET AS), Oksvoll, Norway

Volha Shapaval (committee coordinator)

Associate Professor, Norwegian University of Life Sciences, Ås, Norway

Summary

Wastewater treatment facilities serve an important purpose in public sanitation. Wastewater treatment plants (WWTP) are built at the end of sewerage systems to purify the wastewater before it enters natural water bodies. Carbon, nitrogen and phosphorus have to be removed from wastewater to avoid oxygen depletion, eutrophication and excretion of toxins. Wastewater treatment has also caused some adverse environmental impacts due to energy consumption, use of chemicals and environmental emissions. In a few modern wastewater treatment plants, resource recovery and water reuse are included as a holistic approach. However, the wastewater treatment process needs to be optimised through advanced control to achieve better performance in terms of economics, effluent quality and environmental impact.

The performance of wastewater treatment processes can be affected by disturbances, especially by the variation of influent characteristics. Progress in control laws has been made by researchers and practitioners in wastewater treatment process optimisation, as can be seen from the large amount of publications on control simulation. The lack of reliable and affordable online monitoring equipment and the complexity of the biological treatment process have restricted further implementation of control techniques. This thesis integrates process surveillance, data mining, process modelling and molecular biology to narrow the gap between surveillance and control in practice. Generally, the following works were conducted to optimise the wastewater treatment process: (1) characterisation of influent under the impact of seasonal variation and climate effects; (2) development of a combined approach to achieve advanced control; (3) development of interpretable soft sensors for process surveillance; (4) investigation of interactions between microbial community composition and kinetic modelling.

A key step towards optimised wastewater treatment performance is handling the uncertainties of process inputs. In **Paper I**, a stepwise influent characterisation approach based on data mining methods was developed to characterise influent quality and quantity of a wastewater treatment plant. The seasonal differences of influent quality were compared after eliminating the dilution effect in the cold season. Moreover, the correlation between climate factors and influent characteristics was also investigated.

Paper II addresses the core concept of the thesis, where statistical monitoring and process modelling was proposed as a combined approach to achieve model predictive control. The other appended papers focused on either statistical monitoring or process modelling to support this approach. In **Paper II**, the hard-to-measure variables— chemical oxygen demand (COD) and total phosphorus (TP)— were predicted by statistical models. Furthermore, the predicted values were further used as inputs to the process model. The model outputs of intermediate total suspended solids (TSS) and effluent COD fitted the measured data well, which indicates that the method can be used to control the aeration and chemical dosing of the WWTP.

Data mining was tested in a full-scale WWTP for early warning of poor activated sludge settleability. In **Paper III**, the seasonal variation of activated sludge settleability was investigated by studying the correlation of settleability and process disturbances. Three predictive modelling methods were used to build early warning tools for poor activated sludge settleability. Moreover, the proportion of volatile substances of biomass was found playing a central role in seasonal variation of activated sludge. The storage-biodegradation mechanism explains the reason for poor settleability of activated sludge in the cold season.

In **Paper IV**, the microbial community composition of a lab-scale moving bed biofilm reactor (MBBR) system was investigated by applying high-throughput sequencing. Secondly, the ratios of active heterotrophic biomass and autotrophic biomass in each MBBR chamber were estimated by conducting respiration tests. As a result, the interaction of sequencing results and active biomass ratios led to a novel approach for kinetic model parameter estimation. This approach is useful for the biological process modelling presented in **Paper II**.

Paper V is a continuation of **Paper I** and **Paper II**. Soft sensors can be applied to solve surveillance issues in wastewater treatment plants. For influent monitoring, the nonlinearity caused by seasonal variation and climate effect indicates the necessity of nonlinear models for soft sensors. Multivariate Adaptive Regression Splines (MARS) was found as an interpretable nonlinear modelling tool for COD and TP prediction.

Wastewater is purified at the cost of energy consumption, chemical usage, environmental emissions and other associated costs. The balance between sufficient treatment and environmentally-friendly performance is always an issue for the control of wastewater treatment processes. In **Paper VI**, the environmental impacts of wastewater treatment process control

strategies were evaluated by conducting Life Cycle Assessments. Significant reductions of climate changing impact and environmental toxicity were achieved by enhancing primary removal of particles and applying model predictive control. The study underlines that environmental impacts should be considered alongside economics and effluent quality when designing control strategies for wastewater treatment processes.

Sammendrag

Avløpsrenseanlegg (WWTP) innehar en viktig rolle innen offentlig avfallshåndtering. Avløpsrenseanlegg er plassert på enden av avløpsnettet for å forbedre utløpets vannkvaliteten før det slippes ut til resipientene. Karbon, nitrogen og fosfor må fjernes fra avløpsvannet for å forhindre oksygenutarming, eutrofiering og utslipp av giftstoffer. Behandling av avløpsvann kan også skape negative miljøpåvirkninger på grunn av energiforbruk, kjemikalieforbruk og miljøutslipp. I noen få moderne avløpsrenseanlegg er resursgjenvinning og vanngjenbruk inkludert som en holistisk tilnærming. Avløpsbehandlingsprosessen må optimaliseres for å oppnå bedre ytelse innenfor økonomisk effektivitet, utslippskvalitet og miljøpåvirkning.

Ytelsen til avløpsrenseanlegg blir påvirket av forstyrrelser, da spesielt variasjon i karakteristikken til tilløpet. Framskritt i utvikling av metoder for kontrollsystemer i avløpsbehandling har blitt gjort av forskere og praktikere, noe som det kan ses ut ifra de store mengdene publikasjoner innen kontrollsimulering. Mangelen på kostnadseffektivt og pålitelig utstyr for online overvåkning og kompleksiteten på de biologiske behandlingsprosessene har gjort at implementeringen av kontrollteknikker innen avløpsbehandling har vært begrenset. Denne avhandlingen kombinerer prosessovervåkning, datamining, prosessmodellering og molekylærbiologi for å minske gapet mellom overvåkning og prosesskontroll i praksis. Følgende arbeid ble gjennomført for å optimalisere avløpsbehandling: (1) Karakterisering av tilløpskvalitet og -kvantitet med varierende sesong- og klima-forhold; (2) en kombinert tilnærming for å oppnå avansert kontroll; (3) tolkbare virtuelle sensorer for prosessovervåkning; (4) interaksjoner mellom forskjellige mikrobielle komposisjoner og kinetisk modellering.

Et viktig skritt for å forbedre ytelsen til avløpsbehandlingssystemer er håndteringen av usikkerheter i prosesstilførslene. I **artikkel I**, ble metoder som datamining brukt til å karakterisere kvalitet og kvantitet i tilløpet til et avløpsrenseanlegg. Bidraget til **artikkel I** er et forslag til en detaljert trinnvis metode for karakterisering av tilløp. Som et resultat ble kvaliteten av tilløp i tørt klima sammenlignet etter eliminasjon av sesongbaserte fortynningseffekter. I tillegg ble korrelasjonen mellom klima-faktorer og tilløpskarakteristikker undersøkt.

I **Artikkel II**, som adresserer hovedkonseptet i oppgaven, ble statistisk overvåkning og prosessmodellering foreslått som en kombinert løsning for å oppnå prediktiv modellkontroll.

Resten av artiklene fokuserer enten på statistisk overvåkning eller prosessmodellering for å støtte opp under denne tilnærmingen. I **Artikkel II** ble kjemisk oksygenforbruk (COD) og total fosfor (TP) predikert ved bruk av statistiske modeller. De predikerte variablene ble brukt som inndata i prosessmodellene. Modellens beregnede verdier av slamproduksjon og COD ble godt verifisert, noe som indikerer at metoden kan bli brukt for kontroll av lufting og kjemisk dosering.

Bruk av datamining ble videre testet i et fullskala renseanlegg med den hensikt å gi tidlig advarsel om utilfredsstillende sedimenteringsevne til aktivt slam. I **Artikkel III** ble sesongvariasjoners påvirkning av sedimenteringsevnen til aktivt slam utforsket ved å studere korrelasjonen mellom sedimenteringsevnen til aktivslam og prosessforstyrrelser. Det ble laget tre prediktive modeller for bruk i tidlig varsling av dårlig sedimenteringsevne til aktivt slam. I tillegg ble det observert at de flyktige delene av biomassene spiller en viktig rolle i sesongbaserte variasjoner i aktivslam. Mekanismer for biologisk nedbrytning under lagring ble brukt til å forklare de dårlige sedimenteringsevnene til aktivt slam i kalde sesonger.

I **artikkel IV** ble komposisjonen av mikrobielle samfunn undersøkt i en lab-skala Moving Bed Biofilm Reactor (MBBR) ved bruk av høy gjennomstrømmingssekvensering. I tillegg ble heterotrof og autotrof biomasse estimert ved å foreta respirasjonstester. Det viktige funnet er interaksjonen mellom resultatet av sekvensering og aktiv biomasseforhold ledet til en ny tilnærming for estimering av modellparametere i kinetisk modellering. Denne modellen er svært nyttig for modellering av biologiske prosesser og bidrar som en begrunnelse for **Artikkel II**.

Artikkel V er en fortsettelse av **Artikkel I** og **Artikkel II**. Virtuelle sensorer kan bli brukt til å løse problemer med overvåkning av renseanlegg. Ikke-lineariteter i tilløp forårsaket av sesongvariasjoner og klimaeffekter indikerer at det kreves en ikke-lineær modell for å oppnå en tilfredsstillende overvåkning ved bruk av virtuelle sensorer. I **Artikkel V** ble Multivariate Adaptive Regression Splines (MARS) brukt som et tolkbart modellerings-verktøy (ikke-lineært) for COD og TP prediksjon.

Avløpsvann blir renset med energi, kjemiske, miljørelaterte og andre assosierte kostnader. Balansegangen mellom nødvendig rensegrad og redusering av miljøpåvirkning er en konstant problemstilling innen kontrollprosesser i avløpsbehandling. I **Artikkel VI**, ble miljøpåvirkningen av avløpsrenseprosesser med forskjellige kontrollstrategier undersøkt ved å foreta livsløpsanalyser. Ved å forsterke den primære fjerningen av partikler og ved å implementere prediktiv

modellkontroll ble det observert en merkbar reduksjon av klimapåvirkning og utslipp av miljøgifter. I tillegg til økonomi og avløpskvalitet burde også miljøpåvirkning bli betraktet i design av kontrollstrategier for avløpsrensesystemer.

Acknowledgements

Hey, are you looking for your name on this page? Well, I wish you good luck. If it is not here, please just ask “WHY”……

Alright, no more kidding. The serious talk begins.

Whenever I come to the “Acknowledgements” page of a thesis, it is always filled with warm-hearted words: “gratitude”, “appreciate”, “thanks”, “friendship” and “love”. Well, I never excelled at using explicit language to express my emotion, since adolescent age. The feeling of appreciation to the people I met was most often an interior monologue with an imagined voice of myself. However, I would like to take the challenge this time to make those inner mind activities visible.

I am grateful to many people I met in Norway. First of all, I would like to express my gratitude to my main supervisor, *Professor Harsha Ratnaweera*, who initialised this PhD project, secured the funding and was supportive all the time. This PhD thesis would not have reached this stage without the encouragement and guidance from *Harsha*. I am also grateful to my co-supervisors, *Associated Professor Arve Heistad*, *Professor Lars Hem*, and *Professor Knut Kvaal*. *Arve* has made the fascinating wastewater facilities available in the water lab. I got my understanding of wastewater treatment in Norway from *Lars*, who always has answers to my questions. Most of these questions need practical experience to answer, which can hardly be answered by searching the internet. *Knut* is always patient and was so kind to explain the research methods; he also put so much time and energy into commenting on my work.

I am appreciative of being a PhD student at the Norwegian University of Life Sciences (NMBU) and the Faculty of Science and Technology (REALTEK). NMBU encourages interdisciplinary study, which always reminds me to be open-minded towards new knowledge and seemingly incomprehensible ideas. REALTEK provides a friendly environment, where I had a pleasant journey in both studying and working.

I would like to thank the Water Pollution Control Research Group at the Qingdao University of Technology, for receiving me as a visiting student when I carried out my fieldwork in China. Thanks to *Professor Bi Xuejun* for helping me establish the bioreactors and introducing me to the local wastewater treatment plants. The works in Paper III and Paper IV were partially funded by the research projects at the Qingdao University of Technology. I am grateful for the research

funding from the Regnbyge-3M project and the RECOVER project (granted by The Research Council of Norway) in NMBU. I also want to thank the engineers and operators in Solumstrand wastewater treatment plants for their support during sampling and data collection. Special thanks go to Vibeke Olsbu and former master's student Johan Holm.

Happiness accompanied me when I stayed together with other fellow PhD students in the WESH group. Thanks to *Aleksander Hykkerud* for translating the summary of this thesis. I had a memorable trip with *Nataliia Sivchenko* and *Abhilash Nair* in Canada. The time with *Duo Zhang*, *Olga Kulesha*, *Fasil Eregno*, *Melesse Moges* and former PhD students *Wei Liu* and *Lelum Manamperuma* was delightful, and I expect the growing of friendship during the professional and social discussion. I would like to thank the staff *Vegard Nilsen*, *Zakhar Maletskyi* and *Åsmund Skaar* for organising WESH events. Moreover, best wishes to all the master's students who were involved in this PhD work and to those international visiting students who enriched the international environment of the WESH group.

Now I have sent out the cards of "gratitude", "appreciate", "thanks", and "friendship". The one of "love" is reserved for my family. I am deeply thankful to my parents for their love and support. I sincerely thank *Ms Sun Liyuan* for accompanying me on this PhD journey, in most cases remotely.

Ås, April 2018

Xiaodong Wang

Table of Contents

List of Publications

The contents of the following appended papers are integrated into this thesis, which will be referred to by their Roman numerals (I - VI) throughout the text. The published papers are reproduced with permission from the publishers.

Paper I

Wang, X., Kvaal, K., Ratnaweera, H., 2017. Characterization of influent wastewater with periodic variation and snow melting effect in cold climate area. Computers & Chemical Engineering. 106, 202–211. doi:10.1016/j.compchemeng.2017.06.009

Paper II

Wang, X., Ratnaweera, H., Holm, J.A., Olsbu, V., 2017. Statistical monitoring and dynamic simulation of a wastewater treatment plant: A combined approach to achieve model predictive control. Journal of Environmental Management. 193, 1–7. doi:10.1016/j.jenvman.2017.01.079

Paper III

Wang, X., Bi, X., Liu, C., Ratnaweera, H., 2018. Identifying critical components causing seasonal variation of activated sludge settleability and developing early warning tool. Water Science and Technology. 77, 1689–1697. doi:10.2166/wst.2018.053

Paper IV

Wang, X., Bi, X., Hem, L.J., Ratnaweera, H., 2018. Microbial community composition of a multi-stage moving bed biofilm reactor and its interaction with kinetic model parameters estimation. Journal of Environmental Management. 218, 340–347. doi:10.1016/j.jenvman.2018.04.015

Paper V

Wang, X., Kvaal, K., Ratnaweera, H. Explicit and interpretable nonlinear soft sensor models for influent surveillance at a full-scale wastewater treatment plant. (Manuscript submitted to Journal of Process Control).

Paper VI

Wang, X., Bi, X., Hem, L. J., Ratnaweera, H., 2017. Evaluation of surveillance and control strategies for wastewater treatment plants based on Life Cycle Assessment. Paper presented in the IWA Conference on Sustainable Wastewater Treatment and Resource Recovery: Research, Planning, Design and Operation. November 2017, Chongqing.

List of Acronyms

AE1	First aerobic chamber
AE2	Second aerobic chamber
AN	Anoxic chamber
Anammox	Anaerobic ammonium oxidation
ANOVA	Analysis of Variance
AOB	Ammonium oxidizing bacteria
AS	Activated sludge
ASM	Activated sludge model
BNR	Biological nitrogen removal
COD	Chemical oxygen demand
DNB	Denitrification bacteria
DO	Dissolved oxygen
DSVI	Diluted sludge volume index
EBPR	Enhanced biological phosphorus removal
HRT	Hydraulic retention time
LCA	Life Cycle Assessment
MARS	Multivariate Adaptive Regression Splines
MBBR	Moving Bed Biofilm Reactor
MLR	Multiple Linear Regression
MPC	Model predictive control
NH_4-N	Ammonium nitrogen
NOB	Nitrite oxidising bacteria
ORP	Oxidation-reduction potential
OTU	Operational taxonomic units
OUR	Oxygen uptake rate
PAOs	Phosphorus Accumulating Organisms
PCA	Principal Component Analysis
PCR	Polymerase chain reaction
PO_4-P	Orthophosphate
PLS	Partial Least Squares
PLS-DA	Partial Least Squares Discriminant Analysis
PN	Partial nitrification
SBR	Sequencing batch reactor
SCOD	Soluble chemical oxygen demand
TP	Total phosphorus
TSS	Total suspended solids
UCT	University of Cape Town
VFA	Volatile fatty acids
WarmDry	Warm season and dry climate
WWTP	Wastewater treatment plant

List of Figures

List of Tables

1. Introduction

The growth of urbanisation and industrialisation has improved human living standards considerably. At the same time, there are increasing problems of environmental pollution and resource depletion. One of the major challenges is water pollution. Wastewater treatment has become a worldwide solution for water pollution control. With increasing emphasis on resource recovery from wastewater, a few wastewater treatment facilities have integrated nutrient and energy recovery as well as water reuse as a holistic solution.

Wastewater treatment plants (WWTPs) are composed of mechanical treatment processes, chemical treatment processes and biological treatment processes. The particulate fractions can be removed by either mechanical treatment or chemically enhanced solid-water separation. Soluble organic matters and nitrogen are usually removed from wastewater by biological wastewater treatment systems. Soluble phosphorus can be removed from wastewater by either chemical precipitation or biological treatment. With the implementation of the European Directive for Urban Waste Water Treatment (91/271/EEC) in Europe, stringent nitrogen and phosphorus removal requirements were adopted. However, considerable amounts of energy and materials are required to maintain the removal efficiency. For nitrogen removal in conventional wastewater treatment plants (WWTPs), aeration and sometimes external carbon sources are required to remove nitrogen by biological treatment processes (Meneses et al., 2015; Olsson, 2002; Rusten et al., 1995). Chemical phosphorus removal highly relies on coagulant dosing, and some coagulant dosing control strategies have been developed in the past decades (Ratnaweera and Fettig, 2015). Whether the energy and chemicals consumption pays off in terms of the environmental benefits is still a question (Lorenzo-Toja et al., 2016). On the one hand, WWTPs are considered environmentally friendly as the eutrophication potential reduces due to nutrient removal. On the other hand, negative environmental impacts, such as global warming, ozone depletion and acidification potential are caused by energy and chemicals consumption in the WWTPs (Rahman et al., 2016). There is also a trend of defining wastewater as a resource rather than a type of waste because both the society and the environment will benefit from nutrient recovery, water reuse and energy production from wastewater. In the foreseeable future, resource recovery from wastewater will take a major role in practical wastewater treatment. However, the currently operating wastewater treatment processes will not be completely replaced by water resource recovery facilities. It is still

important to optimise wastewater treatment processes for social and environmental benefits, and the knowledge gained in this process can be further used in resource recovery processes.

The operation cost of WWTPs is predicted to be reduced by 20 % – 50 % in the next decade if advanced surveillance and control are applied (Haimi et al., 2009). The control theory has been developed and implemented in various sectors of industrial process control, but advanced control in the wastewater treatment sector has been limited to computer simulation rather than implementation in full scale (Guerrero et al., 2011; Han et al., 2014; Olsson, 2012). The complexity of biological processes and the availability of instrumentation have restricted the application of advanced control in wastewater treatment plants. Apart from the technological challenges, the high cost of initial investment on instrumentations is also a barrier for WWTPs to implement real-time control. Therefore, the control systems have to be simple and efficient enough to motivate decision-makers.

This introductory chapter starts with a review of the development of biological wastewater nitrogen and phosphorus removal (Section 1.1), which provides the background information on the biological wastewater treatment process. Section 1.2 introduces the operational challenges of wastewater treatment processes and the solutions to optimise wastewater treatment processes. The development and limitations of current process optimisation methods are also discussed in Section 1.2. Data mining and process modelling techniques are reviewed in Section 1.3, which are the main methodology of this thesis. Section 1.4 presents the objectives of this thesis.

1.1 Biological nitrogen and phosphorus removal

The biological nitrogen and phosphorus removal system is the single largest energy and material consumer in a modern WWTP (Olsson, 2012). For process surveillance and control, it is important to understand the mechanism of biological nitrogen and phosphorus removal.

1.1.1 Biological nitrogen removal

Biological wastewater treatment processes are applied worldwide for biodegradable substance removal, especially for the removal of soluble substances. Parts of particulate substances may be converted to soluble substances during hydrolysis reaction. Biological wastewater treatment processes can be classified into two main categories: suspended growth (i.e. activated sludge) and attached growth (i.e. biofilm) processes. The Activated Sludge Model No.1 (ASM1) is the first

comprehensive summary of previous knowledge and experience of biological wastewater treatment (Henze et al., 1987). Although ASM1 is based on activated sludge, the kinetic processes in ASM1 are also applicable for biofilm systems (Plattes et al., 2008).

Conventional biological nitrogen removal (BNR) processes include ammonification of organic nitrogen, nitrification and denitrification. In the earlier 1900s, the nitrification process was known as a two-step reaction (Downing and Hopwood, 1964). The autotrophic ammonium oxidising bacteria (AOB) convert ammonium into nitrite, and the nitrite will be converted to nitrate by nitrite oxidising bacteria (NOB). To remove nitrogen from the wastewater, denitrification bacteria (DNB) have to get involved to deoxygenise nitrate to nitrite and nitrogen gas. Denitrification bacteria were assumed as a group of heterotrophs that can use nitrate as electron acceptors in ASM1. Equation 1.1 illustrates the ideal situation of the conventional nitrogen removal process. However, nitrate and nitrite may convert into greenhouse gas in non-ideal situations, such as nitrous oxide (Kampschreur et al., 2009).

$$NH_4^+ \xrightarrow{AOB} NO_2^- \xrightarrow{NOB} NO_3^- \xrightarrow{DNB} NO_2^- \xrightarrow{DNB} N_2 \qquad (1.1)$$

The conventional BNR process needs to be configured with aerobic chambers for nitrification, and anoxic chambers for denitrification. Aeration is necessary to provide oxygen for aerobic reaction. In anoxic chambers, easily biodegradable organic matters (e.g. ethanol, acetate acid) are required to perform as electron donors (Wanner and Gujer, 1984). In practice, external carbon sources are usually dosed to anoxic chambers to provide electron donors for denitrification processes. Energy is the single largest operational cost in biological wastewater treatment (Olsson et al., 2014), and aeration consumes the largest part of energy (Åmand et al., 2013). In addition, external carbon sources contribute considerably to operational costs. In spite of these challenges, BNR processes are widely used nowadays.

A new pathway for nitrogen removal was found in the 1990s (Siegrist et al., 1998). The nitrate phase is bypassed during nitrogen removal, and only low oxygen levels are needed to convert ammonium nitrogen into nitrite partially. The nitrite will react with ammonium in anaerobic condition and they will finally be removed from the system as nitrogen gas. Later, this new pathway was called partial nitrification/anaerobic ammonium oxidation (PN/Anammox). The PN/Anammox became a popular research topic in the wastewater treatment field (Lackner et al.,

2014), due to its potential for significant reduction of energy and chemical cost (Stinson et al., 2013). However, the process can hardly be applied in WWTPs as a mainstream process due to the crucial operational requirement of ammonium concentration, temperature, carbon/nitrogen ratio and nitrate control (Ødegaard, 2016). Therefore, the PN/Anammox based BNR process is not discussed in this thesis.

1.1.2 Biological phosphorus removal

Phosphorus can be removed from wastewater by either chemical precipitation or enhanced biological phosphorus removal (EBPR) processes. EBPR is performed by Phosphorus Accumulating Organisms (PAOs), which was introduced to Activated Sludge Model No. 2 (ASM2) as a development of ASM1 (Henze et al., 1994). In the aerobic condition, PAOs uptake soluble phosphorus and store phosphorus in the form of intracellular poly-phosphorus. The energy for this process is provided by polyhydroxyalkanoates (PHAs), which are intracellular substances produced from volatile fatty acids (VFAs) by PAOs in anaerobic condition. The phosphorus is released into the wastewater from cells after the hydrolysis of poly-phosphorus and the energy for producing PHAs comes from hydrolysis of poly-phosphorus. Thus, EBPR is achievable in wastewater treatment systems by alternating aerobic-anaerobic conditions. The performance of the EBPR process is profoundly affected by the availability of VFAs (Olsson, 2012). The presence of nitrate in the anaerobic reactor will also cause a failure of EBPR because the denitrification bacteria will outperform PAOs in the competition of VFAs (Guerrero et al., 2011).

Simultaneous nitrogen and phosphorus removal can happen in anoxic condition, where nitrate is used as electron acceptors rather than oxygen (Kerrn-Jespersen and Henze, 1993). The denitrifying PAOs generate energy for phosphorus uptake by degrading PHAs. At the same time, nitrate is reduced to nitrogen gas when it receives electrons from PHAs degradation. The kinetic of denitrifying phosphorus removal was presented in Activated Sludge Model No. 2d (ASM2d) (Henze et al., 1999), which is an extension of ASM2.

1.1.3 Biological nitrogen and phosphorus removal processes

A conventional nitrogen removal system will be configured with both aerobic chambers and anoxic chambers. Pre-denitrification is widely used where the inlet wastewater first enters the anoxic chambers. The nitrified mixed liquid is recycled from the end of the aerobic chamber to mix with the inlet wastewater in the anoxic chamber. In the biofilm system, the biomass is fixed growing in

either aerobic chambers or anoxic chambers. The moving bed biofilm reactor (MBBR) is an innovative process of nitrogen removal (Ødegaard, 1994), which combines advantages of the traditional biofilm system and activated sludge system. In Norway, several municipal WWTPs apply the MBBR system with both pre-denitrification and post-denitrification, as shown in Figure 1.1.

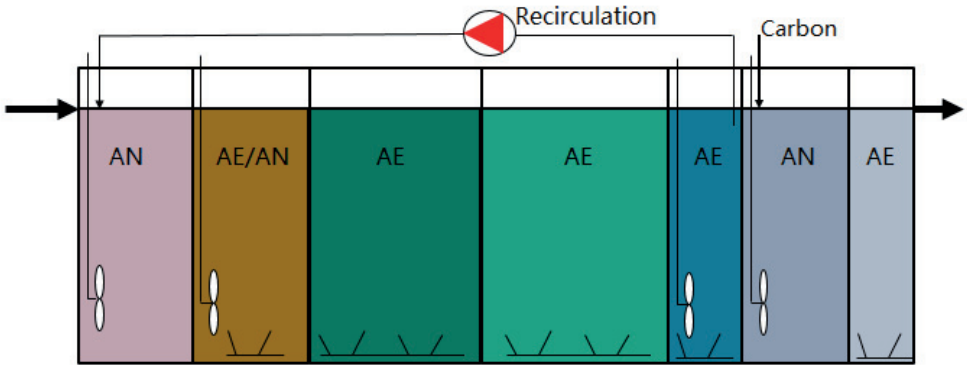

Figure 1.1: The typical moving bed biofilm reactor process configuration with both pre-denitrification and post-denitrification in Norwegian WWTPs. AN is the anoxic chamber, and AE is the aerobic chamber.

To remove nitrogen and phosphorus from the same biological wastewater treatment system, the biomass has to be exposed to an anaerobic-anoxic-aerobic environment (Morgan-Sagastume et al., 1994). One typical example is the University of Cape Town Process (UCT Process) (Sötemann et al., 2002), as shown in Figure 1.2. To avoid the negative effect of nitrate on phosphorus release, the returned activated sludge and nitrified mixed liquid are recycled back to the anoxic chamber for denitrification. An additional recycle stream is added to transport the denitrified mixed liquid back to the anaerobic chamber for poly-phosphorus release and PHAs storage. When the denitrifying PAOs are using nitrates as electron acceptors and PHAs as carbon source, simultaneous nitrogen and phosphorus removal will happen in the anoxic zone (Østgaard et al., 1997). Finally, excessive phosphorus uptake happens in aerobic zone. The phosphorus will be removed from the wastewater treatment system by disposal of waste activated sludge.

Biological phosphorus removal can also be achieved in biofilm systems by exposing the biofilm into an alternating anaerobic–aerobic environment. The most applicable solution for simultaneous nitrogen and phosphorus removal is running the MBBR system as a sequencing batch reactor (SBR)

(Helness, 2007). Besides, continuous MBBR for EBPR has been successfully applied in a full-scale WWTP in Norway by recycling the biofilm carriers.

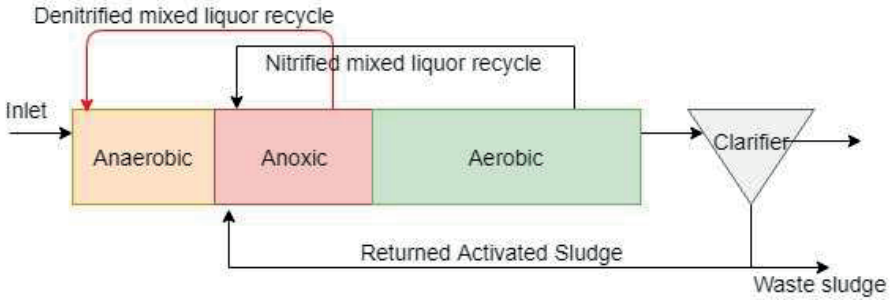

Figure 1.2: The recycle streams of the University of Cape Town (UCT) process.

1.2 Wastewater treatment system optimisation

The major challenges for wastewater treatment process operation are the uncertainties caused by climate change (Hwang and Oleszkiewicz, 2007; Wilen et al., 2006), variation of influent quantity and quality (Bixio et al., 2001; Martin and Vanrolleghem, 2014), and online measurement of process variables (Rieger et al., 2005a). Process optimisation is supposed to bring the process to the optimal status by stabilising the process output and minimising operational cost. Optimisation of wastewater treatment processes is achievable by applying real-time surveillance and control.

In the past decades, advanced control methods for wastewater treatment processes have been studied from several aspects. The control setpoints for carbon, nitrogen and phosphorus removal processes have been studied (Guerrero et al., 2012). Several advanced control strategies were developed for different purposes, e.g. multivariate based coagulant dosing control (Manamperuma et al., 2017), ammonium based aeration control (Åmand and Carlsson, 2012), and carbon source dosing control for nitrogen removal (Stare et al., 2007; Zeng et al., 2008). However, there is always a discussion about "why many control systems fail" (Rieger and Olsson, 2012). Whether the surveillance methods or control law limited the implementation of real-time process optimisation was also an interesting question. Steyer et al. (2006) compared a fuzzy logic controller and a model predictive controller for the anaerobic digestion process, and it turned out that the online monitoring of alkalinity was the restriction rather than the control law. Moreover, an alkalinity prediction model was recommended to replace the expensive alkalinity sensor. Therefore, it is

important to figure out the technological bottleneck that restricts the implementation of real-time optimisation technologies for wastewater treatment systems.

The developments of surveillance and control of wastewater treatment processes are reviewed in the following two subsections, where the limitations are also discussed.

1.2.1 Surveillance of wastewater treatment processes

Online monitoring of state variables is the basic requirement for process control. Commercially available instruments for online monitoring of wastewater treatment processes make real-time surveillance and control possible. Some process variables such as pH, oxidation-reduction potential (ORP), flow rate, conductivity, turbidity, dissolve oxygen (DO), etc., are viewed as easy-to-measure variables due to their short time requirement for measuring and affordable price. These easy-to-measure variables have been applied to control wastewater treatment process for different purposes, e.g. aeration control using ORP and DO sensors for energy saving (Chen et al., 2002); coagulant dosing control using flow rate, turbidity, pH and conductivity sensors (Liu and Ratnaweera, 2016).

A significant development is that nutrient sensors became commercially available in the past two decades (Olsson et al., 2014). Ammonium, nitrate and phosphate sensors have been used for process surveillance in wastewater treatment plants (Machado et al., 2009). Online measurement of nitrate and ammonium nitrogen enables control of the biological nitrogen removal process more accurately (Claros et al., 2012). The most common nutrient sensors are the in situ analysers that were developed based on automated laboratory methods (Haimi et al., 2009). These nutrient analysers require the sample flow free of suspended solids, which means that these analysers need to be used coupled with online filters. Time-delay of the filtration and chemical analysis process extends the drawbacks of these analysers. Fortunately, optical sensors for ammonium and nitrate nitrogen measurement have become commercially available in recent years, but reliable optical sensors for phosphorus measurement can hardly be found on the market. The optical nitrogen sensors are more realistic to be applied for real-time control in full-scale WWTPs due to their chemical-free and short time-delay properties. In spite of this, the WWTP managers and stakeholders would hesitate on whether it is worth the investment, because these sensors are usually more expensive than other commonly used sensors.

Therefore, a major bottleneck of improving automation in WWTPs is the difficulty obtaining real-time data of the necessary state variables (Chai, 2008; Haimi et al., 2009). If fast-response and affordable hardware sensors are not available for the online measurement of carbon and nutrient, indirect data acquisition methods (e.g. prediction models) may be used as alternatives (Corona et al., 2013; Hedegärd and Wik, 2011).

Soft sensors (or software sensors) are groups of models using the combination of easy-to-measure variables to predict hard-to-measure models (Haimi et al., 2015). If prediction models are capable of replacing expensive online sensors, soft sensors can be applied as alternatives to hardware sensors for carbon and phosphorus measurement. Since the pH differences over aeration tanks contain information on ammonium concentration, a soft sensor for ammonium detection was developed based on pH measurements (Ruano et al., 2009). Although several pH sensors can be used to replace ammonium measurement in an aeration tank, ammonium estimation is getting less important with the recent development of affordable optical sensors in the market. Online measurement of chemical oxygen demand (COD) and total phosphorus (TP) are more important because there are long time-delays to measure these two variables. Besides, the prices for COD and TP online instrument are still high based on market investigation. In recent years, soft sensor methods are mostly used for fault detection (Liu et al., 2014a; Samuelsson et al., 2017; Villez et al., 2011) or dealing with time-delays (Xiong et al., 2017), but the hardware sensors cannot be completely replaced in these applications.

The time-delay, initial investment and maintenance cost have restricted the application of COD and TP analysers for control purpose in practice. In this thesis work, data-driven soft sensors based on statistical learning methods for COD and TP detection were developed to replace the hardware measurement completely. In **Paper II**, the correlation between easy-to-measure influent characteristics, COD and TP was investigated, and the most significant variables for influent COD and TP prediction were figured out after principal component analysis. The prediction models for influent COD and TP that could be used to replace the hardware measurement of these two variables were established. Moreover, a new approach for effluent water characteristics prediction was developed by combining statistical models and kinetic models of the treatment process. This work provide possibilities to achieve advanced control of wastewater treatment processes in

practise. Furthermore, an improved statistical method for influent COD and TP prediction was used in **Paper V** to solve the nonlinear variation issues of the WWTP influent.

Model predictive control (MPC) is considered as an advanced control method for wastewater treatment processes, which has been studied theoretically in various literature (Han et al., 2014; Kim et al., 2014; Åmand et al., 2013). Online monitoring of the influent of WWTPs is the key step to achieve MPC, while indirect measurement of contaminants in other streams can be achieved by combining influent prediction data and process models, as shown in **Paper II**.

1.2.2 Control of wastewater treatment processes

The control theory for wastewater treatment processes has been available since the 1970s, when reliable dissolved oxygen sensors were introduced (Olsson and Newell, 1999). The development of instrumentation, control and automation in the past 40 years was reviewed by Olsson et al. (2014), who concluded that there had been tremendous progress in the understanding of process dynamics and control theory. In modern wastewater treatment plants, classical feedback and feedforward control are still popular in aeration control (Rieger et al., 2014; Åmand et al., 2013) and chemical dosing control (Kim et al., 2004; Liu and Ratnaweera, 2016).

There are two types of control algorithms dominating the industrial process control and wastewater treatment, the on-off control and the Proportional-Integral-Derivative (PID) algorithm (Haimi et al., 2009). The on-off controllers can be considered as the simplest error-driven controller, since the control variables have only two values, u_{max} and u_{min}. The selection of u_{max} and u_{min} depends on the sign of the error (e), as shown is Equation 1.2:

$$u = \begin{cases} u_{max} & if\ e > 0; \\ u_{min} & if\ e < 0 \end{cases} \tag{1.2}$$

The on-off control method has been widely used for water level control in wastewater treatment plants (Tchobanoglous et al., 2003). For the water level control, u_{max} is equal to the maximum flow rate of the pump, and u_{min} is 0. This algorithm is simple to be implemented in practice, but the drawback of on-off algorithm is as obvious as its advantage. The control variable is always oscillating around the setpoint with a time-delay, which may cause wear problems for some actuators.

PID is the widely used control algorithm in process control (Åström and Hägglund, 1995). The PID controller consists of three parts, the Proportion term (P), Integral term (I) and Derivative term (D), as shown in Equation 1.3:

$$u = u_0 + K_p \cdot e + \frac{K_p}{T_i}\int_0^t e \cdot dt + K_p \cdot T_d \cdot \frac{de}{dt} \quad (1.3)$$

where K_p is the controller gain, T_i is the integral time, T_d is the derivative time.

These three parts can either be fully utilised or with only the P term, PI term or PD term. The P term enables the controller to respond proportionally to the error (e) between the measurement and the setpoint. The Integral term sums the error of the control signal over time; therefore, the controller will be active as long as the error exists. The Derivative term is activated by the rate of error changing, which contributes to the speed of control action. The Derivative term is not commonly used in industrial process control, because it may be triggered by measurement noise. The PI feedback controllers are the most popular in wastewater treatment (Haimi et al., 2009).

In the 1990s, a lot of efforts have been made in wastewater treatment process control, but many of them were shown only in simulation, as summarised by Olsson (2002) after the first conference on Instrumentation, Control and Automation in 2001 (ICA2001). Later, control scheme for the cycles of sequencing batch reactors was developed based on ORP and pH measurements (Kim et al., 2004). As low-cost sensors, pH and ORP-based control have been used to control either aeration or carbon source dosing in nitrogen removal processes (Martín de la Vega et al., 2012; Ruano et al., 2012, 2009; Won and Ra, 2011). The pH and conductivity sensors are proved vital for coagulant dosing control in either a feedforward or feedback control scheme (Ratnaweera and Fettig, 2015). Another popular application of PI feedback control is the aeration control based on DO setpoints (Machado et al., 2009). Since the wastewater quality variables were not measured in these control methods, a good understanding of process variables (e.g. ammonium) and control variables (e.g. DO) is important. Thanks to the progress in online measurement of nutrient, more accurate control can be applied in recent years. With the possibility of online measurement of ammonium nitrogen, ammonia-based control can be substituted into feedforward and feedback schemes for aeration control (Rieger et al., 2014).

Maciejowski (2002) mentioned in the book “Predictive Control with Constraints” that “Model Predictive Control (MPC) is the only advanced control technique – that is, more advanced than

PID control". The concept of MPC is using one or more predicted future state variables to adjust the actuators to minimise the errors between control variables and the corresponding setpoints. Therefore, MPC can optimise multivariable processes such as wastewater treatment processes. However, the earliest implementation of MPC in real biological wastewater treatment plant that can be found in literature reports was carried out in 2011 (O'Brien et al., 2011; Vrečko et al., 2011). The first documented implementation of MPC in a real biological wastewater treatment process (a pilot MBBR system) is in 2011 (Vrečko et al., 2011). Other recent studies of MPC are either theoretical studies (Gutierrez et al., 2014; Han et al., 2014) or computer simulations (Mulas et al., 2015). The difficulties of applying MPC in practice may be related to the lack of online measurements of some state variables. Another reason may lie in the difficulties in obtaining reliable process models.

In this thesis, the content of **Paper II** is based on the hypothesis that solving process modelling and online measurement issues may enable the implementation of MPC in full-scale WWTPs. The following works in **Paper IV** and **Paper V** are the further investigation of these two issues, respectively.

In recent years, multi-objective optimisation approaches have been taken into consideration, such as including greenhouse gas emission control into the overall control objectives (Flores-Alsina et al., 2011; Sweetapple et al., 2014). The selection of control strategies for wastewater treatment systems has been traditionally driven by either economic-benefit analysis or technology availability. However, the fundamental reason for wastewater treatment has always been environment protection. Whether the wastewater treatment processes are controlled sustainably has drawn the attention of some researchers (Lluis Corominas et al., 2013; Meneses et al., 2015). For instance, significant aeration energy and carbon source can be saved if the nitrogen removal process is controlled by a low DO setpoint, but the greenhouse gas emission will also increase under low DO condition (Kampschreur et al., 2009). Whether the environment will benefit from this type of control is unknown, although the economic benefit is clear. Thus, a comprehensive evaluation including environmental impact assessment is necessary for decision-making. Life cycle assessment of wastewater treatment can be used to evaluate the environmental impacts of different process control strategies (Ontiveros and Campanella, 2013; Rahman et al., 2016).

Paper VI of this thesis applied life cycle assessment (LCA) on control strategies for the typical Norwegian wastewater treatment plant to evaluate the environmental impact. The methodology used in **Paper VI** can serve as the general guideline for determining control strategies.

1.3 Data mining and process modelling in wastewater treatment

Practitioners of wastewater treatment are not only environmental engineers or municipal engineers. Many engineers from other disciplines are involved in this field, such as electrical engineering, automation, chemical engineering and computer technology. Data mining (Haimi et al., 2013; Olsson et al., 2014) and mathematical modelling (Kim et al., 2014; Mannina et al., 2011b) are also important for improving the operation and automation of wastewater treatment processes.

1.3.1 Data mining of wastewater treatment processes

There is a huge potential of using the sensor networks in wastewater treatment plants to optimise WWTP operation (Olsson et al., 2014). The sensor networks provide plenty of data from different locations of the WWTPs, but data-rich is not always equal to information-rich. Data mining is necessary to explore the information hidden behind the large datasets.

Data mining refers to varieties of tools for knowledge retrieval from data. These data mining tools can be classified into two groups, supervised learning and unsupervised learning. Supervised learning is an algorithm for learning a mapping function from inputs to outputs when both input variables and output variables are available. Regression and classification methods are typical examples of supervised learning. Unsupervised learning is a procedure exploring the structure and distribution of the input data without corresponding output variables. The common examples of unsupervised learning are principal components analysis (PCA) and cluster analysis.

Data mining based on statistical learning and multivariate analysis plays multiple functions in wastewater treatment process optimisation. Quantifying the uncertainties (Rieger et al., 2005b) and fault diagnosis (Choi and Park, 2001) are examples of earlier application. Statistical process control has also been introduced to the wastewater treatment industry (Toifl et al., 2010). Principal Component Analysis (PCA) can be used for collinearity detection and correlation analysis (Avella et al., 2011). Predictive techniques such as Partial Least Squares Regression (Liu et al., 2014b), Support Vector Machine Regression (Seshan et al., 2014) and the neural network-based method (Delnavaz et al., 2010; Qiu et al., 2016) are used for the prediction of process variables. Data

mining enables the use of available data for the systematic study of sophisticated systems, e.g. biological wastewater treatment systems. Moreover, using easy-to-measure variables for the prediction of hard-to-measure process variables may significantly reduce the difficulty of process surveillance.

Both supervised learning and unsupervised learning techniques are applied in this study. Principal component analysis is applied to explore the correlation of wastewater characteristic variables (**Paper I**, **Paper II**, **Paper III**, and **Paper V**). Hierarchical cluster analysis is used to group wastewater samples based on the features of wastewater characteristics (**Paper I**). Regression methods are used to predict hard-to-measure variables (**Paper II** and **Paper V**) and early warning for activated sludge settleability (**Paper III**). A special classification method, namely Partial Least Squares Discriminant Analysis (PLS-DA), is applied in **Paper I** to build a classification tool for different influent wastewater. The mathematical procedures and more details of the data mining tools can be found in Chapter 3.

1.3.2 Kinetic modelling and dynamic simulation

Activated sludge Model No. 1 summarised the experience of biological wastewater treatment practice in a mathematical format, where the kinetics of organic matter degradation (heterotrophic growth), nitrification (autotrophic growth) and hydrolysis are explained in the form of Monod equations (Henze et al., 1987). However, the introduction of kinetic model parameters has brought challenges for model calibration. The model parameters such as specific heterotrophic growth rate cannot be measured directly. Estimation methods based on batch tests were proposed in the 1990s (Kappeler and Gujer, 1992; Vanrolleghem et al., 1999). Numerical methods for kinetic model parameter estimation was extensively investigated recently due to the progress of computational power (Cosenza et al., 2014; Mannina et al., 2011a). However, more accurate model calibration methods are still necessary for the dynamic simulation of the biological treatment process, especially for control purpose. The dynamic simulation results may not be sensitive to each of the model parameters because the kinetic models are usually over-parameterised with several kinetics and dozens of model parameters (Cosenza et al., 2014). To achieve the approach developed in **Paper II**, more accurate kinetic model parameter estimation is required. A novel kinetic model parameter estimation method is developed in **Paper IV** based on the molecular biology method.

1.4 Objectives of the study

In a digitalised world, surveillance and control are becoming more important in the optimisation of wastewater treatment processes, especially for the new requirement in nutrient removal and resource recovery. Thus, the overall objective of this thesis is to integrate process surveillance, data mining, kinetic modelling, modern molecular biology methods and their interactions to achieve better control of wastewater treatment plants. In this context, better control of wastewater treatment plants refers to stabilising process performance, decreasing operational cost and reducing environmental impacts. The bottleneck issues that restrict process optimisation are studied in the appended papers of this thesis. The specific objectives of each of the appended papers:

Paper I: Develop a stepwise approach to characterise influent wastewater and investigate the causes of nonlinear variation of influent characteristics.

Paper II: Investigate the possibilities of applying the combined approach of data mining and process modelling to achieve model predictive control.

Paper III: Investigate the capability of data mining techniques in the activated sludge system, by developing early warning tools for activated sludge settleability.

Paper IV: Study the microbial community of an MBBR system and develop a more accurate approach for kinetic model calibration, which can be used to support the approach proposed in **Paper II**.

Paper V: Develop new interpretable nonlinear soft sensor models based on the knowledge obtained in **Paper I** to support the approach proposed in **Paper II**.

Paper VI: Investigate the environmental impact of control strategies for the wastewater treatment plant using LCA, which can be further used to determine guidelines for choosing control strategies.

Moreover, narrowing the knowledge gap of applying data mining methods in the field of wastewater treatment engineering is also the goal of this study.

2. Scope of the Study and Thesis Overview

The thesis is based on six appended papers as referred to by their Roman numerals throughout the thesis. The studied areas of each paper are illustrated in Figure 2.1. The specific scope of work of the appended papers is as follows.

- **Paper I** and **Paper V**: The influent of a full-scale WWTP, which is also the outlet of a combined sewer system.
- **Paper II**: A plant-wide study covers influent, primary treatment, secondary treatment and the effluent.
- **Paper III**: A case study of a full-scale activated sludge system and the corresponding secondary clarifier.
- **Paper IV**: Focus on a lab scale MBBR system.
- **Paper VI**: The overall performance of WWTPs and the environmental impacts on the recipients.

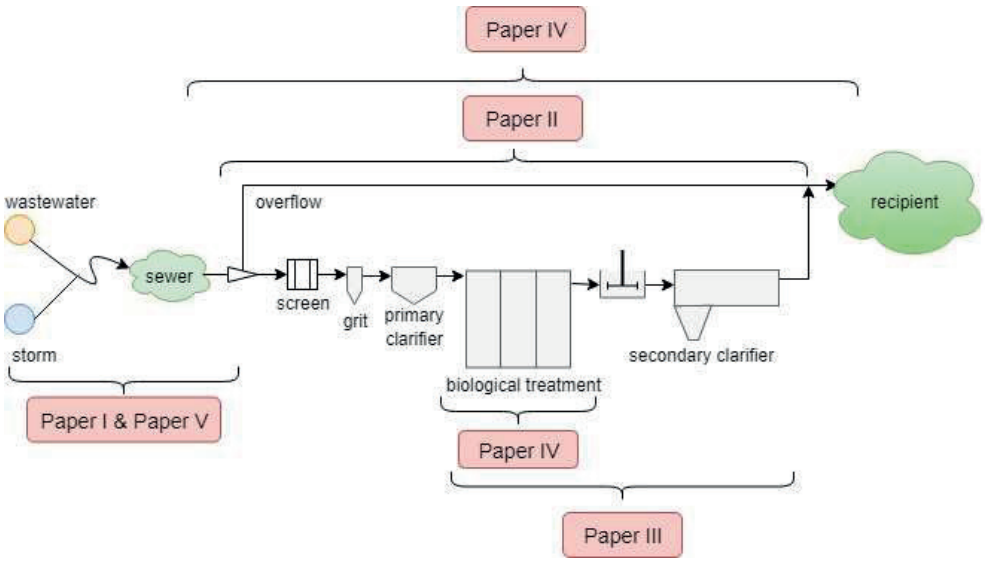

Figure 2.1: Focus area of each paper.

Figure 2.2 shows the interactions of the appended papers. The overall objective of this thesis has been stated in Section 1.4. The following is a summary of each paper:

Paper I: A stepwise approach for influent characterisation.

The daily, weekly and seasonal variation of influent brings uncertainties to the operation of WWTPs. Moreover, the climate (weather) has a significant effect on influent quantity and quality, such as storm impacts caused by rain events or snow melting. The dilution effect of snow melting makes it difficult to characterise seasonal features of influent water, although the seasonal features are essential for advanced control of WWTPs. A stepwise characterisation procedure was stated in **Paper I** based on data mining techniques. A fair comparison of influent characteristics in the cold season and the warm season was carried out when the climate effect was eliminated.

Paper II: Statistical monitoring and dynamic simulation of wastewater treatment process to achieve model predictive control.

There are two obstacles in achieving model predictive control: online carbon and nutrient sensors, and flexible process models. In **Paper II**, a combination of statistical monitoring and dynamic simulation of the wastewater treatment process was used as a solution to achieve model predictive control. Paper II provides a clue to solve the difficulties in advanced process control. The following papers are carried out to further investigate solutions for either statistical monitoring or process modelling.

Paper III: A case study to test the capability of data mining methods for early warning of activated sludge settleability

Multivariate statistics was used as a tool for systematic analysis of sophisticated biological wastewater treatment system. Early warning models for poor activated sludge settleability were developed in **Paper III**. This is also a case study of using statistical monitoring for decision-making.

Paper IV: Investigation of microbial community composition and a new approach for kinetic model calibration.

Microbial community diversity determines the function of a biological wastewater treatment system. In **Paper IV**, the microbial community composition of a multi-stage MBBR system was investigated by high-throughput sequencing. The ratios of heterotroph/autotroph in three function chambers were obtained. Moreover, the ratios of active heterotrophic biomass/autotrophic biomass

were estimated by conducting respiration tests. A novel approach for kinetic parameters estimation was developed by combining the sequencing results and respiration results.

Paper V: Developing nonlinear soft sensor models to support statistical monitoring of wastewater treatment plants

Nonlinear soft sensors for influent monitoring were developed in **Paper V**, which was a further step of **Paper I**. The difficulties of influent monitoring are due to a lack of fast-responding and affordable online analysers for chemical oxygen demand (COD) and total phosphorus (TP). The soft sensor models were developed in the manner of interpretability and nonlinearity.

Paper VI: Environmental impact analysis of control strategies to provide guidelines for control design.

The environmental impacts of two control strategies were compared by applying the Life Cycle Assessment. **Paper VI** concluded that an environmental impact analysis should serve as a guideline for designing WWTP control strategy.

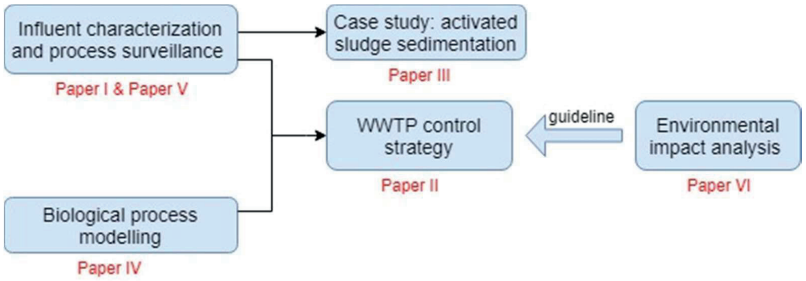

Figure 2.2: The interaction between the appended papers.

3. Methods and Materials

3.1 Data collection

The data of wastewater quantity and quality used in **Paper I**, **Paper II** and **Paper V** are collected from the Solumstrand WWTP, in Drammen, Norway. Three automatic samplers (Teledyne ISCO) were installed at the influent, outlet of biological reactors and the final effluent respectively. The influent of the WWTP was from the combined sewer system, where diluted wastewater was collected, when rain or snow melting happened. The sampling was carried out in both the warm and the cold season.

The activated sludge system in **Paper III** is a biological nitrogen and phosphorus removal system, which is located in Qingdao, China. The inlet samples were collected by an automatic sampler (AS950 AWRS, Hach), which was installed at the outlet of primary clarifiers. The outlet samples were collected at the outlet of secondary clarifiers. The activated sludge samples were collected from the end of the aeration tank.

For the study in **Paper IV**, biofilm samples were collected from every chamber of MBBR during seven days after 40 days of steady-state operation (at 12 ℃). Five carriers were taken randomly from each chamber every other day, and in total 20 carriers were collected from each chamber. Biofilm was scratched from the carriers and stored at -80 ℃ immediately after the carriers were taken out from the MBBR system. The activated sludge (AS) samples were collected from the parallel SBR system at the same time as when biofilm samples were collected.

3.2 Chemical analysis of wastewater samples

COD and soluble COD (SCOD) were analysed using Hach-Lange test kits (LCK 314/514), following the recommended method on spectrophotometer DR 3900. Total suspended solids, ammonium nitrogen, nitrate, nitrite, and orthophosphate and total phosphorus were analysed following Standard Methods (APHA et al., 2012).

3.3 Data mining and statistical analysis

3.3.1 Principal component analysis

Principal Component Analysis (PCA) is a multivariate analytical method used to detect data collinearity and summarise patterns of covariance among variables. The mathematical procedure

of PCA has been well explained and used for fault diagnosing of wastewater treatment process monitoring (Tao et al., 2013). A review of the mathematical procedure is given to provide the background of this statistical method. The dataset $X^{n\times p} = \left[X_1, X_2, \ldots X_p\right]$ represents a data matrix with *n* rows of observation and *p* columns of variables. The goal is to find a smaller set with *k* (k < p) new variables (principal components, PCs), which explains as much as possible of the variability of the original dataset X. The first step is to calculate the covariance matrix Z:

$$Z = \frac{X^T X}{n-1} \tag{3.1}$$

The next step is to calculate the eigenvalues and eigenvectors of the covariance matrix. λ_i $(i = 1,2,\ldots,p)$ is the *i*th eigenvalue of *Z*, and ω_i is the *i*th eigenvector of *Z*. The total numbers of eigenvalues is equal to the numbers of original variables *p*. Both the eigenvalues and eigenvectors are arranged in descending order of the eigenvalues. A loading matrix *W* is formed by the eigenvectors:

$$W = \begin{bmatrix} \omega_{11} & \cdots & \omega_{1p} \\ \vdots & \cdots & \vdots \\ \omega_{p1} & \cdots & \omega_{pp} \end{bmatrix} \tag{3.2}$$

The general form of PCA score matrix is denoted as $S = X \cdot W^T$. For instance, the first principal component (*PC-1*) can be calculated as:

$$PC\text{-}1 = \omega_{11}X_1 + \omega_{21}X_2 + \cdots + \omega_{p1}X_p \tag{3.3}$$

The loading ω_{11}, ω_{21}, …, ω_{p1} coefficients are the eigenvector elements of the largest corresponding eigenvalue λ_1. Therefore, the variance of *PC-1* is maximised. To select *k* principal components that can represent the total variability of the original dataset with reduced dimension, the cumulative percent variance (CPV) principle is applied:

$$CPV = \frac{\sum_{i=1}^{k} \lambda_i}{\sum_{i=1}^{p} \lambda_i} \times 100\% \tag{3.4}$$

For a normalised dataset, the sum of λ_i is equal to the total number of original variables, which is *p* in this case. While for non-normalised dataset, the sum of λ_i is equal to the total variance of the original matrix. Thus, by selecting *k* numbers of principal components with sufficient proportion of CPV, the dimension of the original data matrix is reduced to k new variables (PCs). It is

noteworthy that each of the principal components is independent of each other because the PCs are the products of orthogonal eigenvectors.

In this study, the principal components derived from PCA describe the dominant variation of the wastewater characteristics for further analysis. The PCA method was used in **Paper I**, **Paper II**, and **Paper III** and **Paper V**. Unscrambler® X version 10.4 (CAMO Software, 2016) was used to perform the calculation of PCA.

3.3.2 Cluster analysis

Cluster analysis (or clustering) is another group of unsupervised learning data mining techniques. PCA is used to find a lower dimensional representation of the original dataset, while clustering is used to find homogeneous subgroups among observations with multivariate features (James et al., 2013). The common clustering methods for data mining include K-means clustering and hierarchical clustering (Noiva et al., 2016). The K-means clustering approach allows pre-specifying the desired numbers of clusters. Hierarchical clustering does not need to define the final numbers of clusters, which is an advantage for the data whose subgroup information is completely unknown. Therefore, hierarchical clustering approach is applied in this study to explore the subgroup information and nonlinearity of influent wastewater. Another advantage of hierarchical clustering is that the result is presented in a graphical way, namely dendrogram. The dendrogram shows the grouping results at different levels of similarities. The procedure for hierarchical cluster analysis of data with *n* observations is as follows (James et al., 2013).

1. Pairs the observations and a total of $\frac{n(n-1)}{2}$ pairs of observation can be obtained.
2. Calculate the dissimilarity of each of the pairs in terms of Euclidean distance. For a data matrix with *n* observations and *p* variables $X^{n\times p}$, the Euclidean distance between the *i*th and *(i+1)*th observation is $\sqrt{\sum_{j=1}^{p}\left(X_{i,j}-X_{i+1,j}\right)^2}$, where $j = 1,2,\cdots,p$. In this step, each observation is treated as a cluster, and there are in total *n* clusters.
3. For $i = n, n-1, \cdots, 2$:
    i. Compare all the pairwise dissimilarities among *i* clusters, and merge the most similar pair of clusters (smallest Euclidean distance) as one cluster. Now there are *i-1* clusters.
    ii. Repeat the procedure from Step 1 until there are only two clusters left.

This iteration procedure can be easily executed in any programming language. In this study, R was selected to perform this procedure. The R package *ape* was applied to plot the dendrogram in R environment.

In **Paper I**, influent wastewater samples of the wastewater treatment plant collected during the wet climate period were diluted by snowmelt, while other samples collected in freezing conditions were not affected by snowmelt. Hierarchical cluster analysis was applied to look for subgroups of the data based on wastewater characteristics. Ward's method with Euclidean distance was used to perform the clustering (Singh et al., 2005; Merriam et al., 2015). However, as Xiao et al. (2012) mentioned, the limitation of cluster analysis is that it may produce conceptually meaningless clusters. Therefore, it is important to pre-assess the input data before clustering. The scores of most significant principal components were used as input data for clustering, which screened out the noises in the raw dataset. In the cold season, there are only two climate categories: Dry climate influent and Wet climate influent. The results of cluster analysis would be well acceptable if the two clusters given by cluster analysis featured as a larger amount of diluted influent (Wet climate) and a lower quantity with higher concentration (Dry climate).

3.3.3 Multiple Linear Regression

Multiple Linear Regression (MLR) is a simple and very useful approach for predicting a response variable based on multiple predictors. For a data matrix with p predictors X and a response Y, the general form of MLR can be written as:

$$\hat{Y} = \beta_0 + \beta_1 X_1 + \beta_2 X_2 + \cdots + \beta_p X_p + \varepsilon \tag{3.5}$$

where $\hat{Y}$ is the prediction of real response Y. The model parameter $\beta_i (i = 0,1, \cdots p)$ is estimated by applying least square estimation. The objective of least square estimation is to find a set of β_i that minimise the sum squares of residual error ε

$$RSS = \sum_{i=1}^{n} \varepsilon_i^2 = \sum_{i=1}^{n} \left(Y - \hat{Y}\right)^2 = \sum_{i=1}^{n} (Y - \beta X)\,)^2 \tag{3.6}$$

thus, calculating the partial derivative of RSS to find the proper β_i which minimises RSS. Finally, the model parameters can be calculated from the known data X and Y. The estimated model parameters $\hat{\beta}$ in matrix form:

$$\hat{\beta} = (X^T X)^{-1} X^T Y \tag{3.7}$$

There is always a risk of overfitting an MLR model. In this study, PCA was performed before MLR to select the most significant variables as predictors. Secondly, the backward stepwise selection method was applied to avoid overfitting based on Akaike's information criterion (AIC) to obtain the "shrunk model" with only significant variables (Akaike, 1974). Multiple Linear Regression (MLR) was used for predictive purposes in **Paper II**, **Paper III** and **Paper V**. The leverage correction method was used to validate the MLR models in **Paper II** and **Paper III**, while cross-validation with 12 segments was used in **Paper V**.

3.3.4 Partial Least Squares Regression and Partial Least Squares Discriminant Analysis

Partial Least Squares (PLS) is a methodology that can be used for both regression and discriminant analysis (PLS-DA) (Indahl et al., 2007). Both Partial Least Squares Regression (PLSR) and Partial Least Squares Discriminant Analysis (PLS-DA) are supervised learning techniques. The PLSR procedure looks similar to PCA calculation stated in Subsection 3.3.1. The difference is that the loading vectors are the eigenvectors of the covariance matrix of predictors X and response Y, while PCA loadings are calculated from the covariance matrix of X variables. In general, PCA approach looks for the representative with maximised variance of the original dataset, but PLSR looks for the representative with maximised covariance of the predictors and the response variables. The mathematical procedure will not be repeated here. PLSR was used to build an early warning model for activated sludge settleability in **Paper III**.

Partial Least Squares Discriminant Analysis is a useful classification method initially proposed by Barker and Rayens (2003), which applies the PLSR procedure by substituting the response variables into a dummy matrix. In **Paper I**, PLS-DA was used to build a classifier based on historical data and the category variable – Climate. The category variable Climate with "Dry" and "Wet" entries was converted to a dummy matrix with entries as "0" and "1", while the wastewater characteristics data formed another matrix – the X matrix. PLS-DA algorithm maximises the covariance of these two matrices and extracts dominant eigenvectors of the covariance matrix (Barker and Rayens, 2003; Nocairi et al., 2005). The final classification was performed based on the scores of PLS-DA, which is computed from dominant eigenvectors and original values of wastewater characteristics.

The dummy matrix was computed in R, and then it was used to perform PLS-DA in Unscrambler X version 10.4 (CAMO Software, 2016).

3.3.5 Multivariate Adaptive Regression Splines

The statistical learning method Multivariate Adaptive Regression Splines (MARS) was applied to develop nonlinear soft sensor models in **Paper V**. MARS was initially presented by Friedman (1991) as a nonlinear regression method. It can be viewed as an integration of piecewise linear regression, which captures nonlinearity by adding knots to input variables to break the curve into piecewise basis functions. The general form of the MARS model is expressed as:

$$Y = \beta_0 + \sum_{i=1}^{M} \beta_i \cdot h_i(\boldsymbol{X^n}) + \varepsilon \tag{3.8}$$

where $h_i(\boldsymbol{X})$ is the basis function representing each piece of local linear regression, and β_i is the associated coefficient. The coefficients β were estimated based on the least squares method. The basis functions have the following form:

$$h(x)_+ = \begin{cases} x-k, & if\ x > k \\ 0, & otherwise \end{cases};$$

$$h(x)_- = \begin{cases} k-x, & if\ x < k \\ 0, & otherwise \end{cases} \tag{3.9}$$

where k is a univariate knot. Thus, the MARS method produces continuous models. The determination of basis functions was a data-driven process. MARS can apply both forward stepwise and backward stepwise to select inputs. In this study, second order terms and interaction terms are involved and are selected automatically. The cross-validation method was applied to verify MARS models in the same way as it is used for MLRs. The "earth" package was applied in R to build MARS models (Milborrow, 2018).

3.3.6 Other statistical methods

Analysis of Variance (ANOVA) was performed to study the seasonal difference of influent in **Paper I**. F statistic was calculated along with ANOVA to test if the means of two groups are significantly different. The null hypothesis for the F test is that there is no significant difference between the means of the two groups. If the first group has $n_1$observations and the second group has n_2 observations, the F-value is:

$$F = \frac{n_1(\overline{X_1} - \bar{X})^2 + n_2(\overline{X_2} - \bar{X})^2}{\left(\sum_{j=1}^{n_1}\left(X_{1j} - \overline{X_1}\right)^2 + \sum_{j=1}^{n_2}\left(X_{2j} - \overline{X_2}\right)^2\right) \Big/ (n_1 + n_2 - 2)} \tag{3.10}$$

where $\overline{X_1}$ is the mean of the first group and $\overline{X_2}$ is the mean of the second group. The F-value will be large if the between-group variability is relatively large compared with the within-group variability. The p-value along with an ANOVA test is the probability value when the null hypothesis is true. It is quite common to use a significant level 0.05 for ANOVA tests, which means the null hypothesis should be rejected if the p-value is smaller than 0.05. The conclusion should be that the means of the two groups are significantly different. All the ANOVA tests were performed in R.

Another regression method – support vector machine regression (SVMR) – was also used to compare with the results of MLR and PLSR in **Paper III**. The mathematical procedures of PLSR and SVMR have been well explained in literature (Seshan et al., 2014). Unscrambler X version 10.4 was used to perform the calculation of SVMR..

3.4 Wastewater treatment process modelling

In **Paper II**, the steady-state model of the MBBR system was developed based on Activated Sludge Model 1 (Henze et al., 1987). The function of the steady state model was to determine model parameters. Average influent wastewater characteristics of 120 samples was applied as the model input. Table 4.1 shows the kinetic models of biochemical reactions. In **Paper II**, anoxic growth of heterotrophs was excluded, because there is no anoxic reaction in this MBBR system. Hence, only the aerobic reaction was modelled. The notation of the state variables and process parameters are given in Table 4.2.

3.5 Lab-scale MBBR system

A multi-stage lab-scale MBBR system was set up for the study in **Paper IV**. As is shown in Figure 3.1, domestic wastewater was transported from a primary clarifier of the WWTP to a storage tank that provided constant flow of influent to the MBBR system. The MBBR system consisted of three functional chambers: Anoxic chamber (AN), first aerobic chamber (AE1), and second aerobic chamber (AE2). Each chamber of the bioreactor was filled with suspended plastic bio-carriers. The density of carriers was 0.95 $g \cdot cm^{-3}$ and the specific surface area of the carriers was 600 $m^2 \cdot m^{-3}$. The volume of each chamber was 5 litres. The quantity of carriers in each chamber was 0.32 m^2, in terms of surface area. Dissolved oxygen (DO) in AE1 and AE2 was always higher than 6 $mg \cdot L^{-1}$ to avoid mass transfer limitation among inner layers of biofilm (Ødegaard, 2006). Carriers in upper stream chambers cannot be transported to the downstream chambers because the

opening between each chamber was much smaller than the diameter of the carriers. The hydraulic retention time in each chamber was 2 hours, and the total hydraulic retention time was 6 hours. Nitrified liquid was recycled back to AN for denitrification, with a recycle ratio of 1:1.

To create a steady-state condition for this study, the concentrations of chemical oxygen demand (COD) and ammonium nitrogen ($NH_4^+ - N$) of the inlet wastewater were adjusted to 700 $mg \cdot L^{-1}$ and 50 $mg \cdot L^{-1}$ respectively, by adding sodium acetate and ammonium chloride. The laboratory MBBR system was setup inside the laboratory, where an air conditioner was used to maintain the temperature at 12 ℃. In parallel, an activated sludge (AS) system was running as a sequencing batch reactor (SBR) with the same daily loading rate, to provide the necessary frame of reference. An SBR cycle was four hours (one hour of anoxic reaction, two hours of aerobic reaction, and one hour for sedimentation and refilling, 6 cycles per day). After each cycle, 50 % of the supernatant was discharged to regain space for refilling influent. The sludge age was kept as 18 days during the entire test period. Both the MBBR and activated sludge systems operated for 40 days before this study was carried out.

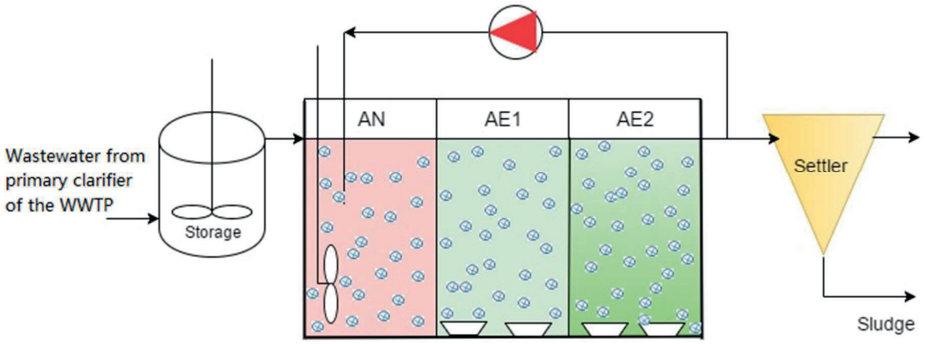

Figure 3.1: The flow diagram of the laboratory scale wastewater treatment system. In the MBBR system, AN, AE1 and AE2 represent anoxic chamber, first aerobic chamber and second anoxic chamber, respectively. Figure from **Paper IV**.

3.6 High-throughput sequencing

DNA was extracted from 1.5 mL of AN, AE1, AE2 and AS samples respectively, using PowerSoil DNA Isolation Kits (Mo Bio Laboratories, USA) according to manufacturer's instruction. The extracted DNA was checked using 1 % agarose gel electrophoresis. The V3-V4 region of the 16S rRNA gene was amplified from extracted DNA using universal primers 338F

(ACTCCTACGGGAGGCAGCA) and 806R (GGACTACNNGGGTATCTAAT) (Du et al., 2017). The mixture of 4 μL of 5× FastPfu Buffer, 2 μL of dNTP (2.5 mM), 0.4 μL of each primer (5 μM), 0.5 μL of DNA and 0.4 μL of Fastpfu Polymerase (TransStart Fastpfu DNA Polymerase, China) were used to perform PCR in a GeneAmp 9700 (Applied Biosystems, USA) PCR system. The thermal cycling was carried out by following these steps as: Initial denaturation at 95 ℃ for 2 minutes, followed by 25 cycles at 95 ℃ for 30 seconds, 55 ℃ for 30 seconds, 72 ℃ for 30 seconds and final extension at 72 ℃ for 5 minutes (Ma et al., 2013; Matar et al., 2017).

After amplification, the triplicate amplicons from each sample were pooled and checked by 2 % gel electrophoresis, followed by purification using AxyPrep DNA Gel Extraction Kit (Axgen, USA) according to manufacturer's instructions (Li and Lu, 2017). The PCR products were quantified on the QuantiFluor-ST Fluorometer (Promega, USA). Finally, high-throughput sequencing was performed on an Illumina Miseq platform at Yuanxubio Co., Ltd. (Shanghai, China).

The sequencing data were trimmed and analysed using Mothur software. Considering the length of the V3-V4 region, sequences shorter than 300 bp were removed. Chimeric sequences were removed using the Uchime program and the resulting sequences were classified using SILVA database as reference. After discarding the low quality sequences, an average of 42 453 effective sequences were obtained with an average length of 420 – 423 bp for each of the four samples (AN, AE1, AE2 and AS). For community analysis, the sequences were clustered into operational taxonomic units (OTUs) with 0.03 cutoff by Mothur program version 1.38.0. More information can be found in the supplementary material.

3.7 Respiration test and active biomass determination

In **Paper IV**, Oxygen uptake rates (OURs) were measured to quantify the active heterotrophic and autotrophic biomass in each chamber of the MBBR system according to Ochoa et al. (2002). Respiration tests were performed in a closed respiration beaker under three conditions (Table 3.1) to obtain: (1) endogenous OUR_1; (2) the sum of oxygen consumption rate of autotrophic biomass together and endogenous respiration of heterotrophic biomass, OUR_2; (3) heterotrophic respiration, OUR_3, with Allythiourea (ATU) added to inhibit nitrification. The OUR of heterotrophic biomass $OUR_H = OUR_3$, and OUR of autotrophic biomass $OUR_A = OUR_2 - OUR_1$. Tap water was used in addition to chemicals as listed in Table 3.1. Dissolved oxygen (DO) was measured by a portable

DO sensor (Hach HQ40D). DO values lower than 6 $mg \cdot L^{-1}$ were not used for OUR calculation, because autotrophic respiration may be restrained due to lower oxygen transfer efficiency among the inner biofilm layers (Ødegaard, 2006).

The mass balance equations of heterotrophs and autotrophs can be derived from ASM1, as shown in Equations 3.11 and 3.12.

Table 3.1: Respiration test procedure for OUR determination of active biomass in biofilm.

OUR	Ammonium	Carbon source	ATU
Endogenous, OUR_1	No	No	No
Autotrophic, OUR_2	Yes, 20 mg $N \cdot L^{-1}$	No	No
Heterotrophic, OUR_3	Yes, 20 mg $N \cdot L^{-1}$	Yes, 250 mg $COD \cdot L^{-1}$	Yes, 20 mg $ATU \cdot L^{-1}$

$$\frac{dS_o}{dt} = \mu_{H,Max} \cdot \frac{1-Y_H}{Y_H} \cdot \left(\frac{S_s}{K_s+S_s}\right) \cdot \left(\frac{S_o}{K_{o,H}+S_o}\right) \cdot X_H \quad (3.11)$$

$$\frac{dS_o}{dt} = \mu_{A,Max} \cdot \frac{4.57-Y_A}{Y_A} \cdot \left(\frac{S_{NH}}{K_{NH}+S_{NH}}\right) \cdot \left(\frac{S_o}{K_{o,A}+S_o}\right) \cdot X_A \quad (3.12)$$

3.8 Life Cycle Assessment

Life Cycle Assessment (LCA) is performed to compare the environmental impacts of different control strategies in **Paper VI**. The scope of the LCA included only the operation of the WWTP. LCA evaluation includes direct emission and indirect emission. Greenhouse gas (e.g. CO_2, CH_4), eutrophication nutrient in the outlet (e.g. TN, TP) and sludge management are the main sources of direct emission. The resources and emissions during electricity generation and chemical production were included in the final evaluation. The detailed methodology of LCA for wastewater treatment has been explained well in literature (Flores-Alsina et al., 2010; Foley et al., 2010; Rahman et al., 2016). SimaPro 8.0 was used to calculate the environmental impact of WWTP operation strategies, where the Ecoinvent database (www.ecoinvent.ch) was applied.

4. Results and Discussion

4.1 Influent characterisation

The surveillance of influent variation is essential for the control of wastewater treatment plants. In **Paper I**, the characteristics of influent in the warm season and cold season were investigated (Figure 4.1). Figure 4.1a showed the 5-day continuous measurement of influent flow rate, chemical oxygen demand (COD) and soluble chemical oxygen demand (SCOD) observed in the warm season and dry climate (WarmDry condition). The peak values of both wastewater quantity and contaminants concentration appeared at the same time of the day during the warm season. The influent flow, COD and SCOD followed the same propagation pattern: started rising after 9:00 in the morning and reached the peak at around 13:00. After slightly decreasing in the afternoon, both wastewater quality and quantity increased to another smaller peak in the evening. The flow, COD and SCOD decreased sharply to a lower level after 23:00 until the next morning. The influent in the cold season shows a difference in pattern when there was a sudden rising of flow rate, which may be a storm event caused by snow melting. The propagation trend of the influent quantity and quality was altered due to the dilution effect, as shown in Figure 4.1b. Snow melting is difficult to predict, which causes difficulty in comparison of the seasonal differences of dry climate influent.The results indicate the nonlinearity of influent variation, which was further explained in **Paper V**.

Influent variation was caused by the joint effect of human activities and climate conditions (Plósz et al., 2009). Distinguishing the wet climate influent becomes more difficult in the cold season because it is not realistic to know the amount of snowmelt or when the snow melting started (Moghadas et al., 2015). In **Paper I**, a statistical learning approach was proposed to distinguish the dry climate influent and wet climate influent. The approach has four steps:

1. Conduct the first ANOVA test to compare the raw influent data in the warm season and cold season. The results cannot indicate the real seasonal differences, because it is highly affected by climate factors.
2. Perform principal component analysis on the cold season data. The first two principal components (PC-1 and PC-2) explain 96 % of the total variability. Therefore, the scores of PC-1 and PC-2 can be used to represent the original dataset with reduced dimension.

3. Use the scores of PC-1 and PC-2 to perform hierarchical clustering. The observations (influent wastewater) are divided into two subgroups (clusters) by hierarchical clustering. Based on the features of these two clusters, one cluster is recognised as the dry climate influent, while the other cluster consists of wet climate influent.
4. Build a classification model based on PLS-DA to classify future influent, with which the previous steps can be bypassed for future classification.

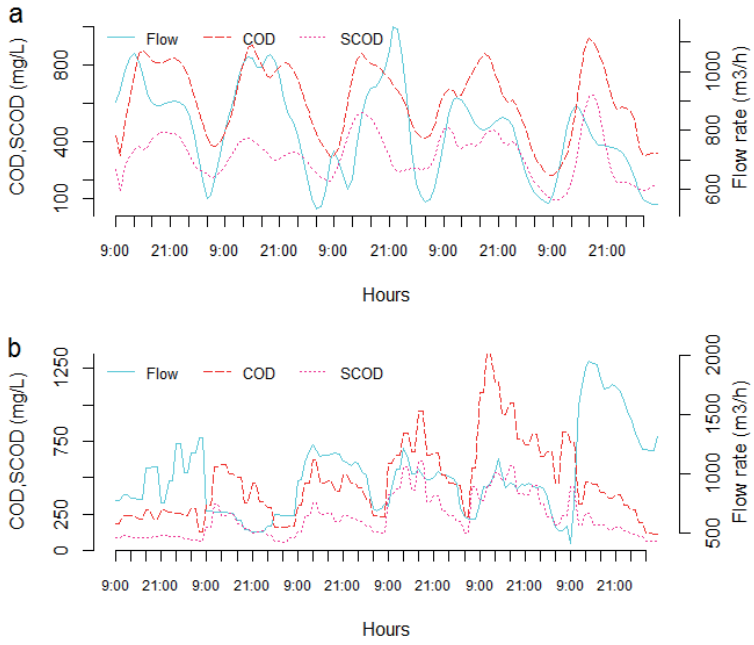

Figure 4.1: The influent flow rate, COD and SCOD of (a) 5-day observations in warm season; (b) 6-day observations in cold season. Figure from **Paper I**.

The details of the stepwise approach for the classification of dry climate and wet climate influent can be found in the appended **Paper I**. The key step of this approach is to find two clusters with different features of wastewater characteristics. Since there are so many influent variables, principal component analysis was used to reduce the dimension and derive the dominant variability of the original dataset. PCA was carried out on the data of cold season (9 variables, 144 observations), and the results are shown in Figure 4.2. The first principal component (PC-1) and the second principal component (PC-2) explained 96 % of the total variance of the dataset (Figure

4.2a), which indicates that these two PCs contains the main variability of the dataset. Figure 4.2b further explained the loading of original variables on the plane of PC-1 and PC-2. Flow, COD, SCOD and TSS are the most significant variables that determined the variation of PC-1 and PC-2. Higher PC-1 values represent higher flow rates and lower chemical composition. PC-2 is a component standing for chemical composition. Higher PC-2 scores indicate higher COD, SCOD and TSS. Thus, the scores of PC-1 and PC-2 can be used as input variables for clustering.

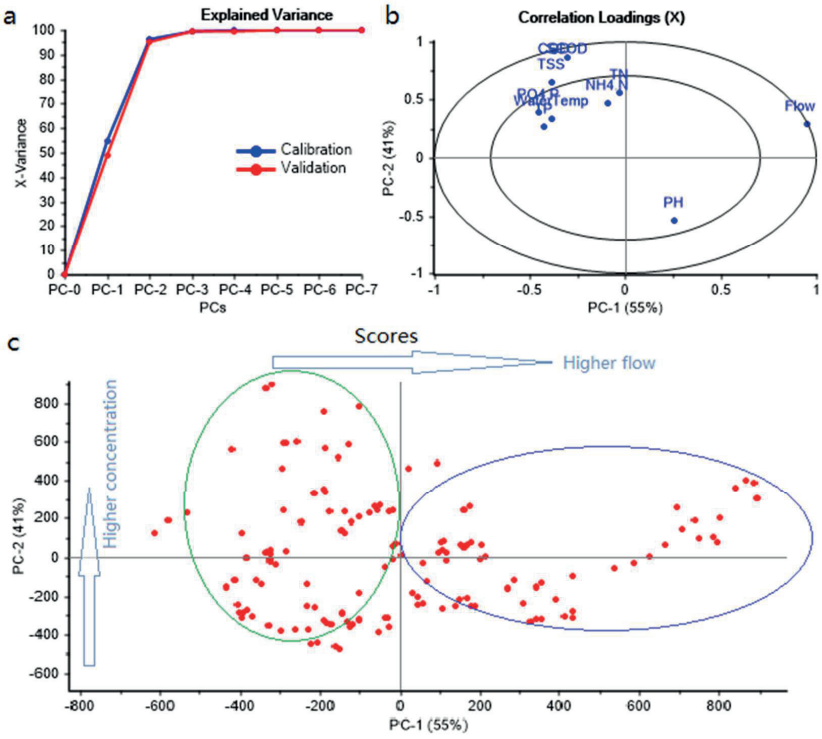

Figure 4.2: Principal component analysis of wastewater characteristics in cold season. (a) The proportion of explained variance by principal components. The blue and red curve represent model calibration results and cross validation results. (b) Correlation loading plot of wastewater characteristic variables on the plane formed by PC-1 and PC-2. (c) Cross-validated scores of all the observations in cold season. Figure from **Paper I**

Figure 4.3 is a dendrogram, which is the result of hierarchical clustering. The names of all the influent samples are located at the external edge of the circle in Figure 4.3. Following the steps of hierarchical clustering (Subsection 3.3.2), the influent with similar features is grouped into one cluster. The term hierarchical refers to different dissimilarity levels. The quantity of clusters

decreases with the increasing of dissimilarity levels. At last, two clusters are formed at the highest dissimilarity level. The cluster with a higher flow rate and lower COD concentrations is labelled in blue colour in Figure 4.3. The observations in red colour are dry climate influent.

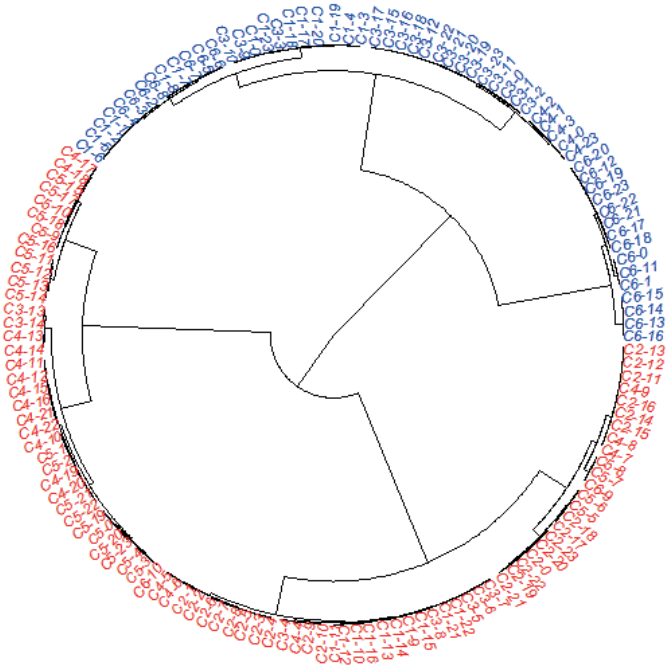

Figure 4.3: Two clusters were obtained by applying the statistical learning approach. The names of observations such as "C1-1" represent Cold climate, sampling Day 1, at one o'clock. The wet climate observations are in blue, and dry climate samples are in red. Figure from **Paper I**.

To compare the differences of influent characteristics between cold season and warm season, climate effects should be eliminated to compare only the dry climate influent. Therefore, the dry climate influent in the cold season (ColdDry) and the warm season (Warm) were compared after cluster analysis, as shown in Figure 4.4. F-statistic values are obtained from ANOVA tests. Whether the difference between the two groups is significant can be verified by comparing the corresponding F-statistic and the significance level in an F-distribution table. Each of the p-values in Figure 4.4 is the probability of being confident to say that the two groups are significantly different. The more commonly used method is to check whether the p-value is below the significant level 0.05. The ANOVA test showed that the differences of flow rate, total suspend solid (TSS),

COD, ammonium nitrogen (NH_4-N) and pH were not significant at significance level 0.05. However, significant seasonal differences were found between orthophosphate (PO_4-P) and total phosphorus (TP). The nonlinearity of phosphorus increased the difficulty for phosphorus prediction, which leads to the works in **Paper V**.

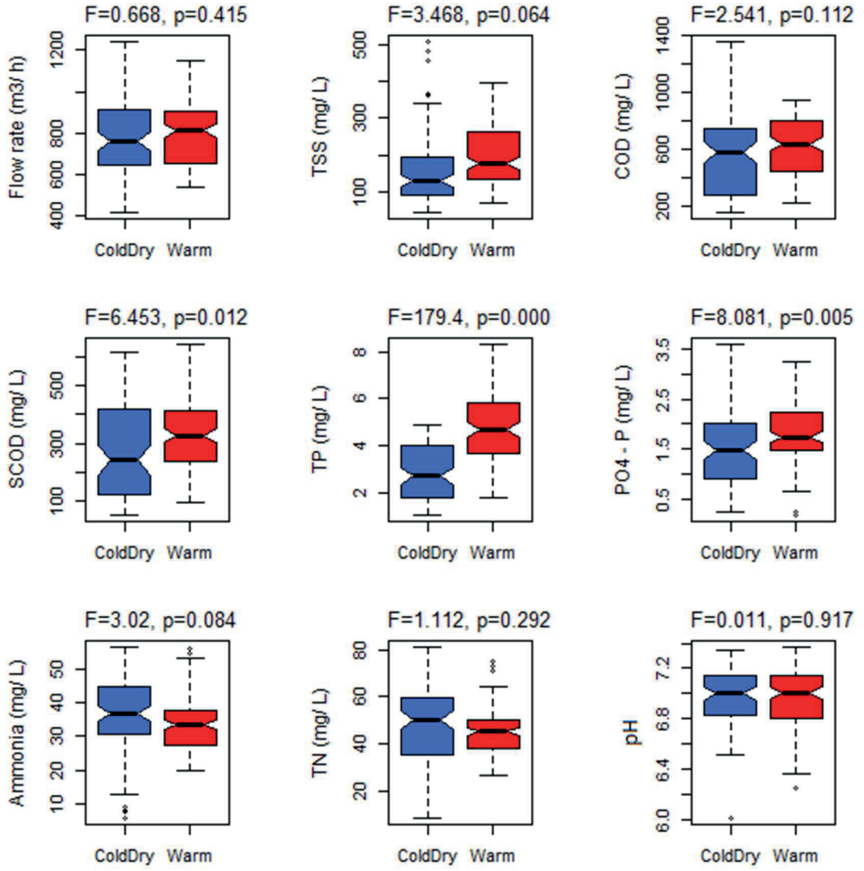

Figure 4.4: The comparison of dry climate influent in the cold season (ColdDry) and the warm season (Warm). Figure from **Paper I**.

The online measurement of influent variables is essential to achieve advanced process control (Kim et al., 2016; Solon et al., 2016). COD and TP are two hard-to-measure variables due to either slow response or high investment cost. Soft sensors would be the alternative solution to hardware sensors for real-time monitoring of hard-to-measure variables. The periodical variation and climate

effect brought challenges to the development of soft sensor models for COD and TP prediction. See further discussion about this issue in **Paper I** and **Paper V**.

Internet of Things (IoT) is considered as the smart solution for many "big challenges", which integrates several digital and physical things for data mining and communication. In **Paper I**, scatter matrix plot are used together with correlation analysis to study the relationship between climate factors and wastewater characteristics. In Figure 4.5, the Pearson correlation coefficients are added to the upper panel of the plot. The air temperature has the highest correlation coefficient with flow rate ($r = 0.49$), and moderate negative correlation with COD ($r = -0.20$). Although air temperature may contribute to snow melting when the air temperature is high enough, the high correlation between air temperature and flow rate is not caused by snow melting. The reason is that the snowmelt will affect water temperature significantly, but the water temperature is not correlated with air temperature in this plot ($r = 0.0069$). The air temperature starts to rise after sunrise, and at the same time water consumption increases due to human habit. This may be the explanation of the high correlation between air temperature and flow rate. The negative correlation of flow and water temperature (r = -0.27) indicates the effect of snow melting, because the cold snowmelt would not only increase the flow rate, but also decrease the water temperature. Solar radiation was highly correlated with COD (r = 0.39) and flow rate (r = 0.35). The correlation between solar radiation and flow rate can be deduced from the effect of solar radiation on snow melting. However, the positive correlation of solar radiation and COD is due to simultaneous daily variation. This is because both COD and solar radiation are higher in the daytime and lower in the night. Snow depth data are discrete daily average values with only 0 cm, 2 cm and 3 cm during the observation period. It is difficult to draw any conclusions related to the snow depth, which also reveals the importance of data quality for data mining. The flow rate may be positively correlated with COD in a dry climate and negatively correlated in a wet climate due to dilution effect, and the net-correlation is very low due to the combined effect.

Overall, the climate data can be useful for influent prediction. This study revealed how climate data can contribute to urban water management to some extent, but long term observation is necessary for further studies.

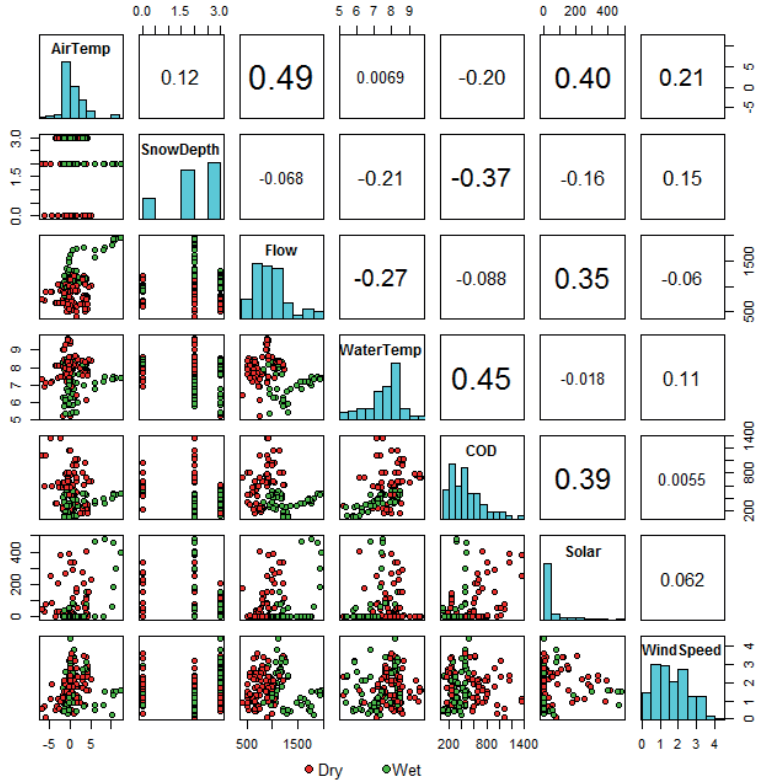

Figure 4.5: Scatter matrix and correlation analysis between climate factors and influent characters in the cold season. The variables in the plot are air temperature (AirTemp), snow depth (Snowdepth), flow rate (Flow), water temperature (WaterTemp), COD, Solar radiation (Solar) and wind speed (WindSpeed). The values on the upper panel are the Pearson correlation coefficients of the corresponding variables. Figure from **Paper I**.

4.2 Statistical monitoring and process modelling

Model predictive control (MPC) is considered as an advanced real-time control approach for processes (Han et al., 2014; Kim et al., 2014; Åmand et al., 2013), but much fewer cases have applied the advanced control in full-scale WWTPs in comparison to just computer simulation. The application of MPC is not limited by the control theory itself. The main challenges include having a process model with sufficient understanding of the process and obtaining reliable real-time data of necessary state variables (Olsson et al., 2014). Since the influent wastewater can be characterised by applying statistical learning methods, statistical monitoring and process modelling was proposed as a combined approach to achieve model predictive control in **Paper II**.

The Solumstrand Wastewater Treatment Plant, Drammen, Norway, was selected as the research object. The process configuration of this WWTP was shown in Figure 4.6. The influent from a combined sewer passes through screens and enters grit traps. There was no primary clarifier in this WWTP. Rather, the influent enters the high rate moving bed biofilm reactors (MBBRs) directly after grit removal. The extremely compact high-rate MBBRs were designed with low hydraulic retention time (HRT) for soluble COD removal (Ødegaard, 2006). The final solid–water separation was done by the ballasted flocculation and separation tanks. This WWTP was chosen for this study because this biological system was simpler than the nutrient removal systems, which makes the process modelling and MPC implementation more realistic.

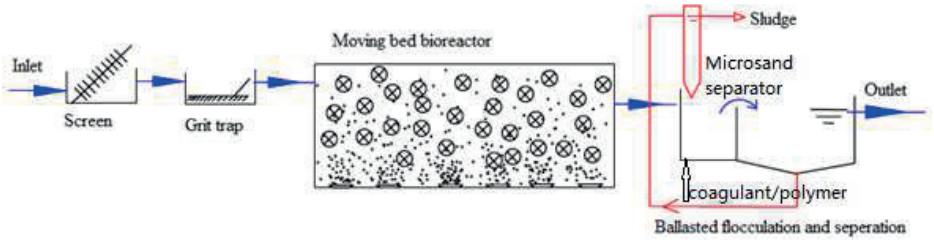

Figure 4.6: Process diagram of Solumstrand WWTP. The influent goes through screens, grit chambers, high rate MBBRs and finally get clarified in the ballasted clarifiers. **Figure from Paper II**.

The main energy consumer in this WWTP was the air compressors for the MBBRs. Chemical consumption is also necessary because coagulants or polymers are required to remove phosphorus and enhance the removal of solids in the ballasted flocculation chamber. Therefore, the main operational costs for wastewater purification in this WWTP were electricity for air supply and chemicals for flocculation. The model predictive control strategy could be used to optimise aeration and chemical dosing. However, online measurements of the inlet COD and the MBBR process model were necessary to perform MPC for aeration control. The TP and TSS data of ballasted clarifier inlet (or the outlet of MBBRs) were required to determine the coagulant dosage.

Online measurement of TSS was no longer difficult in wastewater treatment plants. However, it was still difficult to measure COD and TP online by affordable fast-response sensors. Prediction of COD and TP based on easy-to-measure variables was adopted as the online monitoring strategy in this study.

Multivariate statistical analysis is one of the fundamental tools to figure out significant information from complex systems. First of all, PCA was applied on the influent quality and quantity variables. On the PCA loading plot (Figure 2b in **Paper II**), COD, SCOD, OP, Flow rate, TP and TSS locate closely with each, which reveals the collinearity of these variables. That means, one easy-to-measurement variable from this group can represent their commonly shared variability. Thus, Flow rate can be used as one of the predictors for COD and TP prediction. Although TSS is also an easy-to-measure variable, it was not selected as a predictor because its collinearity with Flow rate will increase the risk of overfitting. The maintenance cost of a TSS sensor is higher than the flow sensor, which is also the reason for choosing Flow rate rather than TSS. Variables from other locations can be used as additional predictors to provide the missing variability of COD and TP. At last, Flow rate, pH and NH_4-N were selected as predictors for COD and TP prediction. Multiple Linear Regression (MLR) is used to establish prediction models following PCA. Equations 4.1 and 4.2 were the MLR models used for COD and TP prediction in **Paper II**, respectively. The model parameters are estimated using the standard least squares estimation method. The possibility of using statistical models to provide real-time data for control purpose was discussed in **Paper II**. The extended prediction models for soft sensor development based on the same dataset was further discussed in **Paper V**.

$$COD_{in} = 2708.2170 + 0.6806 \cdot Flow + 11.4423 \cdot Ammonia_{in} - 443.7516 \cdot pH_{in} \quad (4.1)$$

$$TP_{in} = 0.5548 + 0.0067 \cdot Flow + 0.0443 \cdot Ammonia_{in} - 0.3926 \cdot pH_{in} \quad (4.2)$$

Statistical monitoring was supposed as an alternative to hardware sensors in obtaining hard-to-measure variables. The influent variables can be predicted by multivariate statistical methods, because the pattern of influent can be traced back to regular daily human activities. However, the regular pattern will no longer exist after the wastewater passes through the treatment facilities because the removal of contaminants in the reactors alters the influent pattern. Thus, kinetic models are needed to predict the outlet quality of the wastewater treatment process. The well proved Activated Sludge Model No 1 (ASM1) can be used to model the kinetics of biochemical reactions (Henze et al., 1987). The kinetic models applied from ASM1 are listed in Table 4.1. The symbols of state variables and model parameters are explained in Table 4.2.

Table 4.1: Kinetic process models from ASM1 used to describe the biological behaviour of MBBR system. Table from **Paper II**.

j	Process	Process rate, ρ_j
1	Aerobic growth of heterotrophs	$\rho_1 = \mu_H \left(\frac{S_S}{K_S+S_S}\right)\left(\frac{S_S}{K_{O,H}+S_S}\right) X_{B,H}$
2	Aerobic growth of autotrophs	$\rho_2 = \mu_A \left(\frac{S_{NH}}{K_{NH}+S_{NH}}\right)\left(\frac{S_O}{K_{O,A}+S_O}\right) X_{B,A}$
3	Decay of heterotrophs	$\rho_3 = b_H X_{B,H}$
4	Decay of autotrophs	$\rho_4 = b_A X_{B,A}$
5	Ammonification of soluble organic nitrogen	$\rho_5 = k_a S_{ND} X_{B,A}$
6	Hydrolysis of entrapped	$\rho_6 = k_h \frac{X_h/X_{B,H}}{K_X+(X_S/X_{B,H})}\left[\left(\frac{S_O}{K_{O,A}+S_O}\right)+\eta_h\left(\frac{K_{O,H}}{K_{O,H}+S_O}\right)\left(\frac{S_{NO}}{K_{NO}+S_{NO}}\right)\right] X_{B,H}$
7	Hydrolysis of entrapped organic nitrogen	$\rho_7 = k_h \frac{X_h/X_{B,H}}{K_X+(X_S/X_{B,H})}\left[\left(\frac{S_O}{K_{O,A}+S_O}\right)+\eta_h\left(\frac{K_{O,H}}{K_{O,H}+S_O}\right)\left(\frac{S_{NO}}{K_{NO}+S_{NO}}\right)\right] X_{B,H}(X_{ND}/X_S)$

Table 4.2: State variables and model parameters of biological model

Notation	Definition	Unit
	State variables	
S_s	Soluble biodegradable COD	mg COD L^{-1}
X_S	Particulate biodegradable COD (slowly biodegradable)	mg COD L^{-1}
S_{NH}	Ammonium nitrogen in bulk liquid	mg N L^{-1}
S_{NO}	Soluble nitrate and nitrite nitrogen	mg N L^{-1}
S_{ND}	Soluble degradable organic nitrogen	mg N L^{-1}
$X_{B,H}$	Active heterotrophic biomass	mg COD L^{-1}
$X_{B,A}$	Active autotrophic biomass	mg COD L^{-1}
X_{ND}	Particulate biodegradable organic nitrogen	mg N L^{-1}
S_O	Oxygen	mg COD L^{-1}
	Kinetic parameters	
μ_H	Maximum specific growth rate for heterotrophic biomass	day $^{-1}$

K_S	COD half-saturation coefficient for heterotrophic biomass	mg COD L^{-1}
$K_{O,H}$	Oxygen half-saturation coefficient for heterotrophic biomass	mg COD L^{-1}
K_{NO}	Nitrate half-saturation coefficient for heterotrophic biomass	mg N L^{-1}
b_H	Decay coefficient for heterotrophic biomass	day $^{-1}$
η_H	Correction factor for hydrolysis under anoxic conditions	-
k_h	Maximum specific hydrolysis rate	g COD (g COD · day)$^{-1}$
K_X	Half-saturation coefficient for hydrolysis of X_S	g COD (g COD)$^{-1}$
μ_A	Maximum specific growth rate of autotrophic biomass	day $^{-1}$
K_{NH}	Ammonium half-saturation coefficient for autotrophic biomass	mg N L^{-1}
b_A	Decay coefficient for autotrophic	day $^{-1}$
$K_{O,A}$	Oxygen half-saturation coefficient for autotrophic biomass	mg COD L^{-1}
k_a	Ammonification rate	L (mg COD · day)$^{-1}$
f_{bN}	Nitrogen content of biomass	g N (g COD)$^{-1}$

The steady-state model was used at the first step for model calibration (Ekama, 2009), and sensitivity analysis was used to determine the model parameters. More information about model calibration and values of model parameters can be found in the appended **Paper II**. The model can be used for dynamic simulation of the process performance.

Two main challenges for model predictive control are now presented with solutions: using statistical monitoring methods to obtain hard-to-measure influent variables; and using the kinetic model to obtain the outlet wastewater quality. The combination of these two solutions was tested by dynamic simulation, using predicted COD and TP as the inputs to the process model. The results of the simulation are shown in Figure 4.7. The model output of TSS, COD and ammonium fitted well with measured data. However, the model output TP was much higher than the measured values. The microorganism in MBBR system assimilated most of the phosphorus brought by the

influent, but the anabolism related to phosphorus removal was not included in the ASM based models. The TP and TSS concentration in the MBBR outlet determines coagulant dosage in the flocculation tank. In this case, phosphorus removal by chemical precipitation required negligible coagulant, because soluble phosphorus was already transformed to particulate phosphorus in the biomass. In other words, the coagulant dosage was mainly determined by the TSS of the MBBR outlet. Therefore, the combined approach of statistical monitoring and dynamic simulation is capable of enabling model predictive control.

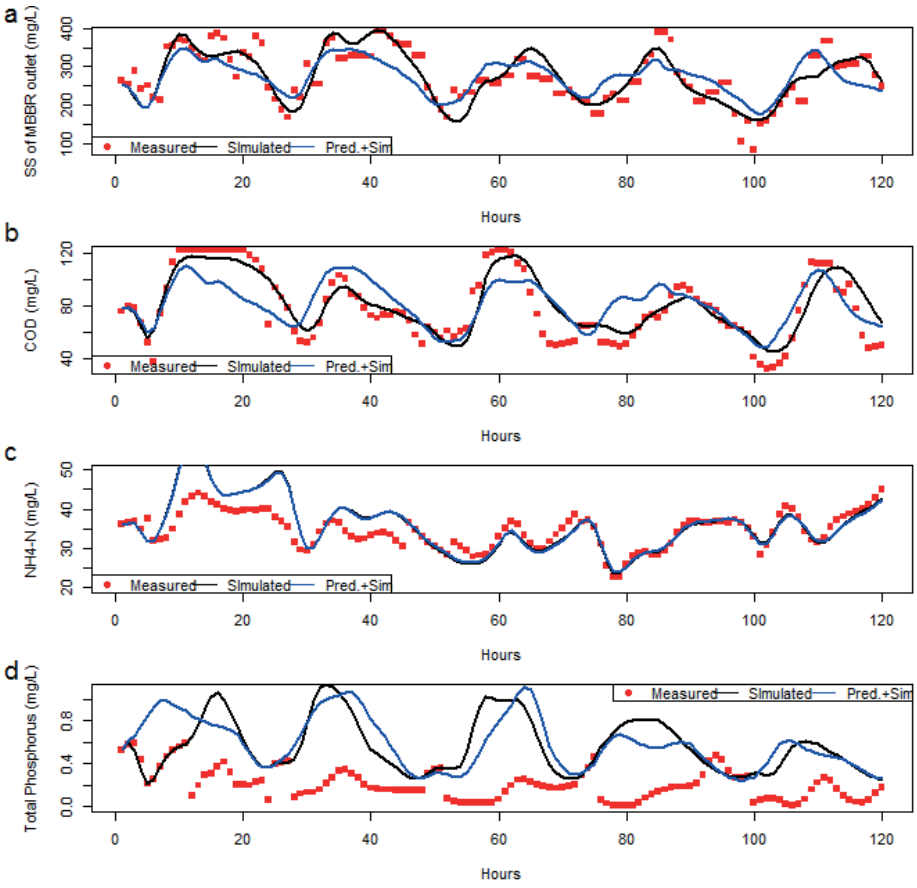

Figure 4.7: Dynamic simulation results of the wastewater treatment process. (a) Suspended solids of MBBR outlet; (b) effluent COD; (c) effluent ammonium; (d) effluent TP. The red, black and blue curves represent the measured data, simulated data based on measured influent, and simulated data based on predicted influent data, respectively. Figure from **Paper II.**

It is also interesting to know if this approach is applicable to a nitrogen removal process. Since the high-rate WWTP was not designed for nitrogen removal, the nitrification and denitrification processes in ASM1 were not applied in this simulation. However, both the aerobic autotrophic growth (nitrification) model and anoxic heterotrophic growth (denitrification) model are in the same form of Monod Equation as aerobic heterotrophic growth (organic substance removal). The same approach can be extended to simulate the nitrification/denitrification process, but proper calibration is necessary.

4.3 Case studies for process surveillance

Statistical learning was applied to characterise influent in **Paper I**. How the statistical methods can be further used in other aspects to optimise WWTP operations in full-scale was the main focus of **Paper III** and **Paper V**.

Seasonal variation of activated sludge settleability was observed in a full-scale WWTP in Qingdao, China. As shown in Figure 4.8, higher diluted sludge volume index (DSVI) of activated sludge was found during the cold season, and lowest DSVI was always found during the warm season. Higher DSVI indicated poor activated sludge settleability during the cold season, which caused higher TSS in the effluent and sometimes led to process failure. An early warning system is important for this WWTP to avoid process failure.

Activated sludge settleability was dependent on several factors, such as substance loading rates (Guo et al., 2014; F. Ye et al., 2011), filamentous bulking (Schuler and Jassby, 2007; Wagner et al., 2015), biomass density (Jones and Schuler, 2010; Schuler and Jang, 2007), and extracellular polymeric substances (Li et al., 2015). All of these factors are the consequences of influent variation and operational condition changing. Therefore, influent variables and operational variables (e.g. temperature, solid retention time) should be employed as inputs for building an early warning tool.

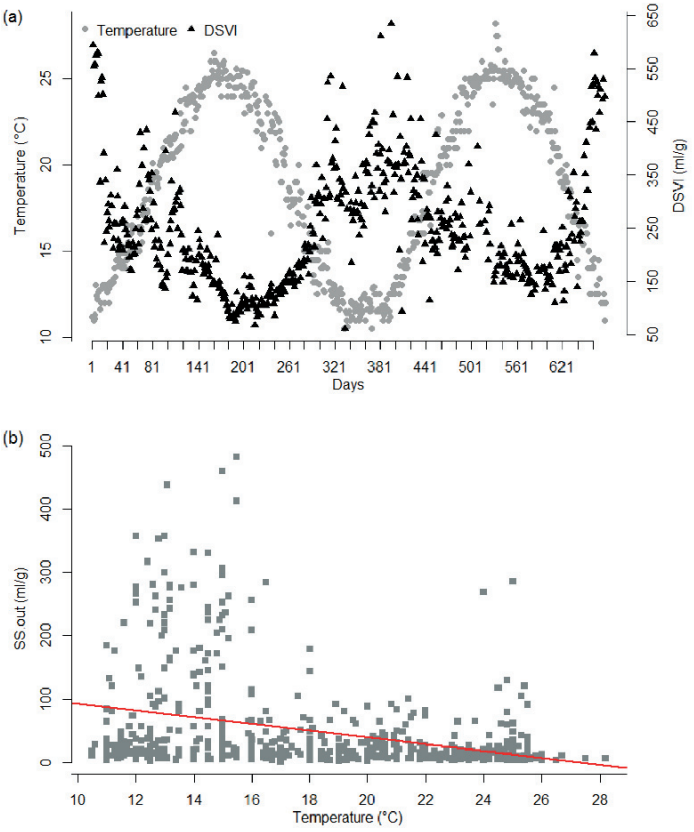

Figure 4.8: (a) Seasonal variation of DSVI in two years; (b) Scatter plot of TSS in the outlet versus temperature. Figure from **Paper III**.

Ten variables that represent influent characteristics, contaminant loadings as well as environmental and operational conditions were analysed together with DSVI by principal component analysis. The results are shown in Figure 4.9. Eleven new independent variables (principal components) were generated by PCA. Figure 4.9a shows the variance explained by the first seven principal components (PCs). The rest of the PCs represented less than 0.1 % of the total variance of the dataset, which can be ignored. PC-1 and PC-2 together represented almost 100 % of the variation of the entire dataset, which suggested the high collinearity of the original variables. It is also a reminder that there is a high risk of overfitting an MLR model if the original variables are applied

directly as inputs of the MLR. Moreover, Figure 4.9b is the loading plot of original variables that are projected to the plane formed by the first principal component (PC-1) and second principal component (PC-2). DSVI, MLSS and Temperature are the most significant variables that represent the main variability of the original dataset because they have higher PC-1 or PC-2 loadings. The other variables located in the inner circle of Figure 4.9b were not significant variables because they had either too low PC-1 or PC-2 loading. Therefore, the variation of Temperature and MLSS may be the reason for DSVI seasonal variation.

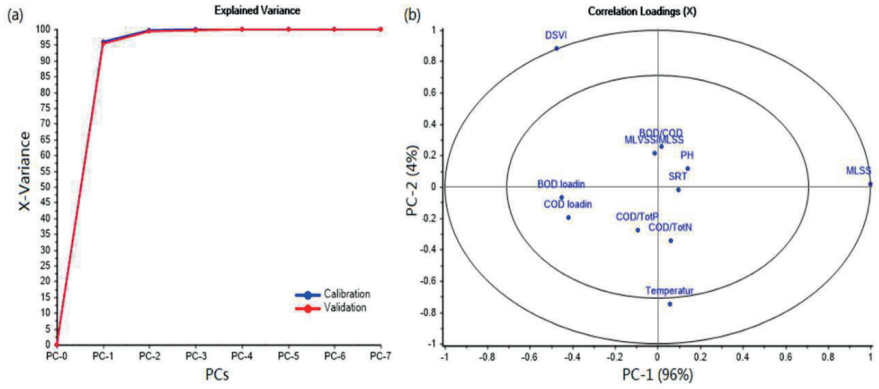

Figure 4.9: Principal component analysis (PCA) of DSVI and the other ten variables: BOD/COD ratio, pH, MLVSS/MLSS ratio, SRT, MLSS, BOD loading, COD loading, COD/Total Phosphrus ratio, COD/Total Nitrogen ratio, Temperature and MLSS. (a) The proportion of total variance being explained by different numbers of principal components; (b) Correlation loading plot projected to the plane of PC-1 and PC-2. Figure from Paper **III**

Based on the PCA results, Temperature and MLSS can be used to build a prediction model for DSVI for early warning purpose. An MLR model was established as below:

$$DSVI = 724.6323 - 14.6889 \cdot Temperature - 0.0953 \cdot MLSS \quad (4.3)$$

The prediction validated by leverage correction indicates that the predicted DSVI can explain 64 % variability of the measured DSVI. The prediction accuracy was not high enough compared with those models based on filamentous bulking (Smets et al., 2006; Liu et al., 2016b). However, this study aims to investigate the original causes of the seasonal variation of activated sludge settleability rather than predicting the status of activated sludge, e.g. filamentous bulking or non-filamentous bulking. Considering the uncontrollable disturbances and the complexity of the full-scale system, the R-square of more than 0.64 was fine to indicate the tendency of settleability changing.

Two other multivariate prediction methods (Multiple Linear Regression and Partial Least Squares, Support Vector Machine) were compared with PCA+MLR method. All these three methods result in similar prediction accuracy, but the MLR model based on PCA has the best interpretability. See more details in **Paper III**.

The nonlinearity of influent variation was caused by both seasonal variation and climate change, as stated in **Paper I**. In **Paper V**, a nonparametric spline regression method – multivariate adaptive regression spline (MARS) – was used to predict influent COD and TP. The model is listed in Table 4.3 (Table S3 in the supplementary material of **Paper V**).

Table 4.3: MARS models for global COD and TP prediction. Table from supplementary material of **Paper V**.

	Knots	Interaction terms	Model
COD	6	No	$\mathrm{COD} = 1050.91058 - 0.43835 \cdot \mathrm{h}(852.625 - \mathrm{Flow}) - 0.08277 \cdot \mathrm{h}(\mathrm{Flow} - 852.625) + 1345.01256 \cdot \mathrm{h}(\mathrm{WaterTemp} - 8.5) - 5.67291 \cdot \mathrm{h}(8.6 - \mathrm{WaterTemp}) - 1357.16268 \cdot \mathrm{h}(\mathrm{WaterTemp} - 8.6) - 11.46400 \cdot \mathrm{h}(\mathrm{TSS} - 342) - 1.48832 \cdot \mathrm{h}(360.25 - \mathrm{TSS}) + 15.28556 \cdot \mathrm{h}(\mathrm{TSS} - 360.25) - 7.55469 \cdot \mathrm{h}(NH_4\text{–N} - 31.2419) - 0.17383 \cdot \mathrm{h}(2335.04 - NH_4\text{–}N^2) + 36.21696 \cdot \mathrm{h}(49.5616 - pH^2) - 24.28355 \cdot \mathrm{h}(pH^2 - 49.5616)$
TP	9	Yes	$TP = -3.8348229 - 0.0028527 \cdot \mathrm{h}(\mathrm{Flow} - 1307.1) + 0.1800591 \cdot \mathrm{h}(53.5239 - NH_4\text{–N}) - 0.5625588 \cdot \mathrm{h}(NH_4\text{–N} - 53.5239) + 0.0000206 \cdot \mathrm{h}(TSS^2 - 129780) + 0.0008343 \cdot \mathrm{h}(8624.06 - \mathrm{Flow} * \mathrm{WaterTemp}) - 0.0001379 \cdot \mathrm{h}(\mathrm{Flow} * \mathrm{WaterTemp} - 8624.06) - 0.0003182 * \mathrm{h}(14893.5 - \mathrm{Flow} * NH_4\text{–N}) + 0.0001098 * \mathrm{h}(\mathrm{Flow} * NH_4\text{–N} - 14893.5) - 0.0035335 * \mathrm{h}(935.74 - \mathrm{WaterTemp} * \mathrm{TSS}) + 0.0024327 * \mathrm{h}(\mathrm{WaterTemp} * \mathrm{TSS} - 935.74) - 0.0957721 * \mathrm{h}(64.08 - \mathrm{WaterTemp} * \mathrm{pH}) - 0.0008502 * \mathrm{h}(4191.85 - \mathrm{TSS} * NH_4\text{–N}) + 0.0004916 * \mathrm{h}(\mathrm{TSS} * NH_4\text{–N} - 4191.85) + 0.0056016 * \mathrm{h}(1056.13 - \mathrm{TSS} * \mathrm{pH}) - 0.0061045 * \mathrm{h}(\mathrm{TSS} * \mathrm{pH} - 1056.13)$

The results show that MARS is a capable tool for COD and TP prediction, with sufficient prediction accuracy in terms of RMSE and R^2 (Results presented in **Paper V**). James et al (James

et al., 2013) has pointed out the importance of interpretability of statistical learning, where statistical learning should not be viewed as black boxes. Compared with neural network based methods and other machine learning methods, the MARS method has advantages of interpretability and applicability in process surveillance (Kuter et al., 2018; Xing et al., 2018).

The case studies in both **Paper III** and **Paper V** show that statistical learning algorithms provide support for the surveillance and control of wastewater treatment processes. The digitalisation of WWTPs will be achieved when the surveillance technology for wastewater treatment processes is upgraded by data mining and multivariate statistical analysis.

4.4 Interaction of microbial community composition and biological process modelling

As mentioned in **Paper II**, robust process surveillance and biological process modelling methods are two of the most critical barriers towards achieving advanced control of wastewater treatment processes. The previous sections have focused on process surveillance and plant-wide modelling for control purposes. In this subsection, the attention will move to the microbial community and its interaction with biological process modelling (**Paper IV**).

Modern molecular biological technology has enabled researchers and practitioners to investigate the microbial structure of biomass. In recent years, the microbial community diversity of wastewater treatment biomass has been studied at the molecular level (Jo et al., 2016; T. Liu et al., 2016; Xu et al., 2017). Since the microbial community of activated sludge system has already been well investigated in various scientific reports (Flowers et al., 2013; Ju et al., 2014; Liang et al., 2010), a lab-scale multi-stage moving bed biofilm reactor (MBBR) was selected for this study. Moving bed biofilm reactors (MBBRs) have been widely applied in wastewater treatment plants over the last decades (Di Trapani et al., 2011; Ødegaard, 2006), but the microbial community diversity of biofilm in each chamber of multi-stage has rarely been reported.

In **Paper IV**, the multi-stage MBBR system was operated in steady state during the experiment period. The microbial community diversity of biofilm in each of the three chambers and a paralleled activated sludge (AS) system was investigated by applying high-throughput sequencing. Figure 4.10 indicated that *Proteobacteria* and *Bacteroidetes* were the dominant phyla in both biofilm and activated sludge (AS) samples. This result complied with other literature reports about

activated sludge (Ma et al., 2013; L. Ye et al., 2011). *Nitrospirae* is highly correlated with nitrification efficiency (Lin et al., 2016). *Nitrospirae* was found in the first aeration chamber (AE2) but is hardly detectable in AN or AE1. This indicated that the lower organic loading environment in AE2 favoured the growth of *Nitrospirae* and other autotrophic bacteria. At the class level, *Alphaproteobacteria, Betaproteobacteria, Flavobacteriia*, and *Gammaproteobacteria* were the four largest classes in all the samples, taking up 52 % - 75 % of the total microbes (Figure 4.10 b). *Clostridia* in AE2 (7.1 %) were much higher compared with that in AE1 (1.2 %), AN (2.6 %), and AS (2.2 %). *Clostridia* proportion was 4.5 % - 13 % in biofilm (Biswas et al., 2014), and 0.1 % - 5.73 % in activated sludge (Ma et al., 2015), suggesting that *Clostridia* may be in favour of attached growing. In this study, all the microbes detected in the activated sludge system can be found in the MBBR system at the class level. Jo et al. (2016) concluded that both the microbial community diversity and its composition differed between the biofilm and activated sludge among membrane bioreactors. Although the composition of AS microbial community differed from any of the biofilm community, the proportion of each class was within the corresponding range of biofilm community composition. Comparison of the microbial community composition of biofilm from multi-stage MBBR systems is hardly found in scientific publications, even though the MBBR system has been widely used. See more details in the appended **Paper IV**. The results extended microbial community studies to biofilm of different functional chambers of the MBBR system.

One reason for performing high-throughput sequencing was to figure out the ratio of heterotrophs and autotrophs of biofilm in each chamber. Some of the bacteria can be identified as autotrophs, e.g. *Nitrospirae*. However, the difficulty encountered here was that the taxonomic information was not sufficient to classify the other bacteria into heterotrophs or autotrophs. A manual method based on significance tests was applied for the classification. The hypothesis was that a significantly higher composition of autotrophic nitrifying bacteria existed in the nitrification chamber (AE2) because the nitrification performance associates with higher autotrophic nitrifying bacteria composition (Liebig et al., 2001; Quan et al., 2013). Thus, if the proportion of an operational taxonomic unit (OTU) from AE2 was significantly higher than that from other chambers, the corresponding bacteria would be classified as autotrophs. The other unidentified OTUs would then be classified as heterotrophs. Those unidentified OTUs were left as unknown. The results based on this classification method are shown in Figure 4.11. The proportion of autotrophs in the biofilm of AE2 was 15.4 %, which is significantly higher than that in AE1 (4.3 %) and AN (0.8 %). Ma et

al. (2015) found that the proportion of autotrophs in activated sludge system was 0.5 % - 4 %, which was also measured by the high-throughput sequencing method. However, autotrophs in biomass might be easily underestimated by the sequencing method due to taxonomy complexity (Bassin et al., 2017; L. Ye et al., 2011). The classification method used in this study has estimation errors, but it compensates the underestimated autotroph errors. Therefore, the results in Figure 4.11 are accepted as the true proportion of heterotrophs and autotrophs.

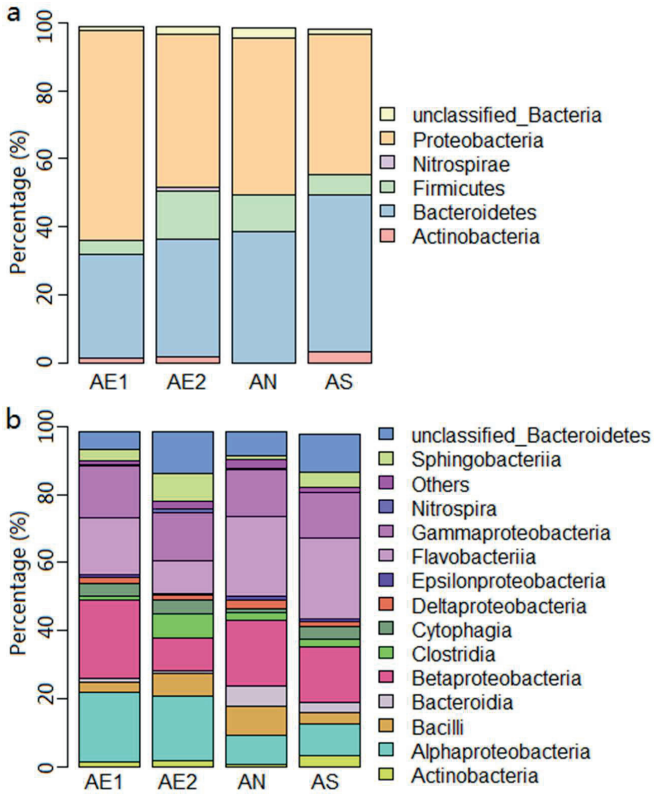

Figure 4.10: Microbial community composition in each function chamber of the MBBR system and a paralleled activated sludge system at (a) Phylum level; (b) Class level. The biofilms were sampled from the first aeration chamber (AE1), second aeration chamber (AE2) and anoxic chamber (AN). Activated sludge samples were from the activated sludge system (AS). Figure from **Paper IV**.

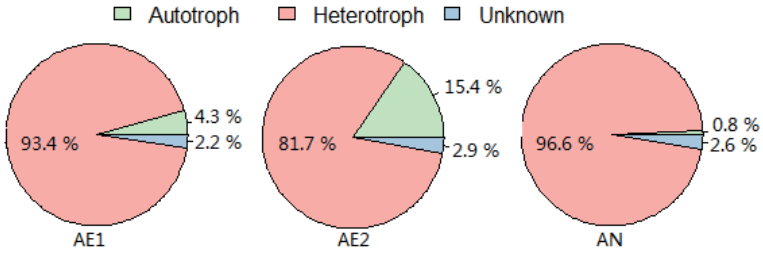

Figure 4.11: The proportion of heterotrophs and autotrophs in AE1, AE2 and AN of MBBR system. Figure from **Paper IV**.

Respiration tests were carried out to measure oxygen uptake rates (OURs) of biomass according to the method stated in **Paper IV**. The biofilms taken from AE1, AE2, and AN were used to perform respiration tests, as shown in Figure 4.12. The rapid decreasing of dissolved oxygen (DO) in the heterotrophic stage (Figure 4.12a and 4.12c) indicated that there are much larger amounts of heterotrophic biomass in AE1 and AN than in AE2. Faster decreasing DO during autotrophic respiration is found in Figure 4.12b, which indicates higher amounts of autotrophic biomass in the biofilm of AE2.

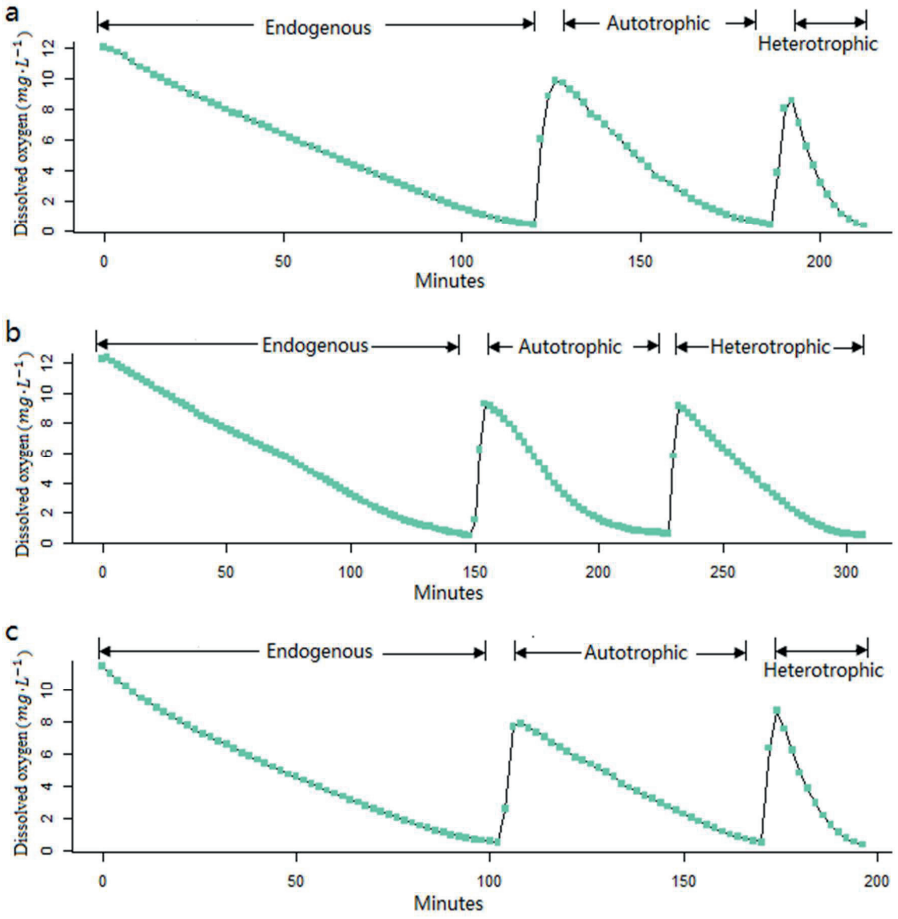

Figure 4.12: Respiration tests of biofilm taken from (a) AE1, (b) AE2 and (c) AN of the lab-scale MBBR system. Figure from **Paper IV**.

During the steady-state operation, the DO was always maintained higher than 6 $mg \cdot L^{-1}$ to avoid oxygen transfer limitation in the biofilm (Ødegaard, 2006). Secondly, the trends of DO decreasing were straight lines when DO decreased from 8.2 to 6 $mg \cdot L^{-1}$. Therefore, the segments 8.2~6 $mg \cdot L^{-1}$ were used to calculate the steady-state OURs.

In this study, the changing of DO values from saturation to around 6 $mg \cdot L^{-1}$ was straight lines (Figure 6), which suggested constant oxygen uptake rates for the corresponding biomass in this condition. Therefore, only one OUR value of each respiration period is derived from Figure 4.12.

The heterotrophic OURs and autotrophic OURs of biofilm are listed in Table 4.4. Heterotrophic biomass in AE1 had the highest OUR (36.72 $mg\ O_2 \cdot L^{-1} \cdot h^{-1}$), and autotrophic biomass from AN had the lowest OUR (1.66 $mg\ O_2 \cdot L^{-1} \cdot h^{-1}$). The highest autotrophic OUR was found from biofilm in AE2 (7.65 $mg\ O_2 \cdot L^{-1} \cdot h^{-1}$). The OUR values were not normalised to specific oxygen uptake rates (SOURs) because the non-normalised OUR values can be further used to calculate the amount of active heterotrophic biomass and autotrophic biomass.

Table 4.4: The OURs of active heterotrophic biomass and autotrophic biomass of biofilm in each chamber of the MBBR system. Table from **Paper IV**.

	AE1	AE2	AN
Heterotrophic, OUR_H $(mg\ O_2 \cdot L^{-1} \cdot h^{-1})$	36.72	9.03	32.40
Autotrophic, OUR_A $(mg\ O_2 \cdot L^{-1} \cdot h^{-1})$	6.97	7.65	1.66

The quantity of active heterotrophic biomass (X_H) and active autotrophic biomass (X_A) were calculated based on simplified ASM models (Ochoa et al., 2002), as shown in Equation 4.4.

$$(a)\ \ X_H = \frac{1}{\mu_{H,Max}} \cdot \frac{Y_H}{1-Y_H} \cdot OUR_H\,,\ \ (b)\ \ X_A = \frac{1}{\mu_{A,Max}} \cdot \frac{Y_A}{4.57-Y_A} \cdot OUR_A \qquad (4.4)$$

where the kinetic parameters at 12℃ are: $\mu_{H,Max} = 3.5\ day^{-1}$, $\mu_{A,Max} = 0.3\ day^{-1}$, and the stoichiometric parameters are $Y_H = 0.67\ g\ COD \cdot (g\ COD)^{-1}$, and $Y_A = 0.24\ g\ COD \cdot (g\ N)^{-1}$. See the calculation procedure in **Paper IV**. The calculated active heterotrophic biomass and active autotrophic biomass are shown in Table 4.5. The biofilm in AE1 was composed with the highest heterotrophic biomass proportion (94.3 %), and the biofilm in AE2 had the highest quantity of autotrophic biomass (33.9 $mg\ COD \cdot L^{-1}$). It is noteworthy that heterotrophic biomass was still dominant in AE2 though most biodegradable matters had been removed before the flow entered AE2. The substances for heterotrophic growth in AE2 may come from hydrolysis of slowly biodegradable particles, lysis of microorganisms and metabolic products (Namkung and Rittmann, 1986; Okabe et al., 1995). Fernandes et al. (Fernandes et al., 2013) measured the biomass distribution of activated sludge, which showed that 12.2 % of the active biomass was autotrophic biomass. Biomass distribution of biofilm was different in each chamber. Overall, the ratios of active heterotrophic and autotrophic biomass in biofilm from different functional chambers provided a reference for further study of the MBBR system.

Table 4.5: Calculated active heterotrophic biomass and autotrophic biomass quantity and ratio from Equation 4.4. Table from **Paper IV**.

	AE1	AE2	AN
Heterotrophic biomass ($mg\ COD \cdot L^{-1}$)	511.2	125.7	451.0
Autotrophic biomass ($mg\ COD \cdot L^{-1}$)	30.9	33.9	7.4
Heterotrophs ratio	94.3 %	78.8 %	98.4 %
Autotrophs ratio	5.7 %	21.2 %	1.6 %

The ratio of autotrophic biomass in each chamber was higher than the corresponding autotroph bacteria proportion in Figure 4.11. Noticeable bias of estimated biomass distribution can be found, because the kinetic model parameters ($\mu_{H,Max}$ and $\mu_{A,Max}$) were calculated from the reference values of ASM1 without calibration. Sensitivity analysis was usually used to calibrate kinetic models of biological wastewater treatment systems (Cosenza et al., 2014; Eldyasti et al., 2012). However, model calibration using sensitivity analysis costs time and requires computational power, because the ASM was over-parameterised and the model outputs are less sensitive to the changing of kinetic parameters (Liwarska-Bizukojc et al., 2011).

In **Paper IV**, a novel approach for kinetic model parameters estimation was developed. From Equation 4.4, the ratio of $\mu_{H,Max}/\mu_{A,Max}$ can be written as a function of X_H/X_A. If we accept that the ratio of heterotrophs/autotrophs can be used to represent the biomass ratio X_H/X_A, the relationship of kinetic model parameters can be easily obtained. The proportional relationships of $\mu_{H,Max}$ and $\mu_{A,Max}$ were established for each functional chamber of MBBR system, as listed in Table 4.6. When sensitivity analysis is applied to calibrate biological process models, kinetic parameters are usually less sensitive than stoichiometric (Liwarska-Bizukojc et al., 2011). Therefore, such a proportional relationship of kinetic model parameters will make it much easier for model calibration.

Table 4.6: Relationship of kinetic parameters $\boldsymbol{\mu_{H,Max}}$ and $\boldsymbol{\mu_{A,Max}}$based on the estimation approach in **Paper IV**.

	AE1	AE2	AN
Kinetic parameters	$\mu_{H,Max} = 8.88\,\mu_{A,Max}$	$\mu_{H,Max} = 8.17\mu_{A,Max}$	$\mu_{H,Max} = 6.14\mu_{A,Max}$

4.5 Environmental impact analysis of control strategies

Although wastewater treatment plants contribute significantly to environmental protection, the amounts of energy and materials consumption by wastewater treatment plants should not be ignored. The energy and materials consumption will increase the negative environmental impacts of wastewater treatment plants, such as global warming, ozone depletion, and human toxicity. For a wastewater treatment plant, different control strategies will lead to different environmental impacts. For instance, a certain amount of aeration energy will be saved when the WWTP applied a low DO setpoint. But, on the other hand, there will be higher nitrous oxide (N_2O) emission when the nitrification process is operating at low DO level (Kampschreur et al., 2009). N_2O is a greenhouse gas which has a 300 times stronger effect than carbon dioxide (IPCC, 2011). Whether the energy saved by low DO control strategy can compensate for the negative effect of N_2O emission needs to be figured out. Most of the research works in the control of WWTPs are technology-driven and encourage economic benefits (Rahman et al., 2016). However, the ultimate goal of a WWTP is to protect the environment, which should not be ignored from the decision-making for control strategies. In recent years, life cycle assessment (LCA) has been used as an environmental impact evaluation tool for different wastewater treatment processes (Krzeminski et al., 2017; Lorenzo-Toja et al., 2015) and effluent disposal standards (Rahman et al., 2016). LCA could also be applied to evaluate the environmental impacts of different control strategies for wastewater treatment plants (Meneses et al., 2015). Therefore, a preliminary study of environmental impacts of different control strategies was conducted based on mass balance calculation of typical Norwegian wastewater treatment plants (**Paper VI**). The purpose of Paper VI is to integrate environmental impact analysis into the optimisation of wastewater treatment processes since environmental impact analysis can serve as a general guideline for the selection of control strategies.

Wastewater treatment can be viewed as using energy and material to exchange for purified water. As shown in Figure 4.13, direct emissions of waste and toxic compounds happen in the WWTP during wastewater treatment. Indirect emissions occur during the production and transport of energy and materials (Ll Corominas et al., 2013). The eutrophication risk will be reduced with more nutrients removed from wastewater, but the environment may suffer from other associated environmental problems due to energy and material consumption. Global warming, ozone depletion and acidification potential were found to be rising due to the application of a more

stringent nutrient removal standard (Rahman et al., 2016). An advanced control strategy should drive the WWTP to achieve the effluent disposal standard with the lowest environmental cost. Therefore, it is critical to review the plant-wide control strategy in a more comprehensive manner. In **Paper VI**, Life Cycle Assessment (LCA) was applied to analyse the plant-wide control strategy of the typical wastewater treatment process configuration in Norway.

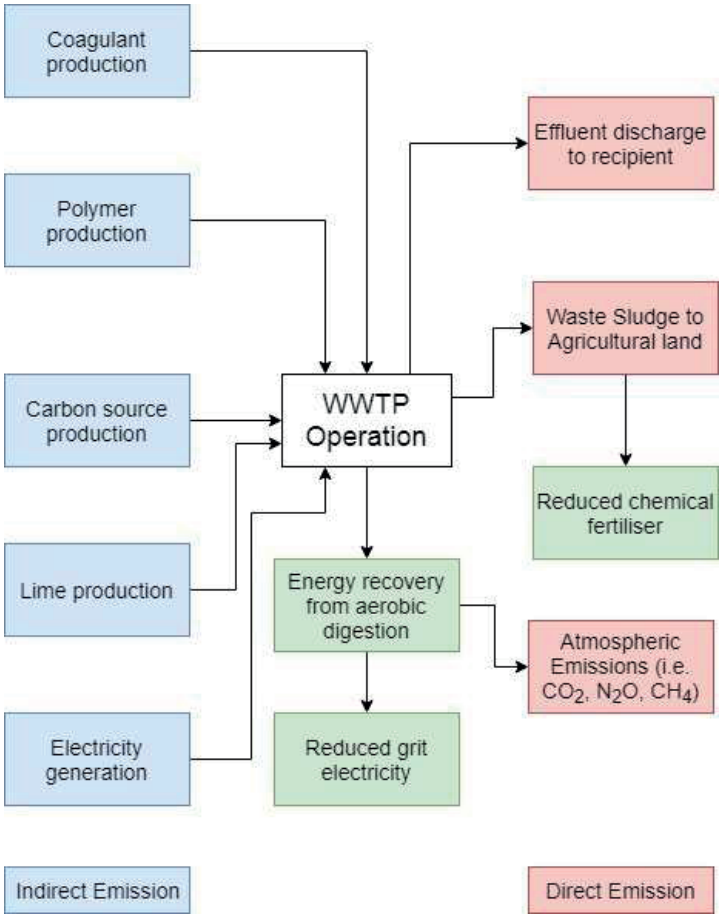

Figure 4.13: The required inputs from the environment to the wastewater treatment process and the outputs of the process. The process outputs include both direct emissions and indirect emissions. Figure from **Paper VI**.

Figure 4.14 illustrates a typical wastewater treatment process configuration in some of the large WWTPs in Norway. This type of WWTP uses MBBR systems for carbon and nitrogen removal, where both pre-denitrification and post-denitrification are applied. In this scenario, ferric chloride

and polymer were added to the MBBR outlet for phosphorus and suspended solids removal. Around 50 % of nitrogen can be removed through pre-denitrification, according to Rusten et al. (1995), another 40 % could be removed by adding sodium acetate as an external carbon source.

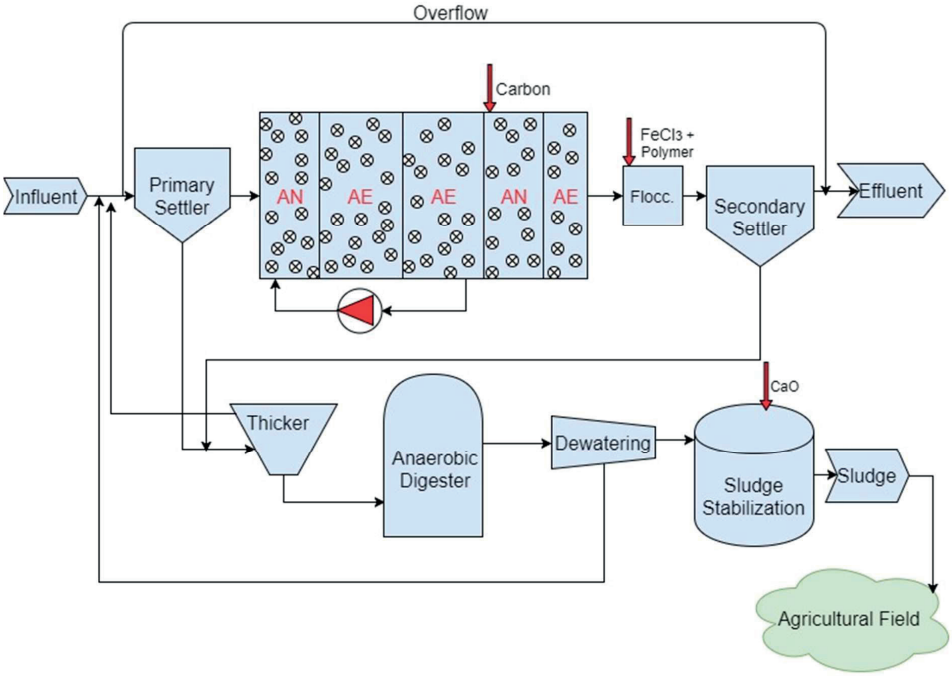

Figure 4.14: The wastewater treatment process configuration used for Life Cycle Assessment in **Paper VI**.

Two types of control strategies were compared in **Paper VI**. The conventional control applied DO feedback control for aeration and flow proportional control for coagulant dosing. The advanced control strategy applied MPC to control aeration and external carbon dosing.

For the advanced control method, the airflow was controlled as a function of influent flow (Q_{in}), primary settled COD (COD_{PS}), inlet ammonium ($NH_4^+ - N$) and dissolved oxygen (DO). COD and soluble COD can be predicted by using soft sensor methods as stated in **Paper V**. Carbon dosing is controlled as a function of flow (Q_{in}), recycle rate ($r_{recycle}$), $NH_4^+ - N$, and DO. Moreover, the advanced control strategy also enhanced particle removal from primary settlers by dosing ferric chloride before the wastewater entered the primary setter. Ødegaard (2016) has shown that enhancing primary removal of particles in front of the biological stage would increase

energy efficiency. In this case, the particulate organic matters settle as primary sludge and are finally recovered as CH_4 in the digester. The detailed mass balance calculation of these two types of control strategy can be found in Table 3 of **Paper VI**. A simplified list of inputs and outputs which served as inventory for LCA can be found in Table 4.7. Significant energy saving can be achieved by applying advanced control. Although direct emissions of greenhouse gases were well studied (Corominas et al., 2012; Flores-Alsina et al., 2011; Guo and Vanrolleghem, 2014), indirect emission of N_2O due to sludge decomposition in the agriculture field was not clear. Therefore, N_2O emission was not considered in this study.

Table 4.7: Daily energy and material inputs to the process and emissions to the final recipient, including emissions to the water body (marine), air, and soil (agriculture field). Table from **Paper VI**.

	Conventional control	Advanced control	Unit
Energy input	6000	5280	kWh/d
$FeCl_3$ dosing	974.4	835.2	kg/d
Acetic acid input	163.9	228.2	kg/d
Total CO_2 emission to air	8242.7	6719.8	kg/d
Nitrogen emission to air	625	591.1	kg/d
CH_4 production	4.97	9.94	m^3/d
COD emission to water body	717.9	713.8	kg/d
Nitrogen emission to water body	180	169	kg/d
Phosphorus emission to water body	6.5	4.8	kg/d
Organic compound to soil	3212.5	2846.7	kg/d
Nitrogen emission to soil	327.6	364.9	kg/d
Phosphorus emission to soil	76.8	92.8	kg/d

The LCA results of applying two different control strategies are shown in Figure 4.15, which concludes the differences between applying two different types of control strategy in terms of environmental impacts. There is no difference in eutrophication impact because both control strategies are applying the same effluent discharging standard. However, the differences of environmental impact lie in other aspects. The negative impact on global warming and toxicity compound emission was significantly reduced due to the application of advanced control. Most electricity in Norway is produced from hydropower. Thus, the reduction of electricity by advanced

control did not contribute to fossil depletion significantly. The higher fossil depletion impact by advanced control is caused by the higher transport usage of fossil for carbon source. Since WWTPs were initially built to protect the environment, the operation strategy should be an economical option that maximises environmental benefits.

Therefore, environmental impact analysis tells how a WWTP should be controlled to achieve the goal of environmental protection. In a full-scale WWTP, plenty of treatment lines and internal streams require surveillance and control. The specific surveillance and control techniques would be capable to optimise limited numbers of streams. For plant-wide optimisation, environmental impact analysis should be applied from the scratch to investigate the interactions between different streams and treatment lines, and individual surveillance and control approach for specific purpose should be designed following the general framework concluded from environmental impact analysis.

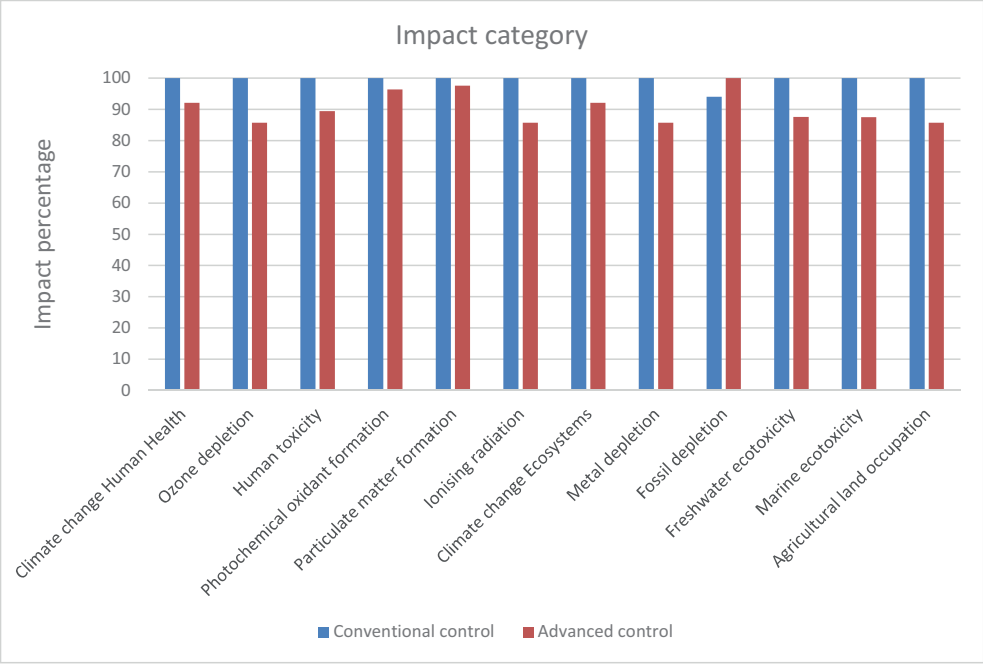

Figure 4.15: Comparison of impact categories of the conventional control strategy and advanced control. Figure from **Paper VI**.

5. Conclusions and Outlook

With the purpose of optimising wastewater treatment processes to reduce operational costs and the environmental impacts of wastewater treatment, this study has the ambition to integrate process surveillance, data mining, kinetic modelling, molecular biology method and environmental impact analysis to optimise wastewater treatment processes. This thesis is also intended to contribute to the advancement of knowledge in wastewater treatment modelling and better methods for process surveillance. The following main conclusions are drawn from the works in the thesis. Outlook for future works is attached to the associated conclusion.

By combining PCA and cluster analysis in series, an improved understanding of influent characterisation was achieved. In the cold season, the dry climate influent and wet climate influent were sorted by applying the unsupervised statistical learning algorithm. It enabled the comparison of the dry climate influent in the warm season and the dry climate influent in the cold season, after the climate effect was eliminated. The influent in the cold season was usually concluded as having a higher flow rate and lower concentration, when compared with that in the warm season. However, after eliminating the snow melting effect, the influent in the cold season is more or less the same as that in the warm season. A classification tool was built based on PLS-DA, which can be directly used in future works.

The implementation of model predictive control in practice is usually limited due to a lack of online analysers and the complexity of the biological wastewater treatment process. Statistical prediction of influent COD and total phosphorus was initially achieved by applying PCA and MLR. Further improvement was done by applying the MARS algorithm which considers the fact of nonlinearity. The intermediate process outlet and the final effluent values were obtained by applying predicted influent values into the process model. Therefore, the calibration of process models is also critical. This study considered the dynamic of both online monitoring and the process. In future works, the dynamics of process actuators should also be included to carry out process control at full scale.

Multiple Linear Regression (MLR), Partial Least Squares Regression (PLSR) and Support Vector Machine Regression (SVMR) were adopted to develop an early warning tool for activated sludge settleablity. The prediction accuracy was almost the same with these three methods, while MLR

had the best interpretability. The proportion of volatile biomass was found playing a central role in seasonal variation of settleability, which can be explained by the storage-biodegradation mechanism. Monitoring and control of volatile biomass content is essential for activated sludge system operation. In practice, chemically enhanced oxidation and dosing inorganic flocculated substances can be further tested to reduce the volatile content proportion.

Microbial diversity and microbial composition of biofilm were found to be different in different function chambers of the MBBR system. Although heterotrophs were the dominant bacteria in the second aerobic chamber, significantly higher proportions of autotrophs were found compared with the anoxic chamber and the first aerobic chamber. The knowledge obtained at the molecular level can be used to supervise modelling of the biological treatment process. If the microbial diversity can be monitored in dynamic changing situations, such information can be further derived to assist process operation and design.

Life Cycle Assessment was applied to analyse the environmental impacts of two different environmental control strategies in wastewater treatment plants. Significant reduction of climate change impact and environmental toxicity was achieved by enhancing primary removal of particles and applying model predictive control in a case study. It is beneficial to integrate environmental impacts in the evaluation of wastewater treatment process performance. The goal of integrating environmental impact analysis to process optimisation is to guide the selection of control strategies. Lower environmental impact control strategies should be selected to make plant-wide control decisions.

The application of data mining enables an economical approach to process surveillance, which motivates practitioners to work towards building more intelligent wastewater treatment processes. Since the composition of the microbial community interacted with process modelling, a new process modelling approach can be achieved. Whenever process optimisation takes place, the environmental impacts should be considered as important as reducing operational costs and stabilising effluent quality. Overall, the knowledge gained by integrating process surveillance, data mining, process modelling, microbial community investigation and environmental impact analysis will benefit wastewater treatment operation, design and digitalisation.

References

Akaike, H., 1974. A new look at the statistical model identification. IEEE Trans. Autom. Control 19, 716–723. doi:10.1109/TAC.1974.1100705

APHA, AWWA, WEF, 2012. Standard methods for the examination of water and wastewater, 22nd ed. American Public Health Association, Washington, D.C.

Avella, A.C., Görner, T., Yvon, J., Chappe, P., Guinot-Thomas, P., de Donato, P., 2011. A combined approach for a better understanding of wastewater treatment plants operation: Statistical analysis of monitoring database and sludge physico-chemical characterization. Water Res. 45, 981–992. doi:10.1016/j.watres.2010.09.028

Barker, M., Rayens, W., 2003. Partial least squares for discrimination. J. Chemom. 17, 166–173. doi:10.1002/cem.785

Bassin, J.P., Rachid, C.T.C.C., Vilela, C., Cao, S.M.S., Peixoto, R.S., Dezotti, M., 2017. Revealing the bacterial profile of an anoxic-aerobic moving-bed biofilm reactor system treating a chemical industry wastewater. Int. Biodeterior. Biodegrad. 120, 152–160. doi:10.1016/j.ibiod.2017.01.036

Biswas, K., Taylor, M.W., Turner, S.J., 2014. Successional development of biofilms in moving bed biofilm reactor (MBBR) systems treating municipal wastewater. Appl. Microbiol. Biotechnol. 98, 1429–40. doi:10.1007/s00253-013-5082-8

Bixio, D., Van Hauwermeiren, P., Thoeye, C., Ockier, P., 2001. Impact of cold and dilute sewage on pre-fermentation - A case study. Water Sci. Technol. 43, 109–117.

CAMO Software, 2016. The Unscrambler X [WWW Document]. CAMO Softw. AS. URL http://www.camo.com/rt/Products/Unscrambler/unscrambler.html

Chai, Q., 2008. Modeling, estimation, and control of biological wastewater treatment plants. Telemark University College.

Chen, K.C., Chen, C.Y., Peng, J.W., Houng, J.Y., 2002. Real-time control of an immobilized-cell reactor for wastewater treatment using ORP. Water Res. 36, 230–238. doi:10.1016/S0043-1354(01)00201-9

Choi, D.-J., Park, H., 2001. A hybrid artificial neural network as a software sensor for optimal control of a wastewater treatment process. Water Res. 35, 3959–3967. doi:10.1016/S0043-1354(01)00134-8

Claros, J., Serralta, J., Seco, a., Ferrer, J., Aguado, D., 2012. Real-time control strategy for nitrogen removal via nitrite in a SHARON reactor using pH and ORP sensors. Process Biochem. 47, 1510–1515. doi:10.1016/j.procbio.2012.05.020

Corominas, L., Flores-Alsina, X., Snip, L., Vanrolleghem, P.A., 2012. Comparison of different modeling approaches to better evaluate greenhouse gas emissions from whole wastewater treatment plants. Biotechnol. Bioeng. 109, 2854–2863. doi:10.1002/bit.24544

Corominas, L., Foley, J., Guest, J.S., Hospido, A., Larsen, H.F., Morera, S., Shaw, A., 2013. Life cycle assessment applied to wastewater treatment: State of the art. Water Res. 47, 5480–5492.

doi:10.1016/j.watres.2013.06.049

Corominas, L., Larsen, H.F., Flores-Alsina, X., Vanrolleghem, P.A., 2013. Including Life Cycle Assessment for decision-making in controlling wastewater nutrient removal systems. J. Environ. Manage. 128, 759–767. doi:10.1016/j.jenvman.2013.06.002

Corona, F., Mulas, M., Haimi, H., Sundell, L., Heinonen, M., Vahala, R., 2013. Monitoring nitrate concentrations in the denitrifying post-filtration unit of a municipal wastewater treatment plant. J. Process Control 23, 158–170. doi:10.1016/j.jprocont.2012.09.011

Cosenza, A., Mannina, G., Vanrolleghem, P. a., Neumann, M.B., 2014. Variance-based sensitivity analysis for wastewater treatment plant modelling. Sci. Total Environ. 470–471, 1068–1077. doi:10.1016/j.scitotenv.2013.10.069

Delnavaz, M., Ayati, B., Ganjidoust, H., 2010. Prediction of moving bed biofilm reactor (MBBR) performance for the treatment of aniline using artificial neural networks (ANN). J. Hazard. Mater. 179, 769–75. doi:10.1016/j.jhazmat.2010.03.069

Di Trapani, D., Christensso, M., Ødegaard, H., 2011. Hybrid activated sludge/biofilm process for the treatment of municipal wastewater in a cold climate region: a case study. Water Sci. Technol. 63, 1121–1129.

Downing, A.L., Hopwood, A.P., 1964. Some observations on the kinetics of nitrifying activated sludge plants. Schweizerische Zeitschrift für Hydrol. 26, 271–288. doi:https://doi.org/10.1007/BF02504050

Du, R., Cao, S., Li, B., Niu, M., Wang, S., Peng, Y., 2017. Performance and microbial community analysis of a novel DEAMOX based on partial-denitrification and anammox treating ammonia and nitrate wastewaters. Water Res. 108, 46–56. doi:10.1016/j.watres.2016.10.051

Ekama, G.A., 2009. Using bioprocess stoichiometry to build a plant-wide mass balance based steady-state WWTP model. Water Res. 43, 2101–2120. doi:10.1016/j.watres.2009.01.036

Eldyasti, A., Nakhla, G., Zhu, J., 2012. Development of a calibration protocol and identification of the most sensitive parameters for the particulate biofilm models used in biological wastewater treatment. Bioresour. Technol. 111, 111–21. doi:10.1016/j.biortech.2012.02.021

Fernandes, H., Hoffmann, H., Antonio, R. V., Costa, R.H.R., 2013. The role of microorganisms in a full-scale sequencing batch reactor under low aeration and different cycle times. Water Environ. Res. 86, 800–809. doi:10.2175/106143013X13807328848450

Flores-Alsina, X., Corominas, L., Snip, L., Vanrolleghem, P.A., 2011. Including greenhouse gas emissions during benchmarking of wastewater treatment plant control strategies. Water Res. 45, 4700–4710. doi:10.1016/j.watres.2011.04.040

Flores-Alsina, X., Gallego, A., Feijoo, G., Rodriguez-Roda, I., 2010. Multiple-objective evaluation of wastewater treatment plant control alternatives. J. Environ. Manage. 91, 1193–1201. doi:10.1016/j.jenvman.2010.01.009

Flowers, J.J., Cadkin, T. a., McMahon, K.D., 2013. Seasonal bacterial community dynamics in a full-scale enhanced biological phosphorus removal plant. Water Res. 47, 7019–7031. doi:10.1016/j.watres.2013.07.054

Foley, J., de Haas, D., Hartley, K., Lant, P., 2010. Comprehensive life cycle inventories of alternative wastewater treatment systems. Water Res. 44, 1654–1666. doi:10.1016/j.watres.2009.11.031

Friedman, J.H., 1991. Multivariate Adaptive Regression Splines. Ann. Stat. 19, 1–67.

Guerrero, J., Guisasola, A., Comas, J., Rodríguez-Roda, I., Baeza, J.A., 2012. Multi-criteria selection of optimum WWTP control setpoints based on microbiology-related failures, effluent quality and operating costs. Chem. Eng. J. 188, 23–29. doi:10.1016/j.cej.2012.01.115

Guerrero, J., Guisasola, A., Vilanova, R., Baeza, J.A., 2011. Improving the performance of a WWTP control system by model-based setpoint optimisation. Environ. Model. Softw. 26, 492–497. doi:10.1016/j.envsoft.2010.10.012

Guo, J., Peng, Y., Yang, X., Wang, Z., Zhu, A., 2014. Changes in the microbial community structure of filaments and floc formers in response to various carbon sources and feeding patterns. Appl. Microbiol. Biotechnol. 98, 7633–7644. doi:10.1007/s00253-014-5805-5

Guo, L., Vanrolleghem, P.A., 2014. Calibration and validation of an activated sludge model for greenhouse gases no. 1 (ASMG1): Prediction of temperature-dependent N_2O emission dynamics. Bioprocess Biosyst. Eng. 37, 151–163. doi:10.1007/s00449-013-0978-3

Gutierrez, G., Ricardez-Sandoval, L.A., Budman, H., Prada, C., 2014. An MPC-based control structure selection approach for simultaneous process and control design. Comput. Chem. Eng. 70, 11–21. doi:10.1016/j.compchemeng.2013.08.014

Haimi, H., Corona, F., Mulas, M., Sundell, L., Heinonen, M., Vahala, R., 2015. Shall we use hardware sensor measurements or soft-sensor estimates? Case study in a full-scale WWTP. Environ. Model. Softw. 72, 215–229. doi:10.1016/j.envsoft.2015.07.013

Haimi, H., Mulas, M., Corona, F., Vahala, R., 2013. Data-derived soft-sensors for biological wastewater treatment plants: An overview. Environ. Model. Softw. 47, 88–107. doi:10.1016/j.envsoft.2013.05.009

Haimi, H., Mulas, M., Sahlstedt, K., Vahala, R., 2009. Advanced Operation and Control Methods of Municipal Wastewater Treatment Process in Finland, Helsinki University of Technology, Water and Wastewater Engineering. Espoo.

Han, H.G., Qian, H.H., Qiao, J.F., 2014. Nonlinear multiobjective model-predictive control scheme for wastewater treatment process. J. Process Control 24, 47–59. doi:10.1016/j.jprocont.2013.12.010

Hedegärd, M., Wik, T., 2011. An online method for estimation of degradable substrate and biomass in an aerated activated sludge process. Water Res. 45, 6308–6320. doi:10.1016/j.watres.2011.09.003

Helness, H., 2007. Biological phosphorus removal in a moving bed biofilm reactor. Norwegian University of Science and Technology.

Henze, M., Grady, C.P.L.J., Gujer, V., Marais, G. v. R., Matsuo, T., 1987. Activated Sludge Model No. 1. IAWPRC Scientific and Technical Reports No. 1.

Henze, M., Gujer, W., Mino, T., Matsuo, T., Wentzel, M.C., Marais, G. v. R., 1994. Activated Sludge No. 2, IAWQ Scientific and Technical Reports, No.3. IAWQ, London.

Henze, M., Gujer, W., Mino, T., Matsuo, T., Wentzel, M.C., Marais, G.V.R., Van Loosdrecht, M.C.M., 1999. Activated Sludge Model No.2d, ASM2d. Water Sci. Technol. 39, 165–182. doi:10.1016/S0273-1223(98)00829-4

Hwang, J.H., Oleszkiewicz, J. a, 2007. Effect of cold-temperature shock on nitrification. Water Environ. Res. 79, 964–968. doi:10.2175/106143007X176022

Indahl, U.G., Martens, H., Næs, T., 2007. From dummy regression to prior probabilities in PLS-DA. J. Chemom. 21, 529–536. doi:doi:10.1002/cem.1061

IPCC, 2011. Climate Change 2001: the Scientific Basis. Cambridge, UK.

James, G., Witten, D., Hastie, T., Tibshirani, R., 2013. An Introduction to Statistical Learning: with Applications in R. Springer-Verlag New York. doi:10.1007/978-1-4614-7138-7

Jo, S.J., Kwon, H., Jeong, S.Y., Lee, C.H., Kim, T.G., 2016. Comparison of microbial communities of activated sludge and membrane biofilm in 10 full-scale membrane bioreactors. Water Res. 101, 214–225. doi:10.1016/j.watres.2016.05.042

Jones, P.A., Schuler, A.J., 2010. Seasonal variability of biomass density and activated sludge settleability in full-scale wastewater treatment systems. Chem. Eng. J. 164, 16–22. doi:10.1016/j.cej.2010.07.061

Ju, F., Guo, F., Ye, L., Xia, Y., Zhang, T., 2014. Metagenomic analysis on seasonal microbial variations of activated sludge from a full-scale wastewater treatment plant over 4 years. Environ. Microbiol. Rep. 6, 80–89. doi:10.1111/1758-2229.12110

Kampschreur, M.J., Temmink, H., Kleerebezem, R., Jetten, M.S.M., van Loosdrecht, M.C.M., 2009. Nitrous oxide emission during wastewater treatment. Water Res. 43, 4093–4103. doi:10.1016/j.watres.2009.03.001

Kappeler, J., Gujer, W., 1992. Estimation of Kinetic parameters of heterotrophic biomass under aerobic conditions and characterization of wastewater for activated sludge modelling. Water Sci. Technol. 25, 125–139.

Kerrn-Jespersen, J.P., Henze, M., 1993. Biological phosphorus uptake under anoxic and aerobic conditions. Water Res. 27, 617–624. doi:https://doi.org/10.1016/0043-1354(93)90171-D

Kim, H., Lim, H., Wie, J., Lee, I., Colosimo, M.F., 2014. Optimization of modified ABA2 process using linearized ASM2 for saving aeration energy. Chem. Eng. J. 251, 337–342. doi:10.1016/j.cej.2014.04.076

Kim, J.-H., Chen, M., Kishida, N., Sudo, R., 2004. Integrated real-time control strategy for nitrogen removal in swine wastewater treatment using sequencing batch reactors. Water Res. 38, 3340–3348. doi:10.1016/j.watres.2004.05.006

Kim, M., Kim, Y., Kim, H., Piao, W., Kim, C., 2016. Evaluation of the k-nearest neighbor method for forecasting the influent characteristics of wastewater treatment plant. Front. Environ. Sci. Eng. 10, 299–310. doi:10.1007/s11783-015-0825-7

Krzeminski, P., Leverette, L., Malamis, S., Katsou, E., 2017. Membrane bioreactors - A review on recent developments in energy reduction, fouling control, novel configurations, LCA and market prospects. J. Memb. Sci. 527, 207–227. doi:10.1016/j.memsci.2016.12.010

Kuter, S., Akyurek, Z., Weber, G.W., 2018. Retrieval of fractional snow covered area from MODIS data by multivariate adaptive regression splines. Remote Sens. Environ. 205, 236–252. doi:10.1016/j.rse.2017.11.021

Lackner, S., Gilbert, E.M., Vlaeminck, S.E., Joss, A., Horn, H., van Loosdrecht, M.C.M., 2014. Full-scale partial nitritation/anammox experiences - An application survey. Water Res. 55, 292–303. doi:10.1016/j.watres.2014.02.032

Li, A.J., Li, X.Y., Gu, J.D., 2015. Characteristics of free cells and aggregated flocs for the flocculation and sedimentation of activated sludge. Int. J. Environ. Sci. Technol. 581–588. doi:10.1007/s13762-015-0896-9

Li, J., Lu, X., 2017. Performance and Microbial Diversity in a Low-Energy ANF-WDSRBC System for the Post-Treatment of Decentralized Domestic Wastewater. Water 9, 1–12. doi:10.3390/w9050330

Liang, Z., Das, A., Beerman, D., Hu, Z., 2010. Biomass characteristics of two types of submerged membrane bioreactors for nitrogen removal from wastewater. Water Res. 44, 3313–3320. doi:10.1016/j.watres.2010.03.013

Liebig, T., Wagner, M., Bjerrum, L., Denecke, M., 2001. Nitrification performance and nitrifier community composition of a chemostat and a membrane-assisted bioreactor for the nitrification of sludge reject water. Bioprocess Biosyst. Eng. 24, 203–210. doi:10.1007/s004490100234

Lin, J., Zhang, P., Li, G., Yin, J., Li, J., Zhao, X., 2016. Effect of COD/N ratio on nitrogen removal in a membrane-aerated biofilm reactor. Int. Biodeterior. Biodegrad. 113, 74–79. doi:10.1016/j.ibiod.2016.01.009

Liu, T., Liu, S., Zheng, M., Chen, Q., Ni, J., 2016. Performance assessment of full-scale wastewater treatment plants based on seasonal variability of microbial communities via high-throughput sequencing. PLoS ONE. 11(4), 1–15. doi:10.1371/journal.pone.0152998

Liu, W., Ratnaweera, H., 2016. Improvement of multi-parameter-based feed-forward coagulant dosing control systems with feed-back functionalities. Water Sci. Technol. 74, 491–499. doi:10.2166/wst.2016.180

Liu, Y., Chen, J., Sun, Z., Li, Y., Huang, D., 2014a. A probabilistic self-validating soft-sensor with application to wastewater treatment. Comput. Chem. Eng. 71, 263–280. doi:10.1016/j.compchemeng.2014.08.008

Liu, Y., Chen, J., Sun, Z., Li, Y., Huang, D., 2014b. A probabilistic self-validating soft-sensor with application to wastewater treatment. Comput. Chem. Eng. 71, 263–280. doi:10.1016/j.compchemeng.2014.08.008

Liu, Y., Guo, J., Wang, Q., Huang, D., 2016. Prediction of Filamentous Sludge Bulking using a State-based Gaussian Processes Regression Model. Sci. Rep. 6, 31303. doi:10.1038/srep31303

Liwarska-Bizukojc, E., Olejnik, D., Biernacki, R., Ledakowicz, S., 2011. Calibration of a complex activated sludge model for the full-scale wastewater treatment plant. Bioprocess Biosyst. Eng. 34, 659–670. doi:10.1007/s00449-011-0515-1

Lorenzo-Toja, Y., Vazquez-Rowe, I., Chenel, S., Marin-Navarro, D., Moreira, M.T., Feijoo, G., 2015. Eco-efficiency analysis of Spanish WWTPs using the LCA+DEA method. Water Res. 68, 637–650. doi:10.1016/j.watres.2014.10.040

Lorenzo-Toja, Y., Alfonsín, C., Amores, M.J., Aldea, X., Marin, D., Moreira, M.T., Feijoo, G., 2016. Beyond the conventional life cycle inventory in wastewater treatment plants. Sci. Total Environ. 553, 71–82. doi:10.1016/j.scitotenv.2016.02.073

Ma, J., Wang, Z., Yang, Y., Mei, X., Wu, Z., 2013. Correlating microbial community structure and composition with aeration intensity in submerged membrane bioreactors by 454 high-throughput pyrosequencing. Water Res. 47, 859–869. doi:10.1016/j.watres.2012.11.013

Ma, Q., Qu, Y., Shen, W., Zhang, Z., Wang, J., Liu, Z., Li, D., Li, H., Zhou, J., 2015. Bacterial community compositions of coking wastewater treatment plants in steel industry revealed by Illumina high-throughput sequencing. Bioresour. Technol. 179, 436–443. doi:10.1016/j.biortech.2014.12.041

Machado, V.C., Gabriel, D., Lafuente, J., Baeza, J.A., 2009. Cost and effluent quality controllers design based on the relative gain array for a nutrient removal WWTP. Water Res. 43, 5129–5141. doi:10.1016/j.watres.2009.08.011

Maciejowski, J.M., 2002. Predictive Control with Constraints. Technology & Engineering, Pearson Education.

Manamperuma, L., Wei, L., Ratnaweera, H., 2017. Multi-parameter based coagulant dosing control. Water Sci. Technol. 75, 2157–2162. doi:org/10.2166/wst.2017.058

Mannina, G., Cosenza, A., Vanrolleghem, P.A., Viviani, G., 2011a. A practical protocol for calibration of nutrient removal wastewater treatment models. J. Hydroinformatics 13, 575. doi:10.2166/hydro.2011.041

Mannina, G., Trapani, D. Di, Viviani, G., Ødegaard, H., 2011b. Modelling and dynamic simulation of hybrid moving bed biofilm reactors: Model concepts and application to a pilot plant. Biochem. Eng. J. 56, 23–36. doi:10.1016/j.bej.2011.04.013

Martin, C., Vanrolleghem, P.A., 2014. Analysing, completing, and generating influent data for WWTP modelling: A critical review. Environ. Model. Softw. 60, 188–201. doi:10.1016/j.envsoft.2014.05.008

Martín de la Vega, P.T., Martínez de Salazar, E., Jaramillo, M. a, Cros, J., 2012. New contributions to the ORP & DO time profile characterization to improve biological nutrient removal. Bioresour. Technol. 114, 160–7. doi:10.1016/j.biortech.2012.03.039

Matar, G.K., Bagchi, S., Zhang, K., Oerther, D.B., Saikaly, P.E., 2017. Membrane biofilm communities in full-scale membrane bioreactors are not randomly assembled and consist of a core microbiome. Water Res. 123, 124–133. doi:10.1016/j.watres.2017.06.052

Meneses, M., Concepción, H., Vrecko, D., Vilanova, R., 2015. Life Cycle Assessment as an

environmental evaluation tool for control strategies in wastewater treatment plants. J. Clean. Prod. 107, 653–661. doi:10.1016/j.jclepro.2015.05.057

Merriam, E.R., Petty, J.T., Strager, M.P., Maxwell, A.E., Ziemkiewicz, P.F., 2015. Complex contaminant mixtures in multistressor Appalachian riverscapes. Environ. Toxicol. Chem. 34, 2603–2610. doi:10.1002/etc.3101

Mevik, B.H., Wehrens, R., 2007. The pls package: Principal component and partial least squares regression in R. J. Stat. Softw. 18, 1–23. doi:10.1159/000323281

Milborrow, S., 2018. Earth: Multivariate Adaptive Regression Splines (Derived from mda:mars by Trevor Hastie and Rob Tibshirani. Uses Alan Miller's Fortran utilities with Thomas Lumley's leaps wrapper). Version 4.6.1, R Package. [online] https://cran.r-project.org/package=earth.

Moghadas, S., Gustafsson, a-M., Muthanna, T.M., Marsalek, J., Viklander, M., 2015. Review of models and procedures for modelling urban snowmelt. Urban Water J. 9006, 1–16. doi:10.1080/1573062X.2014.993996

Morgan-Sagastume, J., Jiménez, B., Noyola, A., 1994. Anaerobic-anoxic-aerobic process with recycling and separated biomass for organic carbon and nitrogen removal from wastewater. Environ. Technol. 15, 233–243. doi:10.1080/09593339409385424

Mulas, M., Tronci, S., Corona, F., Haimi, H., Lindell, P., Heinonen, M., Vahala, R., Baratti, R., 2015. Predictive control of an activated sludge process: An application tothe Viikinmäki wastewater treatment plant. J. Process Control 35, 89–100. doi:10.1016/j.jprocont.2015.08.005

Namkung, E., Rittmann, B.E., 1986. Soluble microbial products (SMP) formation kinetics by biofilms. Water Res. 20, 795–806. doi:https://doi.org/10.1016/0043-1354(86)90106-5

Nocairi, H., Qannari, E.M., Vigneau, E., Bertrand, D., 2005. Discrimination on latent components with respect to patterns. Application to multicollinear data. Comput. Stat. Data Anal. 48, 139–147. doi:10.1016/j.csda.2003.09.008

Noiva, K., Fernández, J.E., Wescoat, J.L., 2016. Cluster Analysis of Urban Water Supply and Demand: Toward Large-Scale Comparative Sustainability Planning. Sustain. Cities Soc. doi:10.1016/j.scs.2016.06.003

O'Brien, M., Mack, J., Lennox, B., Lovett, D., Wall, A., 2011. Model predictive control of an activated sludge process: A case study. Control Eng. Pract. 19, 54–61. doi:10.1016/j.conengprac.2010.09.001

Ochoa, J.C., Colprim, J., Palacios, B., Paul, E., Chatellier, P., 2002. Active heterotrophic and autotrophic biomass distribution between fixed and suspended systems in a hybrid biological reactor. Water Sci. Technol. 46, 397–404.

Okabe, S., Hirata, K., Watanabe, Y., 1995. Dynamic changes in spatial microbial distribution in mixed-population biofilms: experimental results and model simulation. Water Sci. Technol. 32, 67–74.

Olsson, G., 2012. ICA and me--a subjective review. Water Res. 46, 1585–624.

doi:10.1016/j.watres.2011.12.054

Olsson, G., 2002. Lessons learnt at ICA2001. Water Sci. Technol. 45, 1–8.

Olsson, G., Carlsson, B., Comas, J., Copp, J., Gernaey, K. V, Ingildsen, P., Jeppsson, U., Kim, C., Rieger, L., Rodríguez-Roda, I., Steyer, J.-P., Takács, I., Vanrolleghem, P. a, Vargas, A., Yuan, Z., Åmand, L., 2014. Instrumentation, control and automation in wastewater - from London 1973 to Narbonne 2013. Water Sci. Technol. 69, 1373–1385. doi:10.2166/wst.2014.057

Olsson, G., Newell, B., 1999. Wastewater Treatment Systems: Modelling, Diagnosis and Control. IWA Publishing, London, UK.

Ontiveros, G.A., Campanella, E.A., 2013. Environmental performance of biological nutrient removal processes from a life cycle perspective. Bioresour. Technol. 150, 506–512. doi:10.1016/j.biortech.2013.08.059

Plattes, M., Henry, E., Schosseler, P.M., 2008. A zero-dimensional biofilm model for dynamic simulation of moving bed bioreactor systems: Model concepts, Peterson matrix, and application to a pilot-scale plant. Biochem. Eng. J. 40, 392–398. doi:10.1016/j.bej.2008.01.011

Plósz, B.G., Liltved, H., Ratnaweera, H., 2009. Climate change impacts on activated sludge wastewater treatment: a case study from Norway. Water Sci. Technol. 60, 533–541. doi:10.2166/wst.2009.386

Qiu, Y., Liu, Y., Huang, D., 2016. Date-Driven Soft-Sensor Design for Biological Wastewater Treatment Using Deep Neural Networks and Genetic Algorithms. J. Chem. Eng. Japan 49, 925–936. doi:10.1252/jcej.16we016

Quan, X., Gu, L., Qian, Y., Pei, Y., Yang, Z., 2013. Characterization of nitrification performance and microbial community in a MBBR and integrated GBBR-MBBR treating heavily polluted river water. Environ. Eng. Manag. J. 12, 1335–1344.

Rahman, S.M., Eckelman, M.J., Onnis-Hayden, A., Gu, A.Z., 2016. Life-Cycle Assessment of Advanced Nutrient Removal Technologies for Wastewater Treatment. Environ. Sci. Technol. 50, 3020–3030. doi:10.1021/acs.est.5b05070

Ratnaweera, H., Fettig, J., 2015. State of the art of online monitoring and control of the coagulation process. Water (Switzerland) 7, 6574–6597. doi:10.3390/w7116574

Rieger, L., Jones, R.M., Dold, P.L., Bott, C.B., 2014. Ammonia-Based Feedforward and Feedback Aeration Control in Activated Sludge Processes. Water Environ. Res. 86, 63–73. doi:10.2175/106143013X13596524516987

Rieger, L., Olsson, G., 2012. Why Many Control Systems Fail. J. Water Environ. Technol. 24, 42–45. doi:10.2175/193864711802764779

Rieger, L., Thomann, M., Gujer, W., Siegrist, H., 2005a. Quantifying the uncertainty of on-line sensors at WWTPs during field operation. Water Res. 39, 5162–5174. doi:10.1016/j.watres.2005.09.040

Rieger, L., Thomann, M., Gujer, W., Siegrist, H., 2005b. Quantifying the uncertainty of on-line

sensors at WWTPs during field operation. Water Res. 39, 5162–5174. doi:10.1016/j.watres.2005.09.040

Ruano, M.V., Ribes, J., Seco, A., Ferrer, J., 2012. An advanced control strategy for biological nutrient removal in continuous systems based on pH and ORP sensors. Chem. Eng. J. 183, 212–221. doi:10.1016/j.cej.2011.12.064

Ruano, M. V., Ribes, J., Seco, A., Ferrer, J., 2009. Low cost-sensors as a real alternative to on-line nitrogen analysers in continuous systems. Water Sci. Technol. 60, 3261–3268. doi:10.2166/wst.2009.607

Rusten, B., Hem, L.J., Ødegaard, H., 1995. Nitrogen removal from dilute wastewater in cold climate using moving-bed biofilm reactors. Water Environ. Res. 67, 65–74. doi:10.2175/106143095X131204

Samuelsson, O., Björk, A., Zambrano, J., Carlsson, B., 2017. Gaussian process regression for monitoring and fault detection of wastewater treatment processes. Water Sci. Technol. 75, 2952–2963. doi:10.2166/wst.2017.162

Schuler, A.J., Jang, H., 2007. Causes of Variable Biomass Density and Its Effects on Settleability in Full-Scale Biological Wastewater Treatment Systems. Environ. Sci. Technol. 41, 1675–1681. doi:10.1021/es0616074

Schuler, A.J., Jassby, D., 2007. Filament content threshold for activated sludge bulking: Artifact or reality? Water Res. 41, 4349–4356. doi:10.1016/j.watres.2007.06.021

Seshan, H., Goyal, M.K., Falk, M.W., Wuertz, S., 2014. Support vector regression model of wastewater bioreactor performance using microbial community diversity indices: Effect of stress and bioaugmentation. Water Res. 53, 282–296. doi:10.1016/j.watres.2014.01.015

Siegrist, H., Reithaar, S., Koch, G., Lais, P., 1998. Nitrogen loss in a nitrifying rotating contactor treating ammonium-rich wastewater without organic carbon. Water Sci. Technol. doi:10.1016/S0273-1223(98)00698-2

Singh, K.P., Malik, A., Mohan, D., Sinha, S., Singh, V.K., 2005. Chemometric data analysis of pollutants in wastewater - A case study. Anal. Chim. Acta 532, 15–25. doi:10.1016/j.aca.2004.10.043

Smets, I.Y., Banadda, E.N., Deurinck, J., Renders, N., Jenné, R., Van Impe, J.F., 2006. Dynamic modeling of filamentous bulking in lab-scale activated sludge processes. J. Process Control 16, 313–319. doi:10.1016/j.jprocont.2005.06.011

Solon, K., Flores-Alsina, X., Mbamba, C.K., Ikumi, D., Tait, S., Volcke, E.I.P., Brouckaert, C.J., Ekama, G., Vanrolleghem, P., Batstone, D.J., Gernaey, K.V., Jeppsson., U., 2016. Plant-wide modelling of phosphorus transformations in wastewater treatment systems: Effect of control and operational strategies. Water Res. 113, 97–110. doi:10.1016/j.watres.2017.02.007

Stare, A., Vrecko, D., Hvala, N., Strmcnik, S., 2007. Comparison of control strategies for nitrogen removal in an activated sludge process in terms of operating costs: A simulation study. Water Res. 41, 2004–2014. doi:10.1016/j.watres.2007.01.029

Steyer, J.P., Bernard, O., Batstone, D.J., Angelidaki, I., 2006. Lessons learnt from 15 years of ICA

in anaerobic digesters. Water Sci. Technol. 53, 25–33. doi:10.2166/wst.2006.107

Stinson, B., Murthy, S., Bott, C., Wett, B., Al-Omari, A., Bowden, G., Mokhyerie, Y., De Clippeleir, H., 2013. Roadmap Toward Energy Neutrality & Chemical Optimization at Enhanced Nutrient Removal Facilities, in: Proceedings of the WEF/IWA Conference: Nutrient Removal and Resource Recovery. Vancouver, pp. 702–731. doi:https://doi.org/10.2175/193864713813525888

Sweetapple, C., Fu, G., Butler, D., 2014. Multi-objective optimisation of wastewater treatment plant control to reduce greenhouse gas emissions. Water Res. 55, 52–62. doi:10.1016/j.watres.2014.02.018

Sötemann, S.W., Vermande, S., Wentzel, M.C., Ekama, G.A., 2002. Comparison of the Performance of an External Nitrification Biological Nutrient Removal Activated Sludge System With a Uct Biological Nutrient Removal Activated Sludge System. Water SA Spec. Ed. WISA Proc. 105–113.

Tao, E.P., Shen, W.H., Liu, T.L., Chen, X.Q., 2013. Fault diagnosis based on PCA for sensors of laboratorial wastewater treatment process. Chemom. Intell. Lab. Syst. 128, 49–55. doi:10.1016/j.chemolab.2013.07.012

Tchobanoglous, G., Burton, F.L., Stensel, H.D., 2003. Wastewater Engineering: Treatment and Reuse. Metcalf & Eddy, Inc., McGraw-Hill Education.

Toifl, M., Diaper, C., O'Halloran, R., 2010. Review of process and performance monitoring techniques applicable to large and small scale wastewater recycling systems. CRIRO: Water for a Healthy Country National Research Flagship.

Vanrolleghem, P.A., Spanjers, H., Petersen, B., Ginestet, P., Takacs, I., 1999. Estimating (combinations of) Activated Sludge Model No. 1 parameters and components by respirometry. Water Sci. Technol. 39, 195–214. doi:10.1016/S0273-1223(98)00786-0

Villez, K., Srinivasan, B., Rengaswamy, R., Narasimhan, S., Venkatasubramanian, V., 2011. Kalman-based strategies for Fault Detection and Identification (FDI): Extensions and critical evaluation for a buffer tank system. Comput. Chem. Eng. 35, 806–816. doi:10.1016/j.compchemeng.2011.01.045

Vrečko, D., Hvala, N., Stražar, M., 2011. The application of model predictive control of ammonia nitrogen in an activated sludge process. Water Sci. Technol. 64, 1115–1121.

Wagner, D.S., Ramin, E., Szabo, P., Dechesne, A., Pl??sz, B.G., 2015. Microthrix parvicella abundance associates with activated sludge settling velocity and rheology - Quantifying and modelling filamentous bulking. Water Res. 78, 121–132. doi:10.1016/j.watres.2015.04.003

Wanner, O., Gujer, W., 1984. Competition in biofilms. Water Sci. Technol. 17, 27–44.

Wilen, B.M., Lumley, D., Mattsson, A., Mino, T., 2006. Rain events and their effect on effluent quality studied at a full scale activated sludge treatment plant. Water Sci. Technol. 54, 201–208. doi:10.2166/wst.2006.721

Won, S.G., Ra, C.S., 2011. Biological nitrogen removal with a real-time control strategy using moving slope changes of pH(mV)- and ORP-time profiles. Water Res. 45, 171–178.

doi:10.1016/j.watres.2010.08.030

Xiao, F., Halbach, T.R., Simcik, M.F., Gulliver, J.S., 2012. Input characterization of perfluoroalkyl substances in wastewater treatment plants: Source discrimination by exploratory data analysis. Water Res. 46, 3101–3109. doi:10.1016/j.watres.2012.03.027

Xing, W., Wang, W., Shao, Q., Yong, B., 2018. Identification of dominant interactions between climatic seasonality, catchment characteristics and agricultural activities on Budyko-type equation parameter estimation. J. Hydrol. 556, 585–599. doi:10.1016/j.jhydrol.2017.11.048

Xiong, W., Li, Y., Zhao, Y., Huang, B., 2017. Adaptive soft sensor based on time difference Gaussian process regression with local time-delay reconstruction. Chem. Eng. Res. Des. 117, 670–680. doi:10.1016/j.cherd.2016.11.020

Xu, D., Liu, S., Chen, Q., Ni, J., 2017. Microbial community compositions in different functional zones of Carrousel oxidation ditch system for domestic wastewater treatment. AMB Express 7, 40. doi:10.1186/s13568-017-0336-y

Ye, F., Ye, Y., Li, Y., 2011. Effect of C/N ratio on extracellular polymeric substances (EPS) and physicochemical properties of activated sludge flocs. J. Hazard. Mater. 188, 37–43. doi:10.1016/j.jhazmat.2011.01.043

Ye, L., Shao, M.F., Zhang, T., Tong, A.H.Y., Lok, S., 2011. Analysis of the bacterial community in a laboratory-scale nitrification reactor and a wastewater treatment plant by 454-pyrosequencing. Water Res. 45, 4390–4398. doi:10.1016/j.watres.2011.05.028

Zeng, W., Peng, Y., Wang, S., Peng, C., 2008. Process control of an alternating aerobic-anoxic sequencing batch reactor for nitrogen removal via nitrite. Chem. Eng. Technol. 31, 582–587. doi:10.1002/ceat.200700468

Ødegaard, 1994. A new moving bed biofilm reactor - application and results. Water Sci. Technol. 29, 157–165.

Ødegaard, H., 2016. A road-map for energy-neutral wastewater treatment plants of the future based on compact technologies (including MBBR). Front. Environ. Sci. Eng. 10, 2. doi:10.1007/s11783-016-0835-0

Ødegaard, H., 2006. Innovations in wastewater treatment: The moving bed biofilm process. Water Sci. Technol. 53, 17–33. doi:10.2166/wst.2006.284

Østgaard, K., Christensson, M., Lie, E., Jönsson, K., Welander, T., 1997. Anoxic biological phosphorus removal in a full-scale UCT process. Water Res. 31, 2719–2726. doi:10.1016/S0043-1354(97)00125-5

Åmand, L., Carlsson, B., 2012. Optimal aeration control in a nitrifying activated sludge process. Water Res. 46, 2101–2110. doi:10.1016/j.watres.2012.01.023

Åmand, L., Olsson, G., Carlsson, B., 2013. Aeration control - A review. Water Sci. Technol. 67, 2374–2398. doi:10.2166/wst.2013.139

Åström, K.J., Hägglund, T., 1995. PID controllers: theory, design and tuning, Instrument Society of America. Research Triangle Park, NC, USA. doi:1556175167

Appended Papers

Paper I

Wang, X., Kvaal, K., Ratnaweera, H., 2017. Characterization of influent wastewater with periodic variation and snow melting effect in cold climate area. Computers & Chemical Engineering. 106, 202–211. doi:10.1016/j.compchemeng.2017.06.009

Computers and Chemical Engineering 106 (2017) 202–211

Contents lists available at ScienceDirect

Computers and Chemical Engineering

journal homepage: www.elsevier.com/locate/compchemeng

Characterization of influent wastewater with periodic variation and snow melting effect in cold climate area

Xiaodong Wang*, Knut Kvaal, Harsha Ratnaweera

Faculty of Science and Technology, Norwegian University of Life Sciences, P.O. Box 5003-IMT, 1432 Aas, Norway

ARTICLE INFO

Article history:
Received 6 December 2016
Received in revised form 27 May 2017
Accepted 6 June 2017
Available online 9 June 2017

Keywords:
Climate
Cluster analysis
Discriminant analysis
Principal component analysis
Snow melting
Wastewater characteristics

ABSTRACT

The daily, weekly and seasonal variation of influent characteristics of wastewater treatment plants (WWTPs) highly affects the performance of wastewater treatment. In cold climate area, snow melting happens frequently in cold season and affects wastewater characteristics significantly. The dilution effect of snow melting in cold season makes it impossible to compare cold season influent and warm season influent fairly. To enable the study of influent seasonal variation, a stepwise approach was developed to determine whether the WWTP influent wastewater contains snowmelt (wet climate) or not (dry climate). This study investigated the daily, weekly and seasonal variation of WWTP influent, and provided evidence of climate effect on influent characteristics by analyzing the correlation of climatic information and wastewater characteristics. A classification model was developed to further discriminate climate conditions of influent, which will be applied to develop scenario-based soft sensor as well as support WWTP surveillance and control.

1. Introduction

The majority of existing sewer systems in European countries are combined sewer systems (Ashley et al., 2008). In spite of the continual improvement of wastewater treatment technology, combined sewer overflow brings increasingly environmental problems for both storm water management and wastewater treatment (Weyand, 2002). In the winter of some European countries, snowmelt increases the inlet flow of wastewater treatment plants (WWTPs) dramatically and the wastewater temperature may be decreased to 4 °C (Plósz et al., 2009). The European Council Directive 91/271/EEC has defined a threshold of 12 °Cthat 70% nitrogen should be removed by WWTPs. However, in cold climate area, when the combined effect of increasing influent flow and lower temperature caused by snow melting exceeds the treatment capacity, a part of the incoming wastewater bypasses the treatment process and the wastewater was discharged to natural environment without sufficient treatment (Haimi et al., 2009). As results of cold and dilution effect caused by snow melting, the nutrient removal efficiency was observed to be reduced obviously (Bixio et al., 2001).

As is suggested by Hwang and Oleszkiewicz (Hwang and Oleszkiewicz, 2007), special precautions are required in case of sudden snow melting when operating biological wastewater treatment. However, unlike rainfall event, it is difficult to detect when the snow melting starts or stops in the winter of cold climate countries. Snow melting is more likely to happen when the daily temperature is above −1.5 °C (Plósz et al., 2009), but combined sewer systems may receive varying amount of snowmelt from hour to hour within the same day. The wastewater quality and quantity in combined sewer systems are combined effects of human activities and climate conditions. As a result, the influent wastewater quality and quantity to full-scale wastewater treatment plants (WWTPs) are varying hourly, daily, weekly and seasonally (Butler, 1993; Tunçal et al., 2009). Since references related to urban snow melting modelling are rather limited (Moghadas et al., 2015), how climate and human activities interact to determine influent wastewater characteristics of WWTPs was seldom studied. The knowledge gap of this issue leads to passive control of wastewater treatment process, because the variation of wastewater characteristics is not predictable due to climate change and human activities.

Online monitoring and control enable WWTPs to manage the uncertainties caused by periodical variation and combined sewer overflow (Olsson, 2012). Soft sensors are reported as an promising tool to monitor hard-to-measure variables to achieve advanced control of WWTPs (Haimi et al., 2015; Liu et al., 2014). Previous study has developed soft sensors to predict chemical oxygen demand (COD) and total phosphorus (TP) of WWTP influent under dry climate condition (Wang et al., 2017), but the prediction accuracy will decrease when snowmelt appears in the influent. To enable advanced control as well as soft sensor monitoring of wastewater treatment process, it is necessary to characterize

* Corresponding author.
E-mail addresses: xiaodong.wang@nmbu.no, xiaodong.wang01@outlook.com (X. Wang).

http://dx.doi.org/10.1016/j.compchemeng.2017.06.009
0098-1354/

influent of WWTPs in both dry climate condition and wet climate condition. However, it is difficult to determine whether the wastewater contains snowmelt or not, because the domestic influent itself is varying from hour to hour. If the dry influent (without snowmelt) and wet influent (with snowmelt) of WWTP can be distinguished in advance by online measurement, scenario-based soft sensors could be developed to support real time control of WWTPs.

This study presents the daily, weekly and seasonal characteristics of influent wastewater of a WWTP in Norway, which provides a systematic study of influent characteristics in cold climate area. The purpose of statistical analysis was to develop an onsite decision-making technique that can continuously determine if the influent wastewater was collected in dry climate or wet climate. The ultimate goal was to provide influent characteristics of different seasons and climate to support WWTP surveillance and control. The terminology related to "season" and "climate" in this paper was defined in Table 1.

2. Materials and methods

2.1. Wastewater sampling

Data of influent wastewater characteristics of a Norwegian WWTP were collected in 2015 and 2016. As is shown in Table 2, the periods of observation included randomly selected days during warm season and cold season, including both workdays and weekends. An automatic sampler (Teledyne ISCO) was placed at the influent of the WWTP to collect and store wastewater samples hourly during the sampling period. In addition, online sensors were used to measure flow rate and water temperature. The WWTP was connected to the combined sewer system, which brought large amount of snow melting water during winter. The sampling period during cold season contains both dry climate, and wet climate samples. All the warm season samples were collected during dry climate period.

The two sampling periods cannot cover the total variation of wastewater characteristics, because unusual climate events happen occasionally and they are different in each year. However, we intended to provide a stepwise methodology to determine whether the influent was generated in dry or wet climate, and build a classifier to further support scenario-based soft sensors development. The sample quantity was sufficient to serve for model calibration and validation.

2.2. Analysis of wastewater samples

Wastewater chemical characteristics: total suspended solids (TSS), total phosphorus (TP), *ortho*-phosphate (PO_4-P), total nitrogen (TN), ammonia (NH_4-N), chemical oxygen demand (COD), soluble chemical oxygen demand (SCOD), and pH were measured according to standard methods (ApH A et al., 2012). Temperature (WaterTemp) and influent flow were monitored by online instruments.

2.3. Climate data

To study the impact of climate change on wastewater characteristics, we collected climate data from Norwegian weather website www.yr.no, which provided temperature, snow depth and wind speed data. Storm event did not happened during sampling days, but snowing and snow melting took place in the cold season. Solar radiation should be considered as one of the contributor of snow melting. Therefore, global radiation data were collected from Norwegian Institute of Bio-economy Research (NIBIO, 2016) to analyze the relation between snow melting and solar radiation.

2.4. Statistical analysis

In this context, "Climate" is a category variable with two entries, Dry and Wet. It is difficult to decide whether the influent was generated in Dry climate or Wet climate by measurement or physical feeling, because snow melting was happening quietly and invisibly. The climate category of influent can be determined bas generated in Dry climate or Wet climate by measurement or physical feeling, because snow melting was happening quietly and invisibly. The climate category of influent can be determined by its multiple features, such as flow rate, COD and water temperature. To assign the climate category to the influent, we applied principal component analysis and cluster analysis to separate the cold season dataset into two subsets, which are latterly confirmed as Dry climate influent and Wet climate influent.

Wastewater chemical constituents and inlet flow rate usually propagate with the similar trend and correlated with each other (Avella et al., 2011). Principal component analysis (PCA) is a multivariate analytical method used for detecting data collinearity and summarize patterns of covariance among variables. The mathematical procedure of PCA has been well explained and used for fault diagnosing of wastewater treatment process monitoring (Tao et al., 2013). In this study, the principal components derived from PCA describe the dominant variation of the wastewater characteristics for further analysis. The original dataset was divided into 24 segments to perform cross-validation to validate the PCA model.

Samples collected during wet climate were diluted by snow melting, but others were collected during freezing hours without any snowmelt. In this study, hierarchical cluster analysis was applied to divide the data into separated groups based on the wastewater characteristics. Ward's method with Euclidean distance was used to perform the cluster analysis (Singh et al., 2005; Merriam et al., 2015). However, as Xiao (Xiao et al., 2012) mentioned, the limitation of cluster analysis is that it can give a result no matter what kinds of input are used. It is therefore important to pre-assess the input data before clustering. Thus, we used scores of most significant principal components as input data for clustering, which screened out disturbances of the raw dataset.

In the circumstance of cold season, there are only two climate categories: Dry climate influent and Wet climate influent. The results of cluster analysis would be well acceptable, if the two clusters given by cluster analysis featured as larger amount of diluted influent (Wet climate) and normal amount of higher concentration influent (Dry climate). After evaluation of the results of cluster analysis, the two clusters was accept as Dry climate and Wet climate, and the category variable "Climate" was formed accordingly. Thus, the Dry climate wastewater characteristics in cold season can be found out and compared with that in warm season. Analysis of variance (ANOVA) was performed to study the seasonal variation of Dry climate influent.

To support online monitoring and control of wastewater treatment process, it is necessary to establish a classification function, which will continuously assign climate categories to new influent data onsite in cold season. In this study, we applied partial least squares discriminant analysis (PLS-DA) to build a classifier based on historical data and the category variable – Climate. Partial least squares (PLS) is an methodology that can be used for both regression (PLSR) and discriminant analysis (PLS-DA). The category variable Climate with "Dry" and "Wet" entries were converted to a dummy matrix with entries as "0" and "1", while the wastewater characteristics data formed another matrix – the X matrix. PLS-DA algorithm maximizes the covariance of these two matrixes and extracts dominant eigenvectors of covariance matrix (Barker and Rayens, 2003; Nocairi et al., 2005). The final classification was performed based on the scores of PLS-DA, which are computed from dominant eigenvectors and original values of wastewater

Table 1
Description of the terminologies used in this study.

Terminology	Description
Warm season	The period within a year when and the influent wastewater temperature is above 12 °C.
Cold season	The period within a year when and the influent wastewater temperature is lower than 12 °C.
Dry climate	The period when there is neither rainfall nor snowmelt in WWTP influent.
Wet climate	The period when the WWTP influent is diluted by rainfall or snowmelt.
Cold dry period	The period when there is no snowmelt in the influent during cold season
Cold wet period	The period when the WWTP influent is diluted by snowmelt during cold season.
Warm dry period	The period when there is no rain water in the WWTP influent during warm season.
Warm wet period	The period when WWTP influent is diluted by rain water. Not applicable in this study.

Table 2
The periods of observation and the number of samples.

Season	Observation period	Diluted by precipitation	Number of sampling days	Sample quantity
Warm	May 2015–June 2015	No dilution	5	120
Cold	January 2016–March 2016	Diluted by Snow melting	6	144

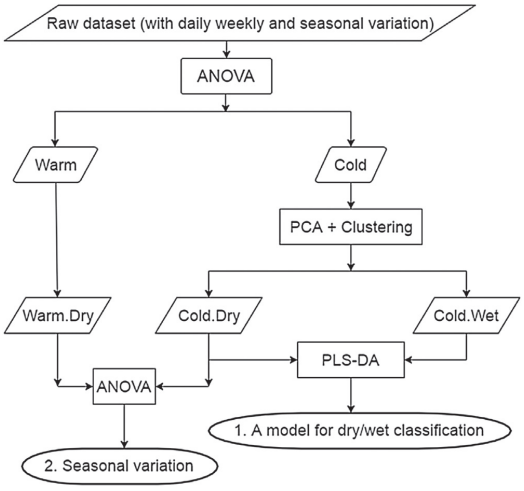

Fig. 1. The workflow to determine dry or wet climate condition of influent, and build a classifier based on predetermined knowledge. The seperation of dry and wet influent provides basis to compare the seasonal differences of wastewater chracteristics in dry climate.

characteristics. Nowadays, the PLS-DA methodology has been well developed and used in multiple fields (Indahl et al., 2007; Liland and Indahl, 2009).

We used Unscrambler® X version 10.4 (CAMO Software, 2016) to perform all the calculation of PCA, cluster analysis, and PLS-DA. Cross-validation with 24 segments were used to validate these models. Besides, correlation analysis, analysis of variance (ANOVA), and scatter matrix were performed in R program to study the seasonal, daily and hourly effects as well as climate effects. The workflow of this approach is shown in Fig. 1.

3. Results and discussion

3.1. Influent wastewater variation

The uncertainties of influent wastewater quality and quantity bring challenges to wastewater treatment process monitoring, modelling and control (Olsson, 2012). The uncertainties of influent wastewater characteristics include daily, weekly and seasonal variation. The daily, weekly and seasonal variation of influent wastewater quality and quantity of this WWTP are shown in Figs. 2–4, respectively.

Fig. 2a shows the time series data of flow rate, COD and soluble COD (SCOD) of the WWTP influent in warm season. The influent flow, COD and SCOD followed the same propagation pattern: started rising after 9:00 in the morning and reach the peak at around 13:00. After slightly decreasing in the afternoon, both wastewater quality and quantity increased to another smaller peak in the evening. The flow, COD and SCOD decreased sharply to a lower level after 23:00 until the next morning. Obviously, wastewater quantity and quality follows the same daily pattern. However, the peak hour observed in this WWTP appeared later than those on literatures (Almeida et al., 1999; Butler, 1993), which may be caused by different living habits in Scandinavian counties.

The cold season influent shows higher variability compared with warm season influent. As is shown in Fig. 2b, the fifth day presented highest COD and lowest flow among all the sampling days, while the sixth day has extreme high flow and relevant lower concentration due to snow melting. Due to the unpredictable snow melting effect, it is difficult to summarize the daily variation pattern in cold season. It is necessary to classify wet climate (with snowmelt) and dry climate (without snowmelt) influent for process control and soft sensor development.

Fig. 3 shows the comparison of wastewater on workdays and weekends. In terms of a significant level of 0.05, ANOVA test shown that flow rate, TSS and total phosphorus concentration were significantly higher on workdays than that on weekends, whereas the other parameters were not significantly different. Since orthophosphate concentration was almost equal on workdays as that on weekend, the higher total phosphorus was a consequence of higher suspended solids on workdays. Overall, the results suggest that workdays and weekends require different control strategies for wastewater treatment process, because the total mass loading of substances were different, especially the total suspended solids and total phosphorus.

The characteristics of the WWTP's influent in warm season and cold season are summarized in Fig. 4. Analysis of variance (ANOVA) was carried out to test if the differences of cold and warm season were significant. The flow rate in cold season was higher than that in warm season ($p < 0.05$), because snow melting generated large amount of wastewater flow into combined sewer systems (Wilen et al., 2006). As a result of dilution, significantly lower TSS, COD, SCOD, TP, and orthophosphate were observed in cold season ($p < 0.05$). In contrast, the differences of total nitrogen and ammonia are not significant at the significant level of 0.05 (p value equals 0.453 and 0.616, respectively), which indicate higher total nitrogen mass loading in cold seasons than that in warm seasons. Literature

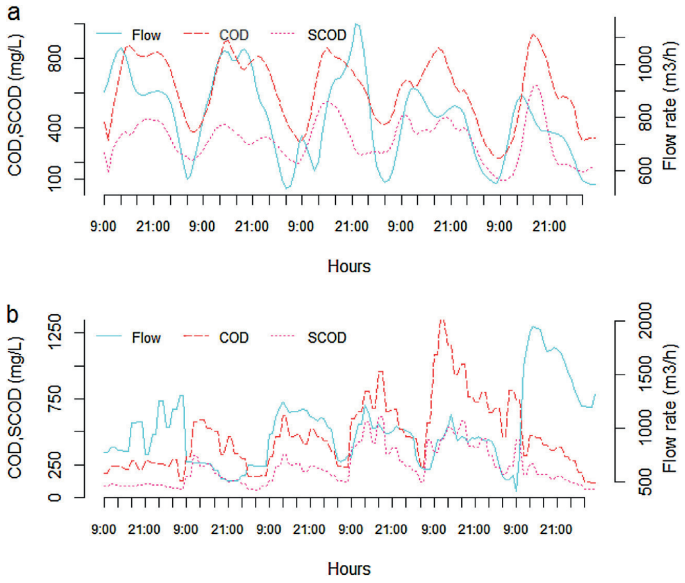

Fig. 2. The Influent wastewater flow, COD and SCOD of each hour during observation days: (a) five days observation in warm season and (b) six days observation in cold season.

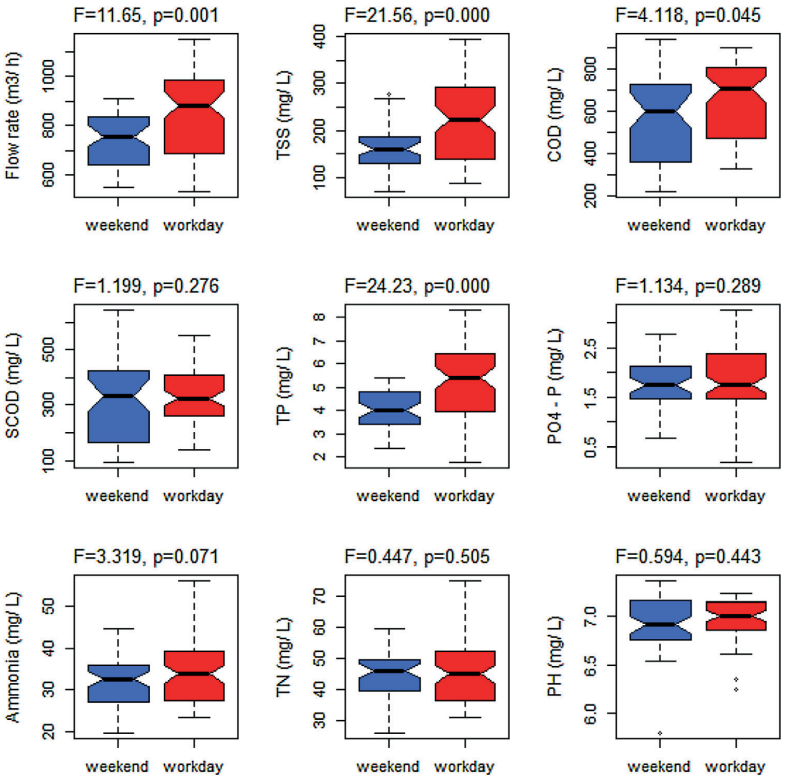

Fig. 3. Boxplot and ANOVA test of wastewater characteristics on workdays and weekends.

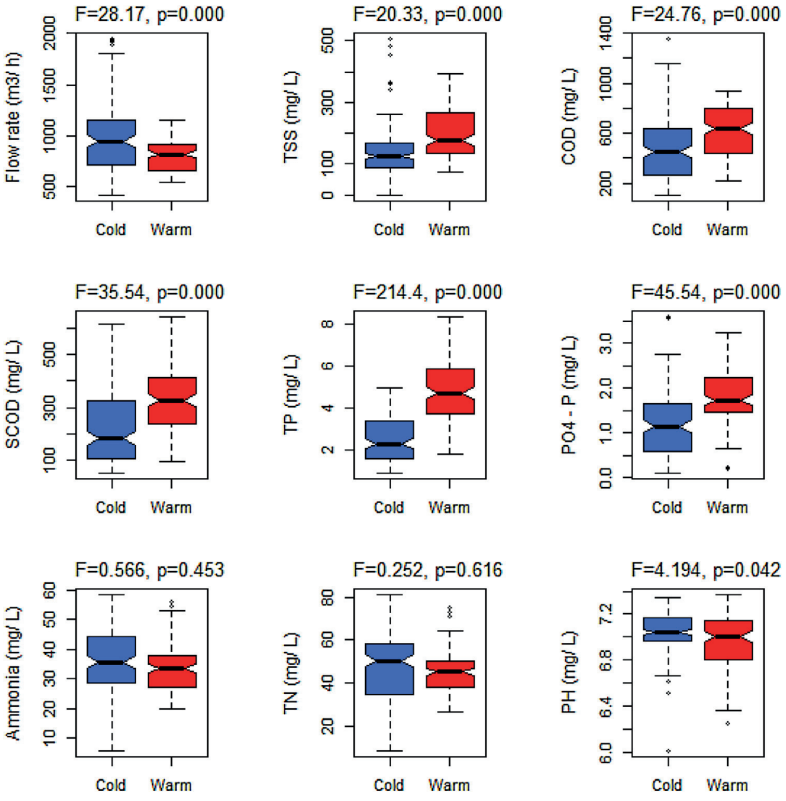

Fig. 4. Boxplot and ANOVA test of wastewater characteristics in warm season and cold season.

suggested that the surface runoff washed off amounts of nitrogen matters to streams (Bhat et al., 2007). Consequently, snow melting brought nitrogen from earth surface to the sewer system and leads to higher mass of nitrogen and ammonia to the WWTP.

Overall, there are significant differences of wastewater characteristics in warm season and cold season. However, the data of cold season contain both dry climate and wet climate (snow melting) periods, which increased the difficulty to draw conclusion of seasonal variation. To figure out the impacts of climate and human activity on wastewater composition, it is necessary to split the cold season dataset into dry climate subset and wet climate subset for further study.

3.2. Separation of dry and wet climate influent in cold season

Wet climate in this study represented snow melting periods in cold season. Rainfall events can be easily perceived either by weather forecast or physical feeling, but snow melting in cold climate area is unpredictable and the efforts on urban snowmelt modelling are rather limited (Moghadas et al., 2015). In spite of this, we developed a stepwise approach to distinguish influent with snowmelt water from dry climate wastewater using principal component analysis (PCA) and cluster analysis

PCA was carried out on the data of cold season (9 variables, 144 observations), and the results are shown in Fig. 5. Two principal components (PCs) explained 96% of the total variance of the dataset (Fig. 5a), which indicated high collinearity of the original variables. Fig. 5b further explained the loading of original variables on the plane of first principal component (PC-1) and second principal component (PC-2). Flow, COD, SCOD and TSS are the most significant variables that determined the variation of PC-1 and PC-2. Furthermore, higher PC-1 values represent higher flow rates and lower chemical composition. PC-2 is a component standing for chemical composition. Higher PC-2 scores indicate higher COD, SCOD and TSS. PCA reduced the dimension of the nine-variable dataset into two PCs, since the first two components retained 96% of the total variance (55% for PC-1 and 41% for PC-2).

The cross-validated scores of all the observations were plotted on the plane formed by PC-1 and PC-2, as is shown in Fig. 5c. Wet climate influent should have higher PC-1 scores and lower PC-2 scores. On the contrary, more concentrated dry climate wastewater scored higher on PC-2 and lower on PC-1. The group of observations in the blue circle of Fig. 5c have higher PC-1 scores, while the green circle group scored lower PC-1 values. More observations in green circle have higher PC-2 scores than that in blue circle indicating that influent related to lower flow were more likely being high concentrated. The PCA results provide a preliminary classification of dry/wet climate wastewater. However, there are a few observations scored lower in both PC-1 and PC-2, which requires more PCs to interpret. Nevertheless, PC-1 and PC-2 represented 96% of the total variance, which is sufficient to be applied in this case.

Followed by PCA, we used the scores of PC-1 and PC-2 as input information for cluster analysis. PCA scores rather than original values of wastewater characteristics were used due to that we want to screen out noise of the raw data and use the dominant differences of wet and dry climate. Hierarchical cluster analysis was carried out

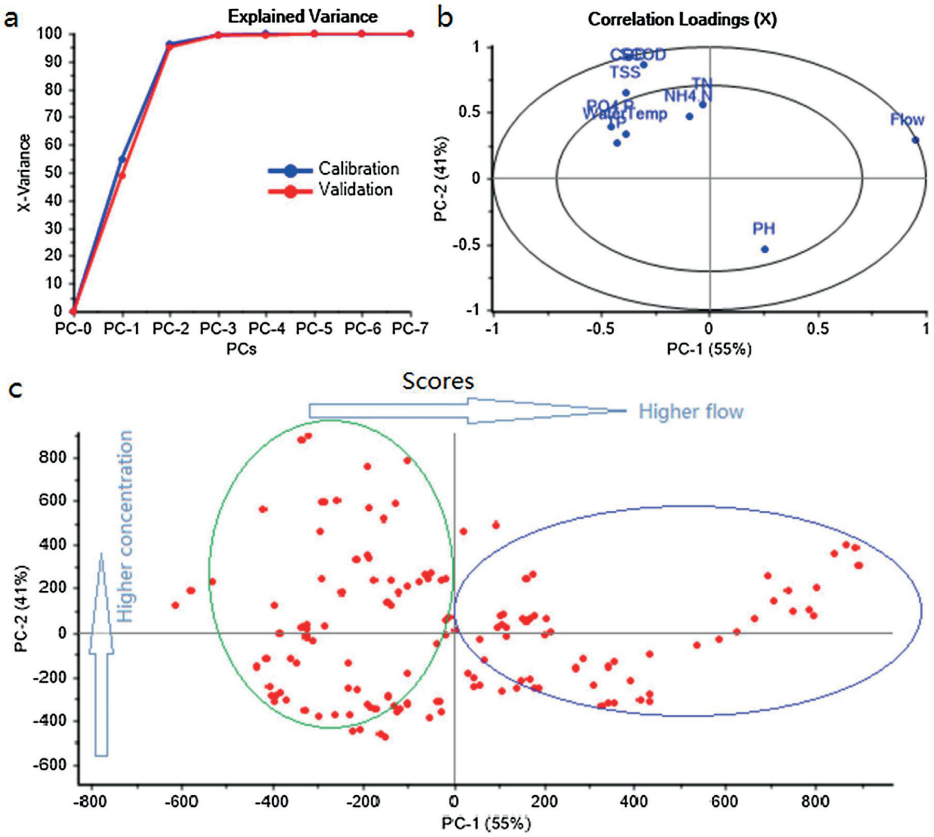

Fig. 5. Principal component analysis of wastewater characteristics in cold season. (a) The proportion of explained variance by principal components. The blue and red curve represent model calibration results and cross validation results. (b) Correlation loading plot of wastewater characteristic variables on the plane formed by PC-1 and PC-2. (c) Cross validated scores of all the observations in cold season. (For interpretation of the references to colour in this figure legend, the reader is referred to the web version of this article.)

to separate observations into different groups. By applying Ward's method and the Euclidean distance as a factor of dissimilarity, the influent was divided into two major groups (Fig. 6). The dendrogram presented in Fig. 6 is the visual result of clustering, where the upper cluster (blue) has higher PC-1 values and lower PC-2 values, while the lower cluster (red) has lower PC-1 scores and higher PC-2 scores. In the hierarchical cluster analysis, the cold season influent can also be divided into four clusters in a relevant shorter Euclidean distance, as is shown in Fig. 6. The observations in these four clusters correspond to the scores in the four regions of Fig. 5c. That said, a few high PC-2–score influent observations merged with some lower PC-2–score observations as one cluster (blue in Fig. 6), due to their relatively higher PC-1 scores. While the negative PC-2 observations merged together with some positive PC-2–score observations and formed another cluster (red in Fig. 6), caused by their negative PC-1 scores. The result was reasonable because the influent flow in the night of dry climate (after 23:00) was much lower than daily average, and the COD and TSS concentration were still relative high at peak hours of wet climate, regardless of dilution by snowmelt.

We were expecting for two climate categories: Dry climate and Wet climate. The two clusters presented by cluster analysis represented normal domestic wastewater and diluted wastewater, which fulfilled the expected grouping strategy. Thus, a category variable "Climate" was built, and entries of this variable – "Dry" and "Wet" were assigned to each observation accordingly.

3.3. Seasonal wastewater characteristics in dry climate

When dry climate influent was find out from cold season, it is natural to study the differences between warm season wastewater and cold-dry wastewater characteristics. Because only dry climate data were observed in warm season, disturbance of climate has been eliminated. ANOVA test was performed to determine whether the seasonal differences are significant. As is shown in Fig. 8, the differences of flow rate, TSS, COD, ammonia, total nitrogen and pH are not significant ($p > 0.05$), indicating relative similar wastewater quality and quantity. However, total phosphorus and orthophosphate in warm season are significantly higher than that in cold-dry season at a significant level of 0.05. Norway applied strict regulation of phosphorus concentration for detergents. Phosphorus in laundry and dishwasher detergents is rather limited. However, other phosphorus sources such as shower gel, shampoo, and human waste lead to the seasonal variation of phosphorus in wastewater. Another interesting phenomenon is that the total COD concentration was not significantly different ($p > 0.05$), but soluble COD

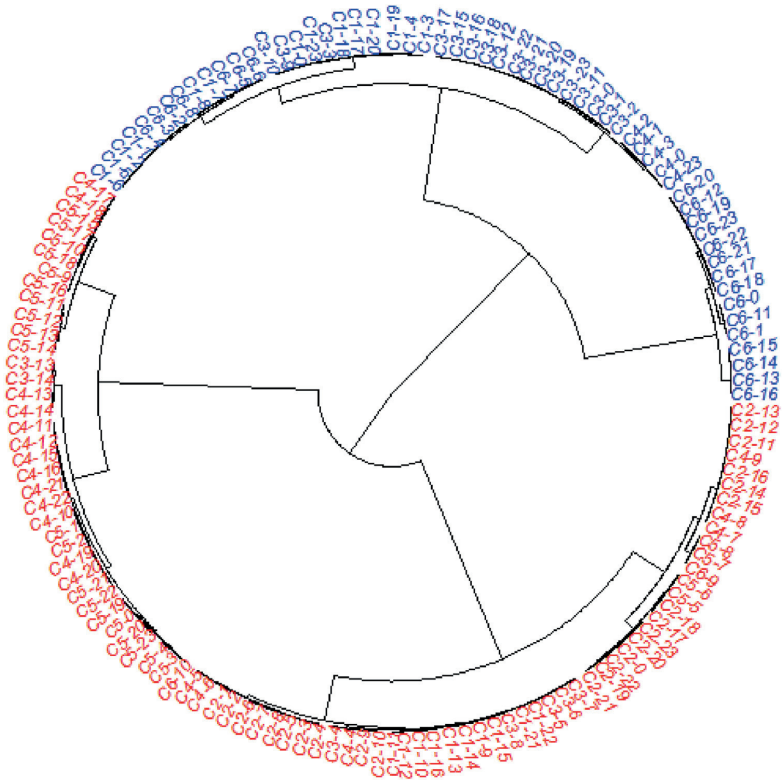

Fig. 6. Dendrogram of cluster analysis based on the scores of PCA. The names of observations such as "C1-1" represent Cold climate, sampling Day 1, at one o'clock. The wet climate observations are in blue color, and dry climate samples are in red. (For interpretation of the references to colour in this figure legend, the reader is referred to the web version of this article.)

(SCOD) was lower in cold-dry season than that in warm season ($p < 0.05$). Activated sludge model No. 2 (ASM2) shown that hydrolysis rate is an exponential function of temperature (Henze et al., 1994). The lower SCOD concentration in cold season may be caused by lower hydrolysis rate in cold season. However, Bixio et al. (2001) had observed higher soluble COD in cold season due to lower biodegrading rate, which contrasted the results of this work. The SCOD generation and consumption is a coupled effect of hydrolysis and biodegradation in sewer systems. The results and conclusion may differ if the hydraulic retention time, oxygen level are different. Therefore, further study is required to investigate the dominate mechanism of the hydrolysis and consumption of COD in sewer systems under different conditions.

3.4. Classifier development

For the sake of reducing operation cost and securing outlet quality, the aeration of biological treatment system and chemical dosing can be controlled according to climate condition and periodical influent variation (Martin and Vanrolleghem, 2014). Online monitoring of influent using soft sensor technology requires prejudgement of climate conditions (Vega et al., 2014). Therefore, it is essential to develop a classification model that is able to discriminate dry or wet climate influent continuously for future data. To make it easier to determine climate condition of influent in practice, partial least squares discriminant analysis (PLS-DA) was applied to develop a classification tool. As a supervised learning algorithm, PLS-DA requires a predefined category variable to train the classification model at the beginning. However, it is not straightforward to determine whether the climate condition for influent is dry or wet, because snow melting can hardly be detected by online equipment. Alternatively, the "Dry" and "Wet" labels of influent obtained from cluster analysis were applied to supervise classifier construction.

Table 3
Confusion matrix of PLS-DA. The correctly discriminated results are in the diagonal of upper-left to down-right.

Predicted\True	Dry	Wet
Dry	83	11
Wet	2	48
Accuracy	0.9097	

As is explained previously, the category variable of wet and dry climate was converted to a dummy matrix with only "0" and "1" as entries. Then we performed PLS-DA with the dummy matrix as response, and wastewater flow, temperature and chemical compositions used as input. Fig. 7 shows the cross-validated score plot of PLS-DA, which indicates that there was an obvious boundary between wet climate and dry climate wastewater. Furthermore, the confusion matrix of validated PLS-DA results (Table 3) indicates that 83 of 85 dry climate observations were correctly classified, and 48 of 59 wet climate observations were correctly classified. The classification accuracy of PLS-DA was 91%, which is sufficient high to use

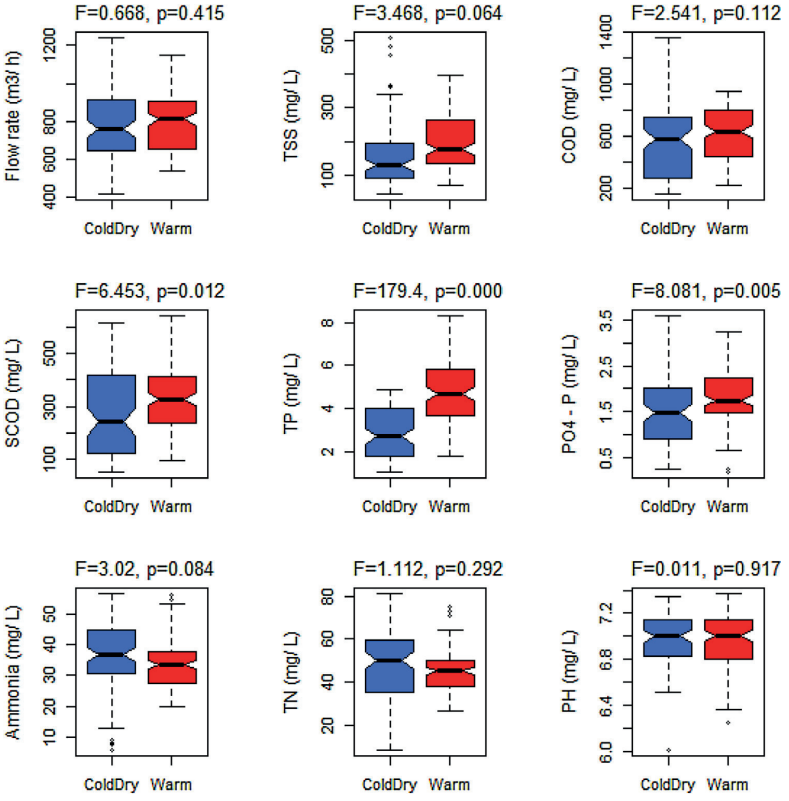

Fig. 7. Boxplot and ANOVA test of dry climate wastewater characteristics (no rain event or snow melting) in warm and cold season.

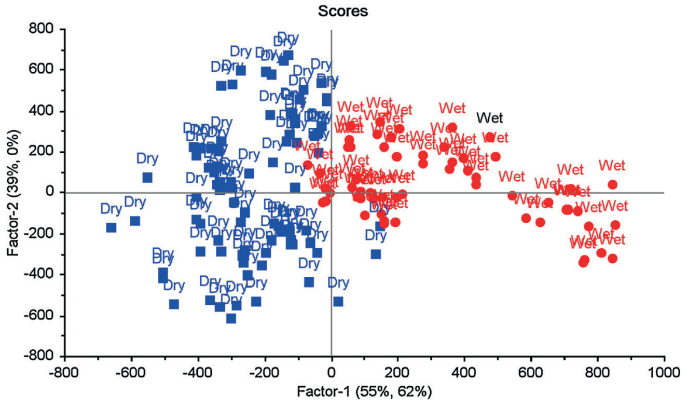

Fig. 8. PLS-DA score plot. Both Factor-1 and Factor-2 are linear combination of wastewater characteristic variables.

this model to classify influent of the WWTP. Overall, the climate condition can be classified by an explicit PLS-DA classifier based on the "Dry" and "Wet" labels obtained from previous cluster analysis, and the classifier can be used to support scenario-based soft sensor development (Haimi et al., 2015).

It has to be notified that the accuracy of classification actually represents the similarity of the classification results and clustering results. The clustering results are estimates of climate conditions but not the actual state of reality. Although an explicit classifier will provide convenience for further application in WWTP control, potential risk of over optimistic classification does exist if the "Dry" and "Wet" conditions were not well clustered and may lead to wrong judgement of climate condition. Therefore, cluster analy-

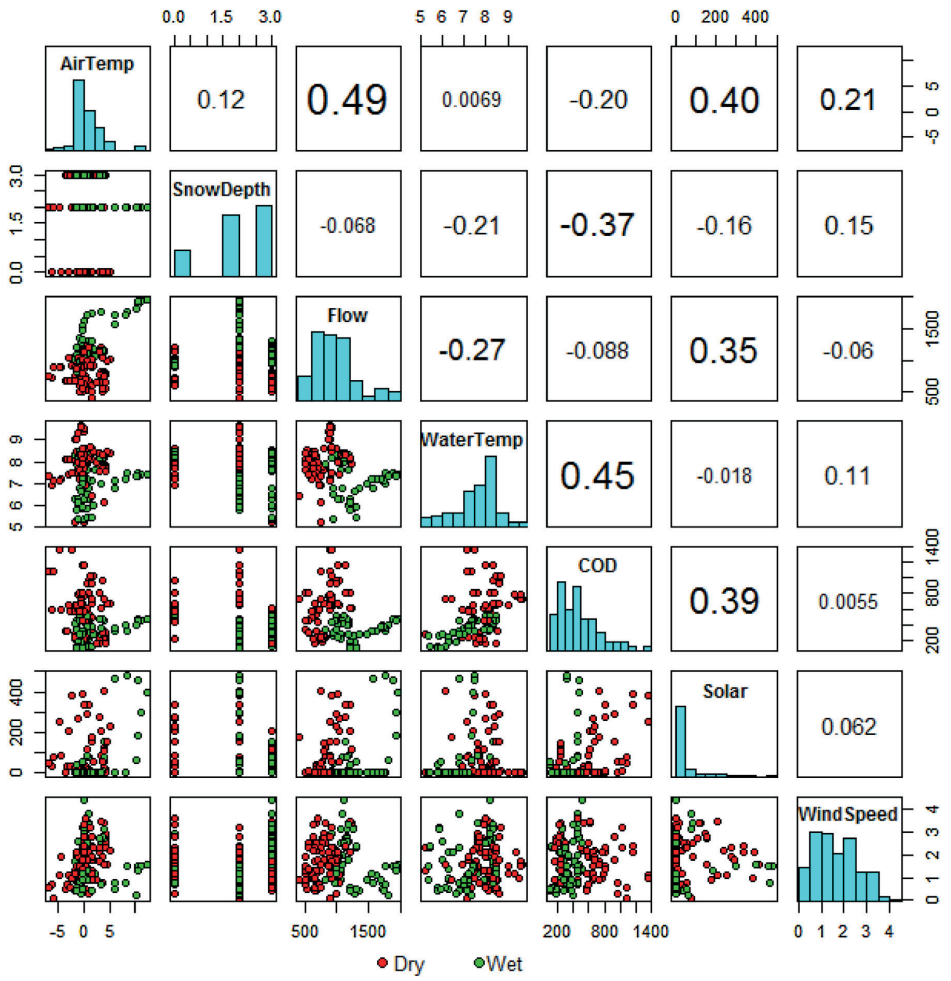

Fig. 9. Scatter matrix and correlation analysis of air temperature (AirTemp), snow depth (SnowDepth), flow rate (Flow), water temperature (WaterTemp), COD, Solar radiation (Solar) and wind speed (WindSpeed) in cold season.

sis plays a central role in this approach and more efforts should be put into assigning climate condition to influent precisely.

3.5. Relationship of climatic factors and wastewater characteristics in cold season

The influence of snow melting on wastewater quantity and quality reflects the impact of climate on wastewater characteristics in cold season. To study the relationship of wastewater characteristics and climatic factors, air temperature, snow depth, solar radiation and wind speed were selected as factors related to snow melting, according to literature review (Moghadas et al., 2015). Because Flow and COD are the most significant variables representing wastewater characteristics, suggested by previous PCA results, we investigated the relationship of flow, COD and climate parameters. The relationship of wastewater temperature and climate was also studied, due to snow melting effect on wastewater.

Scatter matrix plot coupled with correlation analysis was used to study the relationship of climatic factors and wastewater characteristics, where the correlation coefficients (r) are marked in the upper panel of Fig. 9. Snow depth values are discrete daily average values with only 0 cm, 2 cm and 3 cm during the observation period, which are different with the other hourly data. In spite of this, snow depth negatively correlated with water temperature ($r = -0.21$) and COD ($r = -0.37$). Air temperature had a high positive correlation coefficient with flow ($r = 0.49$), and relative strong negative correlation with COD (-0.20). There was very weak correlation between air temperature and water temperature, indicating that daily variation of air temperature cannot affect influent temperature.

The negative correlation of flow and water temperature ($r = -0.27$) complied the effect of snow melting, because the cold snowmelt would not only increase the flowrate, but also decrease water temperature. Flow rate was almost independent with COD concentration ($r = -0.088$), while their wet climate data (green dot) were positively and linearly correlated. In addition, no overlapping of dry and wet observation was found on the scatter plot of flow and COD (Fig. 9). For this reason, flow and COD are useful information to classify cold and wet climate data. The correlation coefficient

of COD and water temperature is 0.45, which represent relative high positive correlation. When the wastewater was diluted by snowmelt, water temperature and COD concentration decreased simultaneously. Solar radiation was highly correlated with flow (r = 0.35) and COD (r = 0.39). It is natural to understand the contribution of radiation to snow melting during daytime, but the positive relation of COD and solar radiation is partially due to wastewater daily variation. The COD concentration was always lower in the dry night, while solar radiation was almost lower to zero during night, which resulted in higher correlation coefficient of COD and solar radiation. Wind speed correlated weakly with either flow (r = −0.06) or COD (r = 0.0055).

Furthermore, wet climate data (green) shows more obvious linear correlation than that of dry climate (red) in Fig. 9. Compared with wet climate data, the chaos of overall scatter plots indicate that the complex effect of climate on wastewater characteristics. This result revealed the importance of classification of dry and wet climate data. Even though air temperature provide some insight of climate effect on snow melting as well as wastewater characteristics in cold season, more efforts are required from urban snow melting modelling to provide support to wastewater characterization in cold season. The stepwise procedures helped to separate the overall dataset to analyze the relation between climatic information and influent data.

4. Conclusions

This work investigated the daily, weekly and seasonal variation of influent wastewater characteristics of wastewater treatment plants in cold climate area. To solve the difficulty of investigating wastewater characteristics in cold season, a stepwise approach was developed to figure out influent characteristic in dry and wet climate respectively. After cluster analysis, the dry climate wastewater characteristics in cold season were compared with that in warm season. As a result, the flow, total COD, TSS, nitrogen, ammonia and pH were not significantly different in cold and warm seasons. Significantly higher phosphorus were observed during warm season. PLS-DA was used to develop a classifier that enables to continuously discriminate dry or wet climate condition of influent, which is capable to support WWTP surveillance and process control based on online measurement.

Snow melting impact wastewater characteristics significantly. The relationship of wastewater characteristics and climate parameters related to snow melting was investigated. The study provide evidence of that how climatic information is related to WWTP influent, the insights of which can be used to support WWTP operation.

Acknowledgements

This work has been supported by the Regnbyge-3M project (grant number 234974), which is granted by the Oslofjord Regional Research Fund. Besides, the work has also been funded by the RECOVER project, granted by the Reserach Council of Norway (grant number 247612). The authors would like to thank the staffs of Solumstrand WWTP for their supports on site.

References

Almeida, M., Butler, D., Friedler, E., 1999. At-source domestic wastewater quality. Urban Water 1, 49–55, http://dx.doi.org/10.1016/S1462-0758(99)00008-4.

ApH A, AWWA, WEF, 2012. Standard Methods for the Examination of Water and Wastewater, 22nd ed. American Public Health Association, Washington, D.C.

Ashley, R.M., Clemens, F.H.L.R., Tait, S.J., Schellart, A., 2008. Climate change and the implications for modelling the quality of flow in combined sewers. In: 11th International Conference on Urban Drainage, Edinburgh, Scotland, UK, 2008 Climate, Edinburgh, Scotland, UK, pp. 1–10.

Avella, A.C., Görner, T., Yvon, J., Chappe, P., Guinot-Thomas, P., de Donato, P., 2011. A combined approach for a better understanding of wastewater treatment plants operation: statistical analysis of monitoring database and sludge physico-chemical characterization. Water Res. 45, 981–992, http://dx.doi.org/10.1016/j.watres.2010.09.028.

Barker, M., Rayens, W., 2003. Partial least squares for discrimination. J. Chemom. 17, 166–173, http://dx.doi.org/10.1002/cem.785.

Bhat, S., Hatfield, K., Jacobs, J.M., Lowrance, R., Williams, R., 2007. Surface runoff contribution of nitrogen during storm events in a forested watershed. Biogeochemistry 85, 253–262, http://dx.doi.org/10.1007/s10533-007-9131-1.

Bixio, D., Van Hauwermeiren, P., Thoeye, C., Ockier, P., 2001. Impact of cold and dilute sewage on pre-fermentation—a case study. Water Sci. Technol. 43, 109–117.

Butler, D., 1993. The influence of dwelling occupancy and day of the week on domestic appliance wastewater discharges. Build. Environ. 28, 73–79, http://dx.doi.org/10.1016/0360-1323(93)90008-Q.

CAMO Software, 2016. The Unscrambler X [WWW Document]. CAMO Softw. AS, URL http://www.camo.com/rt/Products/Unscrambler/unscrambler.html.

Haimi, H., Mulas, M., Sahlstedt, K., Vahala, R., 2009. Advanced Operation and Control Methods of Municipal. Helsinki University of Technology, Water and Wastewater Engineering, Espoo.

Haimi, H., Corona, F., Mulas, M., Sundell, L., Heinonen, M., Vahala, R., 2015. Shall we use hardware sensor measurements or soft-sensor estimates? Case study in a full-scale WWTP. Environ. Model. Softw. 72, 215–229, http://dx.doi.org/10.1016/j.envsoft.2015.07.013.

Henze, M., Gujer, W., Mino, T., Matsuo, T., Wentzel, M.C., Marais, G.v.R., 1994. Activated Sludge No. 2, IAWQ Scientific and Technical Reports, No.3. IAWQ, London.

Hwang, J.H., Oleszkiewicz, J.A., 2007. Effect of cold-temperature shock on nitrification. Water Environ. Res. 79, 964–968, http://dx.doi.org/10.2175/106143007X176022.

Indahl, U.G., Martens, H., Næs, T., 2007. From dummy regression to prior probabilities in PLS-DA. J. Chemom. 21, 529–536, http://dx.doi.org/10.1002/cem.1061.

Liland, K.H., Indahl, U.G., 2009. Powered partial least squares discriminant analysis. J. Chemom. 23, 7–18, http://dx.doi.org/10.1002/cem.1186.

Liu, Y., Chen, J., Sun, Z., Li, Y., Huang, D., 2014. A probabilistic self-validating soft-sensor with application to wastewater treatment. Comput. Chem. Eng. 71, 263–280, http://dx.doi.org/10.1016/j.compchemeng.2014.08.008.

Martin, C., Vanrolleghem, P.A., 2014. Analysing, completing, and generating influent data for WWTP modelling: a critical review. Environ. Model. Softw. 60, 188–201, http://dx.doi.org/10.1016/j.envsoft.2014.05.008.

Merriam, E.R., Petty, J.T., Strager, M.P., Maxwell, A.E., Ziemkiewicz, P.F., 2015. Complex contaminant mixtures in multistressor Appalachian riverscapes. Environ. Toxicol. Chem. 34, 2603–2610, http://dx.doi.org/10.1002/etc.3101.

Moghadas, S., Gustafsson, A.-M., Muthanna, T.M., Marsalek, J., Viklander, M., 2015. Review of models and procedures for modelling urban snowmelt. Urban Water J. 9006, 1–16, http://dx.doi.org/10.1080/1573062X.2014.993996.

NIBIO, 2016. Agriculture Meteorological Service [WWW Document]. Nor. Inst. Bioeconomy Res, URL http://lmt.bioforsk.no/weatherstations/42/chart.

Nocairi, H., Qannari, E.M., Vigneau, E., Bertrand, D., 2005. Discrimination on latent components with respect to patterns. Application to multicollinear data. Comput. Stat. Data Anal. 48, 139–147, http://dx.doi.org/10.1016/j.csda.2003.09.008.

Olsson, G., 2012. ICA and me—a subjective review. Water Res. 46, 1585–1624, http://dx.doi.org/10.1016/j.watres.2011.12.054.

Plósz, B.G., Liltved, H., Ratnaweera, H., 2009. Climate change impacts on activated sludge wastewater treatment: a case study from Norway. Water Sci. Technol. 60, 533–541, http://dx.doi.org/10.2166/wst.2009.386.

Singh, K.P., Malik, A., Mohan, D., Sinha, S., Singh, V.K., 2005. Chemometric data analysis of pollutants in wastewater—a case study. Anal. Chim. Acta 532, 15–25, http://dx.doi.org/10.1016/j.aca.2004.10.043.

Tao, E.P., Shen, W.H., Liu, T.L., Chen, X.Q., 2013. Fault diagnosis based on PCA for sensors of laboratorial wastewater treatment process. Chemom. Intell. Lab. Syst. 128, 49–55, http://dx.doi.org/10.1016/j.chemolab.2013.07.012.

Tunçal, T., Pala, A., Uslu, O., 2009. Determination of microbial responses to seasonal variations of wastewater composition in the izmir wastewater treatment plant. Fresenius Environ. Bull. 18, 2114–2122.

Vega, P., Revollar, S., Francisco, M., Martín, J.M., 2014. Integration of set point optimization techniques into nonlinear MPC for improving the operation of WWTPs. Comput. Chem. Eng. 68, 78–95, http://dx.doi.org/10.1016/j.compchemeng.2014.03.027.

Wang, X., Ratnaweera, H., Holm, J.A., Olsbu, V., 2017. Statistical monitoring and dynamic simulation of a wastewater treatment plant: a combined approach to achieve model predictive control. J. Environ. Manage. 193, 1–7, http://dx.doi.org/10.1016/j.jenvman.2017.01.079.

Weyand, M., 2002. Real-time control in combined sewer systems in Germany—some case studies. Urban Water 4, 347–354, http://dx.doi.org/10.1016/s1462-0758(02)00031-6.

Wilen, B.M., Lumley, D., Mattsson, A., Mino, T., 2006. Rain events and their effect on effluent quality studied at a full scale activated sludge treatment plant. Water Sci. Technol. 54, 201–208, http://dx.doi.org/10.2166/wst.2006.721.

Xiao, F., Halbach, T.R., Simcik, M.F., Gulliver, J.S., 2012. Input characterization of perfluoroalkyl substances in wastewater treatment plants: source discrimination by exploratory data analysis. Water Res. 46, 3101–3109, http://dx.doi.org/10.1016/j.watres.2012.03.027.

Paper II

Wang, X., Ratnaweera, H., Holm, J.A., Olsbu, V., 2017. Statistical monitoring and dynamic simulation of a wastewater treatment plant: A combined approach to achieve model predictive control. Journal of Environmental Management. 193, 1–7. doi:10.1016/j.jenvman.2017.01.079

Journal of Environmental Management 193 (2017) 1–7

Contents lists available at ScienceDirect

Journal of Environmental Management

journal homepage: www.elsevier.com/locate/jenvman

Research article

Statistical monitoring and dynamic simulation of a wastewater treatment plant: A combined approach to achieve model predictive control

Xiaodong Wang [a, *], Harsha Ratnaweera [a], Johan Abdullah Holm [a], Vibeke Olsbu [b]

[a] Department of Mathematical Sciences and Technology, Norwegian University of Life Sciences, P.O. Box 5003-IMT, 1432 Aas, Norway
[b] Department of Water Supply and Sewerage, Drammen Municipality, Engene 1, 3008 Drammen, Norway

ARTICLE INFO

Article history:
Received 20 June 2016
Received in revised form
29 January 2017
Accepted 31 January 2017

Keywords:
Control
Dynamic simulation
MBBR
Multiple regression
Principal component analysis
Wastewater treatment

ABSTRACT

The on-line monitoring of Chemical oxygen demand (COD) and total phosphorus (TP) restrains wastewater treatment plants to achieve better control of aeration and chemical dosing. In this study, we applied principal components analysis (PCA) to find out significant variables for COD and TP prediction. Multiple regression method applied the variables suggested by PCA to predict influent COD and TP. Moreover, a model of full-scale wastewater treatment plant with moving bed bioreactor (MBBR) and ballasted separation process was developed to simulate the performance of wastewater treatment. The predicted COD and TP data by multiple regression served as model input for dynamic simulation. Besides, the wastewater characteristic of the wastewater treatment plant and MBBR model parameters were given for model calibration. As a result, R^2 of predicted COD and TP versus measured data are 81.6% and 77.2%, respectively. The model output in terms of sludge production and effluent COD based on predicted input data fitted measured data well, which provides possibility to enabled model predictive control of aeration and coagulant dosing in practice. This study provide a feasible and economical approach to overcome monitoring and modelling restrictions that limits model predictive control of wastewater treatment plant.

1. Introduction

Model predictive control (MPC) is considered as an advanced control scheme to optimize wastewater treatment plants (WWTPs) (Kim et al., 2014; Vega et al., 2014). The application of MPC has been reported that 25% aeration cost can be saved in an activated sludge plant (O'Brien et al., 2011). For the successfully use of MPC, real time monitoring of the treatment process and appropriate models which can describe process behaviors are required. However, the application of model predictive control in full-scale WWTPs is limited due to unavailability of capable process model and reliable online analyzers for process monitoring, especially for chemical oxygen demand (COD) and total phosphorus (TP) online measurement. Present literature reports are mainly focus on the selection of control structure (Gutierrez et al., 2014; Stare et al., 2007) and cost function and set point optimization (Vega et al., 2014). Consequently, most control scheme developed in the past is tested using simulation, but much fewer controllers have been implemented in full scale WWTPs (Olsson et al., 2014; Åmand et al., 2013).

Moving Bed Biofilm Reactor (MBBR) is a fluidized biofilm wastewater treatment system, which was widely used during last decades due to its higher treatment efficiency and lower footprint (Di Trapani et al., 2011; Ødegaard, 2006). The separation of biomass produced by MBBR system usually requires coagulant dosing to enhance biomass separation. Therefore, aeration and coagulant dosing control is essential to the performance of wastewater treatment plant with MBBR. For the purpose of improving MBBR plant performance and reduce operation cost, a MBBR model and influent wastewater characteristics are necessary to achieve model predictive control.

Although there is no standard MBBR model available as activated sludge model 1- ASM1 (Henze et al., 1987), modelling and dynamic simulation of MBBR has been carried out based on ASM1 (Mannina et al., 2011; Plattes et al., 2006), which proved that the bio-kinetic model in ASM1 are able to serve as reference for the

* Corresponding author.
E-mail addresses: xiaodong.wang@nmbu.no, xiaodong.wang001@gmail.com (X. Wang).

http://dx.doi.org/10.1016/j.jenvman.2017.01.079
0301-4797/

modelling of MBBR system. Nowadays, fluidized biofilm model are available in simulation tools for wastewater treatment, e.g. STOAT® (WRc, Wiltshire, England), BioWin® (EnviroSim Associates Ltd., Canada). Consequently, modelling and dynamic simulation of a MBBR plant are possible to carry out for model predictive control purpose.

Principal components analysis (PCA) is a multivariable statistical method for detecting data collinearity and reduce dataset dimensions, which plays an essential role in software sensor development (Cecil and Kozlowska, 2010; Haimi et al., 2015). Recently, researchers employed PCA to determine correlation between process variables (Avella et al., 2011) and characterize water quality (Huang et al., 2012). Moreover, multiple regression coupled with PCA was used to monitor WWTP operation and predict process performance (Avella et al., 2011; Liu et al., 2014; Martín de la Vega et al., 2012). Data collected from WWTPs contain useful information and are not always explicit. Therefore, with the application of modern statistical methods, process engineers are able to obtain real-time information without the corresponding online sensors.

The objective of this work was to provide an approach to optimize full-scale WWTP performance and reduce operation cost in practice. This is achieved by a combined approach to enable model predictive control. Furthermore, the study provides wastewater characteristics of a full scale WWTP in Norway, based on which a MBBR model was built. Statistical monitoring of influent wastewater and dynamic simulation of WWTP performance based on predicted influent data was carried out. By applying the approach presented in this work, full-scale WWTPs are able to achieve model predictive control easily and economically.

2. Materials and methods

2.1. Description of the wastewater treatment plant

Solumstrand wastewater treatment plant locates in Drammen, in the south of Norway with the treatment capacity of serving 130 000 person equivalent. As is shown in Fig. 1, the influent wastewater passes through the screen and grit trap to remove large solid and sand. The outlet of grit trap enters MBBR system for biological treatment. The biological treatment of this WWTP is consisted of four parallels, and each parallel has two aerobic MBBRs in series. The MBBR system is filled with bio-carriers with filling rate of 59%, and the specific surface area of bio-carriers is greater than 500 m^2/m^3. The MBBR system only has aerobic zone with short nominal hydraulic retention time (1.6 h), which enables organic matter removal, but ammonia and soluble nitrogen removal are not required in this plant. The outlet of MBBR system carries detached biological particles and enters ballasted flocculation tank for solid separation. The ballasted flocculation and separation, also known as Actiflo (Plum et al., 1998), separates solid and water within a short period due to high settling velocity caused by micro-sand and coagulant dosing. Besides, coagulant dosing should secure phosphorus removal ratio larger than 94%.

2.2. Wastewater characteristics

Influent and effluent wastewater was continuously collected by automatic samplers and the wastewater characteristics was analyzed following Standard Methods for chemical oxygen demand (COD), ammonia, total nitrogen (TN), total phosphorus (TP), soluble phosphorus, and suspended solids (SS) (APHA et al., 2012). The total sample collection period was 120 h. Table 1 lists the average influent wastewater characteristic, which are also the input values of the steady state model.

2.3. Multivariate statistical analysis

Two multivariate statistical methods were applied to achieve statistical monitoring of the WWTP: Principal components analysis (PCA) and multiple regression. The mathematical procedure of PCA for statistical monitoring of WWTP was well explained in literature (Liu et al., 2014). In this work, we applied PCA to study the collinearity and correlation between influent variables, i.e., COD, soluble COD (SCOD), Flow, SS, ammonia (NH_4-N), PH, total nitrogen (TN), orthophosphate (OP) and total phosphorus (TP). The results of PCA were visualized in form of two types of plot: explained variances plot and loading plot. The explained variances plot indicates the proportion of total variance explained by each component, while the loading plot visualizes the correlation between original variables. In addition, if a small amount of principal components explains most variance of the data, it indicates high collinearity of original variables. Moreover, the original variables located closely on the loading plot indicates positive correlation, and variables are negatively correlated if they locate on the opposite of the origin. To verify the PCA model, cross validation method was applied.

Because it is expensive and slow to measure COD and total phosphorus by online analyzers, we applied multiple regression to predict influent COD and total phosphorus based on easily measured variables, e.g. flow rate and PH. Leverage correction method are used to validate the multiple regression model. The Unscrambler® software (Camo software company) was used for all the statistical analysis.

2.4. Model development

As stated above, a steady state model of the MBBR system was developed based on Activated Sludge Model 1 (Henze et al., 1987). The function of the steady state model was to determine model parameters. Average influent wastewater characteristic of 120

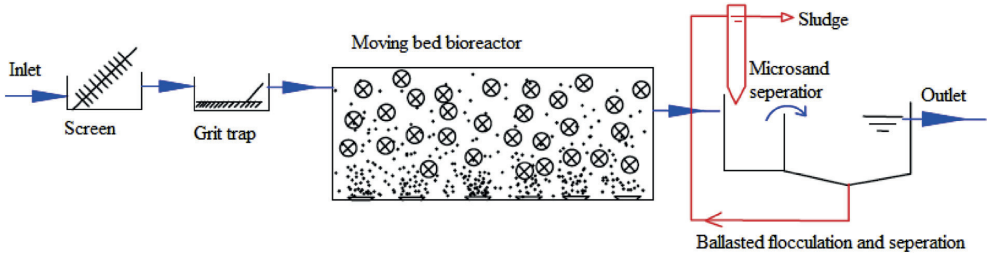

Fig. 1. Schematic diagram of the wastewater treatment plant.

Table 1
Average influent wastewater characteristic, which serves as the input of steady state model.

Symbol	Wastewater Composition	Values	Units
–	Total COD	617	mg COD L^{-1}
–	Volatile fatty acids(VFA)	10	mg COD L^{-1}
S_s	Soluble biodegradable COD	259	mg COD L^{-1}
S_I	Soluble inert COD	56	mg COD L^{-1}
X_S	Particulate biodegradable COD (slowly biodegradable)	218	mg COD L^{-1}
X_I	Particulate inert COD	73	mg COD L^{-1}
X_{vi}	Influent volatile suspended solids	190	mg L^{-1}
X_{ni}	Influent non-volatile solids	10	mg L^{-1}
S_{NH}	Ammonia nitrogen in bulk liquid	33.5	mg N L^{-1}
–	Soluble organic nitrogen	2.88	mg N L^{-1}
S_{NO}	Soluble nitrate and nitrite nitrogen	0	mg N L^{-1}
–	Particulate organic nitrogen	8.62	mg N L^{-1}
S_{ND}	Soluble degradable organic nitrogen	2.88	mg N L^{-1}
–	Soluble unbiodegradable organic nitrogen	0	mg N L^{-1}
X_{ND}	Particulate biodegradable organic nitrogen	6.62	mg N L^{-1}
–	Particulate unbiodegradable organic nitrogen	2	mg N L^{-1}
–	Soluble orthophosphate	1.8	mg P L^{-1}
–	Soluble biodegradable phosphorus	1.8	mg P L^{-1}
–	Soluble unbiodegradable phosphorus	0	mg P L^{-1}
–	Particulate biodegradable phosphorus	2.25	mg P L^{-1}
–	Particulate unbiodegradable phosphorus	0.75	mg P L^{-1}

Table 2
List of basic process model used to describe the biological behavior of MBBR system.

j	Process	Process rate, ρ_j
1	Aerobic growth of heterotrophs	$\rho_1 = \mu_H \left(\frac{S_S}{K_S+S_S}\right)\left(\frac{S_S}{K_{O,H}+S_S}\right)X_{B,H}$
2	Aerobic growth of autotrophs	$\rho_2 = \mu_A \left(\frac{S_{NH}}{K_{NH}+S_{NH}}\right)\left(\frac{S_O}{K_{O,A}+S_O}\right)X_{B,A}$
3	Decay of heterotrophs	$\rho_3 = b_H X_{B,H}$
4	Decay of autotrophs	$\rho_4 = b_A X_{B,A}$
5	Ammonification of soluble organic nitrogen	$\rho_5 = k_a S_{ND} X_{B,A}$
6	Hydrolysis of entrapped	$\rho_6 = k_h \frac{X_S/X_{B,H}}{K_X+(X_S/X_{B,H})}\left[\left(\frac{S_O}{K_{O,A}+S_O}\right)+\eta_h\left(\frac{K_{O,H}}{K_{O,H}+S_O}\right)\left(\frac{S_{NO}}{K_{NO}+S_{NO}}\right)\right]X_{B,H}$
7	Hydrolysis of entrapped organic nitrogen	$\rho_7 = k_h \frac{X_S/X_{B,H}}{K_X+(X_S/X_{B,H})}\left[\left(\frac{S_O}{K_{O,A}+S_O}\right)+\eta_h\left(\frac{K_{O,H}}{K_{O,H}+S_O}\right)\left(\frac{S_{NO}}{K_{NO}+S_{NO}}\right)\right]X_{B,H}(X_{ND}/X_S)$

samples was applied as the model input. Table 2 lists the biological behavior of the MBBR system, based on activated sludge model 1 (ASM1). The full demonstration of process kinetics and stoichiometry can be found in ASM1 (Henze et al., 1987). In this study, we excluded anoxic growth of heterotrophs, because there is no anoxic zone in the MBBR system and only aerobic reaction was modelled. The notation of the state variables and process parameters are given in Table 3.

Table 3
Part of state variables and model parameters of biological model.

Notation	Definition	Units
State variables (other used state variables can be find from Table 1)		
$X_{B,H}$	Active heterotrophic biomass	mg COD L^{-1}
$X_{B,A}$	Active autotrophic biomass	mg COD L^{-1}
S_O	Oxygen	mg COD L^{-1}
Kinetic parameters		
μ_H	Maximum specific growth rate for heterotrophic biomass	day^{-1}
K_S	COD half-saturation coefficient for heterotrophic biomass	mg COD L^{-1}
$K_{O,H}$	Oxygen half-saturation coefficient for heterotrophic biomass	mg COD L^{-1}
K_{NO}	Nitrate half-saturation coefficient for heterotrophic biomass	mg N L^{-1}
b_H	Decay coefficient for heterotrophic biomass	day^{-1}
η_H	Correction factor for hydrolysis under anoxic conditions	–
k_h	Maximum specific hydrolysis rate	g COD (g COD · day)$^{-1}$
K_X	Half-saturation coefficient for hydrolysis of X_S	g COD (g COD)$^{-1}$
μ_A	Maximum specific growth rate of autotrophic biomass	day^{-1}
K_{NH}	Ammonia half-saturation coefficient for autotrophic biomass	mg N L^{-1}
b_A	Decay coefficient for autotrophic	day^{-1}
$K_{O,A}$	Oxygen half-saturation coefficient for autotrophic biomass	mg COD L^{-1}
k_a	Ammonification rate	L (mg COD · day)$^{-1}$
f_{bN}	Nitrogen content of biomass	g N (g COD)$^{-1}$

2.5. Model calibration

The model calibration has been carried out to minimize the difference between the measured and simulated values. As a simplified model for control purpose, the target model output are effluent COD, total phosphorus and ammonia concentration. The SS of MBBR outlet was also interested because it represents sludge production of MBBR system and determines the control of coagulant dosage for biomass separation. Thus, a steady state model with average influent data as input and default ASM1 values were assigned to the model. Latterly, model parameters related to interested variables were calibrated by comparing the steady state output and measured values.

2.6. Dynamic simulation of WWTP performance

We use STOAT to simulate the performance of WWTP. In detail, we employed the "Upflow biological aerated filter" to represent MBBR by setting medium surface area to 500 m^2/m^3. STOAT has no specific model for ballasted flocculation. We selected "chemical P removal" together with "Lamella separator" to represent ballasted flocculation section. Because micro-sand increases the settling velocity to more than 100 m/h, the sludge settling velocity coefficients were calibrated accordingly.

3. Results and discussion

3.1. Principal components analysis (PCA)

We applied PCA to summarize the collinearity and correlation of influent variables. Fig. 2a shows the cumulative explained variance of PCA results, where the blue curve is the results of the fitted PCA model, and the red one shows the results of cross validation. As is shown in Fig. 2a, the first principal component (PC-1) explains 50.1% of total variance of the data (calibrated), while the validated PC-1 explains 41.8% total variance. The first three principal components (PC-1, PC-2 and PC-3) of calibrated and validated results represent 88.9% and 81.9% of total variance, respectively. The results indicate high collinearity of WWTP influent data. Consequently, we can cluster the original variables into three groups and pick one variable from each group to represent the propagation trend of the corresponding group.

Fig. 2b shows the loading of influent variables on the plane formed by PC-1 and PC-2. COD, SCOD, OP, Flow, TP and SS composite the first group with higher PC-1 loading. While PH has negative loading on both PC-1 and PC-2 coordinate, and locates on the opposite of the first group. It indicates that PH is negative correlated with the first group. Moreover, ammonia and total nitrogen forms the third group, which has high negative weight on PC-2. The third group and the first group are almost orthogonal with respect to the origin, which tells that ammonia and total nitrogen contain information that cannot be linearly expressed by variables in the first group. Overall, PCA proved the high collinearity of influent variables and suggested that three original variables were sufficient to represent the variation of influent quality and quantity.

3.2. Multiple regression

Online measurement of influent COD (COD_{in}) and influent TP (TP_{in}) is very important, because COD_{in} and TP are two of the main input factors of the process model and determines whether model predictive control can be achieved or not. However, perspective from process online monitoring and control, COD and TP is slower and more expensive to measure by online analyzers. Therefore, we applied multiple regression method to use easy and fast responding variables (e.g. Flow, PH, ammonia) to predict slower and more expensive variables (COD_{in}, TP_{in}). Recent years multivariate prediction methods partial least squares (Amaral et al., 2013) and artificial neural network (Jing et al., 2015; Lou and Zhao, 2012; Nasr et al., 2012) are reported as useful prediction tools in the field of wastewater treatment. However, from the view of monitoring and control in practice, both partial least squares and artificial neural networks require continuously measurement of all the variables, which would increase the investment on online equipment and maintenance cost. Alternatively, a robust multivariate regression model with pre-selected variables based on PCA is preferred to predict real-time COD_{in} and TP_{in} values.

As is suggested by PCA results in Fig. 2b, we picked one easier measured variable from each of the three groups to predict influent COD_{in} and TP_{in} to avoid overfitting. Therefore, influent flow, ammonia and PH were selected as predictor. Eqs. (1) and (2) are the multiple regression model for influent COD_{in} and TP_{in} respectively:

$$COD_{in} = 2708.2170 + 0.6806Flow + 11.4423Ammonia_{in} - 443.7516PH_{in} \quad (1)$$

$$TP_{in} = 0.5548 + 0.0067Flow + 0.0443Ammonia_{in} - 0.3926PH_{in} \quad (2)$$

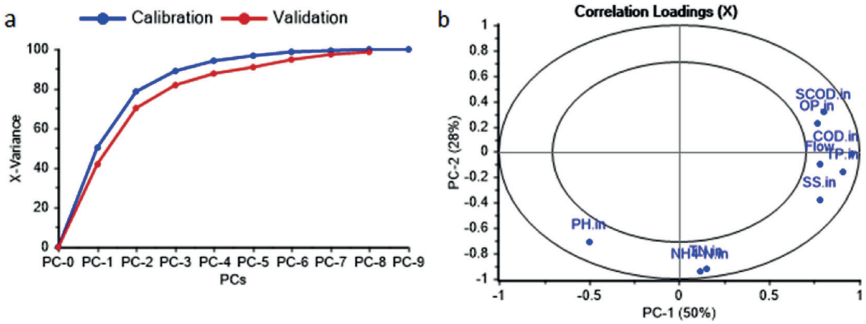

Fig. 2. Principal components analysis of influent flow and wastewater quality. a) Cumulative proportion of total variance of all PCs. The blue and red curve represent the results of PCA model and validated results based on cross-validation, respectively. b) Loading plot of influent variables on the plane of PC-1 and PC-2. The subscript in represent influent. (For interpretation of the references to colour in this figure legend, the reader is referred to the web version of this article.)

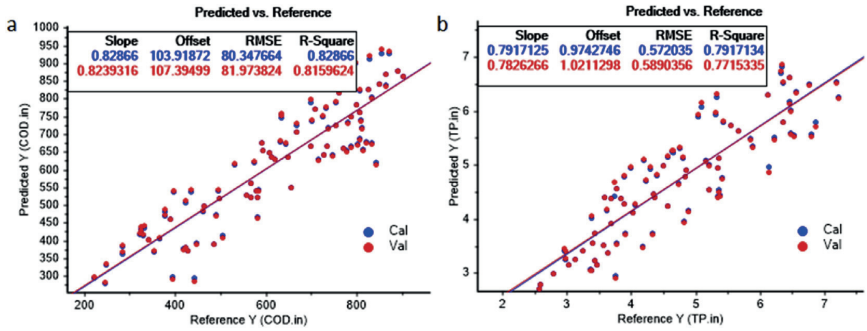

Fig. 3. a) Predicted COD_{in} versus measured COD_{in}; b) Predicted TP_{in} versus measured TP_{in}. The blue values are results of model output, while red values are validated model output based on Leverage Correction. (For interpretation of the references to colour in this figure legend, the reader is referred to the web version of this article.)

The scatter plots of predicted COD_{in} and TP_{in} versus measured COD_{in} and TP_{in} are shown in Fig. 3a and b respectively. The validated prediction based on leverage correction were evaluated in term of R^2. As is shown in Fig. 3a, the linear expression of predicted COD_{in} (Eq. (1)) explains more than 81% of COD_{in} variance. Meanwhile, the predicted TP_{in} as linear expressed in Eq. (2), descripts 77% total variance of measured TP_{in}. Considering the complexity of the full-scale WWTP, prediction accuracy of multiple regression with R^2 greater than 0.7 is acceptable. Thus, the multiple regression model is capable to predict influent COD and TP, which can serve as statistical monitoring tool to provide input values to the process model for model predictive control.

3.3. Process model calibration

As mentioned previously, the model calibration has been carried out to minimize the error of steady state model output and measured data. More specifically, effluent COD, ammonia and the suspended solids (SS) of MBBR outlet were considered as state variables for the seeking of biological kinetic parameters. In addition, the effluent SS was used as state variable to determine setting velocity parameters of the separation tanks. The parameters obtained from calibration step are listed in Table 4. Typical values of model kinetic parameters in ASM1 are given in 10 °C and 20 °C(Henze et al., 1987), but the kinetic parameters in STOAT simulation environment are based on 15 °C. To provide compared modelling result, the equivalent parameter values at 20 °C are calculated. Calibration of temperature dependency of bio-kinetic parameters was based on activated sludge model No. 2 - ASM2 (Henze et al., 1994). However, ASM2 applied Eq. (3) for the calculation of bio-kinetic parameters under different temperature, while Eq. (4) is used in STOAT. To find the equivalent model parameters at 20 °C, the temperature coefficient "θ" in STOAT was calculated from temperature coefficient "a" in ASM2, $\theta = lna$ (Table 5).

$$ASM2: \quad \mu = \mu_{max} \cdot a^{(T-T_{ref})} \tag{3}$$

$$\text{STOAT}: \quad \mu = \mu_{max} \cdot e^{\theta(T-15)} \tag{4}$$

The adopted parameters have been compared with reference values in ASM1. The heterotrophs growth rate (μ_H) and decay rate (b_H) are almost consistent with reference values. However, parameters related to ammonia removal are significantly different with reference values. As the MBBR system is not used to remove ammonia, much lower autotrophic bacteria growth rate (μ_A) was adopted in this model. Besides, a relative higher ammonification rate (k_a) was used to achieve nitrogen balance. However, the reason of higher ammonification in this system is unknown, and further study is necessary to figure out the ammonification mechanism. Overall, the coefficients related to ammonia removal have a higher influence on the model output than those related to COD removal.

3.4. Dynamic simulation

To test the possibility of achieving model predictive control, both predicted influent (multiple regression output) and measured influent data were used as input of wastewater treatment process model to simulate the WWTP. Fig. 4 shows the dynamic simulation results of plant effluent COD, ammonia, TP and suspended solids of MBBR outlet (before separation). SS of MBBR outlet represents sludge production of MBBR. The goodness of fitting in terms of R^2 are given in Table 6. Generally, the model output of SS (Fig. 4a), COD

Table 4
Calibrated process model parameters and reference values from ASM1.

Parameters	Values in STOAT at 15 °C	Parameter unit in STOAT	Equivalent values at 20 °C	Reference values at 20 °C	Parameter unit at 20 °C
μ_H	0.19	h^{-1}	6.40	6	day^{-1}
μ_A	0.008	h^{-1}	0.34	0.8	day^{-1}
b_H	0.0147	h^{-1}	0.50	0.62	day^{-1}
b_A	0.0036	h^{-1}	0.15	–	day^{-1}
k_h	0.07	h^{-1}	2.04	3	day^{-1}
k_a	0.004	h^{-1}	0.12	0.05	day^{-1}
Y_H	0.67	mg COD (mg COD)$^{-1}$	0.67	0.67	mg COD (mg COD)$^{-1}$
Y_A	0.24	mg COD(mg N)$^{-1}$	0.24	0.24	mg COD(mg N)$^{-1}$
f_{bN}	0.005	g N(g COD)$^{-1}$	0.005	–	g N(g COD)$^{-1}$
K	4000	Settling coefficients K and h for the settling velocity equation: $=C^h$, where C represents suspended solids concentration.			
h	1				

Table 5
Temperature coefficients used for the calculation of equivalent MBBR model parameters at 20°C.

Process	θ	a	Degree of dependency
Hydrolysis	0.0392	1.04	Low
Heterotrophs, fermentation	0.0677	1.07	Medium
Nitrification	0.1133	1.12	High

(Fig. 4b) and ammonia (Fig. 4c) are well fitted to the measured data. In particular, the model output based on measured input have higher R^2 values than those based on predicted values. This is reasonable because the predicted influent COD and TP had some errors to real values. The output values of ammonia based on measured influent ammonia overlapped with those based on predicted values (Fig. 4c), because influent ammonia are regarded as easier measured data which is not predicted by multiple regression. However, the simulated phosphorus results were quite higher than measured data (Fig. 4d). Microorganism in MBBR system assimilated more than 1.7 mg/L, but the biological model based on ASM does not contain any anabolism functions related to phosphorus removal. For that reason, the MBBR model passed all the phosphorus content to the separation tank without removal and resulted in higher model output of total phosphorus. On the other hand, the results indicate that phosphorus removal by chemical precipitation requires negligible coagulant in this WWTP, because soluble phosphorus was already transformed to particulate phosphorus in biomass. In other words, only the SS of MBBR outlet determines coagulant dosage into separation tanks.

As is given in Table 6, the R^2 of model output of MBBR suspended solids, effluent COD and ammonia based on predicted influent are 0.507, 0.504 and 0.659, respectively. According to literature report (Avella et al., 2011), correlation coefficients R^2 greater than 0.5 were acceptable to say that model output match measured data well. Furthermore, the SS of MBBR outlet can be used to determine coagulant dosage into the ballasted separation tank, while the model output of effluent COD and ammonia can be used to control real-time airflow to the MBBR system. Therefore, the combined approach of statistical monitoring of influent constituent and process modelling is capable to provide input data for model predictive control of airflow and coagulant dosage.

4. Conclusion

Model predictive control in full-scale wastewater treatment plant has been limited due to on-line monitoring and capable

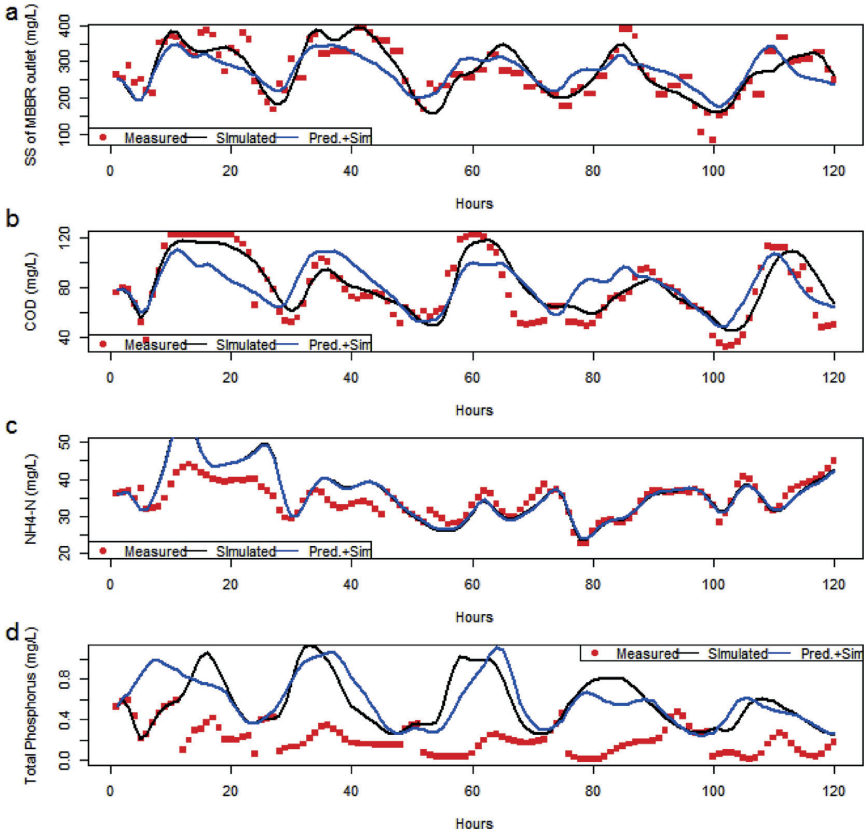

Fig. 4. Dynamic simulation results of a) SS of MBBR outlet; b) effluent COD; c) effluent ammonia; d) effluent total phosphorus. The red, black and blue values represent measured data, simulated data based on measured influent and simulated data based on predicted influent data, respectively. (For interpretation of the references to colour in this figure legend, the reader is referred to the web version of this article.)

Table 6
Goodness of fitting in terms of R^2 of dynamic simulation.

Variables	R^2		
	Measured VS. Simulated	Measured VS. Pred.+Sim.	Simulated VS. Pred.+Sim.
SS_{MBBR}	0.711	0.507	0.713
COD_{outlet}	0.798	0.504	0.527
$Ammonia_{outlet}$	0.666	0.659	0.999
TP_{outlet}	0.003	0.038	0.490

process models. This study provide a combined approach of statistical monitoring and process modelling to achieve model predictive control of the WWTP.

The statistical monitoring of influent COD and total phosphorus (TP) were achieved by combining principle components analysis (PCA) and multiple regression. PCA suggested influent flow, ammonia and PH as predictor variables for COD and TP. Multiple regression shows that the predicted COD and TP allowed description of 81.6% and 77.2% variance of influent COD and TP. A WWTP process model contains MBBR and ballasted separation was built to simulate the performance of a full-scale WWTP. The predicted influent wastewater was used as the input of the process model to simulate the dynamic performance of the treatment process. The results shown that the model was capable to predict sludge production and outlet COD concentration, which determines coagulant dosage and air flow of MBBR system. Therefore, it is possible to apply MPC to control aeration and chemical dosage by applying statistical monitoring of the WWTP. This study provide a convenient and economic approach to achieve better control of wastewater treatment plant.

Acknowledgement

This work has been supported by the Regnbyge-3M project (project number: 234974), which is granted by the Oslo fjord Regional Research Fund, Norway. The authors would also thank the staffs of the Solumstrand WWTP for their supports on wastewater sampling and maintenance of samplers.

References

Amaral, A.L., Mesquita, D.P., Ferreira, E.C., 2013. Automatic identification of activated sludge disturbances and assessment of operational parameters. Chemosphere 91, 705–710. http://dx.doi.org/10.1016/j.chemosphere.2012.12.066.

APHA, AWWA, WEF, 2012. Standard Methods for the Examination of Water and Wastewater, 22nd ed. USA, Washington, DC.

Avella, A.C., Görner, T., Yvon, J., Chappe, P., Guinot-Thomas, P., de Donato, P., 2011. A combined approach for a better understanding of wastewater treatment plants operation: statistical analysis of monitoring database and sludge physico-chemical characterization. Water Res. 45, 981–992. http://dx.doi.org/10.1016/j.watres.2010.09.028.

Åmand, L., Olsson, G., Carlsson, B., 2013. Aeration control - a review. Water Sci. Technol. 67, 2374–2398. http://dx.doi.org/10.2166/wst.2013.139.

Cecil, D., Kozlowska, M., 2010. Software sensors are a real alternative to true sensors. Environ. Model. Softw. 25, 622–625. http://dx.doi.org/10.1016/j.envsoft.2009.05.004.

Di Trapani, D., Christensso, M., Ødegaard, H., 2011. Hybrid activated sludge/biofilm process for the treatment of municipal wastewater in a cold climate region: a case study. Water Sci. Technol. 63, 1121–1129.

Gutierrez, G., Ricardez-Sandoval, L.A., Budman, H., Prada, C., 2014. An MPC-based control structure selection approach for simultaneous process and control design. Comput. Chem. Eng. 70, 11–21. http://dx.doi.org/10.1016/j.compchemeng.2013.08.014.

Haimi, H., Corona, F., Mulas, M., Sundell, L., Heinonen, M., Vahala, R., 2015. Shall we use hardware sensor measurements or soft-sensor estimates? Case study in a full-scale WWTP. Environ. Model. Softw. 72, 215–229. http://dx.doi.org/10.1016/j.envsoft.2015.07.013.

M. Henze, C. Grady, W. Gujer, G. v. R. Marais, T. Matsuo, 1987, Activated Sludge Model No. 1 1987.

M. Henze, W. Gujer, T. Mino, T. Matsuo, M.C. Wentzel, G. v. R. Marais, 1994, Activated Sludge No. 2, IAWQ Scientific and Technical Reports, No.3. IAWQ, London.

Huang, M., Ma, Y., Wan, J., 2012. Modeling a paper-making wastewater treatment process by means of an adaptive network-based Fuzzy inference system and principal component analysis. Ind. Eng. Chem. Res. 51, 6166–6174. http://dx.doi.org/10.1021/ie203049r.

Jing, L., Chen, B., Zhang, B., Li, P., 2015. Process simulation and dynamic control for marine oily wastewater treatment using UV irradiation. Water Res. 81, 101–112. http://dx.doi.org/10.1016/j.watres.2015.03.023.

Kim, H., Lim, H., Wie, J., Lee, I., Colosimo, M.F., 2014. Optimization of modified ABA2 process using linearized ASM2 for saving aeration energy. Chem. Eng. J. 251, 337–342. http://dx.doi.org/10.1016/j.cej.2014.04.076.

Liu, Y., Pan, Y., Sun, Z., Huang, D., 2014. Statistical monitoring of wastewater treatment plants using variational Bayesian PCA. Ind. Eng. Chem. Res. 53, 3272–3282. http://dx.doi.org/10.1021/ie403788v.

Lou, I., Zhao, Y., 2012. Sludge bulking prediction using principle component regression and artificial neural network. Math. Probl. Eng. 2012 http://dx.doi.org/10.1155/2012/237693.

Mannina, G., Trapani, D., Di Viviani, G., Ødegaard, H., 2011. Modelling and dynamic simulation of hybrid moving bed biofilm reactors: model concepts and application to a pilot plant. Biochem. Eng. J. 56, 23–36. http://dx.doi.org/10.1016/j.bej.2011.04.013.

Martín de la Vega, P.T., Martínez de Salazar, E., Jaramillo, M. a, Cros, J., 2012. New contributions to the ORP & DO time profile characterization to improve biological nutrient removal. Bioresour. Technol. 114, 160–167. http://dx.doi.org/10.1016/j.biortech.2012.03.039.

Nasr, M.S., Moustafa, M. a E., Seif, H. a E., El Kobrosy, G., 2012. Application of artificial neural network (ANN) for the prediction of EL-AGAMY wastewater treatment plant performance-Egypt. Alex. Eng. J. 51, 37–43. http://dx.doi.org/10.1016/j.aej.2012.07.005.

O'Brien, M., Mack, J., Lennox, B., Lovett, D., Wall, A., 2011. Model predictive control of an activated sludge process: a case study. Control Eng. Pract. 19, 54–61. http://dx.doi.org/10.1016/j.conengprac.2010.09.001.

Olsson, G., Carlsson, B., Comas, J., Copp, J., Gernaey, K.V., Ingildsen, P., Jeppsson, U., Kim, C., Rieger, L., Rodríguez-Roda, I., Steyer, J.-P., Takács, I., Vanrolleghem, P. a, Vargas, a, Yuan, Z., Åmand, L., 2014. Instrumentation, control and automation in wastewater–from London 1973 to Narbonne 2013. Water Sci. Technol. 69, 1373–1385. http://dx.doi.org/10.2166/wst.2014.057.

Ødegaard, H., 2006. Innovations in wastewater treatment: the moving bed biofilm process. Water Sci. Technol. 53, 17–33. http://dx.doi.org/10.2166/wst.2006.284.

Plattes, M., Henry, E., Schosseler, P.M., Weidenhaupt, A., 2006. Modelling and dynamic simulation of a moving bed bioreactor for the treatment of municipal wastewater. Biochem. Eng. J. 32, 61–68. http://dx.doi.org/10.1016/j.bej.2006.07.009.

Plum, V., Dahl, C.P., Bentsen, L., Petersen, C.R., Napstjert, L., Thomsen, N.B., 1998. The Actiflo method. Water Sci. Technol. 37, 269–275. http://dx.doi.org/10.1016/S0273-1223(97)00778-6.

Stare, A., Vrecko, D., Hvala, N., Strmcnik, S., 2007. Comparison of control strategies for nitrogen removal in an activated sludge process in terms of operating costs: a simulation study. Water Res. 41, 2004–2014. http://dx.doi.org/10.1016/j.watres.2007.01.029.

Vega, P., Revollar, S., Francisco, M., Martín, J.M., 2014. Integration of set point optimization techniques into nonlinear MPC for improving the operation of WWTPs. Comput. Chem. Eng. 68, 78–95. http://dx.doi.org/10.1016/j.compchemeng.2014.03.027.

Paper III

Wang, X., Bi, X., Liu, C., Ratnaweera, H., 2018. Identifying critical components causing seasonal variation of activated sludge settleability and developing early warning tool. Water Science and Technology. 77, 1689–1697. doi:10.2166/wst.2018.053

This is the post-print version of the article. The article can be found online with reference to the following information:
Wang, X., Bi, X., Liu, C., Ratnaweera, H., 2018. Identifying critical components causing seasonal variation of activated sludge settleability and developing early warning tool. Water Science and Technology. 77, 1689–1697. doi:10.2166/wst.2018.053

Identifying critical components causing seasonal variation of activated sludge settleability and developing early warning tool

Xiaodong Wang[a], Xuejun Bi[b, *], Changqing Liu[b], Harsha Ratnaweera[a, b]

[a] Department of Mathematical Sciences and Technology, Norwegian University of Life Sciences, P.O. Box 5003-IMT, 1432 Aas, Norway

[b] Qingdao Technological University, Research Center of Urban Aqua Environmental Pollution Control in Qingdao, Qingdao, 266033, China, Fushun Road 11, 266033 Qingdao, China

*Corresponding author

ABSTRACT

Settleability of activated sludge is one of the most common problems that restricts the efficiency of activated sludge system. Obvious seasonal variation of settleability was found in the activated sludge system of a full scale wastewater treatment plant (WWTP) during two years of observation. Principal component analysis (PCA) was applied to study the correlation between diluted sludge volume index (DSVI), operational and environmental factors. As a result, temperature and mixed liquid suspended solids (MLSS) were found as the most significant variables relating with DSVI variation. Multivariate regression, partial least squares regression and support vector machine regression were applied to develop early warning models for DSVI prediction. The multivariate regression model was proved as a simple and easy-to-interpret early warning tool to be applied in practice. Based on the ratio of volatile substances in biomass, the original cause of seasonal variation of settleability was further discussed by referring the storage-biodegradation mechanism. Moreover, the results of this work also suggested that modern statistical techniques were important to investigate complicated engineering problems. This study provided insights of seasonal variation of activated sludge settleability by systematic investigation of long-term data of a full scale WWTP.

Keywords: activated sludge; early warning; principal component analysis; settleability; substance storage; wastewater treatment

INTRODUCTION

The flocs of activated sludge are formed by microorganisms, which grow in biological wastewater treatment systems, while the size, shape and microbial composition of flocs will vary due to changes of operational and environmental conditions. Poorly formed activated sludge flocs settle slower in sedimentation tanks

and may lead to poor solid-water separation or even process failure. Activated sludge settling remains one of the most common problems that restricted the efficiency of biological wastewater treatment.

The causes of poor settleability have been studied from several aspects, such as filamentous bulking (Arelli et al., 2009), biomass density (Schuler et al., 2001; Jones and Schuler, 2010) and the role of extracellular polymeric substances (Ding et al., 2015). On the one hand, these works well explained the biomass structure and physiochemical characteristics of settling flocs. On the other hand, they reflected the difficulties in figuring out the original causes of variable settleability of activated sludge.

Diluted sludge volume index (DSVI) is an empirical indicator of activated sludge settleability. Seasonal variation of DSVIs has been reported in full-scale wastewater treatment plant (WWTP) (Jones and Schuler, 2010). Jassby et al. (2014) combined biomass density and filament content in biomass to explain the variation of DSVI, and a settleability model was developed as a function of biomass density and filament content. However, the original causes of variable settleability of activated sludge were influent characteristics, operational and environmental factors of the biological system, rather than the physiochemical property or bio-structure of biomass. For early warning purpose in practice, it is important to develop a DSVI prediction model based on the original causes of the variation of activated sludge settleability.

Multivariate statistical methods are getting additional attention in the optimization of wastewater treatment system. Principle component analysis (PCA) was increasingly used in complexity analysis of full-scale WWTPs (Avella et al., 2011) and pattern detection (Amaral et al., 2013). Partial least squares regression (PLSR) is a useful tool to perform prediction (Amaral et al., 2013). Support vector machine regression (SVMR) and multivariate regression had been proved as capable tool for wastewater treatment process surveillance (Liu et al., 2016a; Wang et al., 2017). These multivariate statistical methods can also be used to develop early warning tool for poor settleability of activated sludge. Moreover, the correlation of DSVI and other environmental or operational variables may be figured out by conducting a comprehensive study by applying multivariate statistics.

The aim of this work is to figure out the impact factors of settleability from the complexity of full-scale activated sludge system, and to suggest an early warning tool for poor sludge settleability. This work was performed to explain how operational and environmental factors affect biomass settling and provide better understanding of seasonal variation of activated sludge settleability for troubleshooting.

This is the post-print version of the article. The article can be found online with reference to the following information:
Wang, X., Bi, X., Liu, C., Ratnaweera, H., 2018. Identifying critical components causing seasonal variation of activated sludge settleability and developing early warning tool. Water Science and Technology. 77, 1689–1697. doi:10.2166/wst.2018.053

METHODS AND MATERIALS

Activated sludge system and data collection

The wastewater treatment plant (WWTP) locates in Qingdao, China, where the temperature in biological reactor varies from 10.5 ℃ to 28.2 ℃. The WWTP receives municipal wastewater from the city Qingdao, and the effluent is discharged to marine recipient after treatment. The WWTP is configured with primary treatment, secondary treatment and tertiary treatment, where secondary treatment is performed by an activated sludge system. Following by secondary treatment, flocculation and filtration system consist tertiary treatment. The activated sludge system was an enhanced biological phosphorus removal (EBPR) system equipped with anaerobic, anoxic and aerobic chambers, which enabled the biological treatment stage to remove nitrogen and phosphorus. The settled activated sludge was recycled back to anaerobic chamber from the secondary clarifiers. The activated sludge sedimentation of the biological system was observed for over a two-year period.

Influent samples were collected from the outlet of primary settler by an automatic sampler, which fetched a sample every hour and mixed 24 samples together as daily average sample for lab analysis. Effluent samples were collected from the outlet of secondary clarifier. The measurement of all the contaminants was carried out according to the standard methods (APHA et al., 2012). Diluted sludge volume index (DSVI) were measured immediately after the mixed liquid obtained from the end of aeration tank according to Lee et al. (1983). Other operational data were either obtained from surveillance system or calculated from pre-known data. The range of these data and some variables used in this study were listed in Table 1.

Table 1 Potential disturbances of activated sludge settleability used for this study

Disturbance (variables)	Notation	Unit	Min	Mean	Max	Standard deviation
Influent flow rate	Flow.in	m^3/h	13 722	44305	64935	6540
Temperature of bio-reactor	Temperature	℃	10.50	18.93	28.20	4.93
Influent pH	pH		7.08	7.87	8.94	0.25
Influent chemical oxygen demand	COD.in	mg/l	126.0	424.1	2249.1	149.1
Influent biological oxygen demand	BOD.in	mg/l	65.0	186.4	748.0	65.53
Influent total nitrogen	TotN.in	mg/l	26.15	62.74	113.53	10.70
Influent total phosphorus	Tot.in	mg/l	1.00	6.18	31.80	2.10

This is the post-print version of the article. The article can be found online with reference to the following information:
Wang, X., Bi, X., Liu, C., Ratnaweera, H., 2018. Identifying critical components causing seasonal variation of activated sludge settleability and developing early warning tool. Water Science and Technology. 77, 1689–1697. doi:10.2166/wst.2018.053

Total suspended solids in influent	SS.in	mg/l	25.0	181.3	756	130.5
Influent ammonium	Ammonia.in	mg/l	18.80	53.71	90.75	10.55
Influent chloride	Chloride.in	mg/l	99.26	334.43	1825.0	192.3
Influent Alkalinity	Alkalinity.in	mg/l	75.08	335.25	675.68	143.06
BOD/COD ratio	BOD/COD		0.22	0.45	0.56	0.10
Suspended solids of secondary clarifiers outlet	SS.out	mg/l	1.00	35.16	482.0	74.3
Sludge concentration (Mixed liquid suspended solids)	MLSS	mg/l	938	2023	5372	472
Diluted sludge volume index	DSVI	ml/g	62	251.2	634	114
Volatile matter ratio in sludge	MLVSS/MLSS		0.52	0.74	0.94	0.03
COD/Nitrogen ratio	COD/TotN		2.26	6.79	19.81	1.91
COD/Phosphorus ratio	COD/TotP		20.11	71.06	469.46	25.35
COD loading	COD loading	kg COD/ (kgMLSS.day)	0.05	0.48	2.00	0.27
BOD loading	BOD loading	kg BOD/ (kgMLSS.day)	0.03	0.21	0.67	0.13
Sludge retention time	SRT	days	0.98	18.73	184.3	25.00

Statistical analysis

Principal component analysis (PCA) is a multivariate statistical method for studying covariance of variables and detecting collinearity of dataset. The mathematical procedure had been well explained by Tao et.al. (2013). We applied PCA to study the correlation between DSVI and other environmental/operational variables. To develop early warning tools of poor activated sludge settleability, three methods were adopted and compared: multivariate regression, partial least squares regression (PLSR) and support vector machine regression (SVMR). Multivariate regression is already a commonly used statistical method. PLSR is also a regression method, which has the advantage to avoid overfitting when there are too many variables. SVMR is a machine learning algorithm, which can be used to perform both linear and non-liner modelling. The mathematical procedures of PLSR and SVMR had been well explained in literature (Mevik and Wehrens, 2007; Seshan et al., 2014). All these multivariate analyses were performed in Unscramber X version 10.4 (CAMO Software, 2016).

This is the post-print version of the article. The article can be found online with reference to the following information:
Wang, X., Bi, X., Liu, C., Ratnaweera, H., 2018. Identifying critical components causing seasonal variation of activated sludge settleability and developing early warning tool. Water Science and Technology. 77, 1689–1697. doi:10.2166/wst.2018.053

RESULTS AND DISCUSSION

Settleability variation and the consequences

Significant variation of activated sludge settleability was observed during the two-year period. As is shown in Figure 1a, higher DSVIs appeared in cold season when the temperature of the biological reactor was lower than 15 ℃, while lower DSVI values were observed in warm season when the temperature was higher than 23 ℃. Generally, when the DSVIs were higher than 350 mL/g, the poorly settled activated sludge would be washed out of the sedimentation tank. As a consequence, extremely high effluent SS was quite often observed during cold season when the influent temperature was lower than 15 ℃ (Figure 1b). The result agreed well with Jones and Schuler (2010), who investigated four full-scale WWTPs in New Mexico, US, and similar variation of activated sludge settleability was found in their study.

The results in Figure 1 provide evidence of the seasonal variation of activated sludge settleability, indicating the impact of temperature on activated sludge property. The bacterial community of activated sludge varied in a seasonal pattern (Flowers et al., 2013), which may be a possible explanation of the seasonal variation of settleability. However, the variable characteristics of activated sludge were the combined effect of operational conditions, influent characteristics and environmental conditions (Ju et al., 2014; Jo et al., 2016). To figure out the original causes of seasonal variation, a systematic investigation based on multivariate statistical analysis was carried out.

This is the post-print version of the article. The article can be found online with reference to the following information:
Wang, X., Bi, X., Liu, C., Ratnaweera, H., 2018. Identifying critical components causing seasonal variation of activated sludge settleability and developing early warning tool. Water Science and Technology. 77, 1689–1697. doi:10.2166/wst.2018.053

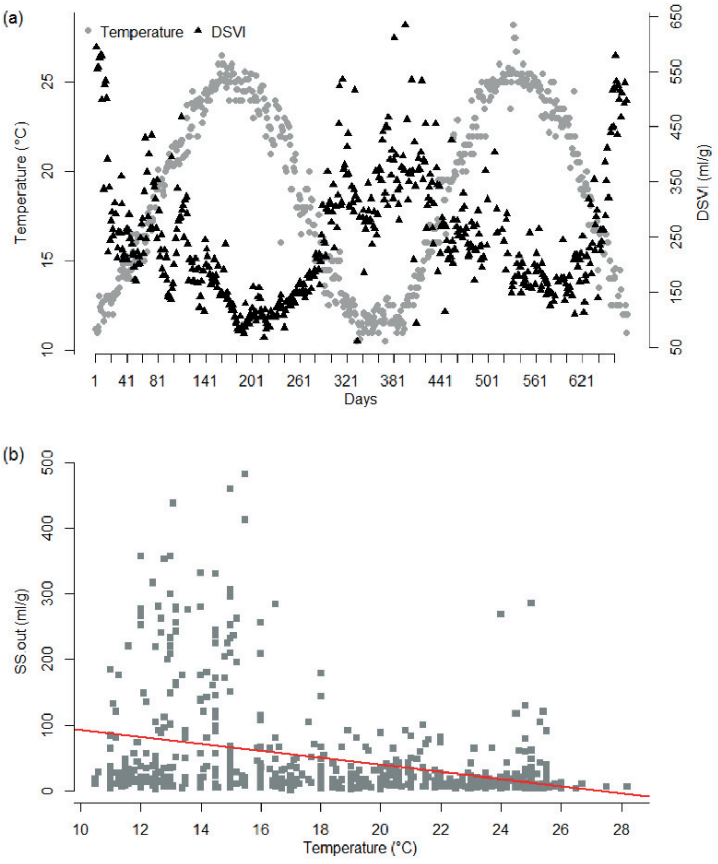

Figure 1 – (a) Variation of sludge volume index (SVI) along with temperature changing in 678 days of monitoring; (b) Scatter plot of secondary clarifier SS outlet versus temperature.

The correlation of 10 variables that represent influent characteristics, contaminant loadings, environmental and operational conditions were assessed together with DSVI by applying principal component analysis (Figure 2). Generally, PCA generated 11 new independent components, which were linear combination of original variables. Figure 2a shows the variance explained by the first seven principal components (PCs). The rest of the PCs represented less than 0.1 % of the total variance of the dataset, which can be ignored.

This is the post-print version of the article. The article can be found online with reference to the following information:
Wang, X., Bi, X., Liu, C., Ratnaweera, H., 2018. Identifying critical components causing seasonal variation of activated sludge settleability and developing early warning tool. Water Science and Technology. 77, 1689–1697. doi:10.2166/wst.2018.053

PC-1 and PC-2 together represented almost 100 % of the variation of the entire dataset, which suggested the high collinearity of the original variables.

Furtherly, Figure 2b shown the loading of original variables on the plane formed by the first principal component (PC-1) and second principal component (PC-2). DSVI, MLSS and Temperature are the most significant variables due to the higher PC-1 or PC-2 loading. These three variables mainly determined the variation of PC-1 and PC-2 as well as the entire original data. Both temperature and MLSS were negatively correlated with DSVI, and therefore they could be used to predict the settleability of activated sludge. Besides, the other variables located in the inner circle of Figure 2b were not significant variables because they had either too low PC-1 or PC-2 loading. It indicated that MLSS and Temperature correlated well with DSVI, while the other variables were not significant to the variation of DSVI in this activated sludge system. Therefore, for early warning purpose, Temperature and MLSS can be used to develop a prediction model for DSVI.

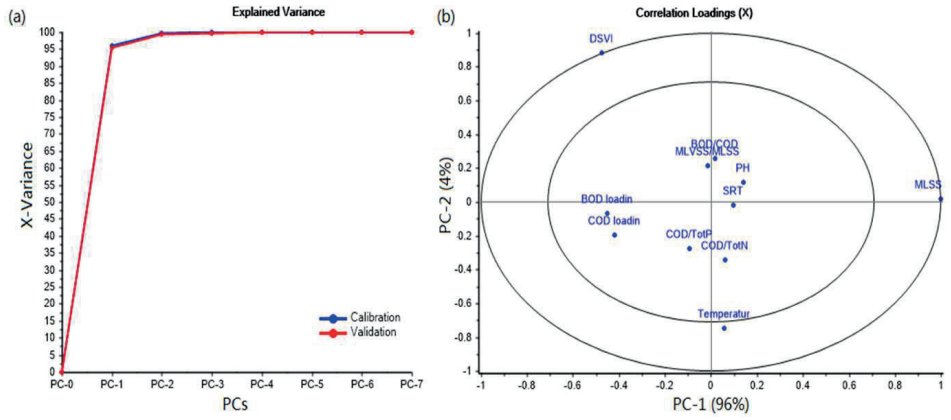

Figure 2. Principal component analysis (PCA) of DSVI and the other ten variables: BOD/COD ratio, pH, MLVSS/MLSS ratio, SRT, MLSS, BOD loading, COD loading, COD/Total Phosphrus ratio, COD/Total Nitrogen ratio, Temperature and MLSS. (a) The proportion of total variance being explained by different numbers of principal components; (b) Correlationg loading plot projected to the plane of PC-1 and PC-2.

Activated sludge settleability prediction for early warning

During the two years operation of the WWTP, we concluded the experience that if activated sludge settleablity got as worse as out of control in cold season, it will never get self-healing until warm season. As a consequence, activated sludge would be washed out of the system together with the supernatant, and it will lead to low removal efficiency of organic matter and ammonia. Therefore, it is necessary to develop

This is the post-print version of the article. The article can be found online with reference to the following information:
Wang, X., Bi, X., Liu, C., Ratnaweera, H., 2018. Identifying critical components causing seasonal variation of activated sludge settleability and developing early warning tool. Water Science and Technology. 77, 1689–1697. doi:10.2166/wst.2018.053

early warning tools to predict DSVI values. Three methods: multivariate regression, partial least squares regression (PLSR) and support vector machine regression (SVMR) were compared to find proper DSVI prediction modelling tools.

As was suggested by PCA in Figure 2b, Temperature and MLSS were selected as predictors to perform linear regression to predict DSVI. Equation (1) is the formula of multivariate regression for DSVI prediction, and the prediction results was shown in Figure 1. The prediction validated by leverage correction indicates that the predicted DSVI can explain 64 % variation of the measured DSVI (Figure 3a). The prediction accuracy was not high enough compared with those models based on filamentous bulking (Smets et al., 2006; Liu et al., 2016b). However, we were aimed to study the original causes of the seasonal variation of activated sludge settleability rather than predicting the status of activated sludge, e.g. filamentous bulking or non-filamentous bulking. Considering the uncontrollable disturbances and the complexity of the full-scale system, the R-square of more than 0.64 was fine to indicate the tendency of settleability changing.

The multivariate regression model was built upon the assumption that the prediction errors had a normal distribution with constant variance. In another word, no pattern should be detected on the residual plot (Figure 3b). The residuals were the differences between predicted DSVI and measured DSVI. However, an obvious pattern was found in Figure 3b, where the residuals were getting greater with the increasing of DSVI. Therefore, the capability of this model was limited, because prediction error would be unnecessary larger for greater DSVI values.

$$DSVI = 724.6323 - 14.6889 \cdot Temperature - 0.0953 \cdot MLSS \quad (1)$$

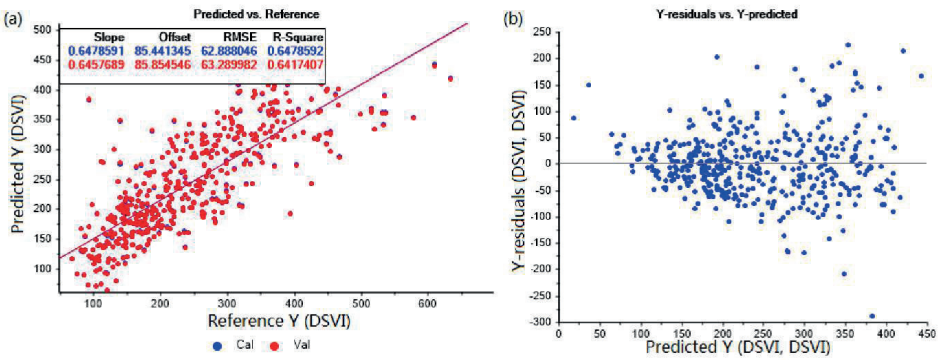

Figure 3 Multivariate regression for DSVI prediction with two explanatory variables: Temperature and MLSS. (a) Predicted DSVI versus the measured DSVI; (b) Residuals plot versus predicted DSVI.

To build a proper early warning tool based on influent characteristics and environmental/operational conditions, partial least squares regression (PLSR) and support vector machine regression (SVMR) were also applied to compare if there was a better solution for DSVI prediction. Figure 4 shows the goodness of fitting of PLSR and SVMR. All the variables listed in Table 1 were employed as explanatory variables to build PLSR and SVMR models, because both PLSR and SVMR can naturally avoid overfitting.

The R^2 of cross validated PLSR model was 0.64 (Figure 4a), while it was 0.67 for SVMR (Figure 4b). Support vector machine captured some nonlinear characteristics of DSVI variation and resulted in better fitting in terms of R^2. Though PLSR and SVMR applied more explanatory variables for model construction, the goodness of fitting was not significantly improved, compared with multivariate regression. The multivariate regression model, Equation (1), used less computational power and it was easier for interpretation. A semi-empirical model of settleability was developed as a function of biomass density and filament content by Jassby et al. (2014). Although that model perform well in DSVI prediction ($R^2 > 0.95$) (Jassby et al., 2014), the complexity of density measurement and filament quantification would limit the usage of the model in practice. Compared with the model developed by Jassby et al., the multivariate regression model in this study lost some accuracy of DSVI prediction. In spite of this, the multivariate regression model indicated the correlation of settleability and its original causes. Secondly, the multivariate regression are more convenient to be adopted as an early warning tool in practice, because the explanatory variables can be easily measured in full-scale WWTPs.

This is the post-print version of the article. The article can be found online with reference to the following information:
Wang, X., Bi, X., Liu, C., Ratnaweera, H., 2018. Identifying critical components causing seasonal variation of activated sludge settleability and developing early warning tool. Water Science and Technology. 77, 1689–1697. doi:10.2166/wst.2018.053

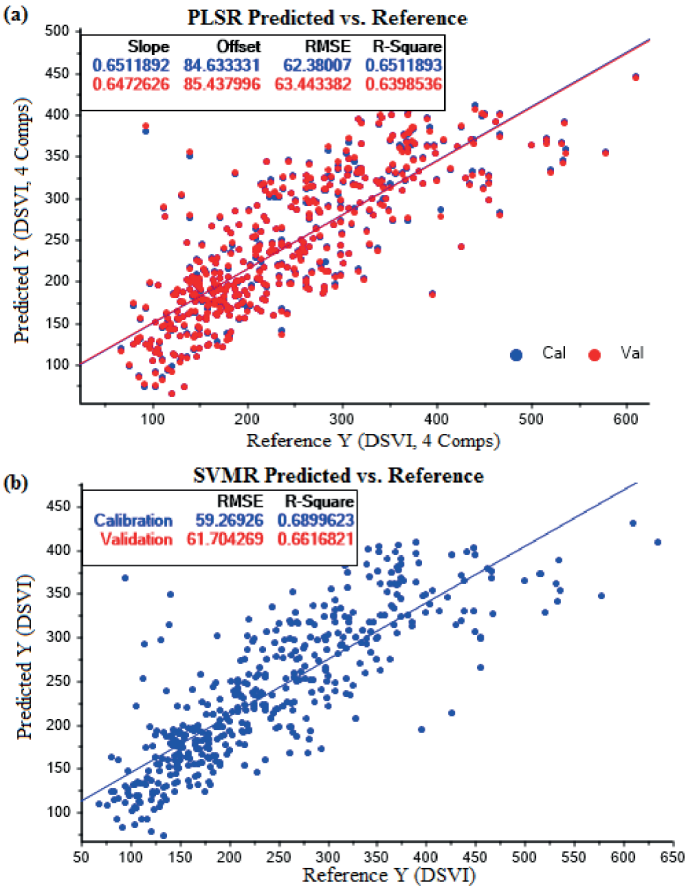

Figure 4 (a) Scatterplot of predicted DSVI by partial least squares regression versus measured DSVI; (b) Scatterplot of predicted DSVI by partial least squares regression versus measured PLSR.

Volatile substances storage and settleability

An interesting finding during two years observation was that the volatile substances of biomass showing a seasonal variation pattern against temperature changing. As is shown in Figure 5, the ratio of MLVSS/MLSS was varied within 0.65 – 0.82. Generally, MLVSS/MLSS was relatively lower in warm season, and it was relatively higher in cold season. The dramatic drop of MLVSS/MLSS in the first 70 days was caused by addition of external coal ash, which was not the natural decreasing of volatile proportion of biomass. The inorganic coal ash was supposed to improve the settling of activated sludge during that period.

This is the post-print version of the article. The article can be found online with reference to the following information:
Wang, X., Bi, X., Liu, C., Ratnaweera, H., 2018. Identifying critical components causing seasonal variation of activated sludge settleability and developing early warning tool. Water Science and Technology. 77, 1689–1697. doi:10.2166/wst.2018.053

Higher settling velocity was usually accompanied with higher inorganic substances in the biomass (Schuler and Jang, 2007; Jassby et al., 2014), because inorganic substances contributed positively to biomass buoyant density (Jones and Schuler, 2010). The seasonal changing of volatile substances in this study agreed with these literature reports. Since temperature was the original cause of seasonal variation of the volatile substances as well as activated sludge settleability, how temperature impact activated sludge settleability via altering volatile substances of biomass was further discussed.

Activated sludge model No. 3 (ASM3) introduced storage of organic substance to split COD flux (Gujer et al., 1999). A study of the distribution of COD flows to direct growth or storage shown that storage contributed 65 % - 92 % of the total COD utilization (Makinia et al., 2006). The temperature-dependent expression of simplified storage and aerobic heterotrophic growth process based on ASM3 is shown as Equation (2) and Equation (3), and the list of symbols were shown in Table 2.

$$\frac{dX_{STO}}{dt} = k_{STO,20℃} \cdot e^{\theta_k (T-20℃)} \cdot \frac{S_s}{K_s + S_s} \cdot X_H \tag{2}$$

$$\frac{dX_H}{dt} = \mu_{H,20℃} \cdot e^{\theta_\mu (T-20℃)} \cdot \frac{{X_{STO}}/{X_H}}{K_{STO} + {X_{STO}}/{X_H}} \cdot X_H \tag{3}$$

Table 2 State variables and model parameters for Equation (2) and Equation (3), based on ASM3.

Notation	Definition	Units
X_H	Heterotrophic biomass	mg COD/L
X_{STO}	Organics stored by heterotrophs	mg COD/L
$k_{STO,20℃}$	Storage rate constant at 20 ℃	g S_S/(g X_H . day)
θ_k	Temperature coefficient for organic storage	$℃^{-1}$
T	Temperature	℃
S_s	Readily biodegradable COD	mg COD/L
$\mu_{H,20℃}$	Max. growth rate of heterotrophs at 20 ℃	d^{-1}
θ_μ	Temperature coefficient for heterotrophic growth	$℃^{-1}$
K_s	Saturation constant for S_s	mg COD/L
K_{STO}	Saturation constant for K_{STO}	mg COD/L

This is the post-print version of the article. The article can be found online with reference to the following information:
Wang, X., Bi, X., Liu, C., Ratnaweera, H., 2018. Identifying critical components causing seasonal variation of activated sludge settleability and developing early warning tool. Water Science and Technology. 77, 1689–1697. doi:10.2166/wst.2018.053

The storage process transforms the soluble COD (S_s) into internal particulate COD (X_{STO}) and stores these in the biomass, which may increase volatile substances of the biomass. Both storage and heterotroph growth process are temperature-dependent, while the growth process is more sensitive to temperature changing than that of storage process. On the one hand, the consumption of stored substance would be significantly slower at cold season, but on the other hand, the formation of volatile substances (storage process) is slightly affected by temperature. Therefore, more volatile substances were accumulated in the biomass and led to higher MLVSS/MLSS ratio. It explains the seasonal variation of MLVSS/MLSS as is indicated in Figure 5. If the inorganic content reaches 50 %, the setting velocity of activated sludge could be 50 % higher than the activated sludge with only 5 % inorganic content (Trelles et al., 2017).

Overall, the seasonal variation of MLVSS/MLSS and the storage-consumption mechanism of volatile substance provided insight to understand the seasonal variation of activated sludge settleability.

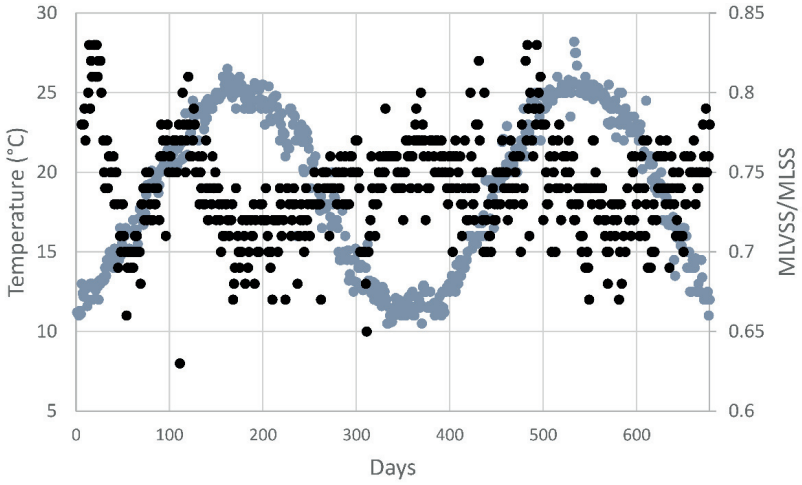

Figure 5 Variation of volatile substances in biomass in terms of terms of MLVSS/MLSS, along with seasonal temperature shifting.

This is the post-print version of the article. The article can be found online with reference to the following information:
Wang, X., Bi, X., Liu, C., Ratnaweera, H., 2018. Identifying critical components causing seasonal variation of activated sludge settleability and developing early warning tool. Water Science and Technology. 77, 1689–1697. doi:10.2166/wst.2018.053

CONCLUSION

- An obvious seasonal variation pattern of activated sludge settleability was found during two years observation in a full-scale WWTP. The DSVI decreased to poor-settling level in cold season, and it would gradually rise to fast-settling level with the increasing of temperature in warm season.
- Principal components analysis shown that temperature and MLSS were the most significant variables correlated with the variation of DSVI in this system. Even though SRT and influent loading rate are important factors determining biological process performance, they are weakly correlated with the variation of activated sludge settleability.
- A multivariate regression model was built to predict DSVI for early warning purpose (R^2 =0.64). The model was simple and easier to be adopted in full-scale WWTPs, but we should be aware of that the prediction capability decreased for higher DSVI prediction.
- Due to the differences in temperature sensitivity of substance storage and biodegradation, volatile content of biomass would increase when temperature decreased in cold season. The negative correlation of volatile content with biomass density led to higher MLVSS/MLSS ratio as well as higher DSVI in cold season. This biomass storage-biodegradation mechanism based on ASM3 provides insight of the seasonal variation of activated sludge settleability.

ACKNOWLEDGEMENTS

This study was financially supported by the National Natural Science Fund of China (No.51078192), the National Water Pollution Control and Treatment Science and Technology Major Project in China (No.2012ZX07203-004) and Qingdao applied basic research project (14-2-4-17-JCH).

REFERENCES

Amaral, A. L., Mesquita, D. P., and Ferreira, E. C. (2013) Automatic identification of activated sludge disturbances and assessment of operational parameters. Chemosphere, **91**(5), 705–710. [online] http://dx.doi.org/10.1016/j.chemosphere.2012.12.066.

APHA, AWWA, and WEF (2012) *Standard methods for the examination of water and wastewater*, Washington, D.C., American Public Health Association.

Arelli, A., Luccarini, L., and Madoni, P. (2009) Application of image analysis in activated sludge to evaluate correlations between settleability and features of flocs and filamentous species. Water Science and Technology, **59**(10), 2029–2036.

Avella, A. C., Görner, T., Yvon, J., Chappe, P., Guinot-Thomas, P., and de Donato, P. (2011) A combined approach for a better understanding of wastewater treatment plants operation: Statistical analysis of monitoring database and sludge physico-chemical characterization. Water Research, **45**(3), 981–992.

CAMO Software (2016) The Unscrambler X. CAMO Software AS. [online] http://www.camo.com/rt/Products/Unscrambler/unscrambler.html.

Ding, Z., Bourven, I., Guibaud, G., van Hullebusch, E. D., Panico, A., Pirozzi, F., and Esposito, G. (2015) Role of extracellular polymeric substances (EPS) production in bioaggregation: application to wastewater treatment. Applied Microbiology and Biotechnology, **99**(23), 9883–9905. [online] http://dx.doi.org/10.1007/s00253-015-6964-8.

Flowers, J. J., Cadkin, T. A., and McMahon, K. D. (2013) Seasonal bacterial community dynamics in a full-scale enhanced biological phosphorus removal plant. Water Research, **47**(19), 7019–7031. [online] http://dx.doi.org/10.1016/j.watres.2013.07.054.

Gujer, W., Henze, M., Mino, T., and Van Loosdrecht, M. (1999) Activated Sludge Model No. 3. Water Science and Technology, **39**(1), 183–193.

Jassby, D., Xiao, Y., and Schuler, A. J. (2014) Biomass density and filament length synergistically affect activated sludge settling: Systematic quantification and modeling. Water Research, **48**(1), 457–465. [online] http://dx.doi.org/10.1016/j.watres.2013.10.003.

Jo, S. J., Kwon, H., Jeong, S. Y., Lee, C. H., and Kim, T. G. (2016) Comparison of microbial communities of activated sludge and membrane biofilm in 10 full-scale membrane bioreactors. Water Research, **101**, 214–225. [online] http://dx.doi.org/10.1016/j.watres.2016.05.042.

Jones, P. A. and Schuler, A. J. (2010) Seasonal variability of biomass density and activated sludge settleability in full-scale wastewater treatment systems. Chemical Engineering Journal, **164**(1), 16–22.

Ju, F., Guo, F., Ye, L., Xia, Y., and Zhang, T. (2014) Metagenomic analysis on seasonal microbial variations of activated sludge from a full-scale wastewater treatment plant over 4 years. Environmental Microbiology Reports, **6**(1), 80–89.

Lee, S.-E., Koopman, B., Bode, H., and Jenkins, D. (1983) Evaluation of alternative sludge settleability indices. Water Research, **17**(10), 1421–1426. [online]

http://www.sciencedirect.com/science/article/pii/0043135483902737.

Liu, T., Liu, S., Zheng, M., Chen, Q., and Ni, J. (2016a) Performance assessment of full-scale wastewater treatment plants based on seasonal variability of microbial communities via high-throughput sequencing. PLoS ONE., **11(4)**, 1–15. [online] http://dx.doi.org/10.1371/journal.pone.0152998.

Liu, Y., Guo, J., Wang, Q., and Huang, D. (2016b) Prediction of Filamentous Sludge Bulking using a State-based Gaussian Processes Regression Model. Scientific Reports, **6**(1), 31303. [online] http://www.nature.com/articles/srep31303.

Makinia, J., Rosenwinkel, K. H., and Phan, L. C. (2006) Modification of ASM3 for the determination of biomass adsorption/storage capacity in bulking sludge control. Water Science and Technology, **53**(3), 91–99.

Mevik, B. H. and Wehrens, R. (2007) The pls package: Principal component and partial least squares regression in R. Journal of Statistical Software, **18**(2), 1–23.

Schuler, A. J. and Jang, H. (2007) Density effects on activated sludge zone settling velocities. Water Research, **41**(8), 1814–1822.

Schuler, A. J., Jenkins, D., and Ronen, P. (2001) Microbial Storage Products, Biomass Density, and Settling Properties of Enhanced Biological Phosphorus Removal Activated Sludge. Water Science and Technology, **43**(1), 173–180.

Seshan, H., Goyal, M. K., Falk, M. W., and Wuertz, S. (2014) Support vector regression model of wastewater bioreactor performance using microbial community diversity indices: Effect of stress and bioaugmentation. Water Research, **53**, 282–296. [online] http://dx.doi.org/10.1016/j.watres.2014.01.015.

Smets, I. Y., Banadda, E. N., Deurinck, J., Renders, N., Jenné, R., and Van Impe, J. F. (2006) Dynamic modeling of filamentous bulking in lab-scale activated sludge processes. Journal of Process Control, **16**(3), 313–319.

Tao, E. P., Shen, W. H., Liu, T. L., and Chen, X. Q. (2013) Fault diagnosis based on PCA for sensors of laboratorial wastewater treatment process. Chemometrics and Intelligent Laboratory Systems, **128**, 49–55. [online] http://linkinghub.elsevier.com/retrieve/pii/S0169743913001445.

Trelles, I. J., Mahamud, M. M., Lavín, A. G., and Díaz, M. (2017) Sludge settling prediction in sequencing

batch reactor plants. Journal of Cleaner Production, **152**, 115–124.

Wang, X., Ratnaweera, H., Holm, J. A., and Olsbu, V. (2017) Statistical monitoring and dynamic simulation of a wastewater treatment plant: A combined approach to achieve model predictive control. Journal of Environmental Management, **193**, 1–7. [online] http://dx.doi.org/10.1016/j.jenvman.2017.01.079.

Paper IV

Wang, X., Bi, X., Hem, L.J., Ratnaweera, H., 2018. Microbial community composition of a multi-stage moving bed biofilm reactor and its interaction with kinetic model parameters estimation. Journal of Environmental Management. 218, 340–347. doi:10.1016/j.jenvman.2018.04.015

Journal of Environmental Management 218 (2018) 340–347

Contents lists available at ScienceDirect

Journal of Environmental Management

journal homepage: www.elsevier.com/locate/jenvman

Research article

Microbial community composition of a multi-stage moving bed biofilm reactor and its interaction with kinetic model parameters estimation

Xiaodong Wang [a, *], Xuejun Bi [b], Lars John Hem [a, c], Harsha Ratnaweera [a, b]

[a] Faculty of Science and Technology, Norwegian University of Life Sciences, P.O. Box 5003-IMT, 1432 Aas, Norway
[b] Qingdao University of Technology, State and Local Joint Engineering Research Center of Urban Wastewater Treatment and Reclamation in China, Fushun Road 11, 266033 Qingdao, China
[c] Oslo Water and Sewage Works, Herslebs Gate 5, 0561 Oslo, Norway

ARTICLE INFO

Article history:
Received 1 November 2017
Received in revised form
6 January 2018
Accepted 3 April 2018

Keywords:
Autotrophic biomass
Heterotrophic biomass
High-throughput sequencing
MBBR
Microbial community
Wastewater treatment

ABSTRACT

Microbial community diversity determines the function of each chamber of multi-stage moving bed biofilm reactor (MBBR) systems. How the microbial community data can be further used to serve wastewater treatment process modelling and optimization has been rarely studied. In this study, a MBBR system was set up to investigate the microbial community diversity of biofilm in each functional chamber. The compositions of microbial community of biofilm from different chambers of MBBR were quantified by high-throughput sequencing. Significantly higher proportion of autotrophs were found in the second aerobic chamber (15.4%), while 4.3% autotrophs were found in the first aerobic chamber. Autotrophs in anoxic chamber were negligible. Moreover, ratios of active heterotrophic biomass and autotrophic biomass (X_H/X_A) were obtained by performing respiration tests. By setting heterotroph/autotroph ratios obtained from sequencing analysis equal to X_H/X_A, a novel approach for kinetic model parameters estimation was developed. This work not only investigated microbial community of MBBR system, but also it provided an approach to make further use of molecular microbiology analysis results.

1. Introduction

Moving bed biofilm reactors (MBBRs) have been widely applied in wastewater treatment plants since last decades (Di Trapani et al., 2014). MBBRs have proved to be successful in both domestic and industrial wastewater treatment, with respect to stable removal efficiency (Delnavaz et al., 2010), compact and high specific biomass concentration (Guo et al., 2010), and high cold-resistant ability (Hoang et al., 2014).

The performance of biological wastewater treatment systems relies on microbial community structure of the biomass (Flowers et al., 2013). With rapid development of molecular biological technology, microbial community diversity of wastewater treatment biomass has been increasingly investigated in recent years (Guo and Zhang, 2012; Jo et al., 2016). Moreover, the relationship of microbial community composition and environmental variables of activated sludge system has been investigated recently using high-throughput sequencing (Xu et al., 2017). Although microbial community of suspended growing activated sludge has been well studied, studies about community differences of fixed growing biofilm in different chambers of MBBR systems were rather limited.

The functional fractions in activated sludge and biofilm were usually classified into two groups: heterotrophic biomass and autotrophic biomass based on metabolic function. The quantity and activity of heterotrophic biomass and autotrophic biomass play central role in organic matter biodegradation and ammonia nitrification. Assessment of heterotrophic biomass and kinetic parameters of activated sludge model No. 1 - ASM1 (Henze et al., 2000) by respiration tests was initially introduced by Kappeler and Gujer (1992). Ochoa et al. (2002) applied the default values of kinetic and stoichiometric parameters to determine active heterotrophic and autotrophic biomass distribution via respiration tests. Hence, respiration tests were increasingly used coupled with kinetic models for biomass distribution quantification (Fernandes et al., 2013; Tsai and Wu, 2005).

* Corresponding author.
E-mail addresses: xiaodong.wang@nmbu.no, xiaodong.wang01@outlook.com (X. Wang).

https://doi.org/10.1016/j.jenvman.2018.04.015
0301-4797/

Simulation results may be biased if kinetic model parameters were adopted without calibration. Since the kinetic model parameters (e.g. heterotrophic growth rate and autotrophic growth rate) are difficult to be measured directly, they were usually estimated by performing batch test in earlier years (Kappeler and Gujer, 1992; Vanrolleghem et al., 1999). With the development of computer and modelling software, these parameters were more often being estimated via numerical approach, such as sensitivity analysis (Mannina et al., 2011b). However, it is quite often that model outputs were not sensitive to some kinetic model parameters, because biological process models was generally over-parameterized with dozens of variables and model parameters (Cosenza et al., 2014). Therefore, if the inner relationship of kinetic parameters could be established, computational power and time can be saved, and more insights of biochemical reaction of biological wastewater treatment may be obtained.

To the best of our knowledge, microbial diversity of biofilms in multi-stage MBBR system is underexplored. In this study, we investigated microbial community composition of different functional chambers of MBBR system. Moreover, the interaction between microbial composition and kinetic modelling provides insight for modelling and optimization of biological wastewater treatment process.

2. Materials and methods

2.1. MBBR system description

A multi-stage laboratory scale MBBR was set up for this study. As is shown in Fig. 1, domestic wastewater was transported from primary clarifier of the WWTP to a storage tank, which provided constant flow of influent to the MBBR system. The MBBR system was consisted by three functional chambers: anoxic chamber (AN), first aerobic chamber (AE1), and second aerobic chamber (AE2). Each chamber of the reactor was filled with suspended plastic biocarriers. The density of carriers was 0.95 $g \cdot cm^{-3}$ and the specific surface area of the carriers was 600 $m^2 \cdot m^{-3}$. The volume of each chamber was 5 liters. The quantity of carriers in each chamber was 0.32 m^2, in terms of surface area. Dissolved oxygen (DO) in AE1 and AE2 was always higher than 6 $mg \cdot L^{-1}$ to avoid mass transfer limitation among inner layers of biofilm (Ødegaard, 2006). Carriers in upper stream chambers cannot be transported to the downstream chambers, because the opening between each chamber was much smaller than the diameter of carriers. The hydraulic retention time in each chamber was 2 h, and the total hydraulic retention time was 6 h. Nitrified liquid was recycled back to AN for denitrification, with recycle ratio of 1:1.

To create steady-state condition for this study, the concentrations of chemical oxygen demand (COD) and ammonia nitrogen ($NH_4^+ - N$) of inlet wastewater were adjusted to 700 $mg \cdot L^{-1}$ and 50 $mg \cdot L^{-1}$ respectively, by adding sodium acetate and ammonium chloride. The laboratory MBBR system was setup inside the laboratory, where an air conditioner was used to maintain the temperature at 12 °C. Besides, to provide necessary references, a paralleled activated sludge (AS) system was running as a sequencing batch reactor (SBR) with the same daily loading rate. A SBR cycle was four hours (one hour of anoxic reaction, two hours of aerobic reaction, and one hour for sedimentation and refilling, 6 cycles per day). After each cycle, 50% of the supernatant was discharged to regain space for refilling influent. The sludge age was kept as 18 days during the entire test period. Both the MBBR and activated sludge systems have been operated for 40 days before this study was carried out.

2.2. Samples collection and wastewater analysis

After 40 days of steady-state operation (at 12 °C), biofilm samples were collected from every chamber of MBBR during a period of seven days. Five carriers were taken randomly from each chamber every other days, and in total 20 carriers were collected from each chamber. Biofilm was scratched from the carriers and stored at −80 °C immediately after the carriers were taken out from MBBR system. The AS samples were collected from the paralleled SBR system at the same time when biofilm samples were collected.

The influent and outlet water quality of each chamber was analyzed once per day. COD and soluble COD (SCOD) were analyzed using Hach-Lange test kits (LCK 314/514), following the recommended method on spectrophotometer DR 3900. Total suspended solids, ammonia nitrogen ($NH_4^+ - N$), nitrate ($NO_3^- - N$), nitrite ($NO_2^- - N$) and orthophosphate ($PO_4^{3-} - P$) were analyzed following Standard Methods (APHA et al., 2012). The seven-day average water quality of influent and outlet of each chamber was shown in Table 1.

2.3. DNA extraction, PCR and high-throughput sequencing

DNA was extracted from 1.5 mL of AN, AE1, AE2 and AS samples respectively using PowerSoil DNA Isolation Kits (Mo Bio Laboratories, USA) according to manufacturer's instruction. The extracted DNA was checked using 1% agarose gel electrophoresis. The V3-V4 region of the 16S rRNA gene was amplified from extracted DNA using universal primers 338F (ACTCCTACGGGAGGCAGCA) and 806R (GGACTACNNGGGTATCTAAT) (Du et al., 2017). The mixture of 4 μL of 5× FastPfu Buffer, 2 μL of dNTP (2.5 mM), 0.4 μL of each

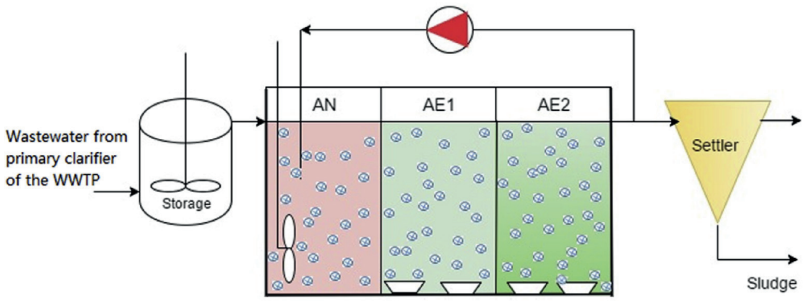

Fig. 1. The flow diagram of the laboratory scale wastewater treatment system. In the MBBR system, AN, AE1 and AE2 represents anoxic chamber, first aerobic chamber and second anoxic chamber, respectively.

Table 1
Average influent and outlet wastewater quality of each MBBR chamber during seven days of biomass sampling (with standard deviations in brackets). The total COD and ammonia of influent were adjusted by adding sodium acetate and ammonium chloride. (The unit of every value is $mg \cdot L^{-1}$).

	Influent	AN outlet	AE1 outlet	AE2 outlet
TSS	260 (±35)	194 (±47)	264 (±63)	242 (±57)
COD	700 (±45)	287 (±106)	329 (±78)	335 (±35)
SCOD	352 (±5)	56 (±15)	19 (±4)	15 (±2)
$NH_4^+ - N$	50 (±0.79)	23.89 (±3.20)	17.27 (±4.15)	4.23 (±1.98)
$NO_3^- - N$	0.83 (±0.11)	3.86 (±2.74)	7.23 (±5.41)	19.23 (±1.52)
$NO_2^- - N$	0.09 (±0.07)	0.02 (±0.04)	0.12 (±0.04)	0.08 (±0.05)
$PO_4^{3-} - P$	4.16 (±1.76)	2.43 (±1.62)	2.33 (±1.09)	2.32 (±1.25)

primer (5 μM), 0.5 μL of DNA and 0.4 μL of Fastpfu Polymerase (TransStart Fastpfu DNA Polymerase, China) were used to perform PCR in a GeneAmp 9700 (Applied Biosystems, USA) PCR system. The thermal cycling was carried out followed the steps as: initial denaturation at 95 °C for 2 min, followed by 25 cycles at 95 °C for 30 s, 55 °C for 30 s, 72 °C for 30 s and final extension at 72 °C for 5 min (Ma et al., 2013; Matar et al., 2017).

After amplification, the triplicate amplicons from each sample were pooled and checked by 2% gel electrophoresis, followed by purification using AxyPrep DNA Gel Extraction Kit (Axgen, USA) according to manufacturer's instructions (Li and Lu, 2017). The PCR products were quantified on the QuantiFluor-ST Fluorometer (Promega, USA). Finally, high-throughput sequencing was performed on an Illumina Miseq platform at Yuanxubio Co., Ltd. (Shanghai, China).

2.4. Processing of sequencing data

The sequencing data were trimmed and analyzed using Mothur software. Considering the length of V3-V4 region, those sequences shorter than 300 bp were removed. Chimeric sequences were removed using Uchime program and the resulting sequences were classified using SILVA database as reference. After discarding the low quality sequences, an average of 42 453 effective sequences were obtained with average length of 420–423 bp for each of the four samples (AN, AE1, AE2 and AS). For community analysis, the sequences were clustered into operational taxonomic units (OTUs) with 0.03 cutoff by Mothur program version 1.38.0. More information can be found in the supplementary material.

2.5. Respiration test and active biomass determination

In this study, we performed respiration tests to quantify active heterotrophic and autotrophic biomass according to Ochoa et al. (2002). Oxygen uptake rate (OUR) of biomass was measured in a closed respiration beaker under three conditions (Table 2), to obtain: (1) endogenous OUR_1; (2) oxygen consumption rate of autotrophic biomass together with endogenous respiration of heterotrophic biomass, OUR_2; (3) and heterotrophic respiration with carbon source and Allythiourea (ATU) to inhibit nitrification, OUR_3. The OUR of heterotrophic biomass $OUR_H = OUR_3$, and OUR of autotrophic biomass $OUR_A = OUR_2 - OUR_1$. Tap water was used in addition with chemicals as listed in Table 2. Dissolved oxygen (DO) was measured by a portable DO sensor (Hach HQ40D). The DO values lower than 6 $mg \cdot L^{-1}$ were not used for OUR calculation, because autotrophic respiration may be restrained due to lower oxygen transfer efficiency among the inner biofilm layers (Ødegaard, 2006).

The mass balance equations of heterotrophs and autotrophs can be derived from ASM1, as is shown in Equation (1) and Equation (2), where the definition of notions were listed in Table 3. Under steady-state condition, Equations (1) and (2) can be simplified into Equations (3a) and (3b) respectively, because either COD or ammonia was sufficient for the corresponding respiration test.

$$\frac{dS_o}{dt} = \mu_{H,\,Max} \cdot \frac{1 - Y_H}{Y_H} \cdot \left(\frac{S_s}{K_s + S_s}\right) \cdot \left(\frac{S_o}{K_{o,H} + S_o}\right) \cdot X_H \tag{1}$$

$$\frac{dS_o}{dt} = \mu_{A,\,Max} \cdot \frac{4.57 - Y_A}{Y_A} \cdot \left(\frac{S_{NH}}{K_{NH} + S_{NH}}\right) \cdot \left(\frac{S_o}{K_{o,A} + S_o}\right) \cdot X_A \tag{2}$$

$$(a)\, X_H = \frac{1}{\mu_{H,Max}} \cdot \frac{Y_H}{1 - Y_H} \cdot OUR_H, \quad (b)\, X_A = \frac{1}{\mu_{A,Max}} \cdot \frac{Y_A}{4.57 - Y_A} \cdot OUR_A \tag{3}$$

2.6. Statistical analysis

Principal coordinate analysis (PCoA) was performed to check the microbial community similarity in Morther 1.38.0. The plot of microbial composition at phylum level and class level was produced in R after removing those phylum accounting less than 1%. The package VennDiagram was employed in R to visualize the overlap relationships of biofilm community. One-way analysis of variance (ANOVA) was used to determine whether bacteria composition in AE2 significantly differ (p-value < 0.05) with corresponding bacteria composition in other groups.

3. Results and discussion

3.1. Microbial community diversity

The sequences obtained from high-throughput sequencing were clustered into 9951 OTUs (operational taxonomic units) at 0.03 nucleotide cutoff. Alpha diversity indices of the pooled four samples AN, AE1, AE2 and AS were shown in Table 4. Good's coverage ranged within 92.86%–95.81%, which suggested that the identified sequences represented the majority of microbial diversity of the corresponding sample (Matar et al., 2017). The relative differences of ACE and Chao 1 values of biofilm from each MBBR chambers were more than 60%, which revealed the differences of microbial diversity in different MBBR chambers. Shannon and Simpson indices suggested that AE2 had a higher diverse microbial community than the biofilm in the other two chambers. Since AE2 is the place mainly for nitrification according to operation results in Table 1, the more diverse microbial community in AE2 may be caused by autotrophic nitrifiers (Young et al., 2017). The diversity

Table 2
Respiration test procedure for OUR determination of active biomass in biofilm.

OUR	Ammonia	Carbon source	ATU
Endogenous, OUR_1	No	No	No
Autotrophic, OUR_2	Yes, 20 mg $N \cdot L^{-1}$	No	No
Heterotrophic, OUR_3	Yes, 20 mg $N \cdot L^{-1}$	Yes, 250 mg $COD \cdot L^{-1}$	Yes, 20 mg $ATU \cdot L^{-1}$

Table 3
Variables and model parameters of active heterotrophic and autotrophic biomass growth models.

Notation	Definition	Units
S_o	Dissolved oxygen	$mg\ COD \cdot L^{-1}$
$\mu_{H,Max}$	Maximum specific growth rate for heterotrophic biomass	day^{-1}
$\mu_{A,Max}$	Maximum specific growth rate for autotrophic biomass	day^{-1}
Y_H	Yield for heterotrophic biomass	$g\ COD \cdot (g\ COD)^{-1}$
Y_A	Yield for autotrophic biomass	$g\ COD \cdot (g\ N)^{-1}$
S_s	Concentration of readily biodegradable COD	$mg\ COD \cdot L^{-1}$
S_{NH}	Ammonia nitrogen	$mg\ N \cdot L^{-1}$
K_s	COD half-saturation coefficient for heterotrophic biomass	$mg\ COD \cdot L^{-1}$
K_{NH}	Ammonia half-saturation coefficient for autotrophic biomass	$mg\ N \cdot L^{-1}$
$K_{o,H}$	Oxygen half-saturation coefficient for heterotrophic biomass	$mg\ O_2 \cdot L^{-1}$
$K_{o,A}$	Oxygen half-saturation coefficient for heterotrophic biomass	$mg\ O_2 \cdot L^{-1}$
X_H	Active heterotrophic biomass	$mg\ COD \cdot L^{-1}$
X_A	Active autotrophic biomass	$mg\ COD \cdot L^{-1}$
a_H	Temperature coefficient for heterotrophs	–
a_A	Temperature coefficient for autotrophs	–

Table 4
Alpha diversity analysis at cutoff 0.03 for biofilm and AS samples.

Sample	OTUs	ACE	Chao 1	Shannon	Simpson	Coverage
AE1	2248	8363.33	5553.665	5.5110	0.0147	0.9457
AE2	3542	14000.72	9007.782	5.7091	0.0140	0.958
AN	4391	22353.76	12844.56	5.5136	0.0219	0.9286
AS	4244	18112.96	11551.54	5.7244	0.0193	0.9546

difference of activated sludge and biofilm was not clear, because the Shannon index of AS was slightly higher than AE2, while ACE, Chao 1 and Simpson indices of AS were within the corresponding index range of biofilm. Principal coordinate analysis (PCoA) was performed to visualize the community similarity (Supplementary material), where AE1 and AE2 located much closer to each other, suggesting that the two types of biofilm in aerobic environment are more similar than mixed cultured activated sludge or anoxic biofilm.

3.2. Bacterial community composition

A total of 27 phyla and 55 classes were identified from the three functional chambers of the MBBR system. In this study, five major phyla (14 major classes) composited 99% of the entire microbial community. The composition of major phyla and classes of both biofilm and AS are shown in Fig. 2a and b, respectively.

Proteobacteria and *Bacteroidetes* were the dominant phyla in both biofilm and AS samples (Fig. 2a), which complied with most of other studies (Ma et al., 2013; Ye et al., 2011). *Nitrospirae* was detected as a major phylum only in AE2 (1.1%). *Nitrospirae* can be hardly detected in AN or AE1 while AS contained less than 0.1%. The phylum *Nitrospirae* is a phylum of nitrite oxidation bacteria (NOB) (Hoang et al., 2014), and the quantity of *Nitrospirae* is highly correlated with nitrification efficiency (Lin et al., 2016). The proportion of *Nitrospirae* in AE2 (1.1%) was equal to that of a previous investigation of eight full-scale WWTPs (Liu et al., 2016). The low organic loading environment in AE2 favored the growing of *Nitrospirae* and other autotrophic bacteria. Another characteristic at phylum level was that *actinobacteria* was not detected in AN. *Actinobacteria* have been reported as heterotrophs (Ye et al., 2011) which can live in both aerobic and non-aerobic environment (Servin et al., 2008). Further investigation of correlations between anoxic biofilm and *actinobacteria* is necessary to figure out the absence of *actinobacteria* in anoxic chamber of MBBR system.

At class level, *Alphaproteobacteria, Betaproteobacteria,*

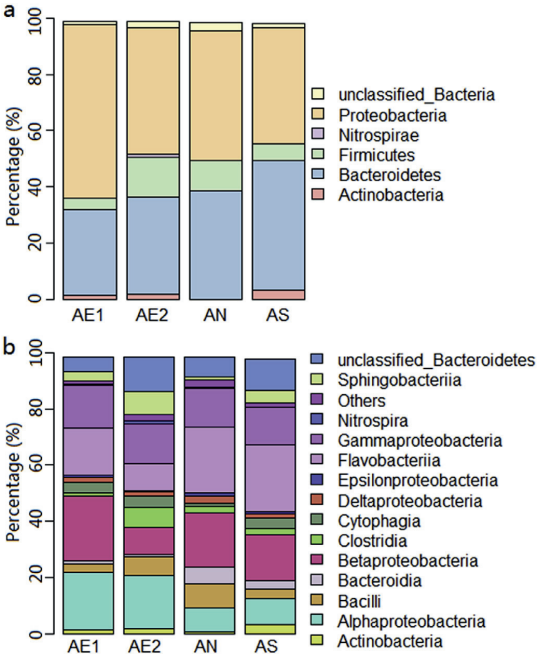

Fig. 2. Microbial community diversity and its composition in each functional chamber of MBBR system and a paralleled activated sludge system at (a) Phylum level; and (b) Class level.

Flavobacteriia, and *Gammaproteobacteria* are the four largest classes in all the samples, which took up 52%–75% of the total microbes (Fig. 2b). *Clostridia* in AE2 (7.1%) were much higher compared with that in AE1 (1.2%), AN (2.6%), and AS (2.2%). *Clostridia* proportion was 4.5%–13% in biofilm (Biswas et al., 2014), and 0.1%–5.73% in activated sludge (Ma et al., 2015), suggesting that Clostridia may be in favor of attached growing. In this study, no specific microbe was found in activated sludge at class level. Jo et al. (2016) concluded that not only microbial community diversity but also its composition were different between the biofilm and activated sludge among membrane bioreactors. Although the composition of AS

microbial community was different with any of the biofilm community, the proportion of each class was within the corresponding range of biofilm community composition.

Since microbial community information of activated sludge system had been well studied in related literatures (Lu et al., 2014; Ma et al., 2013; Ye et al., 2011), we will focus on the multi-stage MBBR system for further discussion in the following text.

A total of 489 genera were identified from the biofilm samples. Fig. 3 shows that 240 genera were shared by the biofilm from each chamber of the MBBR system. AE2 was the most microbial abundant chamber (383 genera) at genus level, while AE1 was the least microbial abundant chamber (319 OTUs) among all three chambers. Comparison of microbial community composition of biofilm from multi-stage MBBR system can be hardly found from scientific publications, even though MBBR system has been widely used. The results extended microbial community studies to biofilm of different functional chambers of MBBR system.

3.3. Proportion of heterotrophs and autotrophs

One of the purposes of performing high-throughput sequencing was to figure out the ratio of heterotrophs and autotrophs in biofilm. The substrate for some well identified bacteria were already known, e.g. *Nitrospirae*, while other autotrophs were difficult to be identified from the taxonomic information obtained previously. Because nitrification performance associated with higher autotrophic nitrifying bacteria composition (Liebig et al., 2001; Quan et al., 2013), we accepted the hypothesis that significantly higher composition of autotrophic nitrifying bacteria existed in nitrification chamber (AE2). Another reason of assuming significantly higher proportion of autotrophs in AE2 is that autotrophic bacteria are in favor of low C/N ratio environment (Kumar et al., 2012; Sun et al., 2014). As most biodegradable COD had been removed in AN and AE1, AE2 became a more favorable place for autotrophs growing. If an OTU proportion from AE2 was significantly higher than that from other biomass samples, the corresponding bacteria would be classified as autotrophs. The other unidentified OTUs were classified as heterotrophs. However, a small fraction of bacteria were neither identified in class or order level, nor their proportions significantly differ with the corresponding OTUs from AE2. These small fractions were left as unknown.

The results based on this classification approach are shown in Fig. 4. The autotroph composition in AE2 was 15.4%, significantly higher than that in AE1 (2.2%). The autotrophs in AN were negligible (0.8%) compared the unknown composition in AN (2.6%).

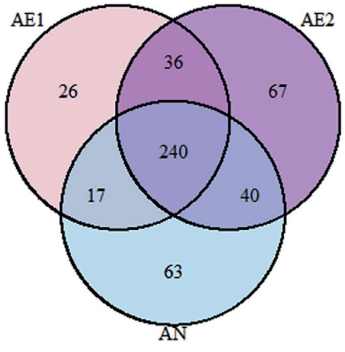

Fig. 3. Overlap of bacterial community at genus level of biofilm from three different functional chambers of MBBR.

Autotrophs occupied 0.5%–4% of total bacteria in full-scale activated sludge system (Ma et al., 2015), measured by high-throughput sequencing methods. However, autotrophs in biomass might be easily underestimated by sequencing method due to taxonomy complexity (Bassin et al., 2017; Ye et al., 2011). For this study, the classification based on statistical significance tests brought estimation errors to the results, but it also avoided underestimating autotroph composition caused by undetected bacteria. We would like to accept the heterotroph/autotroph ratio obtained through this approach.

3.4. Respiration tests and active biomass distribution

Oxygen uptake rates (OURs) of MBBR biofilm were measured by performing respiration tests. The results of respiration of biofilm taken from AE1, AE2, and AN are shown in Fig. 5a, b and c, respectively. Generally, the biomass of AE1 and AN were composed with much larger population of heterotrophs, indicated by the sharp trend slopes of heterotrophic stages (Fig. 5a and c). The sharp decreasing of DO during autotrophic stage of AE2 revealed the existence of larger amount of autotrophs (Fig. 5b).

In this study, the trends of DO decreasing were straight lines when DO decreased from 8.2 to 6 $mg \cdot L^{-1}$. Therefore, the segments 8.2~6 $mg \cdot L^{-1}$ were used to calculate the steady-state OURs. OUR values were calculated as is shown in Table 5. Heterotrophic biomass in AE1 had the highest OUR (36.72 $mg\ O_2 \cdot L^{-1} \cdot h^{-1}$). The OUR of heterotrophic biomass in AN was 32.40 $mg\ O_2 \cdot L^{-1} \cdot h^{-1}$ which achieved the same level as the heterotrophic biomass in AE1. Denitrification biomass were supposed to be the dominant organism in AN, which was mainly composed by heterotrophic bacteria. The highest autotrophic OUR was found from biofilm in AE2 (7.65 $mg\ O_2 \cdot L^{-1} \cdot h^{-1}$). The OUR values were not normalized as specific oxygen uptake rate (SOUR), because the non-normalized OUR values can be used to calculate the amount of active heterotrophic biomass and autotrophic biomass. In this study, the changing of DO values from saturation to around 6 $mg \cdot L^{-1}$ were straight lines (Fig. 5), which suggested constant oxygen uptake rates for the corresponding biomass in this condition. Therefore, only one OUR of each respiration period was derived from Fig. 5.

The quantity of active heterotrophic biomass (X_H) and autotrophic biomass (X_A) can be calculated according to Equation (3a) and Equation (3b), respectively, by applying the default model parameters in ASM1, where $\mu_{H,\ Max,20} = 6\ day^{-1}$, $\mu_{A,Max,20} = 0.8\ day^{-1}$, $Y_H = 0.67g\ COD \cdot (g\ COD)^{-1}$, and $Y_A = 0.24\ g\ COD \cdot (g\ N)^{-1}$. However, these reference values for bacteria growth are given at 20 °C in ASM1, while the MBBR system was running at 12 °C. Therefore, the maximum specific growth rate at 12 °C ($\mu_{H,Max}$ and $\mu_{A,Max}$) should be calculated by applying temperature coefficients. In this study, we used the temperature coefficient suggested by ASM2 (Gujer et al., 1995), where the temperature coefficient for heterotrophs $a_H = 1.07$, and temperature coefficient for autotrophs $a_A = 1.12$. The calculation of $\mu_{H,Max}$ and $\mu_{A,Max}$ are shown in Equation (4) and Equation (5).

$$\mu_{H,Max} = \mu_{H,Max,20} \cdot a_H^{(T-20)} = 3.5 \tag{4}$$

$$\mu_{A,Max} = \mu_{A,Max,20} \cdot a_A^{(T-20)} = 0.3 \tag{5}$$

After calculating the maximum specific growth rates at 12 °C, the biomass distribution in each functional chamber of the MBBR system were obtained (Table 6). AE1 had the highest quantity of total active biomass, where heterotrophic biomass was 511.2 $mg\ COD \cdot L^{-1}$, and autotrophic biomass was 30.9 $mg\ COD \cdot L^{-1}$. Since

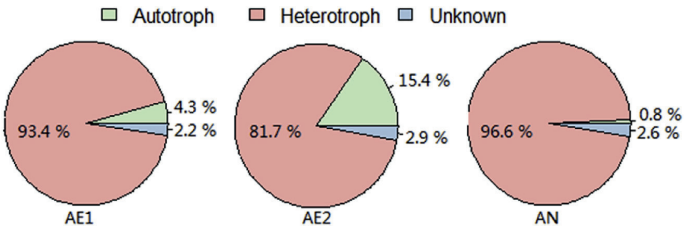

Fig. 4. The proportion of heterotrophic and autotrophic bacteria in AE1, AE2 and AN of MBBR system.

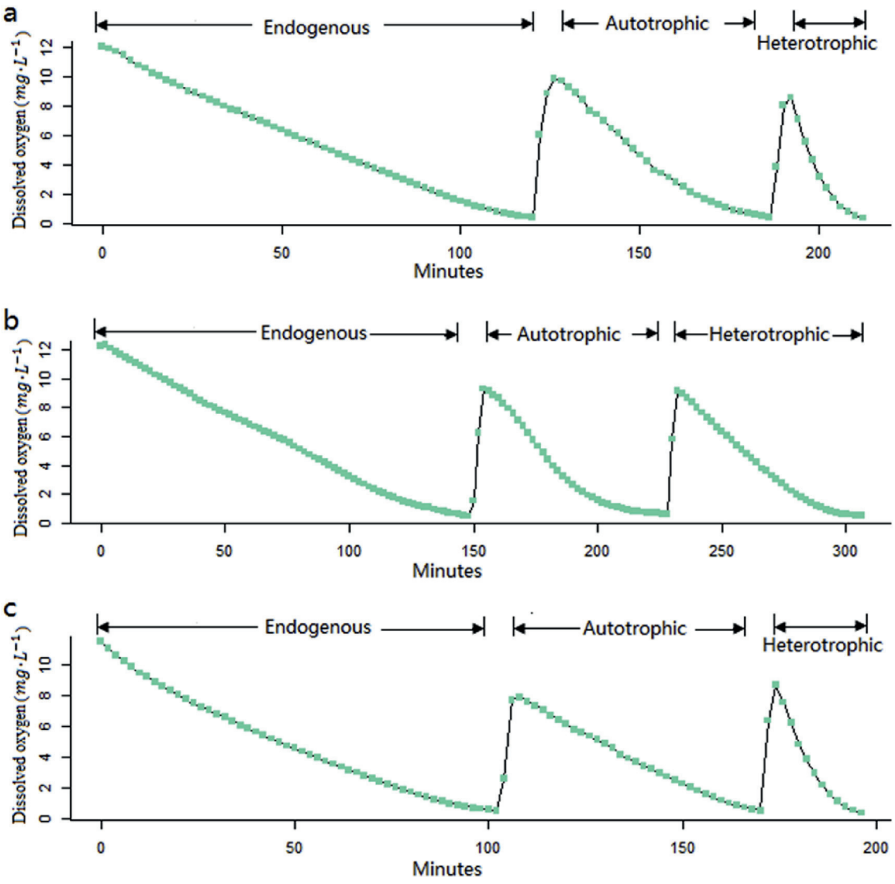

Fig. 5. Respiration test of biofilms taken from (a) AE1, (b) AE2, and (c) AN of the multi-stage MBBR system.

Table 5
OURs of active heterotrophic biomass and autotrophic biomass of biofilm in each functional chamber.

	AE1	AE2	AN
Heterotrophic, OUR_H ($mg\ O_2 \cdot L^{-1} \cdot h^{-1}$)	36.72	9.03	32.40
Autotrophic, OUR_A ($mg\ O_2 \cdot L^{-1} \cdot h^{-1}$)	6.97	7.65	1.66

Table 6
Calculated heterotrophic biomass and autotrophic biomass quantity and ratios, by applying Equation (3) and model parameters in ASM1.

	AE1	AE2	AN
Heterotrophic biomass ($mg\ COD \cdot L^{-1}$)	511.2	125.7	451.0
Autotrophic biomass ($mg\ COD \cdot L^{-1}$)	30.9	33.9	7.4
Heterotrophs ratio	94.3%	78.8%	98.4%
Autotrophs ratio	5.7%	21.2%	1.6%

the substances loading in AE2 was much lower compared with the other chambers, the total active biomass quantity was therefore much lower than that in AE1 and AN. Nevertheless, AE2 had not only the highest autotrophic biomass proportion (21.2%) but also the highest quantity of autotrophic biomass (33.9 $mg\,COD{\cdot}L^{-1}$) among all three chambers. The autotrophic biomass composition in AE1 (5.7%) was less than that of activated sludge (12.2%) reported by Fernandes et al. (2013), but autotrophic biomass in AE2 (21.2%) were much higher. Because biofilm in each chamber is fixed growing, the biomass distribution would be different in each chamber of MBBRs due to environmental selection effect. However, the lack of sufficient literature references makes it difficult to compare biomass distribution of multi-stage MBBR biofilm. It is noteworthy that heterotrophic biomass was still the dominant in AE2 though most biodegradable organic had been removed before the flow entering AE2. The substances for heterotrophic growth in AE2 may come from hydrolysis of slowly biodegradable particles, lysis of microorganism and metabolic products (Namkung and Rittmann, 1986; Okabe et al., 1995). Overall, the respiration tests revealed the biomass distribution of biofilm in different functional chamber of MBBR system. The ratios of active heterotrophic and autotrophic biomass in biofilm from different functional chamber provided reference for further study of multi-stage MBBR system.

3.5. Kinetic model parameters calibration

The estimated values of heterotrophic and autotrophic biomass can represent real active biomass quantity only if the model parameters had been calibrated (Mannina et al., 2011a). Interestingly, the proportions of heterotrophic and autotrophic biomass obtained from respiration tests (Table 6) were comparable with proportions of heterotrophs and autotrophs from sequencing analysis (Fig. 4). The autotrophic biomass ratios obtained from respiration tests in all three chambers were higher than that obtained from sequencing analysis. Noticeable bias of estimated biomass distribution can be found, because the kinetic model parameters ($\mu_{H,Max}$ and $\mu_{A,Max}$) were calculated from the reference values of ASM1 without calibration. Sensitivity analysis was usually used to calibrate kinetic models of biological wastewater treatment system (Cosenza et al., 2014; Eldyasti et al., 2012). However, model calibration using sensitivity analysis cost time and requires computational power, because the ASM was over-parameterized and the model outputs were less sensitive to the changing of kinetic parameters (Liwarska-Bizukojc et al., 2011).

In this study, we were motivated to find a new approach to calibrate model parameters by the interaction of respiration results and sequencing analysis. The ratio of heterotrophic and autotrophic biomass X_H/X_A was a function of $\mu_{H,Max}/\mu_{A,Max}$ according to Equation (3). Thus, the relations of $\mu_{H,Max}$ and $\mu_{A,Max}$ of each chamber were obtained by equalizing X_H/X_A and heterotrophs/autotrophs from sequencing analysis. In AE1, $\mu_{H,Max} = 8.88\,\mu_{A,Max}$, the coefficient is greater than that calculated from the default values in ASM1, where $\mu_{H,Max} = 7.5\,\mu_{A,Max}$. The coefficient for biofilm in AE2 is 8.17 ($\mu_{H,Max} = 8.17\mu_{A,Max}$), which is relatively lower than that for AE1. However, the result for AN ($\mu_{H,Max} = 6.14\mu_{A,Max}$) was not acceptable, because the autotrophic bacteria proportion was even lower than unknown bacteria proportion (Fig. 4). Nevertheless, the proportional relationships of $\mu_{H,Max}$ and $\mu_{A,Max}$ were established for each functional chamber of MBBR system. For sensitivity analysis, kinetic parameters were usually less sensitive than stoichiometric (Liwarska-Bizukojc et al., 2011), which makes it difficult to calibrate kinetic parameters. By establishing the proportional relationship of $\mu_{H,Max}$ and $\mu_{A,Max}$, computational power and time could be saved.

This model parameters calibration approach can be used in practice when a precise process model is required, e.g. soft sensor development. It is also important for both process operation and designing to know the relationship of heterotroph and autotroph growth rate. This calibration approach can be applied whenever it is possible to perform sequencing and respiration tests, but the property of biofilm or activated sludge should be stable during the tests. A well operated biological process would have temporary stable proportion of heterotrophs and autotrophs regardless of daily variation of influent, which provides opportunity to apply this approach.

4. Conclusion

In the multi-stage MBBR system, not only microbial diversity but also its composition were different in each chamber of the MBBR system. The proportion of heterotrophic bacteria and autotrophic bacteria were calculated based on the microbial community composition. The ratios of active heterotrophic biomass and autotrophic biomass (X_H/X_A) were calculated by performing respiration tests. Relationships of kinetic parameters $\mu_{H,Max}$ and $\mu_{A,Max}$ were established by accepting heterotrophs/autotrophs ratios equal to X_H/X_A. The results proved that molecular microbiology analysis data can be further applied to solve practical engineering problems. This approach developed in this study can be further used for biological process modelling and control.

Acknowledgements

The work was supported by the RECOVER project, granted by the Reserach Council of Norway (grant number 247612); and the National Natural Science Fund of China (grant number 51078192).

Appendix A. Supplementary data

Supplementary data related to this article can be found at https://doi.org/10.1016/j.jenvman.2018.04.015.

References

APHA, AWWA, WEF, 2012. Standard Methods for the Examination of Water and Wastewater, twenty-second ed. American Public Health Association, Washington, D.C.

Bassin, J.P., Rachid, C.T.C.C., Vilela, C., Cao, S.M.S., Peixoto, R.S., Dezotti, M., 2017. Revealing the bacterial profile of an anoxic-aerobic moving-bed biofilm reactor system treating a chemical industry wastewater. Int. Biodeterior. Biodegr. 120, 152–160. https://doi.org/10.1016/j.ibiod.2017.01.036.

Biswas, K., Taylor, M.W., Turner, S.J., 2014. Successional development of biofilms in moving bed biofilm reactor (MBBR) systems treating municipal wastewater. Appl. Microbiol. Biotechnol. 98, 1429–1440. https://doi.org/10.1007/s00253-013-5082-8.

Cosenza, A., Mannina, G., Vanrolleghem, P. a., Neumann, M.B., 2014. Variance-based sensitivity analysis for wastewater treatment plant modelling. Sci. Total Environ. 470–471, 1068–1077. https://doi.org/10.1016/j.scitotenv.2013.10.069.

Delnavaz, M., Ayati, B., Ganjidoust, H., 2010. Prediction of moving bed biofilm reactor (MBBR) performance for the treatment of aniline using artificial neural networks (ANN). J. Hazard. Mater. 179, 769–775. https://doi.org/10.1016/j.jhazmat.2010.03.069.

Di Trapani, D., Di Bella, G., Mannina, G., Torregrossa, M., Viviani, G., 2014. Comparison between moving bed-membrane bioreactor (MB-MBR) and membrane bioreactor (MBR) systems: influence of wastewater salinity variation. Bioresour. Technol. 162, 60–69. https://doi.org/10.1016/j.biortech.2014.03.126.

Du, R., Cao, S., Li, B., Niu, M., Wang, S., Peng, Y., 2017. Performance and microbial community analysis of a novel DEAMOX based on partial-denitrification and anammox treating ammonia and nitrate wastewaters. Water Res. 108, 46–56. https://doi.org/10.1016/j.watres.2016.10.051.

Eldyasti, A., Nakhla, G., Zhu, J., 2012. Development of a calibration protocol and identification of the most sensitive parameters for the particulate biofilm models used in biological wastewater treatment. Bioresour. Technol. 111, 111–121. https://doi.org/10.1016/j.biortech.2012.02.021.

Fernandes, H., Hoffmann, H., Antonio, R.V., Costa, R.H.R., 2013. The role of microorganisms in a full-scale sequencing batch reactor under low aeration and different cycle times. Water Environ. Res. 86, 800–809. https://doi.org/10.2175/106143013X13807328848450.

Flowers, J.J., Cadkin, T.A., McMahon, K.D., 2013. Seasonal bacterial community

dynamics in a full-scale enhanced biological phosphorus removal plant. Water Res. 47, 7019–7031. https://doi.org/10.1016/j.watres.2013.07.054.
Gujer, W., Henze, M., Mino, T., Matsuo, T., Wentzel, M.C., Marais, v., G.R, 1995. The activated sludge model No. 2: biological phosphorus removal. Water Sci. Technol. 31, 1–11. https://doi.org/10.1016/0273-1223(95)00175-M.
Guo, F., Zhang, T., 2012. Profiling bulking and foaming bacteria in activated sludge by high throughput sequencing. Water Res. 46, 2772–2782. https://doi.org/10.1016/j.watres.2012.02.039.
Guo, W., Ngo, H.-H., Dharmawan, F., Palmer, C.G., 2010. Roles of polyurethane foam in aerobic moving and fixed bed bioreactors. Bioresour. Technol. 101, 1435–1439. https://doi.org/10.1016/j.biortech.2009.05.062.
Henze, M., Gujer, W., Mino, T., van Loosdrecht, M.C.M., 2000. Activated Sludge Models: ASM1, ASM2, ASM2d and ASM3. Scietific and Technical Report No. 9. IWA Publishing, London, UK.
Hoang, V., Delatolla, R., Abujamel, T., Mottawea, W., Gadbois, A., Laflamme, E., Stintzi, A., 2014. Nitrifying moving bed biofilm reactor (MBBR) biofilm and biomass response to long term exposure to 1 °C. Water Res. 49, 215–224. https://doi.org/10.1016/j.watres.2013.11.018.
Jo, S.J., Kwon, H., Jeong, S.Y., Lee, C.H., Kim, T.G., 2016. Comparison of microbial communities of activated sludge and membrane biofilm in 10 full-scale membrane bioreactors. Water Res. 101, 214–225. https://doi.org/10.1016/j.watres.2016.05.042.
Kappeler, J., Gujer, W., 1992. Estimation of Kinetic parameters of heterotrophic biomass under aerobic conditions and characterization of wastewater for activated sludge modelling. Water Sci. Technol. 25, 125–139.
Kumar, M., Lee, P.Y., Fukusihma, T., Whang, L.M., Lin, J.G., 2012. Effect of supplementary carbon addition in the treatment of low C/N high-technology industrial wastewater by MBR. Bioresour. Technol. 113, 148–153. https://doi.org/10.1016/j.biortech.2011.12.102.
Li, J., Lu, X., 2017. Performance and microbial diversity in a low-energy ANF-WDSRBC system for the post-treatment of decentralized domestic wastewater. Water 9, 1–12. https://doi.org/10.3390/w9050330.
Liebig, T., Wagner, M., Bjerrum, L., Denecke, M., 2001. Nitrification performance and nitrifier community composition of a chemostat and a membrane-assisted bioreactor for the nitrification of sludge reject water. Bioprocess Biosyst. Eng. 24, 203–210. https://doi.org/10.1007/s004490100234.
Lin, J., Zhang, P., Li, G., Yin, J., Li, J., Zhao, X., 2016. Effect of COD/N ratio on nitrogen removal in a membrane-aerated biofilm reactor. Int. Biodeterior. Biodegr. 113, 74–79. https://doi.org/10.1016/j.ibiod.2016.01.009.
Liu, T., Liu, S., Zheng, M., Chen, Q., Ni, J., 2016. Performance assessment of full-scale wastewater treatment plants based on seasonal variability of microbial communities via high-throughput sequencing. PLoS ONE 11 (4). https://doi.org/10.1371/journal.pone.0152998.
Liwarska-Bizukojc, E., Olejnik, D., Biernacki, R., Ledakowicz, S., 2011. Calibration of a complex activated sludge model for the full-scale wastewater treatment plant. Bioprocess Biosyst. Eng. 34, 659–670. https://doi.org/10.1007/s00449-011-0515-1.
Lu, H., Chandran, K., Stensel, D., 2014. Microbial ecology of denitrification in biological wastewater treatment. Water Res. 64, 237–254. https://doi.org/10.1016/j.watres.2014.06.042.
Ma, J., Wang, Z., Yang, Y., Mei, X., Wu, Z., 2013. Correlating microbial community structure and composition with aeration intensity in submerged membrane bioreactors by 454 high-throughput pyrosequencing. Water Res. 47, 859–869. https://doi.org/10.1016/j.watres.2012.11.013.
Ma, Q., Qu, Y., Shen, W., Zhang, Z., Wang, J., Liu, Z., Li, D., Li, H., Zhou, J., 2015. Bacterial community compositions of coking wastewater treatment plants in steel industry revealed by Illumina high-throughput sequencing. Bioresour. Technol. 179, 436–443. https://doi.org/10.1016/j.biortech.2014.12.041.
Mannina, G., Cosenza, A., Vanrolleghem, P.A., Viviani, G., 2011a. A practical protocol for calibration of nutrient removal wastewater treatment models. J. Hydroinf. 13, 575. https://doi.org/10.2166/hydro.2011.041.
Mannina, G., Trapani, D. Di, Viviani, G., Ødegaard, H., 2011b. Modelling and dynamic simulation of hybrid moving bed biofilm reactors: model concepts and application to a pilot plant. Biochem. Eng. J. 56, 23–36. https://doi.org/10.1016/j.bej.2011.04.013.
Matar, G.K., Bagchi, S., Zhang, K., Oerther, D.B., Saikaly, P.E., 2017. Membrane biofilm communities in full-scale membrane bioreactors are not randomly assembled and consist of a core microbiome. Water Res. 123, 124–133. https://doi.org/10.1016/j.watres.2017.06.052.
Namkung, E., Rittmann, B.E., 1986. Soluble microbial products (SMP) formation kinetics by biofilms. Water Res. 20, 795–806. https://doi.org/10.1016/0043-1354(86)90106-5.
Ochoa, J.C., Colprim, J., Palacios, B., Paul, E., Chatellier, P., 2002. Active heterotrophic and autotrophic biomass distribution between fixed and suspended systems in a hybrid biological reactor. Water Sci. Technol. 46, 397–404.
Okabe, S., Hirata, K., Watanabe, Y., 1995. Dynamic changes in spatial microbial distribution in mixed-population biofilms: experimental results and model simulation. Water Sci. Technol. 32, 67–74.
Ødegaard, H., 2006. Innovations in wastewater treatment: the moving bed biofilm process. Water Sci. Technol. 53, 17–33. https://doi.org/10.2166/wst.2006.284.
Quan, X., Gu, L., Qian, Y., Pei, Y., Yang, Z., 2013. Characterization of nitrification performance and microbial community in a MBBR and integrated GBBR-MBBR treating heavily polluted river water. Environ. Eng. Manag. J. 12, 1335–1344.
Servin, J.A., Herbold, C.W., Skophammer, R.G., Lake, J.A., 2008. Evidence excluding the root of the tree of life from the actinobacteria. Mol. Biol. Evol. 25, 1–4. https://doi.org/10.1093/molbev/msm249.
Sun, F., yun, Lv, mei, X., Li, J., Peng, yi, Z., Li, P., Shao, fei, M., 2014. Activated sludge filterability improvement by nitrifying bacteria abundance regulation in an adsorption membrane bioreactor (Ad-MBR). Bioresour. Technol. 170, 230–238. https://doi.org/10.1016/j.biortech.2014.07.092.
Tsai, Y.P., Wu, W.M., 2005. Estimating biomass of heterotrophic and autotrophic bacteria by our batch tests. Environ. Technol. 26, 601–613. https://doi.org/10.1080/09593330.2001.9619500.
Vanrolleghem, P.A., Spanjers, H., Petersen, B., Ginestet, P., Takacs, I., 1999. Estimating (combinations of) Activated Sludge Model No. 1 parameters and components by respirometry. Water Sci. Technol. 39, 195–214. https://doi.org/10.1016/S0273-1223(98)00786-0.
Xu, D., Liu, S., Chen, Q., Ni, J., 2017. Microbial community compositions in different functional zones of Carrousel oxidation ditch system for domestic wastewater treatment. Amb. Express 7, 40. https://doi.org/10.1186/s13568-017-0336-y.
Ye, L., Shao, M.F., Zhang, T., Tong, A.H.Y., Lok, S., 2011. Analysis of the bacterial community in a laboratory-scale nitrification reactor and a wastewater treatment plant by 454-pyrosequencing. Water Res. 45, 4390–4398. https://doi.org/10.1016/j.watres.2011.05.028.
Young, B., Delatolla, R., Kennedy, K., Laflamme, E., Stintzi, A., 2017. Low temperature MBBR nitrification: microbiome analysis. Water Res. 111, 224–233. https://doi.org/10.1016/j.watres.2016.12.050.

Appendix A. Supplementary material

Microbial community of a multi-stage moving bed biofilm reactor and using bacterial composition to supervise kinetic model parameters estimation

Xiaodong Wang [a, *], Xuejun Bi [b], Lars John Hem [a, c], Harsha Ratnaweera [a]

[a] Faculty of Science and Technology, Norwegian University of Life Sciences, P.O. Box 5003-IMT, 1432 Aas, Norway

[b] Qingdao Technological University, State and Local Joint Engineering Research Center of Urban Wastewater Treatment and Reclamation in China, Fushun Road 11, 266033 Qingdao, China

[c] Oslo Water and Sewage Works, Herslebs Gate 5, 0561 Oslo, Norway

*Corresponding author: xiaodong.wang@nmbu.no, xiaodong.wang01@outlook.com

Table S1 Effective sequences number and length of sequences obtained from the four pooled samples.

Sample	Read number	Min. length	Max. length	Average length
AE1	24 016	390	440	422
AE2	48 985	388	439	420
AN	40 733	399	438	424
AS	56 080	375	441	423

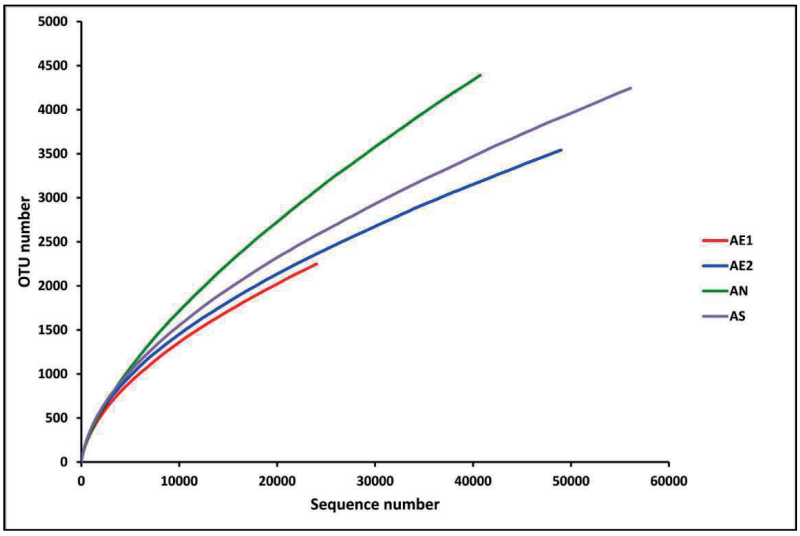

Figure S1 Rarefaction curves of OTUs defined at 3 % distance.

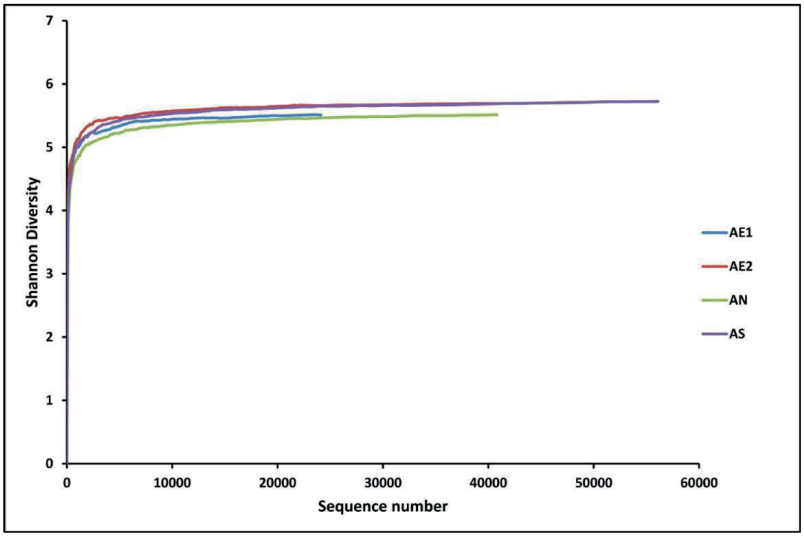

Figure S2 Shannon diversity curve at OUT cutoff 0.03.

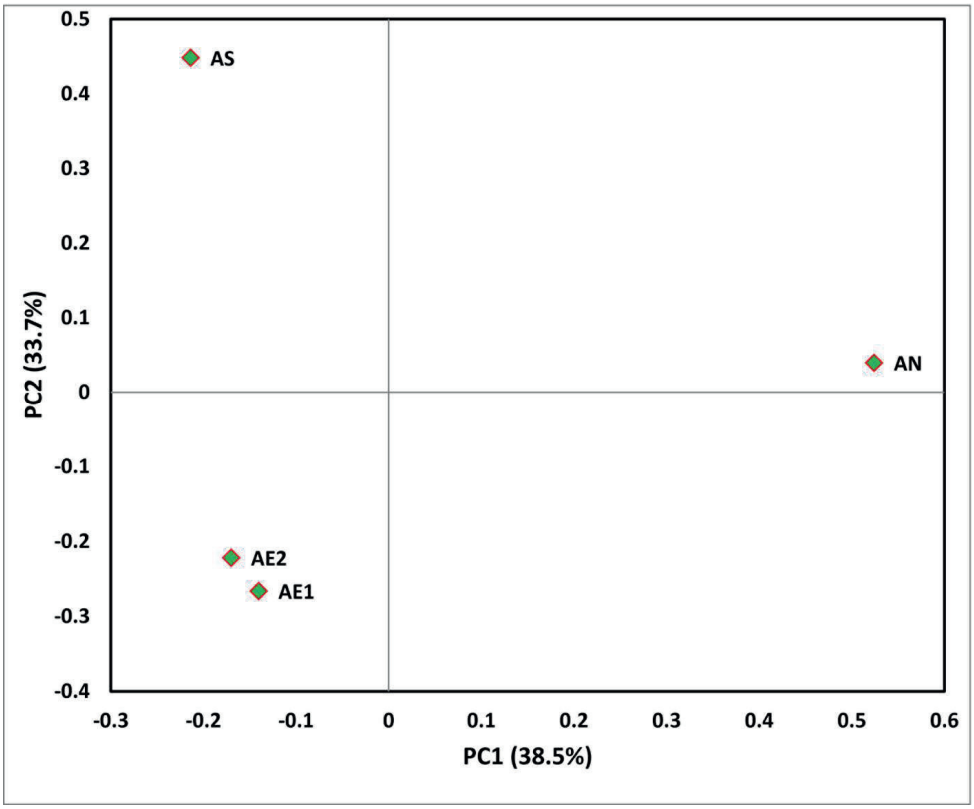

Figure S3 Principal coordinate analysis (PCoA) of biofilm and AS samples to check the similarity of microbial communities.

Paper V

Wang, X., Kvaal, K., Ratnaweera, H. Explicit and interpretable nonlinear soft sensor models for influent surveillance at a full-scale wastewater treatment plant. (Manuscript submitted to Journal of Process Control).

Explicit and interpretable nonlinear soft sensor models for influent surveillance at a full-scale wastewater treatment plant

Xiaodong Wang [a, *], Knut Kvaal[a], Harsha Ratnaweera[a]

[a] Faculty of Science and Technology, Norwegian University of Life Sciences, P.O. Box 5003-IMT, 1432 Aas, Norway

*Corresponding author: xiaodong.wang01@outlook.com, xiaodong.wang@nmbu.no

Abstract

In wastewater treatment plants, the most adopted sensors are those with the properties of low cost and fast response. Soft sensors are alternative solutions to the hardware sensor for online monitoring of hard-to-measure variables, such as chemical oxygen demand (COD) and total phosphorus (TP). The purpose of this study is to obtain a modelling approach which is able to identify the nonlinearity of influent and explain the correlation of inputs-outputs. Thus, the variation of influent characteristics was investigated at the first stage, which provided the basis to build global and local multiple linear regression models. Secondly, a nonlinear modelling tool multivariate adaptive regression splines (MARS) was applied for influent COD and TP prediction. Satisfactory prediction accuracy was obtained in terms of root mean square error (RMSE) and R^2. Unlike other machine learning techniques which are "black box" models, MARS provided interpretable models which explained the nonlinearity and correlation of inputs-outputs. The MARS models can be used not only for prediction, but also to provide insight of influent variation.

Keyword: Multiple linear regression; Multivariate adaptive regression splines; MARS; Nonlinear model; Soft sensor; Wastewater treatment plant

1. Introduction

The increasing requirement of wastewater treatment efficiency and economics have driven more researchers and practitioners to the field of surveillance and control of wastewater treatment plants (WWTPs) [1]. One of the limitations to achieve advanced control of WWTPs is the lack of robust and affordable online measurement instruments for some water quality variables. Fortunately, lack of hardware sensor measurements does not mean lack of information. The inner correlation and propagation trend of multiple wastewater characteristics opens another window to find low-cost solutions for global public health.

With the development of data science and machine learning techniques, more researchers have attempted to obtain unmeasured variable values by data mining and modelling [2–4]. An indirect data retrieval

method, named soft sensor (or virtual sensor) was developed to obtain hard-to-measure variables by manipulating easy-to-measure variables. In WWTPs, the hard-to-measure variables are either associated with a long time-delay or high capital cost [5]. The easy-to-measure process variables are typically pH, conductivity, oxidation/reduction potential (ORP), turbidity, temperature, flowrate and probably ammonium nitrate due to recent technological development [6]. The data-driven soft sensors use easy-to-measure variables as inputs to construct prediction models, and the outputs are usually the hard-to measure variables [7–9]. Chemical oxygen demand (COD) and total phosphorus (TP) are two of the most important water quality variables for wastewater treatment process. However, the online real-time measurement of these two variables were limited due to the cost of the devices and long time-delay for real-time control. Thus, soft sensors become a potential solution for WWTPs to measure these variables online.

In practice, several statistical learning and machine learning algorithms have been applied for soft sensor modelling. The conventional multiple linear regression (MLR) has been used for water quality prediction as interpretable methods [10,11]. MLR models have the advantages of simplicity and easy interpretability, which can be easily programmed for surveillance and control in practice. However, since MLR assumes the linearity of input-output relation, its limits in prediction accuracy have also been addressed in several water related studies [12,13]. Several nonlinear statistical learning and machine learning methods have been tested to build water quality soft sensor models [14–16], and the most studied methods for water quality soft sensor are neural networks [9,17,18]. Nonlinear models can be easily simulated nowadays, but it is still a challenge to apply complicated nonlinear models in practice [1]. Neural networks' capability of prediction and nonlinearity capture were well addressed in various literature, but lack of interpretability has limited their value, because the insight of dataset and natural characteristics of input-output are usually left unexplained as "black boxes" [19]. Another drawback of training the neural networks is the lack of general protocol to determine the structure, i.e. the number of layers and neurons [14,20]. Nevertheless, researchers and practitioners will continue the effort to make data-driven soft sensors more feasible due to their fantastic potential to substitute hardware sensors and overcome measurement delay [21].

Application of sophisticated modelling techniques does not always pay off unless the methods were critically compared with simpler methods [22]. In this study, we attempted to investigate the correlation of predictors and response variables and simultaneously build soft sensors models for chemical oxygen demand (COD) and total phosphorus (TP) of WWTP influent. A global linear model may not work well in different seasonal and climate conditions, even in a selected WWTP. Local models for each of the subsets can be obtained by dividing the general dataset into several subsets based on different conditions.

This is the conventional solution to simultaneously deal with nonlinear prediction and to capture the insights of nonlinear relationships. A well established statistical learning method named Multivariate Adaptive Regression Splines (MARS) developed by Friedman is an alternative solution to achieve the goal of this study [23].

Multivariate adaptive regression splines (MARS) can be used in data mining and prediction for complex and high-dimensional nonlinear data. Kuter et al. applied both MARS and multilayer feedforward artificial neural network (ANN) for fractional snow cover estimation [19]. The MARS approach performed the same as ANN, but was more computationally efficient in model building. Moreover, MARS has been proven as an efficient tool in the prediction of phenol and nitrophenol adsorption [13], classification of satellite images [24], rainfall-runoff simulation [25], and identification of dominant interaction of climatic effect on rainfall and water availability [26]. The advantage of MARS is its ability to automatically add knots to the general curve, which break the global model into piecewise linear polynomial splines. By smoothly connecting spline pieces, the MARS model is able to capture both the linearity and nonlinearity. Therefore, MARS retains the interpretability of linear models, and it is also capable to provide insight of the natural phenomenon.

The primary goal of this study is to derive explicit soft sensor models, which can be used to predict hard-to-measure WWTP influent variables. However, training and validating nonlinear models requires a large quantity of measured data to perform sufficient model runs [27]. Although running these models may not be computationally expensive, it is too expensive and time consuming to obtain a large dataset of influent wastewater quality. Therefore, the secondary goal of this this study is to obtain interpretable nonlinear models with limited full-scale WWTP influent data.

2. Materials and methods

2.1 Dataset and problem description

A multivariate dataset of WWTP influent characteristics was obtained by sampling and analyzing the hourly influent quality and quantity. The dataset was supposed to cover influent characteristics of both warm and cold season in Norway. Due to the high cost of laboratory analysis and time limitation, thes sampling lasted six days in warm season, and five days in cold season. Samples were collected in every hour and 24 samples were collected in each sampling day. In warm season, all of the samples were collected in dry climate condition (no storm event). Melting snow resulted in occasional wet climate condition in cold season. The cold season data were collected in both dry climate and wet climate conditions. The general dataset can be divided into three subsets (Warm-Dry, Cold-Dry and Cold-Wet) by applying a classifier developed in a previous study [28].

There are both easy-to-measure variables and hard-to-measure variables in the dataset. In the context of soft sensor development, the easy-to-measure variables are pH, flow rate (Flow), total suspended solid (TSS), water temperature (WaterTemp), and ammonium nitrate (NH_4-N). The hard-to-measure variables are chemical oxygen demand (COD) and total phosphorus (TP), because online measurement devices for these two variables are expensive and have long time-delays which prevent them from being used for real-time surveillance and control. Therefore, we are interested to study the correlation of these easy-to-measure variables and hard-to-measure variables, and to obtain soft sensor models as alternatives of hardware sensors.

2.2 Global and piecewise multiple linear regression (MLR)

Multiple linear regression (MLR) is the linear model trained based on least square estimation, which is a simple way to interpret the correlations of inputs and outputs. To increase prediction accuracy, high order terms and interaction terms can be involved as inputs. In this study, square terms of original variables and two-effect-interaction terms were applied in MLR models. All the original variables, square terms and interaction terms were included to train an over-fitted model at the first step. Secondly, backward stepwise selection method was applied to eliminate non obligatory prediction terms based on Akaike's information criterion (AIC) to obtain the "shrunk model" with only significant variables [29]. The global MLR models were trained based on the general dataset, and the piecewise local models were trained based on corresponding subsets. At last, every 10-12 observations were randomly selected to form several folds, and these folds were employed to perform cross validation to verify the final model.

2.3 Multivariate adaptive regression splines

Multivariate adaptive regression splines (MARS) was initially presented by Frieman as a nonlinear regression method [23]. It can be viewed as an integration of piecewise linear regression, which captures nonlinearity by adding knots to input variables to break the curve into piecewise basis functions. The general form of the MARS model is expressed as:

$$Y = \beta_0 + \sum_{i=1}^{M} \beta_i \cdot h_i(\boldsymbol{X^n}) + \varepsilon \qquad (1)$$

where $h_i(\boldsymbol{X})$ is the basis function representing each piece of local linear regression, and β_i is the associated coefficient. The coefficients β were estimated based on the least squares method. The basis functions have the following form:

$$h(x)_+ = \begin{cases} x - k, & if\ x > k \\ 0, & otherwise \end{cases};$$

$$h(x)_- = \begin{cases} k - x, & if\ x < k \\ 0, & otherwise \end{cases} \quad (2)$$

where k is a univariate knot. Thus, the MARS method produces continuous models. The determination of basis functions was a data-driven process. MARS can apply both forward stepwise and backward stepwise to select inputs. In this study, second order terms and interaction terms are involved and being selected automatically. The cross validation method was applied to verify MARS models in the same way as it is used for MLRs. The "earth" package was applied in R to build MARS models [30].

Unlike neural network based methods, statistical learning methods such as MARS should not be viewed as black boxes [31]. MARS retained the interpretability to explain the nonlinear correlation of inputs and outputs.

3. Results and discussion

3.1 Variation of wastewater characteristics

The variation of influent quantity and quality of wastewater treatment plants contributes major uncertainties to process operation, designing and modelling [32,33]. Our previous study had shown the daily, weekly and seasonal variation of influent, caused by both human activity and climate [28]. To further investigate the correlation of wastewater quality and quantity, the variation of flowrate and contaminants under different conditions was monitored, as shown in Figure 1. Figure 1(a) showed 5-day continuous measurement of influent flowrate (Flow), COD, TSS and ammonium nitrogen (NH_4-N) during warm season. Only dry climate condition was observed during the sampling days (Warm-Dry condition). Generally, the wastewater contaminants concentration increased or decreased at the same time as the flowrate, which indicated the linearity of influent quality and quantity. The linearity of influent variation in dry climate may be traced back to regular human activity, and it provides the possibility to establish explicit soft sensor models.

However, the variation of influent in dry climate condition and wet climate condition follows different statistical distribution [34]. To capture the influent characteristics in wet climate condition, continuous sampling and measurement of influent quality and quantity was conducted in snow season for six days. This was done as unpredictable snow melting may happen at any time during the day [35,36]. In this study, As shown in Figure 1(b), the wastewater quality propagated differently than influent flowrate when the climate factor was shifted to wet condition due to snowmelt (Figure 1b). The drop and rise feature of influent characteristics during freezing cold time (Cold-Dry condition) was similar to that in Warm-Dry condition. While there was snow melting (Cold-Wet condition), contaminants concentration

decreased due to dilution because flowrate increased dramatically. Figure 1(b) indicates that the climate effect increased the uncertainty of influent variation.

Overall, the nonlinearity of influent characteristics was the combined effect of both human activity and climate. To develop soft sensor models for influent quality prediction, the nonlinearity in different scenarios should be considered.

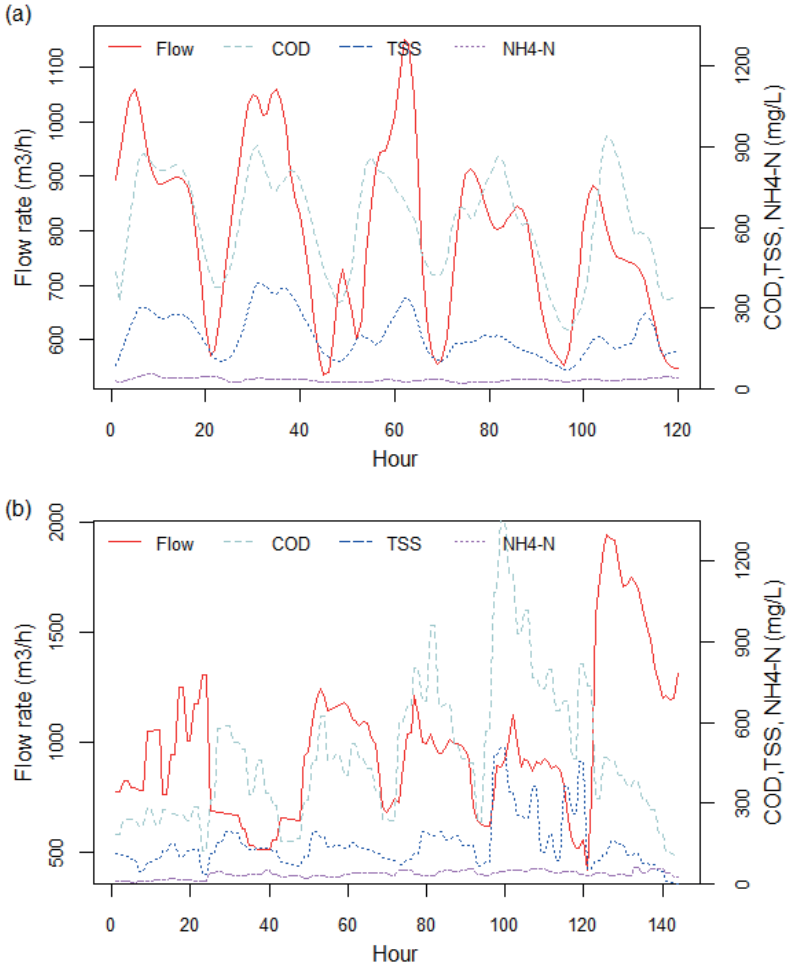

Figure 1 The hourly data of influent flowrate, COD, TSS and ammonium in (a) warm season, no storm events happened during five days observation (Warm-Dry condition);(b) cold season, with both dry and climate conditions.

3.2 Global and piecewise multiple linear regression

Though it is difficult to detect when the wet climate starts due to snow melting, the general dataset can be split into Warm-Dry, Cold-Dry and Cold-Wet subsets by applying statistical learning algorithm according to the previous study [28]. The next step is to investigate the correlation between influent characteristic factors. Since COD and total phosphorus (TP) are not easy to measure directly by online sensors, it is more essential to study the prediction accuracy of COD and TP.

Multiple linear regression (MLR) method was used to build models for COD and TP prediction and study the influence of interaction term on prediction accuracy. Independent variables flowrate (Flow), water temperature (WaterTemp), total suspended solid (TSS), ammonium nitrogen (NH_4-N) and pH were selected as predictors. This is because these variables are relatively easy-to-measure variables in WWTPs. Moreover, quadratic terms and interaction terms were also included to build an over-fitted model with all the possible features as prediction terms. Secondly, backward stepwise selection method was applied to eliminate non obligatory prediction terms based on Akaike's information criterion (AIC) to avoid over-fitting [29]. The selected prediction terms and coefficients for the final models of COD and TP were listed in Table S1 and Table S2 in supplementary material. In this study, we intended to obtain soft sensor models that are applicable in different seasonal and climate conditions. Therefore, regression models for COD and TP prediction was established based on the general dataset (Table S1) and subsets of different conditions (Table S2).

The results of linear multiple linear regression (MLR) modelling was sown in Table 1. For COD predictions, the model built on the general dataset without interaction term was a second order polynomial equation (MLR 1). While the COD model with interaction terms (MLR 2) contains both second order and interaction terms. In total 13 prediction terms were selected by AIC backward stepwise selection. The model performance in terms of RMSE were quite close for MLR1 and MLR2. The cross-validated R^2 of MLR 1 (0.835) was approximately equal to that of MLR 2 (0.847), which indicates limited contribution from interaction term for COD prediction.

Considering the uncertainty of full-scale WWTPs and the criteria of prediction accuracy for wastewater soft sensors in literature [11,15,37], it would be sufficient to build soft sensor for influent monitoring if R^2 is higher than 0.80. Therefore, Model 1 is simple and robust enough to serve as a global model for COD prediction. However, the second order polynomial without interaction term for TP prediction (MLR 3) was not as satisfactory as MLR 1 for COD prediction, but Model 4 with three square terms and seven interaction terms performed much better in terms of RMSE and R^2. The cross-validated R^2 was slightly lower than R^2, which indicated that the model was not over fitted. Therefore, the interaction term was necessary to train a global MLR model for TP prediction.

Unlike global COD models, there was a clear difference in the prediction accuracy for global TP which was caused by interaction terms. Local MLR models were built to study the linearity of TP and its correlation with easy-to-measure variables. RMSE would no longer serve as a fair comparison index, because the TP values in wet climate were significantly lower than that in dry climate. Therefore, the comparison of piecewise MLR models was based on R^2 only in this case.

As shown in Table 1, the MLR model built on Warm-Dry subset (MLR 5) appeared with satisfactory prediction accuracy. While the R^2 of the other piecewise local MLRs did not reach the criteria of 0.80, regardless of interaction terms. Although R^2 of MLRs in cold season can be improved by including interaction terms, the cross-validated R^2 values of MLR 7 and MLR 9 were too low to serve as soft sensor models. The results in Table 1 revealed the higher nonlinearity of TP variation in the influent.

A satisfactory global COD prediction model can be obtained by applying multiple linear regression. For TP prediction, interaction terms were necessary to obtain similar prediction accuracy as the COD MLR model. The piecewise MLRs for TP performed poorly. The nonlinearity of TP requires further study.

Table 1 Mutiple linear regression (MLR) performance for global (using general dataset) and piecewise (subsets of general dataset) COD and TP prediction.

Model	Target variable	Interaction term	Dataset	RMSE	R^2	Cross validation R^2
MLR 1	COD	No	General	98.128	0.840	0.835
MLR 2		Yes	General	92.360	0.859	0.847
MLR 3	TP	No	General	0.919	0.714	0.707
MLR 4		Yes	General	0.658	0.853	0.845
MLR 5		No	Warm-Dry	0.607	0.821	0.813
MLR 6		No	Cold-Dry	0.809	0.532	0.490
MLR 7		Yes	Cold-Dry	0.572	0.766	0.715
MLR 8		No	Cold-Wet	0.365	0.705	0.643
MLR 9		Yes	Cold-Wet	0.317	0.774	0.696

3.3 Multivariate adaptive regression splines

The piecewise MLR models in the last section were built based on the classification of season-climate conditions. Multivariate adaptive regression splines (MARS) can provide smooth piecewise function without specific assumptions of the relationship between predictors and target variables [23]. The knots and splines are automatically selected based on the property of the data rather than being pre-defined. One of the objectives of this work is to develop interpretable models for COD and TP prediction, which can

deal with both linear and nonlinear problems with sufficient accuracy. Although MARS has advantage in interpretability [19], MARS has been used less in the field of water quality and wastewater treatment compared with neural network. Soft sensor models that can provide more explicit information were preferred for the surveillance and control of wastewater treatment process.

As shown in Table S3 in supplementary material, MARS models were built for global influent COD and TP prediction. The MARS model for COD prediction employed square terms but interaction terms were not applied. On the contrary, the application of interaction terms in the TP model reflected that the joint effects of influent variables were significant for TP prediction. The scatter plot of predicted COD and TP by MARS model were shown in Figure 2(a) and Figure 2(b), respectively. The model predicted COD and TP fit the measured data well in a wide range. As shown in Figure 2, the data points were located close to the trend line even for extreme high values, i.e. COD$\geq 800\ mg/L$ and TP$\geq 6\ mg/L$. The prediction performance in terms of RMSE and R2 were listed in Table 2. The RMSE of the MARS model for COD prediction (MARS 1) was 80.4 (Table 2), which is much smaller than that of MLR 1 (98.128) and MLR 2 (92.360). A similar result was also found in TP modelling. The R^2 of MARS 2 and MLR 4 were almost equal for global TP prediction, but the increase of RMSE was significant due to the better capture of nonlinearity. Table 2 also showed the necessary numbers of knots and prediction terms for MARS model construction. The MARS model for TP prediction required more knots and interaction terms to achieve the same R^2 level as that of COD, which indicated the higher nonlinearity of TP propagation. Overall, the accuracy in terms of RMSE for COD and TP were improved by applying MARS method.

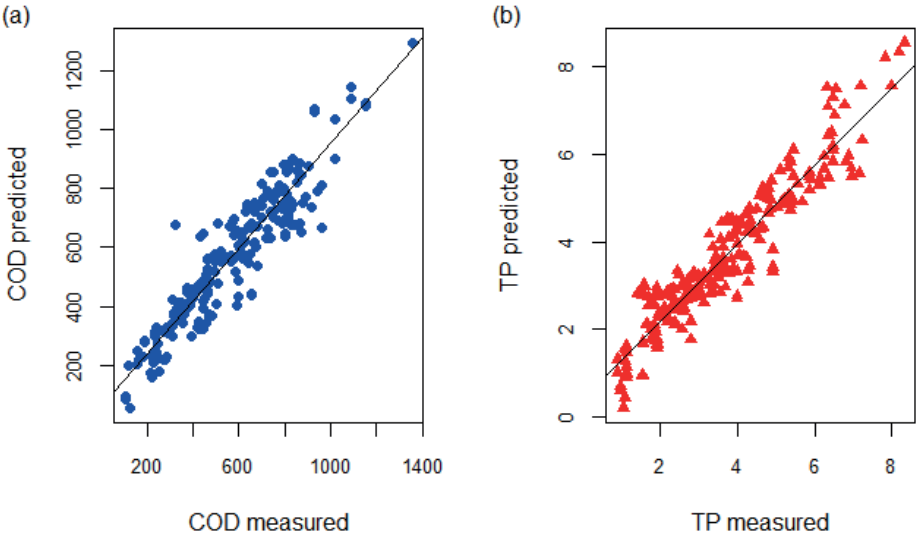

Figure 2 (a) Predicted COD by MARS method versus measured COD; (b) Predicted TP by MARS versus measured TP.

Table 2 Performance of MARS models for global influent COD and TP prediction

Model	Target	Interaction term	Knots	Basis function	RMSE	R^2	Cross Validation R^2
MARS 1	COD	No	6	13	80.439	0.892	0.851
MARS 2	TP	Yes	9	16	0.573	0.889	0.841

3.4 Discussion and outlook of soft sensor modelsw

The fitted COD and TP by global MLR and MARS were compared with the measurement, as is shown in Figure 3. Generally, the difference of prediction performance can be hardly detected from Figure 3. However, the COD prediction by MARS was closer to the measurement for peak hours (Figure 3(a)), which may be the reason of significant lower RMSE of MARS than MLR. For TP prediction, MARS also showed better approaching to the measurement in fluctuating situations in Figure 3(b). Therefore, we can conclude that MARS performed better than MLR for the prediction of extremal values. MARS breaks the general data into several pieces of splines and allows the slope of each piece to be different. The MARS models can capture the extremal situations due to the allowance of several splines. For the global MLR

models with higher order and interaction terms, they always need to be continuous and their first derivatives also need to be continuous. In general, global MLR fit smoother curves (Figure 3), but it did not help improve the fitting of real world data due to nonlinear fluctuation [12]. The improvement of nonlinearity capture is important to reduce measurement error and increase control stability.

It is also instructive to evaluate the numbers of knots and basis functions of the two MARS models. MARS 1 was constructed with 6 knots and 13 basis functions, while MARS 2 has 9 knots and 16 basis functions. To achieve a satisfactory prediction, the TP dataset was broken into smaller pieces of splines by adding more numbers of knots, which reflected higher nonlinearity of TP than COD. The basis functions are second order polynomials. As listed in Table S3, the COD model (MARS 1) has first order and square terms, while the TP model (MARS 2) included interaction terms. The interaction terms suggested that the correlation of TP and an easy-to-measure variable were dependent on the third easy-to-measure variable [31]. Thus, the interaction terms in basis functions were significant for TP prediction, but the interaction effect was not statistical significant for COD prediction.

Compared with machine learning algorithms (e.g. neural networks), MARS is less “black box” for nonlinear predictive modelling. This is because MARS is more informative and interpretable to retrieve the real world knowledge [12,26]. In this study, the knots of MARS were capable of informing where significant changes of TP or COD may happen. Moreover, the three local piecewise MLRs for TP prediction were built on the basis of pre-known knowledge of season-climate conditions, which are highly dependent on the accuracy of data classification. In other words, the TP dataset was firstly classified into three subsets and each of the local MLR models was built on the corresponding subsets. The local MLRs turned out to perform unsatisfactory as global models. Moreover, the MARS model for TP prediction included 9 knots rather than 3 knots, which indicates that the causes of nonlinearity of TP was beyond the effects of seasonal variation or climate impact.

Overall, the MARS models are not only flexible in prediction of hard-to-measure variables, but also provided explicit knowledge for the downstream operation of wastewater treatment process.

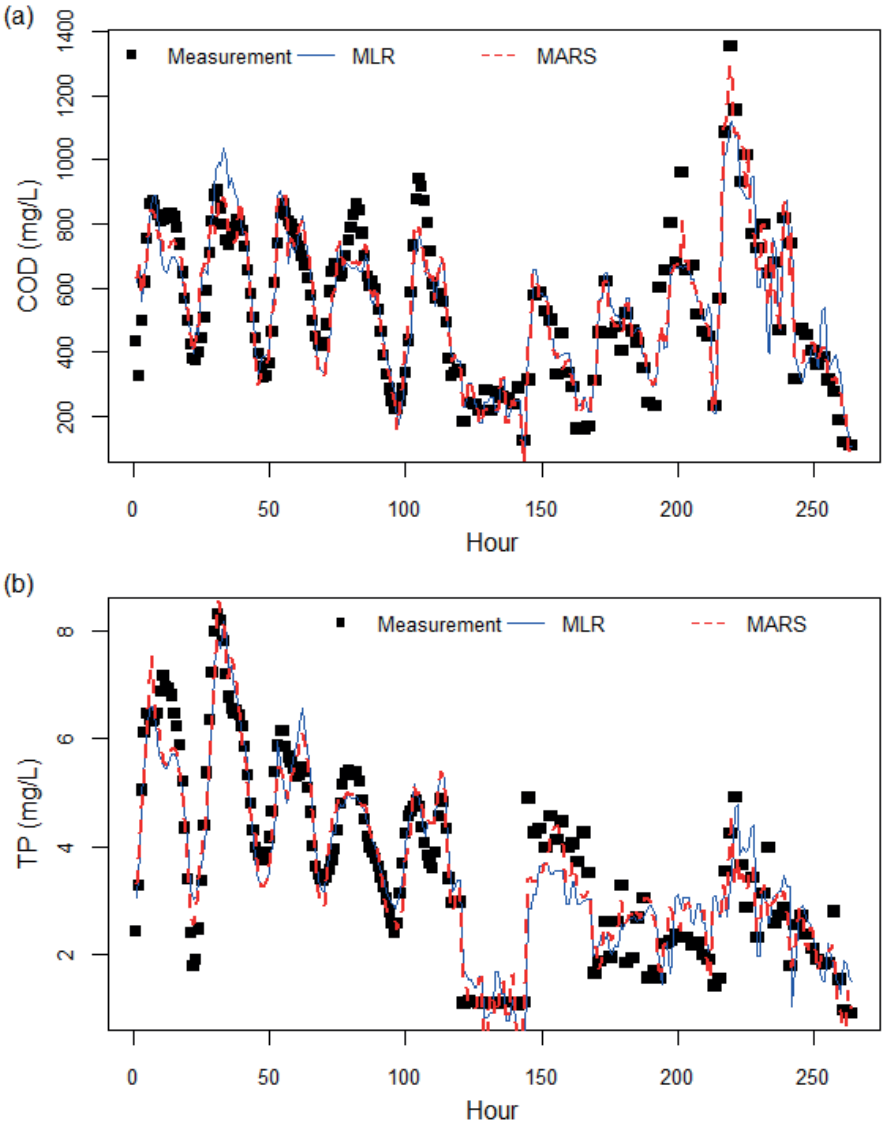

Figure 3 (a) The measured COD and predicted COD by global MLR and MARS; (b) The measured TP and predicted TP by global MLR and MARS.

4. Conclusion

The online monitoring of influent wastewater characteristics is essential for wastewater treatment process surveillance and control. Soft sensor is an alternative solution for online measurement of COD and total

phosphorus (TP) in an economic manner. In this study, we investigated the possibility of using easy-to-measure variables as predictors to construct both global and local soft sensor models for COD and TP prediction. The goal is to build interpretable nonlinear models to serve as soft sensors for the surveillance of wastewater treatment process.

The global MLR models performed similar to the MARS models in terms of R^2 for COD and TP prediction. However, the RMSEs of MARS models were smaller than that of the corresponding MLRs. MARS has the advantage of capturing nonlinearity in fluctuating situations.

Compared with other "black box" modeling techniques, such as neural network, useful information and knowledge can be retrieved from MARS models. The MARS models indicated the points where significant changes happened. Moreover, splines may also suggest the number of groups for pre-classification of the dataset.

Acknowledgements

This work has been supported by the RECOVER project, granted by the Research Council of Norway (grant number 247612).

Appendix A. Supplementary material

Supplementary material related to this article can be found in the online version.

References

[1] G. Olsson, B. Carlsson, J. Comas, J. Copp, K. V Gernaey, P. Ingildsen, U. Jeppsson, C. Kim, L. Rieger, I. Rodríguez-Roda, J.-P. Steyer, I. Takács, P. a Vanrolleghem, A. Vargas, Z. Yuan, L. Åmand, Instrumentation, control and automation in wastewater - from London 1973 to Narbonne 2013, Water Sci. Technol. 69 (2014) 1373–1385. doi:10.2166/wst.2014.057.

[2] W. Yan, P. Guo, Y. Tian, J. Gao, A Framework and Modeling Method of Data-Driven Soft Sensors Based on Semisupervised Gaussian Regression, Ind. Eng. Chem. Res. 55 (2016) 7394–7401. doi:10.1021/acs.iecr.5b04118.

[3] J. Shiri, A. Keshavarzi, O. Kisi, S. Karimi, Using soil easily measured parameters for estimating soil water capacity: Soft computing approaches, Comput. Electron. Agric. 141 (2017) 327–339. doi:10.1016/j.compag.2017.08.012.

[4] H. Seshan, M.K. Goyal, M.W. Falk, S. Wuertz, Support vector regression model of wastewater bioreactor performance using microbial community diversity indices: Effect of stress and bioaugmentation, Water Res. 53 (2014) 282–296. doi:10.1016/j.watres.2014.01.015.

[5] F.A.A. Souza, R. Araújo, J. Mendes, Review of soft sensor methods for regression applications, Chemom. Intell. Lab. Syst. 152 (2016) 69–79. doi:10.1016/j.chemolab.2015.12.011.

[6] H. Haimi, M. Mulas, F. Corona, R. Vahala, Data-derived soft-sensors for biological wastewater treatment plants: An overview, Environ. Model. Softw. 47 (2013) 88–107. doi:10.1016/j.envsoft.2013.05.009.

[7] Y. Liu, J. Chen, Z. Sun, Y. Li, D. Huang, A probabilistic self-validating soft-sensor with application to wastewater treatment, Comput. Chem. Eng. 71 (2014) 263–280. doi:10.1016/j.compchemeng.2014.08.008.

[8] H. Haimi, M. Mulas, F. Corona, S. Marsili-Libelli, P. Lindell, M. Heinonen, R. Vahala, Adaptive data-derived anomaly detection in the activated sludge process of a large-scale wastewater treatment plant, Eng. Appl. Artif. Intell. 52 (2016) 65–80. doi:10.1016/j.engappai.2016.02.003.

[9] J. Fernandez de Canete, P. Del Saz-Orozco, R. Baratti, M. Mulas, A. Ruano, A. Garcia-Cerezo, Soft-sensing estimation of plant effluent concentrations in a biological wastewater treatment plant using an optimal neural network, Expert Syst. Appl. 63 (2016) 8–19. doi:10.1016/j.eswa.2016.06.028.

[10] S. Akilandeswari, B. Kavitha, Comparison of ANFIS and statistical modeling for estimation of chemical oxygen demand parameter in textile effluent, Der Chem. Sin. 4 (2013) 96–99.

[11] M. Ay, O. Kisi, Modelling of chemical oxygen demand by using ANNs, ANFIS and k-means clustering techniques, J. Hydrol. 511 (2014) 279–289. doi:10.1016/j.jhydrol.2014.01.054.

[12] A.T.C. Goh, W.G. Zhang, An improvement to MLR model for predicting liquefaction-induced lateral spread using multivariate adaptive regression splines, Eng. Geol. 170 (2014) 1–10. doi:10.1016/j.enggeo.2013.12.003.

[13] E. Z-Flores, M. Abatal, A. Bassam, L. Trujillo, P. Juárez-Smith, Y. El Hamzaoui, Modeling the adsorption of phenols and nitrophenols by activated carbon using genetic programming, J. Clean. Prod. 161 (2017) 860–870. doi:10.1016/j.jclepro.2017.05.192.

[14] Y. Qiu, Y. Liu, D. Huang, Date-Driven Soft-Sensor Design for Biological Wastewater Treatment Using Deep Neural Networks and Genetic Algorithms, J. Chem. Eng. Japan. 49 (2016) 925–936. doi:10.1252/jcej.16we016.

[15] Y. Liu, Adaptive just-in-time and relevant vector machine based soft-sensors with adaptive differential evolution algorithms for parameter optimization, Chem. Eng. Sci. 172 (2017) 571–

584. doi:10.1016/j.ces.2017.07.006.

[16] B. Szelag, J. Gawdzik, Assessment of the Effect of Wastewater Quantity and Quality, and Sludge Parameters on Predictive Abilities of Non-Linear Models for Activated Sludge Settleability Predictions, Polish J. Environ. Stud. 26 (2017) 315–322. doi:10.15244/pjoes/64810.

[17] M. Zhang, X. Liu, A soft sensor based on adaptive fuzzy neural network and support vector regression for industrial melt index prediction, Chemom. Intell. Lab. Syst. 126 (2013) 83–90. doi:10.1016/j.chemolab.2013.04.018.

[18] D.-J. Choi, H. Park, A hybrid artificial neural network as a software sensor for optimal control of a wastewater treatment process, Water Res. 35 (2001) 3959–3967. doi:10.1016/S0043-1354(01)00134-8.

[19] S. Kuter, Z. Akyurek, G.W. Weber, Retrieval of fractional snow covered area from MODIS data by multivariate adaptive regression splines, Remote Sens. Environ. 205 (2018) 236–252. doi:10.1016/j.rse.2017.11.021.

[20] Y. Liu, J. Guo, Q. Wang, D. Huang, Prediction of Filamentous Sludge Bulking using a State-based Gaussian Processes Regression Model, Sci. Rep. 6 (2016) 31303. doi:10.1038/srep31303.

[21] H. Haimi, F. Corona, M. Mulas, L. Sundell, M. Heinonen, R. Vahala, Shall we use hardware sensor measurements or soft-sensor estimates? Case study in a full-scale WWTP, Environ. Model. Softw. 72 (2015) 215–229. doi:10.1016/j.envsoft.2015.07.013.

[22] O. Samuelsson, A. Björk, J. Zambrano, B. Carlsson, Gaussian process regression for monitoring and fault detection of wastewater treatment processes, Water Sci. Technol. 75 (2017) 2952–2963. doi:10.2166/wst.2017.162.

[23] J.H. Friedman, Multivariate Adaptive Regression Splines, Ann. Stat. 19 (1991) 1–67. http://www.jstor.org/stable/224183.

[24] E. Quirós, Á.M. Felicísimo, A. Cuartero, Testing multivariate adaptive regression splines (MARS) as a method of land cover classification of TERRA-ASTER satellite images, Sensors. 9 (2009) 9011–9028. doi:10.3390/s91109011.

[25] M. Rezaie-Balf, Z. Zahmatkesh, S. Kim, Soft Computing Techniques for Rainfall-Runoff Simulation: Local Non–Parametric Paradigm vs. Model Classification Methods, Water Resour. Manag. 31 (2017) 3843–3865. doi:10.1007/s11269-017-1711-9.

[26] W. Xing, W. Wang, Q. Shao, B. Yong, Identification of dominant interactions between climatic seasonality, catchment characteristics and agricultural activities on Budyko-type equation parameter estimation, J. Hydrol. 556 (2018) 585–599. doi:10.1016/j.jhydrol.2017.11.048.

[27] D. Shahsavani, S. Tarantola, M. Ratto, Evaluation of MARS modeling technique for sensitivity analysis of model output, Procedia - Soc. Behav. Sci. 2 (2010) 7737–7738. doi:10.1016/j.sbspro.2010.05.204.

[28] X. Wang, K. Kvaal, H. Ratnaweera, Characterization of influent wastewater with periodic variation and snow melting effect in cold climate area, Comput. Chem. Eng. 106 (2017) 202–211. doi:10.1016/j.compchemeng.2017.06.009.

[29] H. Akaike, A new look at the statistical model identification, IEEE Trans. Autom. Control. 19 (1974) 716–723. doi:10.1109/TAC.1974.1100705.

[30] Milborrow Stephen, Derived from mda:mars by Trevor Hastie and Rob Tibshirani. Uses Alan Miller's Fortran utilities with Thomas Lumley's leaps wrapper. earth: Multivariate Adaptive Regression Splines, Version 4.6.1, R Packag. (2018). https://cran.r-project.org/package=earth.

[31] G. James, D. Witten, T. Hastie, R. Tibshirani, An Introduction to Statistical Learning: with Applications in R, Springer New York, 2014. https://books.google.no/books?id=at1bmAEACAAJ.

[32] E. Belia, Y. Amerlinck, L. Benedetti, B. Johnson, G. Sin, P.A. Vanrolleghem, K. V. Gernaey, S. Gillot, M.B. Neumann, L. Rieger, A. Shaw, K. Villez, Wastewater treatment modelling: Dealing with uncertainties, Water Sci. Technol. 60 (2009) 1929–1941. doi:10.2166/wst.2009.225.

[33] G. Olsson, ICA and me--a subjective review., Water Res. 46 (2012) 1585–624. doi:10.1016/j.watres.2011.12.054.

[34] M. Talebizadeh, E. Belia, P.A. Vanrolleghem, Influent generator for probabilistic modeling of nutrient removal wastewater treatment plants, Environ. Model. Softw. 77 (2016) 32–49. doi:10.1016/j.envsoft.2015.11.005.

[35] B.G. Plósz, H. Liltved, H. Ratnaweera, Climate change impacts on activated sludge wastewater treatment: a case study from Norway., Water Sci. Technol. 60 (2009) 533–541. doi:10.2166/wst.2009.386.

[36] S. Moghadas, a-M. Gustafsson, T.M. Muthanna, J. Marsalek, M. Viklander, Review of models and procedures for modelling urban snowmelt, Urban Water J. 9006 (2015) 1–16. doi:10.1080/1573062X.2014.993996.

[37] S. Puig, M.C.M. van Loosdrecht, J. Colprim, S.C.F. Meijer, Data evaluation of full-scale wastewater treatment plants by mass balance, Water Res. 42 (2008) 4645–4655. doi:10.1016/j.watres.2008.08.009.

Appendix A. Supplementary material

Table S3 Predictors (including raw variables, second order and interaction terms) selected based on backward backward selection and the model coefficients of the regression model for general conditions.

Predictors	COD without interaction	COD with interaction	TP without interaction	TP with interaction
Intercept	3.131×10^{3}	-3.619×10^{3}	1.372	1.552×10^{1}
Flow	5.593×10^{-1}	-8.431×10^{-3}		-2.988×10^{-2}
WaterTemp	7.504	-9.303×10^{1}	2.238×10^{-1}	-4.568×10^{-1}
TSS	1.425	-2.541	1.299×10^{-2}	1.385×10^{-1}
NH_4-N	6.140	-6.169×10^{1}	9.166×10^{-2}	-3.087×10^{-1}
pH	-4.877×10^{2}	-6.126×10^{2}	-5.178×10^{-1}	-9.547×10^{-1}
$Flow^2$	-2.414×10^{-4}	-2.948×10^{-4}		-2.062×10^{-6}
$WaterTem^2$				
TSS^2		-7.838×10^{-4}	-1.169×10^{-5}	-2.115×10^{-5}
$NH_4\text{-}N^2$			-1.224×10^{-3}	-2.124×10^{-3}
pH^2				
Flow*WaterTemp				-5.576×10^{-4}
Flow*TSS				
Flow*NH_4-N		-3.803×10^{-3}		-4.847×10^{-5}
Flow:*pH		2.408×10^{-1}		-2.620×10^{-3}
WaterTemp*TSS		-7.802×10^{-2}		-1.243×10^{-3}
WaterTemp*NH_4-N				
WaterTemp* pH		1.654×10^{1}		
TSS*NH_4-N				3.308×10^{-4}
TSS*pH				-2.111×10^{-2}
NH_4-N*pH		-7.404		5.238×10^{-2}

Table S4 Model predictors and the corresponding coefficients for total phosphorus prediction models in different condition.

Predictors	Warm-Dry	Cold-Dry	Cold-Dry (interaction)	Cold-Wet	Cold-Wet (interaction)
Intercept	1.079×10^{2}	-1.492×10^{2}	-1.479×10^{2}	-1.434	-1.717×10^{3}
Flow	1.239×10^{-2}	-2.421×10^{-3}	5.791×10^{-3}	2.726×10^{-4}	1.302×10^{-2}
WaterTemp			-2.191×10^{1}		3.632×10^{1}
TSS	1.430×10^{-2}		1.741×10^{-1}	-1.492×10^{2}	3.773×10^{-1}
NH_4-N		1.525×10^{-1}	1.313×10^{-1}	8.095×10^{-2}	-2.646
pH	-3.170×10^{1}	4.474×10^{1}	6.474×10^{1}		4.512×10^{2}
$Flow^2$	-6.876×10^{-6}		-5.798×10^{-6}		1.563×10^{-6}
$WaterTem^2$		2.731×10^{-2}	2.158×10^{-1}	1.946×10^{-2}	
TSS^2		3.356×10^{-6}	-2.853×10^{-5}	-6.632×10^{-5}	-1.131×10^{-4}
$NH_4\text{-}N^2$		-2.045×10^{-3}	-2.779×10^{-3}	-1.010×10^{-3}	-2.008×10^{-3}
pH^2	2.255	-3.327	-6.209		-2.978×10^{1}
Flow*WaterTemp			-2.236×10^{-3}		-2.996×10^{-3}
Flow* TSS					
Flow*NH_4-N					1.412×10^{-4}
Flow*pH					
WaterTemp*TSS			-3.226×10^{-3}		
WaterTemp* NH_4-N					-2.891×10^{-2}
WaterTemp* pH			2.989		-4.721
TSS* NH_4-N			5.328×10^{-4}		
TSS*pH			-2.213×10^{-2}		-4.893×10^{-2}
NH_4-N*pH					3.392×10^{-1}

Table S5 MARS models for global COD and TP prediction.

	Knots	Interaction terms	Model
COD	6	No	$\mathrm{COD} = 1050.91058 - 0.43835 \cdot \mathrm{h}(852.625 - \mathrm{Flow}) - 0.08277 \cdot \mathrm{h}(\mathrm{Flow} - 852.625) + 1345.01256 \cdot \mathrm{h}(\mathrm{WaterTemp} - 8.5) - 5.67291 \cdot \mathrm{h}(8.6 - \mathrm{WaterTemp}) - 1357.16268 \cdot \mathrm{h}(\mathrm{WaterTemp} - 8.6) - 11.46400 \cdot \mathrm{h}(\mathrm{TSS} - 342) - 1.48832 \cdot \mathrm{h}(360.25 - \mathrm{TSS}) + 15.28556 \cdot \mathrm{h}(\mathrm{TSS} - 360.25) - 7.55469 \cdot \mathrm{h}(NH_4\text{–N} - 31.2419) - 0.17383 \cdot \mathrm{h}(2335.04 - NH_4\text{–}N^2) + 36.21696 \cdot \mathrm{h}(49.5616 - pH^2) - 24.28355 \cdot \mathrm{h}(pH^2 - 49.5616)$
TP	9	Yes	$TP = -3.8348229 - 0.0028527 \cdot \mathrm{h}(\mathrm{Flow} - 1307.1) + 0.1800591 \cdot \mathrm{h}(53.5239 - NH_4\text{–N}) - 0.5625588 \cdot \mathrm{h}(NH_4\text{–N} - 53.5239) + 0.0000206 \cdot \mathrm{h}(TSS^2 - 129780) + 0.0008343 \cdot \mathrm{h}(8624.06 - \mathrm{Flow} * \mathrm{WaterTemp}) - 0.0001379 \cdot \mathrm{h}(\mathrm{Flow} * \mathrm{WaterTemp} - 8624.06) - 0.0003182 * \mathrm{h}(14893.5 - \mathrm{Flow} * NH_4\text{–N}) + 0.0001098 * \mathrm{h}(\mathrm{Flow} * NH_4\text{–N} - 14893.5) - 0.0035335 * \mathrm{h}(935.74 - \mathrm{WaterTemp} * \mathrm{TSS}) + 0.0024327 * \mathrm{h}(\mathrm{WaterTemp} * \mathrm{TSS} - 935.74) - 0.0957721 * \mathrm{h}(64.08 - \mathrm{WaterTemp} * \mathrm{pH}) - 0.0008502 * \mathrm{h}(4191.85 - \mathrm{TSS} * NH_4\text{–N}) + 0.0004916 * \mathrm{h}(\mathrm{TSS} * NH_4\text{–N} - 4191.85) + 0.0056016 * \mathrm{h}(1056.13 - \mathrm{TSS} * \mathrm{pH}) - 0.0061045 * \mathrm{h}(\mathrm{TSS} * \mathrm{pH} - 1056.13)$

Paper VI

Wang, X., Bi, X., Hem, L. J., Ratnaweera, H., 2017. Evaluation of surveillance and control strategies for wastewater treatment plants based on Life Cycle Assessment. Paper presented in the IWA Conference on Sustainable Wastewater Treatment and Resource Recovery: Research, Planning, Design and Operation. November 2017, Chongqing

Evaluation of Surveillance and Control Strategies for Wastewater Treatment Plants Based on Life Cycle Assessment

Xiaodong Wang[1, *],Xueun Bi[2], Lars John Hem[1,3],Harsha Ratnaweera[1]

[1] Faculty of Science and Technology, Norwegian University of Life Sciences, P.O.Box 5003-IMT, 1432 Aas, Norway

[2] Qingdao University of Technology, State and Local Joint Engineering Research Center of Urban Wastewater Treatment and Reclamation, Fushun Road 11, 266033 Qingdao, China

[3] Oslo Water and Sewerage Works, Oslo Municipality, P.O.Box 4704 Sofienberg, 0506 Oslo, Norway

Abstract: Two scenarios of wastewater treatment configuration was used to compare the benefits of applying advanced surveillance and control strategies. Scenario 1 is a compact MBBR wastewater treatment plant. By applying advance advanced control of aeration and chemical dosing, electricity consumption can be reduced by 11 %, and coagulant consumption can be reduced by 24 %. Scenario 2 is a nutrient removal wastewater treatment plant (WWTP) based on typical process configuration in Norway. Mass balance calculation and Life cycle assessment was carried to compare two control strategies. LCA results shown that significant environmetal benifits would be acheived by enhancing primary particle removal and model predictive control (MPC).

Keywords: control strategy; Life cycle assessment; Mass balance; wastewater treatment

1. Introduction

The need for advanced control of wastewater treatment plants (WWTPs) can be motivated for several purposes, such as achieving better effluent quality, handling unusual loading variation and reducing operation cost (Olsson, 2012). To achieve advanced control of WWTPs, i.e. model predictive control (MPC), real time monitoring of influent quality and quantity are required. On-line nutrient sensors are getting commonly used and affordable in the last decades, but some wastewater quality variables such as chemical oxygen demand (COD), total Phosphorus (TP) are difficult to be measured on-line, which require statistical monitoring or soft sensors to achieve advanced control (Wang et al., 2017b).

There is always a question from WWTP managements about whether will the price paid on applying advanced surveillance and control (ASAC) can be recovered in a few years. Beside initial investment of the facilities, WWTPs have to spend additional cost on the maintenance of on-line sensors and actuators as well as upgrading the operation team. Even though there are reports that have stated the benefit of applying ASAC (Olsson et al., 2014; Olsson and Jeppsson, 2006; Zanetti et al., 2012), managers and operators of WWTPs are still hesitate to shift the gear to control and automation. As WWTPs were initially built to protect environment, the shift of plant operation mood should be an economical option which can maximize environmental benefits. Indirect environmental impacts of installing ASAC facilities, such as additional consumption of materials, should be better documented. Therefore, it requires comprehensive analysis of the impact of ASAC on WWTPs from an integrated perspective.

In this study, we investigated the mass balance of carbon, nitrogen and phosphorus of wastewater treatment plants based on process configuration in Norway. Comparison of mass balance with and without ASAC was carried out to track the impact of the WWTP on the environment. In recent years, the international standardized methodology for environmental profile assessment – life cycle assessment (LCA), has been increasingly used to analysis the eco-efficient of WWTPs (Lorenzo-Toja et al., 2015; Rahman et al., 2016), but LCA has been rarely used to assess the control strategy impacts. The ultimate goal of this study is to evaluate the balance of environmental and economic impacts of applying advanced surveillance and control in WWTPs from a life cycle perspective. The results of this study will provide objective information for decision making on operation strategy.

2. Materials and Methods

The goal of the life cycle assessment (LCA) part is to compare the environmental impacts of different control options. The scope of the LCA involves the operation of the WWTP, as presented in Figure 1. LCA evaluation includes direct emission and indirect emission. Greenhouse gas (e.g. CO2, CH4), eutrophication nutrient in the outlet (e.g. TN, TP) and sludge management are the main source of direct emission. The resources and emissions during electricity generating and chemical production were included for the final evaluation. The detailed methodology of LCA for wastewater treatment has been well explained in literature

report (Flores-Alsina et al., 2010; Foley et al., 2010; Rahman et al., 2016). SimaPro 8.0 was used to calculate the environmental impact of WWTP operation strategies, where the Ecoinvent database was applied.

Results and Discussion

This paper introduced two surveillance and control solutions for two different wastewater treatment process configuration. The two scenarios of process configuration are based on typical processes of full-scale wastewater treatment plants in Norway.

Scenario 1. Advanced surveillance and control for compact system

A compact wastewater treatment process was chosen as Scenario 1. As is shown in Figure 2, the influent from combined sewer system would go through the screen and grit chamber before entering the biological treatment. MBBR system was applied for biological organic matter removal, with HRT 1.6 hours at full capacity (2000 m^3/day). To save space, Actiflo (Veolia Water Technology, n.d.) was applied for solid-water separation. Microsand, ferric chloride and polymer were dosed and mixed with the outlet of MBBR to assist solid-water separation. Since the recipient water environment was not nitrogen sensitive, nitrogen removal was not required in this WWTP. Electricity accounted 8.25 % of the total operation cost and chemical consumption cost 19.5 %. For such a compact and simple process, the potential of reducing environmental compact is clear: reducing aeration energy consumption and chemical dosage. The traditional control strategy for aeration and chemical dosing is flow proportional control. As results, when storm events or snow melting happed, the influent flow increased dramatically and the municipal wastewater was distilled. Based on the flow proportional rule, both air flow and chemical dosage was increased to an unnecessary high level. Therefore, it is necessary to distinguish dry weather influent and wet weather influent.

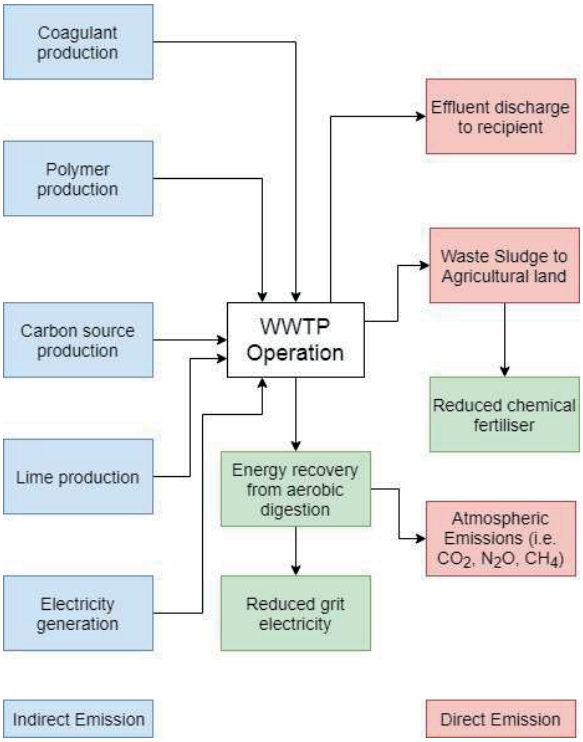

Figure 1 The required inputs from environment to wastewater treatment process and the outputs of the process. The process outputs include both direct emission and indirect emission.

Rain events can be easily predicted based on weather forecast, and influent with snowmelt can be classified according to the PLS-DA methods introduced in our previous study (Wang et al., 2017a). The average influent characteristics of dry weather and wet weather was listed in Table 1. Thus, the proposed control strategy for this scenario is making air flow as the function of both influent flow and COD, and coagulant dosage as a function of flow and other influent variables as previous literature report (Manamperuma et al., 2017).

Table 1 Average influent characteristics in dry weather and wet weather.

	Flow (m^3/h)	Temperature (℃)	TSS (mg/L)	TP (mg/L)	TN (mg/L)	NH_4-N (mg/L)	COD (mg/L)	S-COD (mg/L)	PH
Dry	780	8.0	171	3.9	47.5	35.9	662	225	7.0
Wet	1265	7.1	110	2.9	44.8	32.5	343	127	7.1

The direct emission from the WWTP was not affected significantly by the advanced control solution, because the effluent quality and sludge production was almost equal to that controlled by flow proportional controller. However, electricity consumption can be reduced by 11 %, and coagulant consumption can be reduced by 24 %.

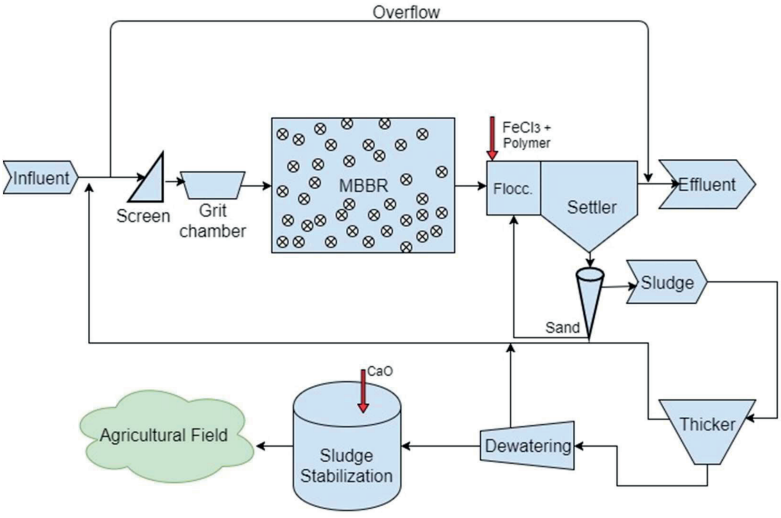

Figure 2 Wastewater treatment process configuration of Scenario 1, based on a full-scale WWTP in Norway.

Scenario 1 provide the results of applying advanced model predictive control (MPC) in the water line of a simple WWTP. While Scenario 2 introduced a typical nutrient removal WWTP in Norway.

Scenario 2. Advanced surveillance and control for nutrient removal system

Figure 3 illustrated a MBBR based nutrient removal process. Similar process configuration was applied in some large WWTPs which discharge the effluent to nutrient sensitive recipients in Norway. The MBBR system applied both pre-denitrification and post-denitrification to make fully use of carbon source in the influent for nitrogen removal. Ferric Chloride and polymer was added to mix with MBBR outlet to assist sedimentation. Some Norwegian WWTPs applied flotation for solid-water separation which can reduce the retention time into 20 minutes (Ødegaard, 2006). DO feed-back control and proportional dosing control of coagulant was

applied as conventional strategy to control aeration and coagulant dosing. Around 50 % nitrogen can be removed through pre-denitrification, according to Rusten et al. (1995), another 40 % could be removed by adding sodium acetate as external carbon source.

We propose to use ammonia based model predictive control (MPC) to control carbon dosing and aeration. Ammonia, PH, suspended solid (SS), conductivity of the influent should be measured by on-line sensors. COD and soluble COD can be predicted using soft sensor methods as stated in previous study (Wang et al., 2017b). The airflow is controlled as a function of influent flow (Q_{in}), primary settled COD (COD_{PS}), inlet ammonia ($NH_4^+ - N$) and dissolved oxygen (DO), as indicated in equation (1). Carbon dosing is controlled as a function of influent flow (Q_{in}), recycle rate ($r_{recycle}$), $NH_4^+ - N$, and DO, as shown in Equation (2).

$$q_{air} = f(Q_{in},\ COD_{PS}, NH_4^+ - N, DO) \quad (1)$$

$$q_{carbon} = f\left(Q_{in}, r_{recycle}, NH_4^+ - N, DO\ \right) \quad (2)$$

Ødegaard (2016) has shown that enhancing primary removal of particles before biological stage would increase energy efficiency. To maximize energy recovery from wastewater, the advanced control strategy applied to enhance particle removal from primary settler. Thus, additional ferric chloride was added to the channel before entering primary setter. In this case, the majority of organic matters would not be converted to CO2, but they will be settled as primary sludge and finally be recovered as CH_4 in the digester. The mass balance calculation of the two control strategies was listed in Table 2.

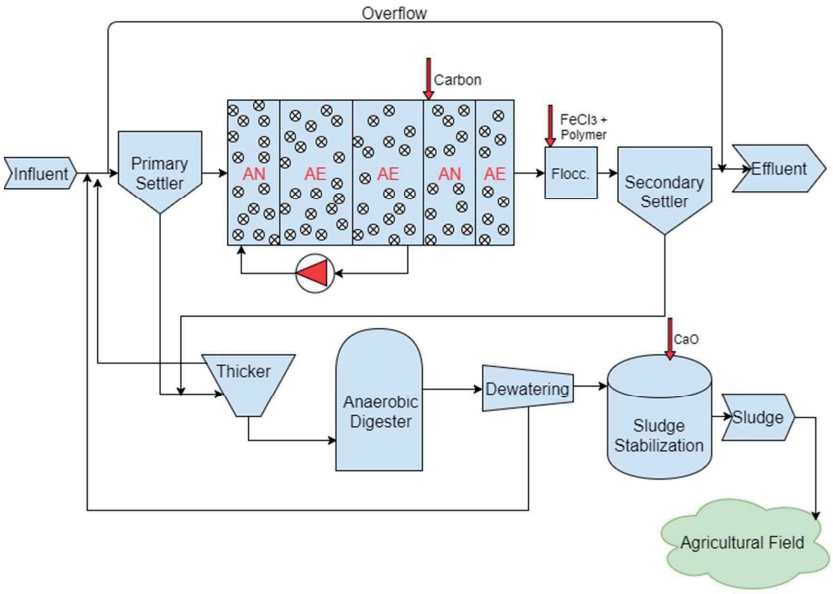

Figure 3 Wastewater treatment process configuration of Scenario 2, based on a typical nutrient removal process in Norway.

Table 2 Mass balance of the WWTP of Scenario 2.

	Conventional control	Advanced control	Unit
Influent Q	24000	24000	m^3/d
Influent COD	13488	13488	kg COD/d
Influent N	1140	1140	kg/d
Influent P	96	96	kg/d
$Primary_{in}$ Q	24960	24960	m^3/d
$Primary_{in}$ COD	13596	13596	kg COD/d
$Primary_{in}$ N	1176.5	1176.5	kg/d
$Primary_{in}$ P	99.8	99.8	kg/d
$Primary_{out}$ Q	24710.4	24336	m^3/d
$Primary_{out}$ COD	8973.4	4758.6	kg COD/d
$Primary_{out}$ N	1000	882.4	kg/d
$Primary_{out}$ P	80.8	20	kg/d

$Primary_{sludge}$ Q	249.6	624	m^3/d
$Primary_{sludge}$ COD	4622.6	8837.4	kg COD/d
$Primary_{sludge}$ N	176.5	294.1	kg/d
$Primary_{sludge}$ P	19	81.8	kg/d
CO_2 from biological treatment	4859.7	2619.1	kg COD/d
N emission	625	591.1	kg/d
Effluent Q	24166.8	24146.7	m^3/d
Effluent COD	717.9	713.8	kg COD/d
Effluent N	180	169	kg/d
Effluent P	6.5	4.8	kg/d
WAS Q	543.6	219	m^3/d
WAS COD	3549.3	2038.5	kg COD/d
WAS N	195	122.3	kg/d
WAS P	74.3	15.2	kg/d
External carbon	153.2	213.3	kg COD/d
$Digester_{in}$ Q	396.6	421.5	m^3/d
$Digester_{in}$ COD	8104.5	10802.1	kg COD/d
$Digester_{in}$ N	364.1	401.4	kg/d
$Digester_{in}$ P	80.3	96.6	kg/d
Methane	2107	4213	kg COD/d
CO2 from digester	1135	2268	kg COD/d
Reject Q	960	960	m^3/d
Reject COD	108	108	kg COD/d
Reject N	36.5	36.5	kg/d
Reject P	3.8	3.8	kg/d
Disposal Sludge COD	4754.5	4213.1	kg COD/d
Disposal Sludge N	327.6	364.9	kg/d
Disposal Sludge P	76.8	92.8	kg/d

According to literature report, the electricity consumption can be as low as 0.25 kWh/m3 to reach 3 mg/L effluent total nitrogen (Ødegaard, 2016). For the new MPC operation mood, most organic compound went to primary sludge and results in lower energy consumption and lower CO2 emission from biological wastewater treatment stage. A simplified process inputs and outputs (emission to final recipients) were listed in Table 3. Significant energy saving and increasing of CH_4 production due to the new control strategy can be found from Table 3. To study the environmental impact of wastewater treatment by applying different control strategy, life cycle assessment was carried out. Among the published LCA and wastewater treatment studies, greenhouse gas (GHG) emissions from the decomposition of sludge applied to agriculture were seldom included (Corominas et al., 2013). Direct emission of GHG from WWTP was already well studied (Corominas et al., 2012; Flores-Alsina et al., 2011; Guo and Vanrolleghem, 2014), but indirect emission of N_2O from agriculture field was not very clear. Therefore, N_2O mission was not included in this LCA study.

Table 3 Summary of daily energy and materials input to the process and emissions to the final recipients, including emission to water body (marine), air, and soil (agriculture field).

	Conventional control	Advanced control	Unit
Energy input	6000	5280	kWh
$FeCl_3$ dosing	974.4	835.2	kg
Acetic acid input	163.9	228.2	kg
Total CO_2 emission to air	8242.7	6719.8	kg
Nitrogen emission to air	625	591.1	kg
CH_4 production	4.97	9.94	m^3
COD emission to water body	717.9	713.8	kg
Nitrogen emission to water body	180	169	kg
Phosphorus emission to water body	6.5	4.8	kg
Organic compound to soil	3212.5	2846.7	kg
Nitrogen emission to soil	327.6	364.9	kg
Phosphorus emission to soil	76.8	92.8	kg

As is shown in Figure 4, by applying the advanced control strategy in a typical system as Scenario 2, significant reduction of global warming impact and toxicity compound emission. The differences in eutrophication impact was not found because both control strategy can enable high nitrogen and phosphorus removal. The higher fossil depletion impact of advanced MPC control was due to the higher transport usage for carbon source. The electricity in Norway was mainly hydropower electricity. Thus, the reduction of electricity by advanced control was not related to fossil depletion. Overall, choosing the right WWTP operation strategy will significantly affect the environmental benefits.

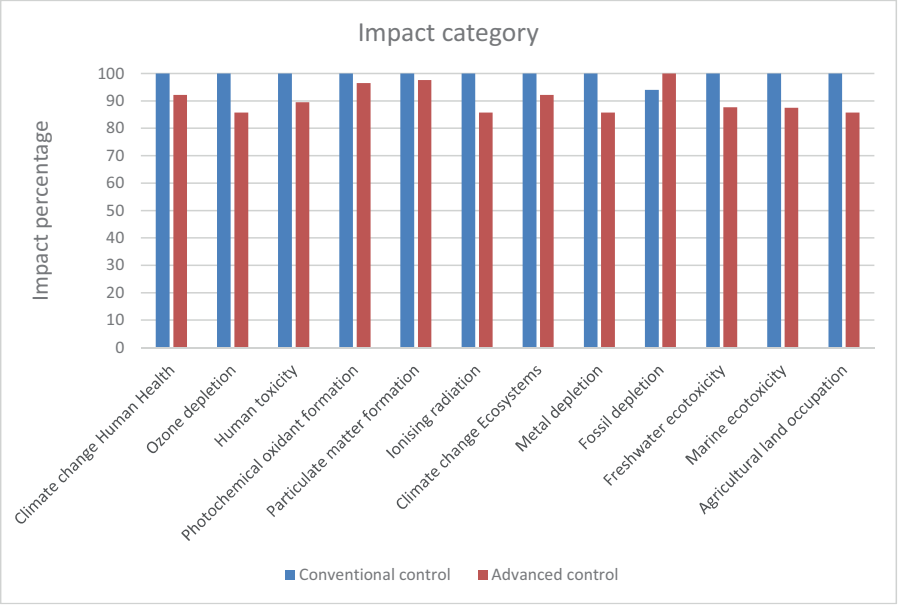

Figure 4 Comparison of impact categories of the conventional control strategy and the advanced control.

Conclusions

Two scenarios of Norwegian wastewater treatment process configuration was introduced to apply advanced control strategy. The benefits of applying right control strategy was stated in this work. For Scenario 2, mass balance and life cycle assessment (LCA) was carried out to evaluate the environmental benefits of applying advanced control strategy of WWTP. By enhancing primary removal of particles and applying MPC, significant reduction of climate

changing impact and environmental toxicity can be achieved.

Acknowledgement

This work was supported by the RECOVER project, granted by The Research Council of Norway (grant number 247612).

References

Corominas, L., Flores-Alsina, X., Snip, L., Vanrolleghem, P.A., 2012. Comparison of different modeling approaches to better evaluate greenhouse gas emissions from whole wastewater treatment plants. Biotechnol. Bioeng. 109, 2854–2863. doi:10.1002/bit.24544

Corominas, L., Foley, J., Guest, J.S., Hospido, A., Larsen, H.F., Morera, S., Shaw, A., 2013. Life cycle assessment applied to wastewater treatment: State of the art. Water Res. 47, 5480–5492. doi:10.1016/j.watres.2013.06.049

Flores-Alsina, X., Corominas, L., Snip, L., Vanrolleghem, P.A., 2011. Including greenhouse gas emissions during benchmarking of wastewater treatment plant control strategies. Water Res. 45, 4700–4710. doi:10.1016/j.watres.2011.04.040

Flores-Alsina, X., Gallego, A., Feijoo, G., Rodriguez-Roda, I., 2010. Multiple-objective evaluation of wastewater treatment plant control alternatives. J. Environ. Manage. 91, 1193–1201. doi:10.1016/j.jenvman.2010.01.009

Foley, J., de Haas, D., Hartley, K., Lant, P., 2010. Comprehensive life cycle inventories of alternative wastewater treatment systems. Water Res. 44, 1654–1666. doi:10.1016/j.watres.2009.11.031

Guo, L., Vanrolleghem, P.A., 2014. Calibration and validation of an activated sludge model for greenhouse gases no. 1 (ASMG1): Prediction of temperature-dependent N2O emission dynamics. Bioprocess Biosyst. Eng. 37, 151–163. doi:10.1007/s00449-013-0978-3

Lorenzo-Toja, Y., Vazquez-Rowe, I., Chenel, S., Marin-Navarro, D., Moreira, M.T., Feijoo, G., 2015. Eco-efficiency analysis of Spanish WWTPs using the LCA+DEA method. Water Res. 68, 637–650. doi:10.1016/j.watres.2014.10.040

Manamperuma, L., Wei, L., Ratnaweera, H., 2017. Multi-parameter based coagulant dosing control. Water Sci. Technol. 75, 2157–2162. doi:org/10.2166/wst.2017.058

Olsson, G., 2012. ICA and me--a subjective review. Water Res. 46, 1585–624. doi:10.1016/j.watres.2011.12.054

Olsson, G., Carlsson, B., Comas, J., Copp, J., Gernaey, K. V, Ingildsen, P., Jeppsson, U., Kim, C., Rieger, L.,

Rodríguez-Roda, I., Steyer, J.-P., Takács, I., Vanrolleghem, P. a, Vargas, a, Yuan, Z., Åmand, L., 2014. Instrumentation, control and automation in wastewater--from London 1973 to Narbonne 2013. Water Sci. Technol. 69, 1373–85. doi:10.2166/wst.2014.057

Olsson, G., Jeppsson, U., 2006. Plant-wide control: dream, necessity or reality? Water Sci. Technol. 53, 121. doi:10.2166/wst.2006.083

Rahman, S.M., Eckelman, M.J., Onnis-Hayden, A., Gu, A.Z., 2016. Life-Cycle Assessment of Advanced Nutrient Removal Technologies for Wastewater Treatment. Environ. Sci. Technol. 50, 3020–3030. doi:10.1021/acs.est.5b05070

Rusten, B., Hem, L.J., Ødegaard, H., 1995. Nitrogen removal from dilute wastewater in cold climate using moving-bed biofilm reactors. Water Environ. Res. 67, 65–74. doi:10.2175/106143095X131204

Veolia Water Technology, n.d. Actiflo.

Wang, X., Kvaal, K., Ratnaweera, H., 2017a. Characterization of influent wastewater with periodic variation and snow melting effect in cold climate area. Comput. Chem. Eng. 106, 202–211. doi:10.1016/j.compchemeng.2017.06.009

Wang, X., Ratnaweera, H., Holm, J.A., Olsbu, V., 2017b. Statistical monitoring and dynamic simulation of a wastewater treatment plant: A combined approach to achieve model predictive control. J. Environ. Manage. 193, 1–7. doi:10.1016/j.jenvman.2017.01.079

Zanetti, L., Frison, N., Nota, E., Tomizioli, M., Bolzonella, D., Fatone, F., 2012. Progress in real-time control applied to biological nitrogen removal from wastewater. A short-review. Desalination 286, 1–7. doi:10.1016/j.desal.2011.11.056

Ødegaard, H., 2016. A road-map for energy-neutral wastewater treatment plants of the future based on compact technologies (including MBBR). Front. Environ. Sci. Eng. 10, 2. doi:10.1007/s11783-016-0835-0

Ødegaard, H., 2006. Innovations in wastewater treatment: The moving bed biofilm process. Water Sci. Technol. 53, 17–33. doi:10.2166/wst.2006.284

Errata list

This sheet lists errors found in the submitted version of the thesis and the following changes have been made.

Page number	Paragraph	Change from	Change to
3	1	Ammonia oxidizing bacteria converts	Ammonium oxidizing bacteria convert
4	2	The kinetics denitrifying phosphorus removal was	The kinetic of denitrifying phosphorus removal was
9	2	The developments of instrumentation	The development of instrumentation
10	3	a lot of efforts have been made in wastewater treatment process control have been,	a lot of efforts have been made in wastewater treatment process control,
19	1	diluted wastewater was collected if rain or snow melting happened	diluted wastewater was collected, when rain or snow melting happened
37	Equation 4.1, 4.2	PH	pH
56	Figure 4.15	The title on Y-axis is missing	"Impact percentage" is added to Y-axis.
61	Reference Guerrero, 2012	Rodr??guez-Roda	Rodríguez-Roda
61	Reference Guo, 2014	N2O	N_2O
65	Reference Milborrow 2018	Derived from mda:mars by Trevor Hastie and Rob Tibshirani. Uses Alan Miller's Fortran utilities with Thomas Lumley's leaps wrapper. earth: Multivariate Adaptive Regression Splines. Version 4.6.1, R Packag.	Earth: Multivariate Adaptive Regression Splines (Derived from mda:mars by Trevor Hastie and Rob Tibshirani. Uses Alan Miller's Fortran utilities with Thomas Lumley's leaps wrapper). Version 4.6.1, R Package. [online] https://cran.r-project.org/package=earth.
68	Reference Toifl 2010	Review of process and performance monitoring techniques applicable to large and small scale wastewater recycling systems.	Review of process and performance monitoring techniques applicable to large and small scale wastewater recycling systems. CRIRO: Water for a Healthy Country National Research Flagship.

ISBN: 978-82-575-1515-7
ISSN: 1894-6402

Norwegian University
of Life Sciences

Postboks 5003
NO-1432 Ås, Norway
+47 67 23 00 00
www.nmbu.no

99221 / ANDVORDGRAFISK.NO